

C-H BORYLATION OF TERMINAL ALKYNES, THE REDUCTIVE CYCLIZATION
OF ALKYNYLBORONATES, AND THE SYNTHESIS AND ANALYSIS OF
PINCER-LIGATED RHODIUM COMPLEXES

A Dissertation

by

CHRISTOPHER JAMES PELL

Submitted to the Office of Graduate and Professional Studies of
Texas A&M University
in partial fulfillment of the requirements for the degree of

DOCTOR OF PHILOSOPHY

Chair of Committee,	Oleg V. Ozerov
Committee Members,	Michael B. Hall
	François P. Gabbaï
	Perla B. Balbuena
Head of Department,	Simon W. North

December 2017

Major Subject: Chemistry

Copyright 2017 Christopher J. Pell

ABSTRACT

Due to the utility of organoboron reagents in the synthesis of pharmaceuticals and other industrially relevant compounds, the transition metal-catalyzed C-H borylation of organic molecules has become a very popular area of research. Since the Ozerov group's initial discovery of an iridium complex that can perform catalytic dehydrogenative borylation of terminal alkynes (DHBTA), we have made further investigations into the C-H borylation of terminal alkynes and the synthetic applications of the alkynylboronate products.

Here we describe a pincer-ligated palladium complex as the first group 10 catalyst for DHBTA. Unlike the iridium systems, the palladium catalyst also catalyzed a competing alkyne hydrogenation reaction, which could be suppressed using elemental mercury or phosphines as additives. We then turned our attention to (PNP)Ir complexes as catalysts for the DHBTA of 1,6-enynes and 1,6-diynes. These substrates could be borylated and isolated in moderate to excellent yields, and they could serve as substrates for rhodium-catalyzed reductive cyclization to form five-membered cyclic compounds containing pendant C-B bonds. It was found that borylated 1,6-diynes tethered by amines or an ether linkage would form 3,4-bis(methylpinacolboryl)-substituted pyrroles or furans during reductive cyclization.

Investigations into C-C coupling catalyzed by pincer-ligated rhodium complexes will also be discussed. First, we describe the synthesis of a series of PCP-based pincer-ligated rhodium complexes and how they performed as catalysts for stereoselective

alkyne dimerization. While stereoselectivity was not achieved with any of the PCP-ligands on rhodium, these systems were faster and longer-lived than the (PNP)Rh alkyne dimerization catalysts previously reported by our group. Later, the fate of (PNP)Rh as a potential catalyst for Negishi coupling will be discussed. It was observed that although (PNP)Rh could perform all three fundamental steps in Negishi coupling (oxidative addition of an aryl halide, transmetallation, and reductive elimination), it was not a suitable catalyst. This was due to rhodium's ability to insert into the carbon-zinc bond of the organozinc reagent to form a catalytically inactive species.

Finally, the synthesis, characterization, and electronic structure of complexes of (PNP)Rh bearing small perfluorocarbon ligands will be described.

DEDICATION

To Mom and Dad for showing me that hard work pays off.

ACKNOWLEDGEMENTS

I would like to thank my research advisor Dr. Oleg Ozerov for his guidance over the past five years as well as during my 2011 summer semester as an REU student. I appreciate his time and all the opportunities that he has provided me. His mentorship has allowed me to develop into a successful chemist and an independent thinker. I would also like to thank my committee members Dr. Michael Hall, Dr. François Gabbai, and Dr. Perla Balbuena.

I would also like to thank the Ozerov research group, especially my elders who mentored me in navigating graduate school and becoming a better chemist: Sam Timpa, Morgan MacInnis, Chun-I Lee, Loren Press, Billy McCulloch, Jessica DeMott, Yanjun Zhu, Rafael Huacuja, Rodrigo Ramirez, Jill Davidson, and Chandra Mouli Palit. I also appreciated having Wei-Chun Shih as a classmate, and I am proud to see Bryan Foley continue the project of alkyne C-H borylation. To all of those still working in the Ozerov group, I wish you the best of luck.

Above all, I would like to thank my family who stood by me and made all of my accomplishments possible. Thanks to my mom, dad, and Tom for instilling in me all the values that have helped me succeed in graduate school. Finally, I would like to thank the love of my life, Yanyan Wang, who inspires me to be a better person.

I am proud to have spent time at Texas A&M University. The spirit and traditions of A&M are contagious, and I am glad that I have become a part of this community.

CONTRIBUTORS AND FUNDING SOURCES

This work was supervised by a thesis committee consisting of Professor Oleg V. Ozerov, Professor François P. Gabbaï, and Professor Michael B. Hall of the Department of Chemistry and Professor Perla B. Balbuena of the Department of Chemical Engineering.

Assistance with automated flash column chromatography for the work in Chapter 3 was provided by Yanyan Wang and Professor Donald J. Darensbourg (Department of Chemistry, TAMU).

The XRD structures in Chapter 5 were solved by Wei-Chun Shih during his time as a graduate student in the Department of Chemistry at Texas A&M University. The XRD structures in Chapter 6 were solved by David Herbert during his time as a postdoctoral research associate in the Department of Chemistry at Texas A&M University. The synthesis and characterization of some compounds in Chapter 6 were completed by Yanjun Zhu (Department of Chemistry, TAMU), and several experiments were conducted by Rafael Huacuja (Department of Chemistry, TAMU). All computational analysis in Chapter 6 was performed by Professor Russel P. Hughes of the Department of Chemistry at Dartmouth College.

All other work conducted for this dissertation was completed by the student independently.

This work was made possible in part by the U.S. National Science Foundation (grants CHE-0944634, CHE-1300299, and CHE-1565923 to O. V. O.) and the Welch

Foundation (grant A-1717 to O. V. O.). Its contents are solely the responsibility of the authors and do not necessarily represent the official views of the U.S. National Science Foundation or the Welch Foundation.

NOMENCLATURE

Ar	Aryl
BArF ₂₀	Tetrakis(pentafluorophenyl)borate
B ₂ pin ₂	Bis(pinacolato)diboron
BINAP	2,2'-Bis(diphenylphosphino)-1,1'-binaphthyl
BIPHEP	2,2'-Bis(diphenylphosphino)-1,1'-biphenyl
Boc	<i>tert</i> -Butoxycarbonyl
CAAC	Cyclic (alkyl)(amino) carbene
COD	Cyclooctadiene
COE	Cyclooctene
Cp	Cyclopentadienyl
Cp*	1,2,3,4,5-Pentamethylcyclopentadienyl
DBA	Dibenzylideneacetone
DFT	Density Functional Theory
DHBTA	Dehydrogenative Borylation of Terminal Alkynes
Dipp	2,6-diisopropylphenyl
Et	Ethyl
FLP	Frustrated Lewis Pair
HBpin	Pinacolborane, 4,4,5,5-tetramethyl-1,3,2-dioxaborolane
HBdan	1,8-naphthalenediaminatoborane
ⁱ Pr	<i>iso</i> -propyl
MIDA	<i>N</i> -methylimidodiacetic acid

NBO	Natural Bond Order
NBS	<i>N</i> -bromosuccinimide
n-Bu	<i>n</i> -butyl
NHC	<i>N</i> -heterocyclic carbene
NLMO	Natural Localized Molecular Orbitals
NMR	Nuclear Magnetic Resonance
OA	Oxidative Addition
OAc	Acetate
OTf	Triflate
Ph	Phenyl
PMP	1,2,2,6,6-pentamethylpiperidine
py	pyridine
RE	Reductive Elimination
TBE	<i>tert</i> -butyl ethylene, 2,2-dimethyl-3-butene
^t Bu	<i>tert</i> -butyl
THF	Tetrahydrofuran
TM	Transmetallation
Ts	Toluenesulfonamide
WBI	Wiberg Bond Indices
XRD	X-Ray Diffraction

TABLE OF CONTENTS

	Page
ABSTRACT	ii
DEDICATION	iv
ACKNOWLEDGEMENTS	v
CONTRIBUTORS AND FUNDING SOURCES.....	vi
NOMENCLATURE.....	viii
TABLE OF CONTENTS	x
LIST OF SCHEMES	xiv
LIST OF FIGURES.....	xix
LIST OF TABLES	xxii
CHAPTER I INTRODUCTION AND LITERATURE REVIEW	1
1.1 Introduction	1
1.1.1 Introduction to Organoboron Chemistry	1
1.1.2 Synthesis of Organoboron Reagents and the Beginning of C-H Borylation.....	3
1.1.3 Summary – Alkynylboronates in Context	7
1.2 Synthesis of Alkynylboron Compounds	10
1.2.1 Traditional Synthesis of Alkynylboron Reagents	10
1.2.1.1 Synthesis of Alkynylboronates.....	10
1.2.1.2 Synthesis of Ethynyl N-Methylimidodiacetic Acid Boronates	12
1.2.1.3 Synthesis of Alkynyl Trifluoroborate Salts.....	13
1.2.2 Dehydrogenative Borylation of Terminal Alkynes	13
1.2.3 Formation of Alkynyl Triarylborates with Frustrated Lewis Pairs	19
1.2.4 Formation of Alkynylboronates and Tetraalkynylborates Using Amines.....	22
1.3 Applications of Alkynylboronates	24
1.3.1 Synthesis of Multisubstituted Olefins	24
1.3.2 Applications in C-C Coupling Chemistry	29
1.3.3 Synthesis of Cyclic Compounds Containing Pendant C-B Bonds	36

CHAPTER II Pincer-ligated Palladium Catalyzed Dehydrogenative Borylation of Terminal Alkynes	44
2.1 Introduction	44
2.2 Results and Discussion.....	47
2.2.1 Synthesis of Group 10 DHBTA Catalysts.....	47
2.2.2 Catalytic DHBTA Activity with Group 10 Metal (POCOP) Complexes	48
2.2.3 Ligand Screening and Catalyst Optimization.....	54
2.2.4 Substrate Scope	57
2.2.5 Attempts to Diborylate Acetylene	58
2.3 Conclusions	61
2.4 Experimental	61
2.4.1 General Considerations	61
2.4.2 Synthesis and Characterization	62
2.4.3 Stoichiometric Reactions.....	68
2.4.4 Catalytic Reactions.....	72
2.4.5 Characterization of Alkynylboronates.....	78
CHAPTER III Dehydrogenative Borylation of 1,6-Enynes and 1,6-Diynes and Subsequent Reductive Cyclization.....	79
3.1 Introduction	79
3.2 Results and Discussion.....	83
3.2.1 DHBTA of 1,6-Enynes.....	83
3.2.2 DHBTA of 1,6-Diynes	85
3.2.3 Reductive Cyclization of 1,6-Enynes	90
3.2.4 Reductive Cyclization of 1,6-Diynes	99
3.2.5 Subsequent Reactions of Reductive Cyclization Products.....	106
3.3 Conclusions	107
3.4 Experimental	108
3.4.1 General Considerations	108
3.4.2 DHBTA of 1,6-Enynes and 1,6-Diynes	109
3.4.2.1 Synthesis and Characterization of Borylated 1,6-Enynes	109
3.4.2.2 Synthesis and Characterization of 1,6-Diynes	113
3.4.2.3 Synthesis and Characterization of Borylated 1,6-Diynes.....	116
3.4.3 Synthesis of Reductive Cyclization Catalysts	122
3.4.4 Reductive Cyclization of Borylated 1,6-Enynes	123
3.4.4.1 General Procedure for Catalyst Screening	123
3.4.4.2 General Procedure for Substrate Screening	124
3.4.4.3 Synthesis and Characterization of Organic Products	125
3.4.5 Synthesis and Characterization of [2+2+2] Cyclization Product	131
3.4.6 Reductive Cyclization of Borylated 1,6-Diynes.....	134
3.4.6.1 General Procedure for Substrate Screening	134
3.4.6.2 Synthesis and Characterization of Organic Products	135

3.4.7 Additional Experiments.....	146
CHAPTER IV A SERIES OF Pincer-LIGATED RHODIUM COMPLEXES AS CATALYSTS FOR THE DIMERIZATION OF TERMINAL ALKYNES.....	
4.1 Introduction.....	149
4.2 Results and Discussion.....	151
4.2.1 Synthesis of Pincer Ligands and Their Rh Complexes	151
4.2.2 Catalytic Alkyne Dimerization.....	161
4.3 Conclusion.....	166
4.4 Experimental	167
4.4.1 General Considerations	167
4.4.2 Synthesis and Characterization	167
4.4.3 Catalytic Reactions.....	190
CHAPTER V SYNTHESIS OF PNP RHODIUM COMPLEXES CONTAINING RHODIUM-ZINC COVALENT BONDS	
5.1 Introduction.....	191
5.2 Results and Discussion.....	192
5.2.1 Stoichiometric and Catalytic Reactions Relevant to Negishi Coupling.....	192
5.2.2 Reactions of Rh-Zn Bimetallic Complexes with Dihydrogen.....	203
5.3 Conclusion.....	206
5.4 Experimental	207
5.3.1 General Considerations	207
5.3.2 Negishi Coupling Reactions	207
5.3.3 Synthesis and Characterization	209
5.3.4 Reactions with Dihydrogen	216
5.3.5 X-ray Crystallography.....	217
CHAPTER VI SYNTHESIS OF FLUOROCARBENE, FLUOROOLEFIN, AND FLUOROCARBENE COMPLEXES OF RHODIUM.....	
6.1 Introduction.....	220
6.2 Results and Discussion.....	222
6.2.1 Synthesis of CF ₂ , C ₂ F ₄ , and CFCF ₃ Complexes.....	222
6.2.2 Synthesis of Cationic Fluoromethyldiyne	229
6.3 Computational Studies and Discussion	232
6.3.1 DFT Structural Studies	232
6.3.2 Comparison of C ₂ H ₄ and C ₂ F ₄ Ligands	235
6.3.3 Comparison of CH ₂ and CF ₂ Ligands	239
6.3.4 Comparison of CH ⁺ , CF ⁺ , and CCF ₃ ⁺ Ligands.....	241
6.3.5 Degree of Rh-C Multiple Bonding.....	243
6.3.6 Comparison of CF ⁺ , NO ⁺ , and CO Ligands	243
6.3.7 Relative Energies of Isomeric Fluorocarbon Ligands	244

6.4 Conclusions	245
6.5 Experimental	246
6.5.1 General Considerations	246
6.5.2 Synthesis and Characterization	247
6.5.3 X-ray Crystallography	257
6.5.4 Computational Methods	259
CHAPTER VII CONCLUSION	261
REFERENCES	264
APPENDIX A SYNTHESIS OF BORYLATED METALLACYCLOPENTENES AND ATTEMPTS AT PAUSON KHAND CYCLIZATION WITH ALKYNILBORONATES	294
APPENDIX B SYNTHESIS OF (NHC)CU ALKYNIL COMPLEXES	305
APPENDIX C LIST OF PUBLICATIONS RESULTING FROM PHD WORK	310

LIST OF SCHEMES

	Page
Scheme I-1. Hydroboration-oxidation, hydroboration with dialkoxylboranes, and Suzuki Coupling.	2
Scheme I-2. Methods of synthesizing arylboronates from aryl halides.	4
Scheme I-3. Initial reports of Ir-catalyzed dehydrogenative arene borylation by Smith and Hartwig.	5
Scheme I-4. Arylboronic esters as a temporary functional group.	7
Scheme I-5. Dehydrogenative borylation of terminal alkynes and possible competing side reactions.	9
Scheme I-6. Brown's original synthesis of alkynylboronates.	11
Scheme I-7. Synthesis of diborylethyne from trichloroethylene.	12
Scheme I-8. Synthesis of ethynyl <i>N</i> -methylimidodiacetic acid boronates.	12
Scheme I-9. Synthesis of alkynyl trifluoroborate salts.	13
Scheme I-10. DHBTA catalyzed by Ir ¹	14
Scheme I-11. (PNP)Ir DHBTA catalysts and high turnover performance by Ir ³	15
Scheme I-12. DHBTA with 1,8-naphthalenediaminatoborane catalyzed by Zn(OTf) ₂ and pyridine.	16
Scheme I-13. DHBTA catalyzed by (CAAC)CuOTf (101), and the mechanism proposed by Bertrand et al.	18
Scheme I-14. Dehydrogenative formation of an alkynylboratabenzene ligand on lanthanum.	19
Scheme I-15. Borylation of phenylacetylene using B(C ₆ F ₅) ₃ /P ^t Bu ₃ and the proposed mechanism.	20
Scheme I-16. Amine-borane FLP borylation of 1-hexyne, the Lewis base addition to 1-hexyne, and the carboboration of <i>tert</i> -butylacetylene.	22
Scheme I-17. Formation of alkynylboronates from borenium cations.	23

Scheme I-18. Formation of tetraalkynylborate salts from the PMP-BF ₃ adduct.	24
Scheme I-19. Reactions of alkynylboronates with zirconocene to make multisubstituted olefins.	25
Scheme I-20. Zirconium-mediated double allylation of an alkynylboronate and subsequent ring-closing olefin metathesis to yield borylated cyclohexadiene.	26
Scheme I-21. Diboration of alkynyl MIDA boronates and subsequent selective Suzuki coupling.	27
Scheme I-22. Silylboration of an alkynylboronate and subsequent selective cross coupling reactions to form a tetraarylethene.	28
Scheme I-23. IrI-catalyzed DHBTA and dehydrogenative diboration of terminal alkynes.	29
Scheme I-24. Nickel-catalyzed carboboration of an internal alkyne with an alkynylboronate.	29
Scheme I-25. Trifluoromethylation of alkynyl trifluoroborate salts.	30
Scheme I-26. Synthesis of 1,3-diynes from alkynylboron compounds.	31
Scheme I-27. Synthesis of diarylacetylenes from alkynylboron reagents.	32
Scheme I-28. Suzuki coupling of alkynylboron reagents with acid chlorides and 2- chloroacetates and 2-chloroacetamides.	33
Scheme I-29. Copper-mediated coupling of alkynylboronates with acid chlorides, and boron trichloride-assisted coupling of alkynyltrifluoroborate salts with acid chlorides.	34
Scheme I-30. Bronsted acid catalyzed formation of propargyl ethers and secondary alkylacetylenes from alkynyltrifluoroborate salts.	35
Scheme I-31. Trityl ion mediated C-H alkynylation of ethers with alkynyltrifluoroborate salts.	35
Scheme I-32. Potassium alkynyltrifluoroborates as σ -nucleophiles in an interrupted Nazarov reaction.	36
Scheme I-33. Synthesis of allenes from alkynyl trifluoroborate salts in a Petasis reaction.	36

Scheme I-34. Rhodium catalyzed C-H activation and annulation with ethynyl MIDA boronate to synthesize borylated heterocyclic compounds.	37
Scheme I-35. (Top) [2+2+2] cycloaddition with an alkynylboronate and a borylated 1,6-diyne, (Bottom) [2+2+2] cycloaddition with ethynyl MIDA boronate.....	38
Scheme I-36. Synthesis of borylated bicyclic heterocycles from ethynyl MIDA boronates and 2-iodoanilines/phenols.....	39
Scheme I-37. Zirconocene-mediated synthesis of cyclic borylated compounds.....	40
Scheme I-38. Ring closing enyne metathesis of borylated 1,6-enynes followed by a Diels Alder reaction with nitroethylene.....	40
Scheme I-39. Cycloaddition reactions with alkynylboron compounds to form pyrrazoles.....	41
Scheme I-40. Cycloaddition reaction of alkynylboronates with 2-pyrazinones and the directed cycloadditions of potassium alkynyltrifluoroborate salts with 2-pyrones and triazines.	42
Scheme I-41. Cobalt-mediated Pauson Khand reaction of alkynylboronates and norbornadiene.	43
Scheme II-1. General reaction scheme for the dehydrogenative borylation of terminal alkynes (DHBTA).	45
Scheme II-2. Examples of the dehydrogenative formation of pincer-ligated group 10 metal boryl and alkynyl species from the corresponding metal hydride and the proposed mechanisms for pincer-ligated group 10 metal DHBTA.	46
Scheme II-3. Synthesis of (POCOP)M-H complexes and 206c.....	47
Scheme II-4. Proposed mechanism for palladium-catalyzed DHBTA	51
Scheme II-5. Insertion of an alkynylboronate into 206a's Pd-H bond and the protonolysis of 206d and 206e.....	52
Scheme II-6. Additional PCP-type pincer-ligated palladium DHBTA precatalysts.	55
Scheme II-7. Synthesis of 206f and subsequent reaction with HBpin.	59
Scheme III-1. DHBTA and Ir DHBTA catalysts	80
Scheme III-2. Rhodium-catalyzed reductive cyclization of 1,6-enynes and 1,6-diyne as first described by the Krische group.	81

Scheme III-3. Reductive cyclization with borylated 1,6-enynes and 1,6-diynes.	83
Scheme III-4. Rh-catalyzed [2+2+2] cycloaddition of 303B.	96
Scheme III-5. Reported synthesis of pyrroles from <i>N,N</i> -dipropargylamines.	105
Scheme III-6. Oxidation of 309B _{2c} -pyr to form a 3,4-bis(hydroxymethyl)pyrrole.	106
Scheme III-7. Suzuki coupling of 306B _{2c} -exo with 4-fluoroiodobenzene.	107
Scheme IV-1. Alkyne dimerization.	150
Scheme IV-2. Synthesis of bis(phosphinite) ligands.	152
Scheme IV-3. Synthesis of <i>Ortho</i> -methyl PNP (409).	154
Scheme IV-4. Synthesis of rhodium complexes of the <i>Ortho</i> -methyl PNP ligand (409).	155
Scheme IV-5. Direct metalation of (POCOP)-type pincer ligands with [(COD)RhCl] ₂	156
Scheme IV-6. Synthesis of Rh pincer complexes through six-coordinate intermediates.	158
Scheme IV-7. Synthesis of Rh(I) diisopropylsulfide adducts.	159
Scheme IV-8. Synthesis of 404-Rh(H ₂) and 403-Rh(C ₆ H ₁₀).	159
Scheme IV-9. Synthesis of Rh(I) pincer carbonyl complexes.	160
Scheme IV-10. Possible mechanism for alkyne dimerization.	164
Scheme V-1. Mechanism for Pd-catalyzed Negishi coupling compared to a Rh(I)/Rh(III) mechanism.	192
Scheme V-2. (Top) 501-Cl Transmetalation with Ph ₂ Zn, reductive elimination of biphenyl, and oxidative addition of iodobenzene. (Bottom) Dehydrohalogenation of 502 with Ph ₂ Zn and the oxidative addition of iodobenzene.	193
Scheme V-3. Synthesis of 504 and 505.	195
Scheme V-4. (Top) Treatment of 504 with chlorobenzene. (Bottom) Synthesis and hydrolysis of 506 and synthesis of 507.	200

Scheme V-5. Treatment of 506 with phenylhalides and percent conversion to 501-X.	203
Scheme VI-1. Initial observation of (PNP)Rh=CF ₂ , and synthesis of (PNP)Rh=CF ₂ initially performed by Yanjun Zhu.	223
Scheme VI-2. Reactions of 503 with pentafluoroethane and fluoroform to synthesize perfluoroalkylidnes.	225
Scheme VI-3. Synthesis of (PNP)Rh(C ₂ F ₄).	226
Scheme VI-4. Synthesis of (PNP)RhCF ⁺ via fluoride abstraction. Initially performed by Yanjun Zhu.	230
Scheme A-1. Synthesis of A01 and observation of A02.	294
Scheme A-2. Synthesis of A03 from Cp ₂ TiCl ₂ .	297
Scheme A-3. Synthesis of borylated cyclopentenone A04 from A03.	299
Scheme A-4. Synthesis of borylated cyclopentenone A06 with stoichiometric [Rh(CO) ₂ Cl] ₂ .	301
Scheme B-1. Synthesis of B02.	305
Scheme B-2. Synthesis of B04.	306
Scheme B-3. Synthesis of B05.	307

LIST OF FIGURES

	Page
Figure II-1. Photograph of J. Young tubes for entries 3, Table II-1 (right) and 6, Table II-2 (left) after 1 day. A drop of Mercury can be seen in the left tube. The right tube has changed to a red/orange color indicating the presence of Pd nanoparticles.	53
Figure II-2. Reaction mixture concentrations resulting from the treatment of 206f with 2 eq. of pinacolborane.	60
Figure II-3. Stacked ¹ H NMR spectra from Table II-6, entry 3. 4-methylstyrene is not produced until after day 1.	76
Figure III-1. ¹ H- ¹³ C HSQC NMR spectrum of crude 303Bc-endo in CDCl ₃ . Resonances for residual pentane are visible at 0.88 and 1.27 ppm. Cross peak for CH ₂ -Bpin ¹ H- ¹³ C correlations highlighted at (1.43,9.41) and (1.57,9.34).	128
Figure III-2. ¹ H- ¹³ C HMBC spectrum of 302Bd-a indicating the correlation between the proton on C ₂ with C ₅	134
Figure III-3. ¹ H- ¹³ C HSQC NMR spectrum of 309B ₂ c-pyr in CDCl ₃ . Crosspeak highlighted at (2.046,8.218) to show the ¹ H- ¹³ C correlation between CH ₂ -Bpin.	140
Figure IV-1. (PNP)Rh alkyne dimerization catalysts.	151
Figure V-1: Left: ORTEP drawing of 504. The ellipsoids are set at the 50% probability level, and hydrogen atoms and isopropyl methyls have been omitted for clarity. Selected bond distances (Å) and angles (°): Rh1-C1 = 2.048(4), Rh1-Zn1 = 2.3217(6), C7-Zn1-Rh1 = 175.62(14), Zn1-C7 = 1.949(4), N1-Rh1-Zn1 = 73.32(10), Zn1-N1 = 2.664(4), Rh1-N1 = 2.133(3) C1-Rh1-N1 = 178.36(16), P1-Rh1-P2 = 162.62(4), Rh1-P1 = 2.2760(11), Rh1-P2 = 2.2819(11), N1-Zn1-Rh1 = 50.08(8). Zn-N Contact: C1'-Rh1'-N1' = 177.57(16), C1'-Rh1' = 2.025(4), N1'-Rh1' = 2.155(3), Zn1'-Rh1' = 2.3478(7), N1'-Rh1'-Zn1' = 63.21(10), N1'-Rh1' = 2.155(3), P1'-Rh1' = 2.2710(11), Rh1'-P2' = 2.2869(11), P1'-Rh1'-P2' = 162.67(4), N1'-Zn1' = 2.366(4), N1'-Rh1'-Zn1' = 63.21(10), N1'-Zn1'-Rh1' = 54.41(8), C7'-Zn1'-Rh1' = 173.15(13). XRD Structure solved by Wei-Chun Shih.	196
Figure V-2. ORTEP drawing of 505. The ellipsoids are set at the 50% probability level, and hydrogen atoms and methyls are omitted for clarity. Selected	

bond distances (Å) and angles (°): Rh1-Zn1 = 2.3738(5), Rh2-Zn1 = 2.3711(5), Rh1-N1 = 2.117(2), Rh2-N2 = 2.114(2), Rh1-C1 = 2.054(3), Rh2-C33 = 2.049(3), Rh1-Zn1-Rh2 = 177.030(16), C1-Rh1-Zn1 = 89.44(8), C33-Rh2-Zn1 = 89.43(8), C1-Rh1-N1 = 172.80(10), C33-Rh2-N2 = 174.33(10), P1-Rh1-P2 = 155.54(3), P3-Rh2-P4 = 158.44(3). XRD structure solved by Wei-Chun Shih. 197

- Figure V-3. ORTEP Drawing of 507. The ellipsoids are set at the 50% probability level. Hydrogens, methyls, and a molecule of pentane are omitted for clarity. Selected bond distances (Å) and angles (°): Rh1-Cl1 = 2.4403(14), Rh1-Cl2 = 2.6114(15), Rh2-Cl3 = 2.4287(14), Rh2-Cl4 = 2.6102(16), Rh1-N1 = 2.038(5), Rh2-N2 = 2.023(4), N1-Rh1-Cl2 = 92.97(14), N2-Rh2-Cl4 = 91.26(15), Zn1-Cl1 = 2.3045(16), Zn1-Cl2 = 2.2585(16), Zn1-Cl3 = 2.3151(17), Zn1-Cl4 = 2.2385(15), N1-Rh1-Cl1 = 176.71(14), N2-Rh2-Cl3 = 176.04(15), Cl1-Zn1-Cl3 = 106.25(6), Cl2-Zn1-Cl3 = 120.67(6), Cl4-Zn1-Cl3 = 97.11(6). The Rh-H could not be located from the difference Fourier maps. XRD structure solved by Wei-Chun Shih. 202
- Figure V-4. ¹H NMR spectrum resulting from the treatment of 504 with dihydrogen gas. Inset is the hydride region of the ¹H NMR spectrum. 205
- Figure V-5. Crude ¹H NMR spectrum resulting from treating 401-Rh(H₂) with ZnCl₂. Inset is the hydride region of the ¹H NMR spectrum. 206
- Figure VI-1. Perfluoroalkylidenes from Hughes and Baker. Isolated fluorocarbyne by Hughes, the iridium carbyne by Bergman, and matrix-trapped fluorocarbynes by Andrews. 221
- Figure VI-2 ORTEPs of (PNP)Rh=CF₂ (left) and (PNP)Rh(C₂F₄) (right). The ellipsoids are set at the 50% probability level, and hydrogen atoms are omitted for clarity. Selected bond distances (Å) and angles (°) for (PNP)Rh=CF₂: Rh1-C1, 1.821(4); Rh1-N1, 2.043(3); C1-F1, 1.335(4); C1-F2, 1.348(5); N1-Rh-C1, 171.39(15); F2-C1-F1, 100.8(3); Rh1-C1-F2, 130.1(3); Rh1-C1-F1, 128.6. (PNP)Rh(C₂F₄): Rh1-C14, 2.006(3); Rh1-N1, 2.054(3); C14-F1, 1.378(3); C14-F2, 1.361(3); C14-C140, 1.354(7); C14-Rh-C140, 39.4(2); C14-Rh-N1, 160.28(10). XRD structures solved by David Herbert. 228
- Figure VI-3. ORTEP of [(PNP)Rh≡CF][HCB₁₁Cl₁₁]. The ellipsoids are set at the 50% probability level, and hydrogen atoms are omitted for clarity. Selected bond distances (Å) and angles (°): Rh1-C1, 1.702(7); Rh1-N1, 2.019(4); C1-F1, 1.257(8); C1-Rh1-N1, 174.1(3); F1-C1-Rh1, 173.4(7). XRD Structure solved by David Herbert. 231

Figure VI-4. NLMOs for the bonding and antibonding interactions between C ₂ H ₄ (column 1) and C ₂ F ₄ (column 2) and the (PNP)Rh fragment. For clarity the P ⁱ Pr ₂ groups have been replaced by PMe ₂ groups and the aryl part of the pincer truncated to P-CH=CH-N linkers.	237
Figure VI-5. NLMOs for the bonding and antibonding interactions between the CF ₂ ligand and the (PNP)Rh fragment (left) and for the CH ₂ ligand and the (PNP)Rh fragment (right). For clarity the P ⁱ Pr ₂ groups have been replaced by PMe ₂ groups and the aryl part of the pincer truncated to P-CH=CH-N linkers.	240
Figure VI-6. NLMOs for the bonding and antibonding interactions between the CF ⁺ ligand and the (PNP)Rh fragment. For clarity the P ⁱ Pr ₂ groups have been replaced by PMe ₂ groups and the aryl part of the pincer truncated to P-CH=CH-N linkers.	242
Figure VI-7. Resonance forms for the π-system in a linear Rh–X–Y ligand array, with WBI values for the bonds in Rh–C–O, Rh–N–O, and Rh–C–F complexes. All three complexes are isoelectronic and no formal charges are shown.	244
Figure VI-8. (Top) Calculated structures and relative energies for (PNP)Rh(C ₂ F ₄) isomers. (Bottom) Calculated structures and relative energies for proposed structures resulting from fluoride abstraction from (PNP)Rh=C(F)(CF ₃).....	245
Figure A-1. ¹ H NMR of A01 in C ₆ D ₆	296
Figure A-2. ¹ H NMR of A03 in C ₆ D ₆	298
Figure A-3. <i>in situ</i> ¹ H NMR of A04 in CDCl ₃ . Cp ₂ TiCl ₂ is present at 6.58 ppm, and 1,4-dioxane is present at 3.73 ppm.	300
Figure A-4. ¹ H NMR of A06 in C ₆ D ₆ . Bpin decomposition product can be observed at 1.01 and silicone grease is present at 0.29 ppm.	302
Figure B-1. ¹ H NMR of B04 in CDCl ₃ . Residual dichloromethane visible at 5.30 ppm, residual pentane resonances visible at 0.88 ppm and 1.27 ppm. Residual silicone grease visible at 0.07 ppm.	307
Figure B-2. ¹ H NMR spectrum of B05 in CDCl ₃ . Residual dichloromethane visible at 5.30 ppm, residual pentane resonances visible at 0.88 ppm and 1.27 ppm.	309

LIST OF TABLES

	Page
Table II-1. DHBTA catalyst screening with (POCOP)M complexes (M = Ni, Pd, Pt).....	49
Table II-2. The effect of additives on Pd-catalyzed DHBTA of 4-ethynyltoluene.....	54
Table II-3. DHBTA with different (pincer)Pd catalysts.....	56
Table II-4. DHBTA with various alkynes.	58
Table II-5. Comprehensive list of all DHBTA reactions of 4-ethynyltoluene with different (POCOP)Pd catalysts and various additives.	73
Table II-6. Turnover test for 209b.....	75
Table II-7. Higher HBpin:Alkyne Ratios	77
Table III-1. DHBTA of 1,6-enynes.	84
Table III-2. DHBTA of 1,6-diynes.....	86
Table III-3. Reductive cyclization of 303B.....	91
Table III-4. Reductive cyclization of of various borylated 1,6-enynes.....	97
Table III-5. Reductive cyclization of borylated 1,6-diynes.....	100
Table IV-1. Carbonyl stretching frequencies of PCP/POCOP rhodium carbonyl compounds	161
Table IV-2. Conversion of alkyne and the isomeric distribution of the produced enynes.	162
Table IV-3. Geminal/ <i>E</i> enyne isomer ratios for dimerization catalysts.	165
Table V-1. Negishi coupling with 502	194
Table VI-1. Calculated and crystallographic bond lengths (Å) ^a and Wiberg Bond Indices ^b (WBI) for (PNP)Rh compounds.	234
Table A-1. Attempts at stoichiometric and catalytic Pauson Khand reactions with alkynylboronates.....	303

CHAPTER I

INTRODUCTION AND LITERATURE REVIEW

1.1 Introduction

1.1.1 Introduction to Organoboron Chemistry

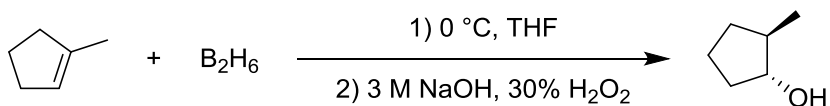
Borylated organic molecules are versatile reagents in synthetic chemistry and their reactivity has provided useful techniques for the synthetic chemist's toolbox. Transformations regarding C-B bonds have been honored with Nobel prizes in chemistry being awarded to Herbert C. Brown¹ in 1979 for his work on hydroboration-oxidation and Akira Suzuki² in 2010 for his work on palladium-catalyzed carbon-carbon coupling reactions. Boron's role in both of these reactions is as a stepping stone to a desired product, and boron does not appear in the final product.

In the original report of hydroboration-oxidation,³ the B-H bond of diborane is added across a C-C double bond and then oxidized with hydrogen peroxide as an anti-Markovnikov synthesis of alcohols (Scheme I-1, top). The B-H bonds of dialkylboranes, such as 9-borabicyclo [3.3.1] nonane (9-BBN) can also easily add across unsaturated C-C bonds without the aid of catalysts.⁴ Advances in hydroboration led to regioselective and chemoselective hydroboration of both alkenes and alkynes with dialkoxylboranes using catalysts (Scheme I-1, middle).^{5,6}

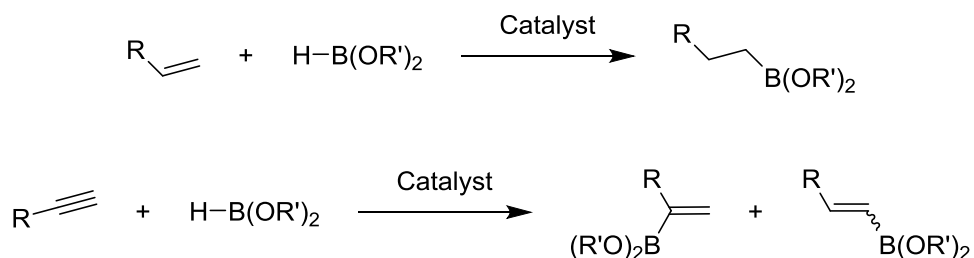
In the case of Suzuki coupling, the C-B functionality is used as a transmetallation agent to create a new C-C bond via palladium coupling catalysis (Scheme I-1, bottom).

The reaction was first discovered using alkenyl boronic esters with alkenyl or alkynyl halides.⁷ The adaptability of the reaction allowed the substrate scope to be rapidly expanded to a number of different organoboranes such as arylboron, alkylboron, and alkynylboron reagents with a number of different organic electrophiles.² The field has also advanced in the level of sophistication of the boron-containing functional group, which has allowed for tailoring the organoboron reagents to favor certain reaction conditions.⁸

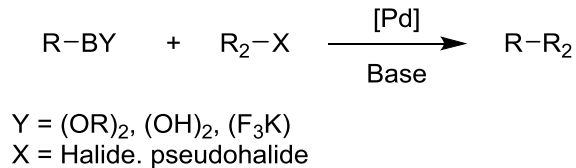
Brown: Original Hydroboration-Oxidation Reaction



Hydroboration with dialkoxylboranes



Suzuki Coupling Reaction



Scheme I-1. Hydroboration-oxidation, hydroboration with dialkoxylboranes, and Suzuki Coupling.

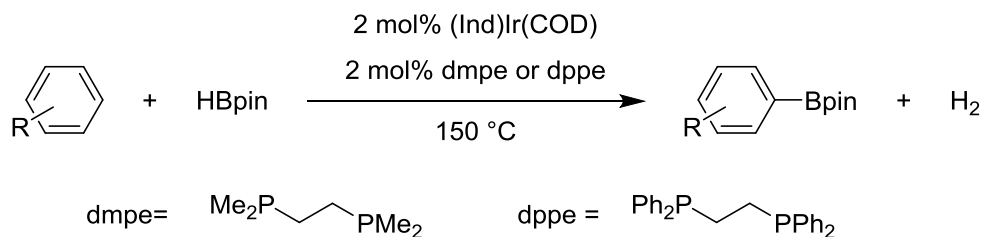
These two reactions have used borylated organic molecules as stepping stones to synthesize molecules of pharmaceutical and industry interest.⁹ It should be noted that in these reactions the organoboron moiety is used as a temporary functional group and is not present in the final product. More recently, boron has been recognized as more than just a means to an end and has been incorporated as a key component in small molecule pharmaceuticals. For instance, crisaborole (Eucrisa) has recently been approved by the Food and Drug Administration as a topical treatment for eczema, and its mode of action is directly dependent on the presence of boron in its structure.¹⁰

1.1.2 Synthesis of Organoboron Reagents and the Beginning of C-H Borylation

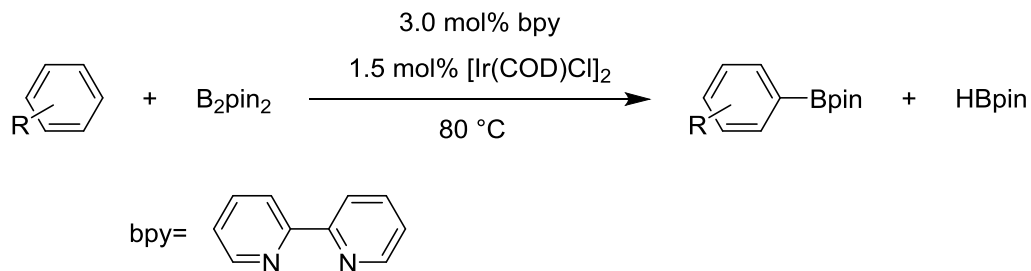
Due to the obvious utility of organoboron reagents, there has been a drive to develop new methods of incorporating C-B bonds into molecules. As shown in Scheme I-1, borylated olefins and alkanes can be accessed via the hydroboration of alkenes and alkynes. Arylboronates are typically formed from aryl halides being treated with a strong organometallic base such as butyl lithium and then reacted with a trialkyl borate reagent (Scheme I-2, top).¹¹ Initially these reactions were conducted in batches, but recent advances in continuous processing flow reactors make this a current popular method for the industrial synthesis of organoboron reagents.¹² Aryl boronic esters can also be accessed via palladium cross coupling with diboron reagents or boranes in a process called Miyuara coupling (Scheme I-2, bottom).¹³ The downside of these two methods is that they require the prefunctionalization of the arene via halogenation, and they are not atom economical due to the stoichiometric production of a salt byproduct.

borylation of arenes with regards to selectivity¹⁸⁻²⁰ and turn over numbers.^{21,22} The method of C-H borylation followed by cross coupling has also been used in the total synthesis of a number of products;^{15,23} most recently it has been used in the 100 kg scale preparation of Doravirine, which is currently being tested for the treatment of HIV/AIDS.²⁴

Smith et al.



Hartwig et. al.

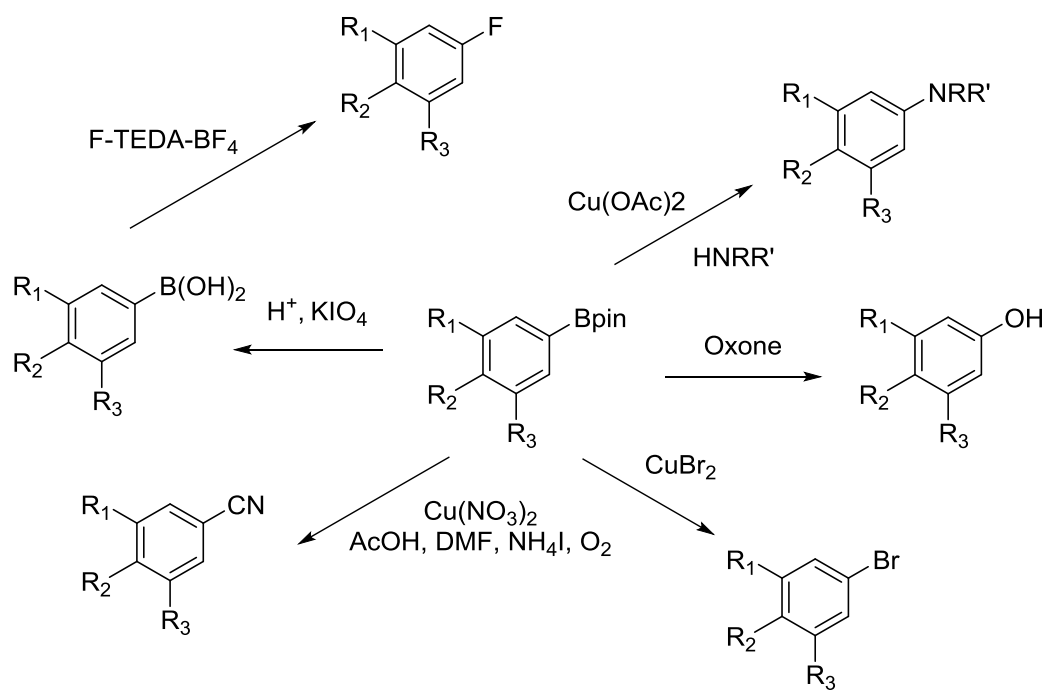


Scheme I-3. Initial reports of Ir-catalyzed dehydrogenative arene borylation by Smith and Hartwig.

The popularity of these dehydrogenative borylation catalysts with synthetic chemists resulted in a deeper investigations into the utility of aryl boronic esters beyond their use as coupling partners in the Suzuki reaction.²³ Arylboronic esters have been shown to be versatile temporary functional groups for a number of transformations to

desirable functional groups where the regioselectivity is dictated by sterics instead of electronics. For instance, C-H borylation followed by oxidation with oxone was used as a straightforward synthesis of 3,5-disubstituted phenols (Scheme I-4).²⁵ C-H borylation was also used as a starting point to access meta halogenated 1,3-disubstituted arenes (Scheme I-4).²⁶

Aryl nitriles,²⁷ arylamines and ethers²⁸ have also been synthesized through a number of methods from aryl boronates (Scheme I-4). There is also a wide array of copper-mediated transformations from boronic acids,²⁹ which can be accessed from the boronic esters via oxidative hydrolysis in the presence of periodate (Scheme I-4).³⁰ One premier transformation from aryl boronic acids is the formation of aryl fluorides,³¹ which is a useful technique for ¹⁸F-labeling of arenes for positron emission tomography (Scheme I-4).³²

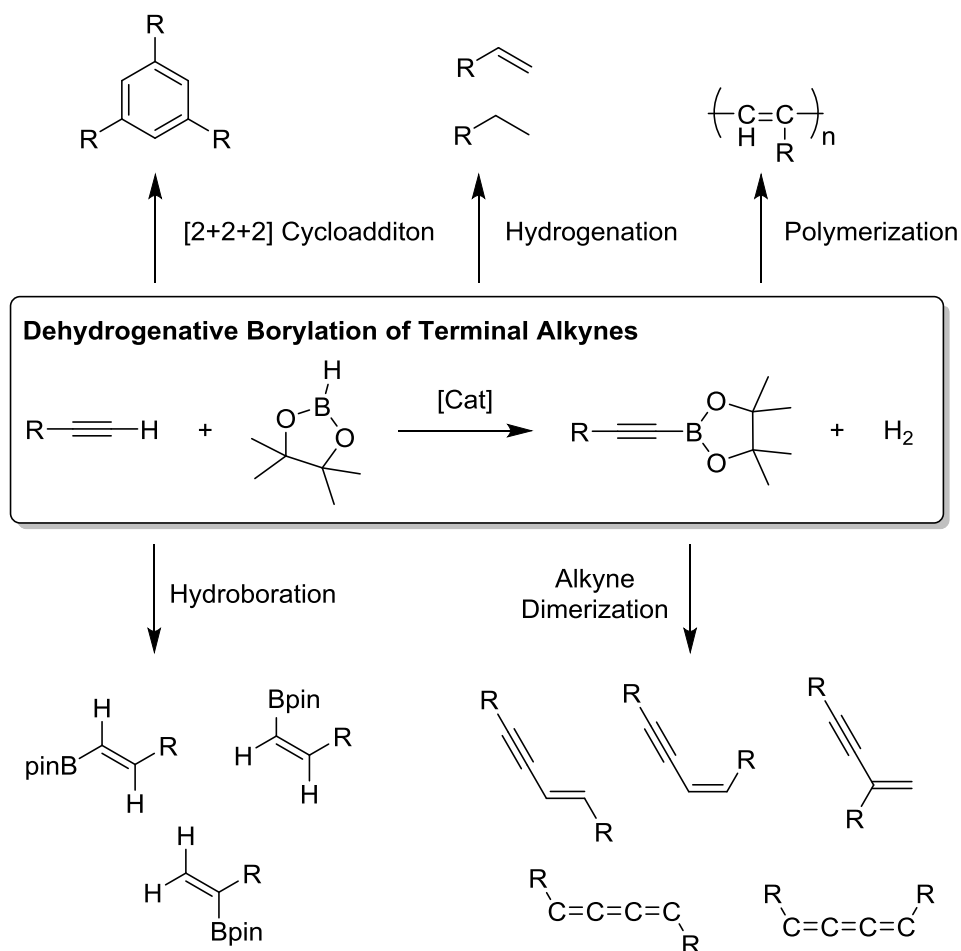


Scheme I-4. Arylboronic esters as a temporary functional group.

1.1.3 Summary – Alkynylboronates in Context

It is evident from the diverse applications of organoboron reagents that the incorporation of C-B bonds into small molecules is a valuable transformation. While arene borylation has become a very sophisticated methodology over the past 15-20 years, there have also been advances in the borylation of a variety of substrates such as alkanes,³³ benzylic C-H bonds,³⁴ allylic C-H bonds,³⁵ and alkenes.³⁶ However, one substrate that eluded the grasp of C-H borylation catalysis until recently was the terminal alkyne.³⁷ The product of the C-H borylation of terminal alkynes is an alkynylboronate (Scheme I-5). This transformation is particularly difficult because the B-H bond of the borane can add across the unsaturated C-C bond of the alkyne in a hydroboration

reaction.⁶ In the presence of transition metals, terminal alkynes can also undergo a number of different autotransformations such as alkyne dimerization to form enynes³⁸ and butatrienes,³⁹ [2+2+2] cycloadditions,⁴⁰ and oligomerizations and polymerizations.⁴¹ Also, if a catalyst can perform C-H borylation of terminal alkynes, then hydrogen gas will be a byproduct which could result in the hydrogenation of the alkyne.⁴² Then there is also the possibility that the products from these reactions could participate in a subsequent reaction. A catalyst capable of performing the C-H borylation of terminal alkynes would have to avoid all of these possible reactions (Scheme I-5).



Scheme I-5. Dehydrogenative borylation of terminal alkynes and possible competing side reactions.

Our group discovered the C-H borylation of terminal alkynes using pincer-ligated iridium catalysts, and two chapters of this thesis will regard the advancement of pincer-ligated transition metal borylation catalysts as well as the application of the alkynylboronate products in cyclization reactions. Alkynylboron reagents are versatile building blocks in organic chemistry, and their synthesis and reactivity has been recently reviewed.^{43,44} The rest of this chapter will highlight the traditional and developing

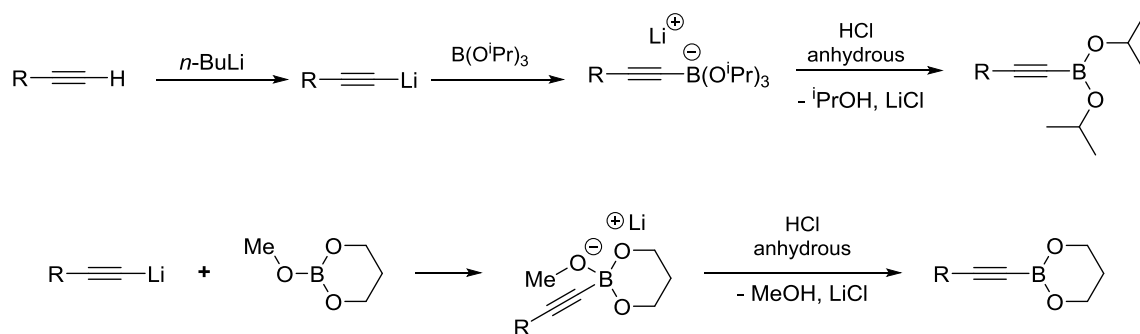
methods used to access alkynylboron reagents as well as highlight the more recent applications of these useful reagents.

1.2 Synthesis of Alkynylboron Compounds

1.2.1 Traditional Synthesis of Alkynylboron Reagents

1.2.1.1 Synthesis of Alkynylboronates

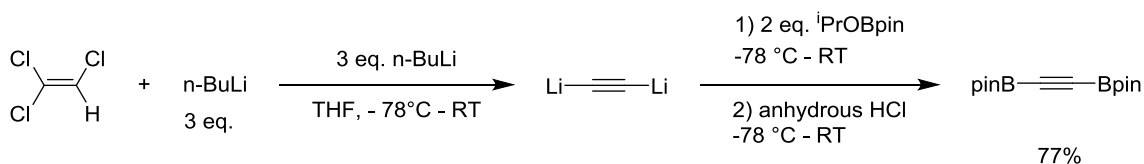
The traditional synthesis of organoboron reagents is typically accomplished via the reaction of a nucleophilic organometallic reagent with a trialkyl borate reagent.¹² This is also the case for the commonly used synthesis of alkynylboronates developed by the Brown group.⁴⁵ In this procedure, a lithium acetylide is reacted with a trialkylborate (Scheme I-6). The lithium borate salt is then treated with anhydrous hydrochloric acid to yield a neutral alkynylboronate. Brown's original report also showed that this synthesis can be accomplished with a cyclic borate (2-methoxy-1,3,2-dioxaborinane). Studies using alkynylboronates have frequently used this general synthesis with other cyclic borates such as isopropoxy pinacolborane.⁴³



Scheme I-6. Brown's original synthesis of alkynylboronates.

There is also a Ag(I)-catalyzed version of this reaction that couples terminal alkynes with isopropoxy pinacolborane and uses Cs_2CO_3 as a base instead of a strong alkali metal base.⁴⁶ However, this catalytic method still requires an acidic workup step for product isolation. The authors report that the alkynylboronates can be isolated through column chromatography; however, in our experience alkynylboronates were wont to undergo hydrolysis when exposed to silica gel.

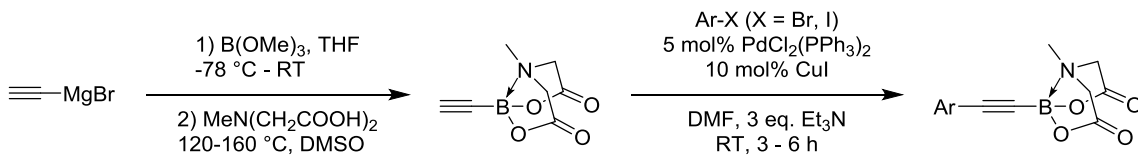
The traditional synthesis of diborylated acetylene requires a slight variation to Brown's method. It was discovered by the Barton group during their research on preceramic polymers that trichloroethylene, when treated with three equivalents of *n*-butyl lithium at $-78\text{ }^\circ\text{C}$, will form dilithium acetylide.⁴⁷ The Therien group applied this method in order to synthesize the convenient building block, diborylethyne (Scheme I-7).⁴⁸ Diborylethyne was originally used in Suzuki coupling to form poly(*p*-phenyleneethyene).



Scheme I-7. Synthesis of diborylethyne from trichloroethylene.

1.2.1.2 Synthesis of Ethynyl *N*-Methylimidodiacetic Acid Boronates

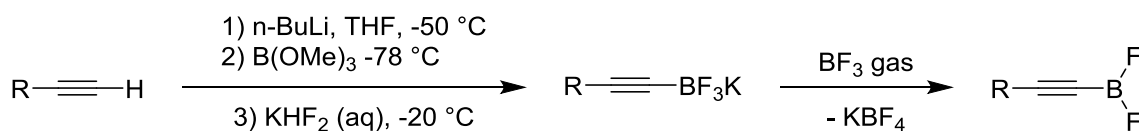
The Burke group has focused on using *N*-methylimidodiacetic acid (MIDA) boronates⁴⁹ in developing a method of iterative cross coupling for the synthesis of complex small molecules. The benefit of the MIDA boronate is that it is a protected boron moiety that is air and moisture stable, usually crystalline, can withstand silica gel chromatography, and can be deprotected to yield an organoboron reagent that will undergo Suzuki coupling *in situ*. In an attempt to synthesize building blocks for stereochemically complex polyolefins, the Burke group developed a method of synthesizing ethynyl MIDA boronate.⁵⁰ This was accomplished by treating trimethylborate with ethynyl Grignard and subsequent transesterification with *N*-methylimidodiacetic acid (Scheme I-8). Fortuitously, the C-B bond linkage in ethynyl MIDA boronate is inert to Sonagashira coupling conditions, which allows the remaining alkynyl C-H bond to be functionalized with a variety of arenes.⁵¹



Scheme I-8. Synthesis of ethynyl *N*-methylimidodiacetic acid boronates.

1.2.1.3 Synthesis of Alkynyl Trifluoroborate Salts

Potassium trifluoroborate salts offer an air and moisture stable organoboron compound.⁵² The first synthesis of alkynyltrifluoroborate reagents was performed by Darses et al. in a one-pot reaction by synthesizing the alkynylboronate from the terminal alkyne and then treating the boronic ester with a saturated solution of potassium bifluoride *in situ* (Scheme I-9).⁵³



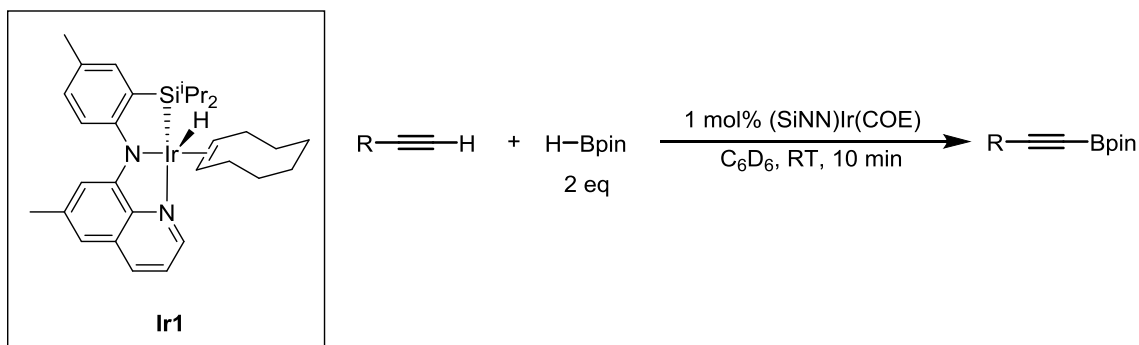
Scheme I-9. Synthesis of alkynyl trifluoroborate salts.

The Frohn research group then observed that alkynyldifluoroboranes could be prepared via a fluoride abstraction by a strong Lewis acid such as boron trifluoride (Scheme I-9).⁵⁴ However, these compounds were too reactive to be isolated, and instead the yields were calculated by ¹⁹F NMR spectroscopy. While these species are too reactive to be isolated, they have been generated *in situ* to be used as nucleophiles.

1.2.2 Dehydrogenative Borylation of Terminal Alkynes

The first example of catalytic dehydrogenative borylation of terminal alkynes (DHBTA) was reported by the Ozerov group using an iridium pincer complex (**Ir1**) that incorporated silyl, amido, and quinolone donors, abbreviated as (SiNN) (Scheme I-10).³⁷ The design of this ligand in regard to C-H borylation was founded on the notion that

iridium catalysts for aromatic C-H borylation involve a hydrogen transfer from the coordinated arene to an Ir-B bond that acts as a base to accept the hydrogen.⁵⁵ It was envisioned that a strongly sigma donating donor (*ie* silyl) incorporated into a pincer ligand would work analogously.



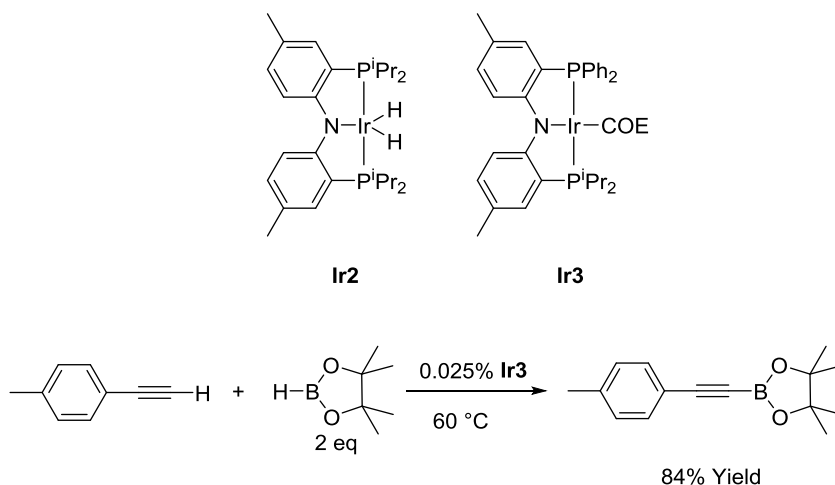
Scheme I-10. DHBTA catalyzed by **Ir1**.

The cyclooctene adduct of the (SiNN)Ir complex was found to borylate a range of terminal alkynes at very mild conditions: 10 minutes at room temperature with 1.0 mol% catalyst loading. The catalyst could efficiently borylate aryl, alkyl, and silyl acetylenes; but the catalyst was limited in its ability to tolerate propargyl ethers.

The system required slow addition of the alkyne and was optimized to use 2 equivalents of pinacolborane (HBpin) with respect to the terminal alkyne. It was noted that higher alkyne:HBpin ratios resulted in lower product yields and the eventual deactivation of the catalyst.

Iridium DHBTA catalysts were further optimized through a screening of similar pincer ligands.⁵⁶ It was discovered that various PNP-ligated iridium complexes, such as

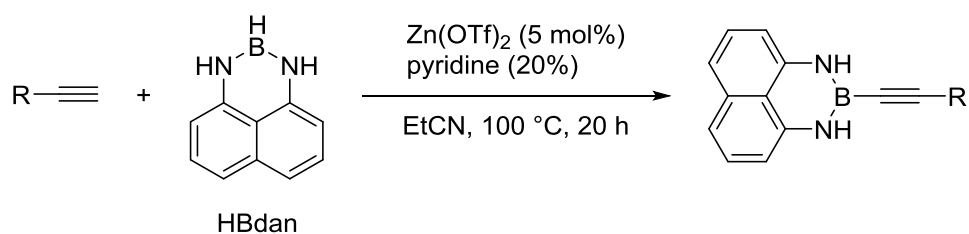
Ir2 and **Ir3** could perform DHBTA, and the asymmetric diarylamido complex (**Ir3**) provided a more efficient catalyst than **Ir1** (Scheme I-11). **Ir3** was found to effectively borylate the same substrate scope as **Ir1**, but could also operate at a much lower catalyst loading. 4-ethynyltoluene could be borylated in 84% yield with 0.025 mol% catalyst loading at 60 °C (Scheme I-11). This corresponds to 3400 turnovers. In addition to its higher rate of reaction, the catalyst was also found to be tolerant of trimethylsilyl propargyl ether and 1,6-enynes. This catalyst system will be discussed further in Chapter III. The Ozerov group has also developed catalysts based on PCP pincer-ligated palladium complexes.⁵⁷ An in depth discussion of these complexes is located in Chapter II.



Scheme I-11. (PNP)Ir DHBTA catalysts and high turnover performance by **Ir3**.

Catalytic zinc triflate and pyridine have also been shown to dehydrogenatively form alkynylboronates (Scheme I-12). This system is not tolerant of HBpin as a borane source and was optimized with 1,8-naphthalenediaminatoborane (HBdan).⁵⁸ However,

this “masked boryl group” allowed for the alkynylboron compounds to be purified via column chromatography. Yields of >80% were reported for a number of alkyl, aryl, and heterocyclic terminal alkynes. Of particular interest, this method could efficiently borylate phenyl propargyl ether and 3-butyn-1-ol. Propargyl ethers were difficult substrates for transition metal DHBTA catalysts.



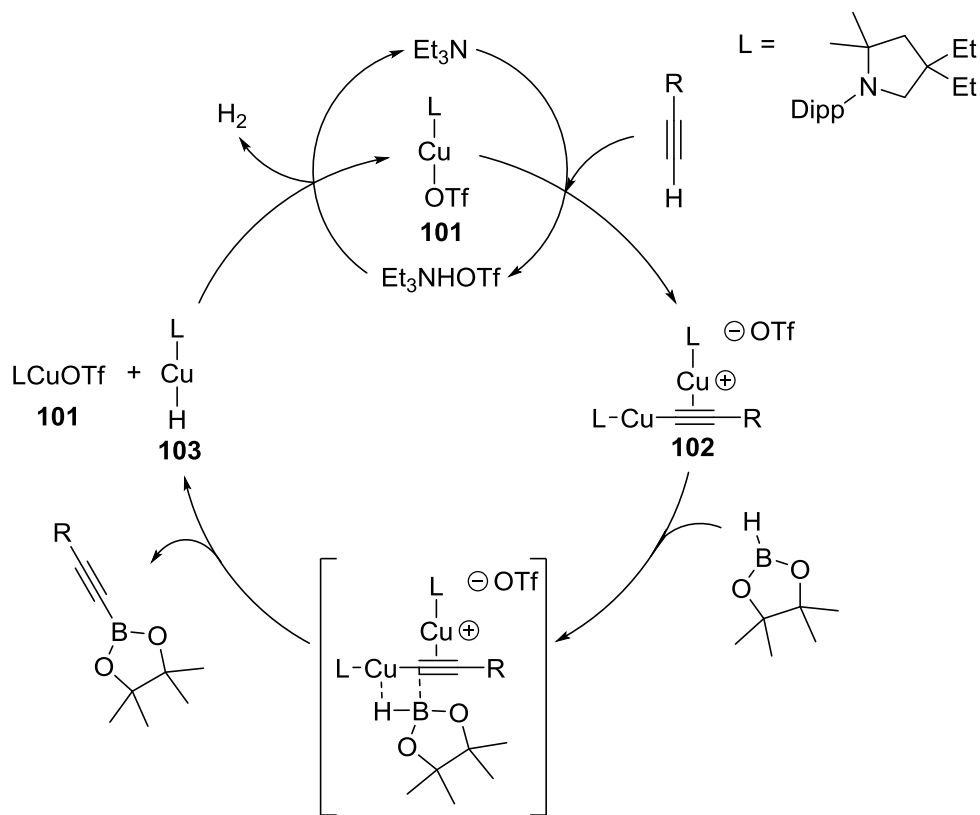
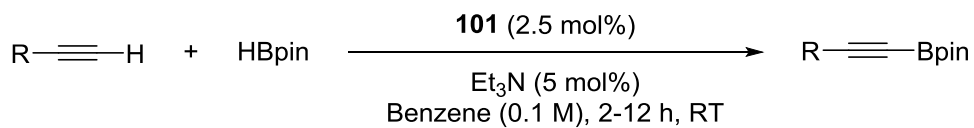
Scheme I-12. DHBTA with 1,8-naphthalenediaminoborane catalyzed by Zn(OTf)₂ and pyridine.

The applications of naphthalenediaminato alkynylboronates were tested for their synthetic utility. While the Bdan group connected to a Csp² atom has been shown to be inert to Suzuki cross coupling,⁵⁹ the alkynylboronates can undergo Csp Suzuki coupling and palladium-free Sonagashira coupling.

The catalytic dehydrogenative formation of alkynylboronates with pinacolborane has also been accomplished with copper triflate bound to a commercially available cyclic (alkyl)(amino)carbene (CAAC) ligand (**101**) (Scheme I-13).⁶⁰ This system could borylate alkyl and aryl alkynes and was also tolerant of trimethyl propargyl ether, which was isolated in an 89% yield. It was noted that electron-rich terminal alkynes (typically alkyl substituted) required reaction times of 12 h as opposed to the 2 h required for less

electron-rich alkynes such as those with aryl or benzyl substituents. The catalytic cycle is postulated to proceed through the formation of a σ,π -bis(copper) acetylide (**102**) as shown in Scheme I-13. The authors hypothesize that the biscopper complex reacts with HBpin to form the alkynylboronate, a copper hydride (**103**), and reform **101**. Compound **103** can then dehydrogenatively react with the ammonium triflate salt to expel H₂ gas and reform another equivalent of **101**. Curiously, the authors did not report a stoichiometric reaction between the isolable **102**⁶¹ and HBpin.

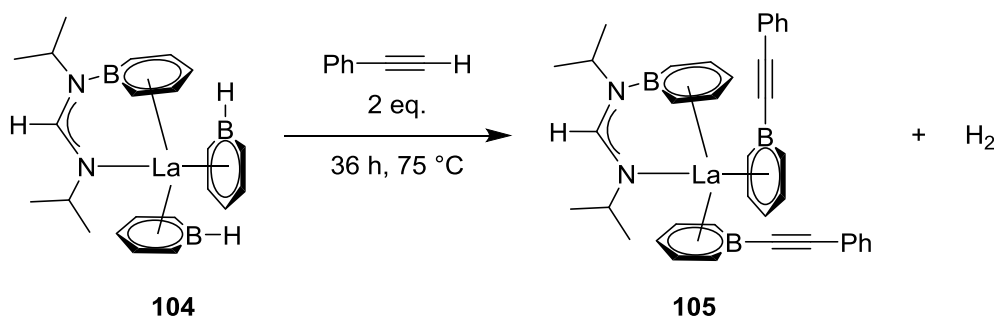
Also of note, by changing the counter anion from a triflate to a phenoxide and removing triethylamine from the reactions, this system was found to favor hydroboration over DHBTA.⁶²



Scheme I-13. DHBTA catalyzed by (CAAC)CuOTf (**101**), and the mechanism proposed by Bertrand et al.

Although the reaction is not catalytic, boratabenzene ligands on lanthanum have been shown to dehydrogenatively borylate terminal alkynes (Scheme I-14).⁶³ Boratabenzenes are aromatic anions that resemble cyclopentadienyl ligands in organometallic chemistry. While studying these ligands on lanthanum, the Chen group discovered that a boratabenzene can undergo dehydrogenative borylation of

phenylacetylene in the coordination sphere of a tris(boratabenzene) lanthanum complex (**104**) to furnish the alkynylated complex (**105**). The reaction was slow, finishing after 36 h at 75 °C. The alkynylboron compounds remain in the coordination sphere of lanthanum after the reaction, precluding any catalytic applications of the lanthanum complex. **104** was found to hydroborylate internal alkynes such as 3-hexyne.



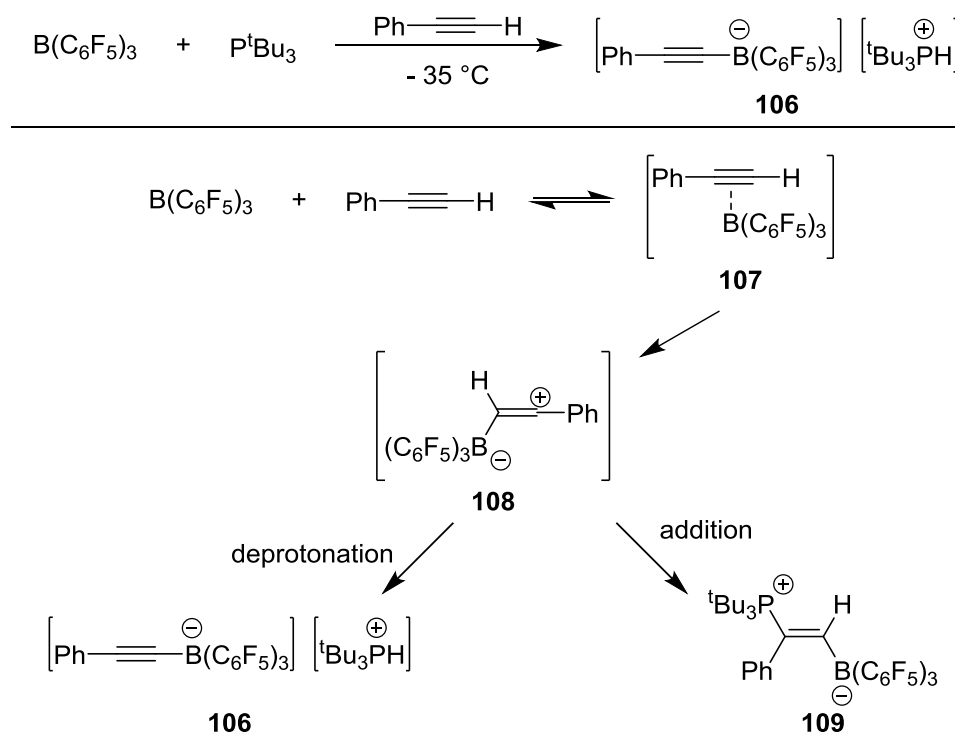
Scheme I-14. Dehydrogenative formation of an alkynylboratabenzene ligand on lanthanum.

1.2.3 Formation of Alkynyl Triarylborationes with Frustrated Lewis Pairs

Although a main-group catalytic system for the borylation of terminal alkynes has not been reported, there have been main-group systems facilitating Csp-B bond formation. Some of these systems use frustrated Lewis pairs (FLPs), which are a combination of a bulky Lewis base with a bulky electrophilic Lewis acid. These bulky Lewis acid-base pairs cannot form a strong adduct and will act as a binary system that has both an open Lewis acidic site and a Lewis basic site.⁶⁴ These systems became very popular after the groups of Stephan and Erker discovered that phosphine-borane FLPs could heterolytically split dihydrogen.⁶⁵ After these discoveries, FLPs were used to

activate other small molecules such as terminal alkynes. FLPs can deprotonate various alkynes and add the alkynyl anion to the trialkylborane to form alkynyl triarylborates. These reagents are not synthetically useful, but the study of the reactivity of alkynes with boranes and main group bases is a worthwhile pursuit.

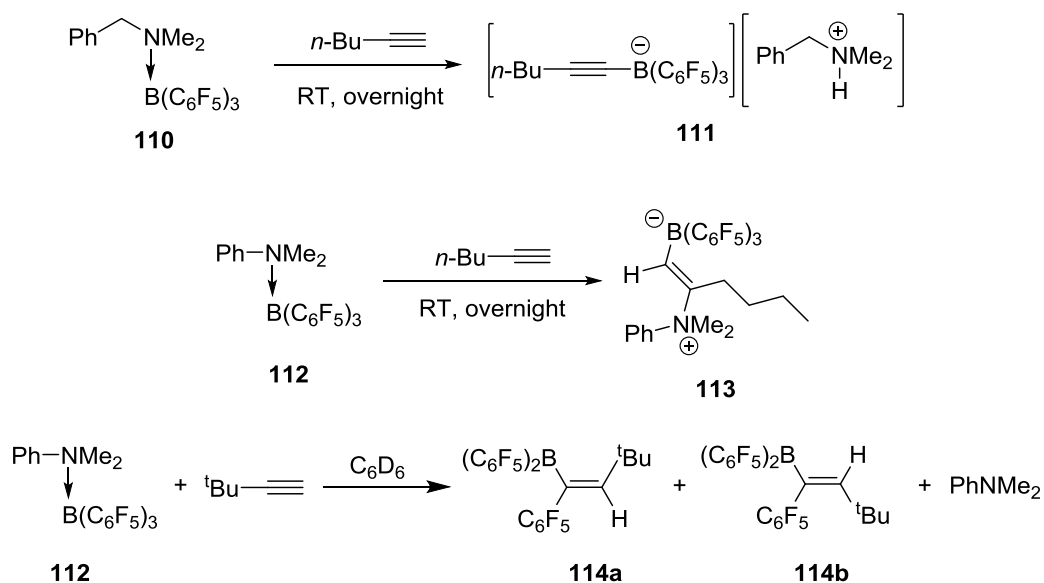
The FLP formed from the combination of $B(C_6F_5)_3$ and P^tBu_3 was observed to activate the terminal C-H bond of phenylacetylene to form the phosphonium alkynyl borate salt **106** (Scheme I-15, top).⁶⁶ A similar reaction with a bulky intramolecular, ethylene-bridged phosphine-borane FLP was performed by the Erker group also lead to a zwitterionic phosphonium alkynyl borate salt similar to **106**.⁶⁷



Scheme I-15. Borylation of phenylacetylene using $B(C_6F_5)_3/P^tBu_3$ and the proposed mechanism.

The mechanism of this transformation has been hypothesized to result from an initial π -interaction of the alkyne with the borane Lewis acid (**107**) (Scheme I-15, bottom). DFT calculations performed by the Berke group showed that this type of complex could undergo electrophilic attack by the alkyne to form a σ -adduct (**108**).⁶⁸ This adduct of an alkyne and a borane activates the alkyne toward nucleophilic attack and increases the acidity of the terminal C-H bond. Depending on the nature of the base and the temperature of the reaction, either deprotonation will occur or the base can act as a nucleophile, which result in a zwitterionic olefinic species (**109**).^{66b} Formation of **109** was observed in <20% yield by Dureen et al. when performing the reaction in Scheme I-15 at room temperature.^{66a}

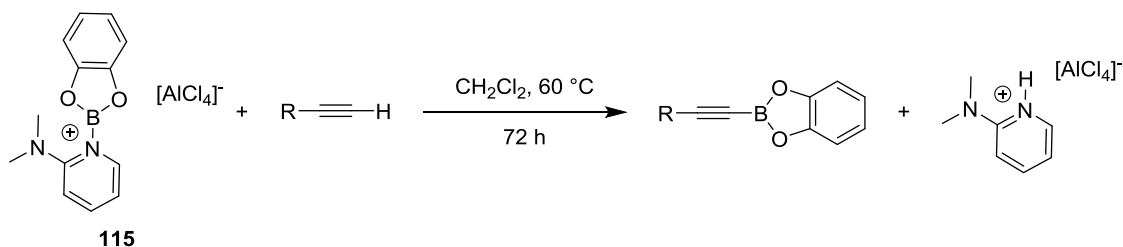
Additionally, the Stephan group investigated amine-borane FLPs and also made similar discoveries about the relative basicity of the amine correlating with the product of the reaction.⁶⁹ If [*N,N*-dimethylbenzylamine][B(C₆F₅)₃] (**110**) is treated with a terminal alkyne, the alkynylborate salt (**111**) is formed (Scheme I-16, top); however, if *N,N*-dimethylaniline (a less basic amine) (**112**) is used, the Lewis base addition product is formed (**113**) (Scheme I-16, middle). A less acidic alkyne such as *tert*-butylacetylene or trimethylsilylacetylene was not deprotonated by **112**, and the reaction resulted in a 1,1-carboboration of the alkyne to form products **114a** and **114b** (Scheme I-16, bottom).



Scheme I-16. Amine-borane FLP borylation of 1-hexyne, the Lewis base addition to 1-hexyne, and the carboboration of *tert*-butylacetylene.

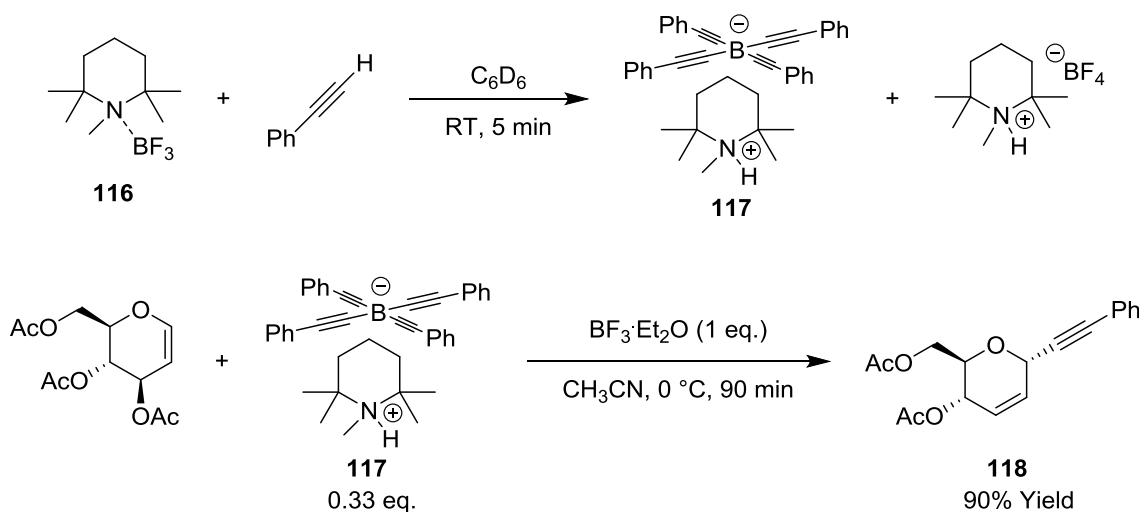
1.2.4 Formation of Alkynylboronates and Tetraalkynylborates Using Amines

While investigating DMAP chelated borenium cations for the haloboration of terminal alkynes, the Ingelsohn group discovered that 2-(*N,N*-dimethylamino)pyridine (2-DMAP) chelated BX_2^+ ($\text{X} = \text{Cl}, \text{Br}$) performed haloboration of terminal and internal alkynes. However, when the X-ligands on boron were chelated together, the addition of the X-B bond across the alkyne was inhibited and the dehydroboration of the terminal alkyne occurred (Scheme I-17). This reactivity was observed with $[(o\text{-catecholato})\text{B}(2\text{-DMAP})][\text{AlCl}_4]$ (**115**), which exclusively formed alkynylboronates when treated with terminal alkynes.⁷⁰



Scheme I-17. Formation of alkynylboronates from borenium cations.

While FLPs using tris(pentafluorophenyl)borane have been known to C-H borylate terminal alkynes since 2009, there has been no reported synthetic application of the resulting alkynyl tris(pentafluorophenyl)borates. The cost of fluorinated triphenylboranes might also outweigh the benefits of any potential applications. However, the Repo group recently used the BF_3 adduct of 1,2,2,6,6-pentamethylpiperidine (PMP) (**116**) to synthesize tetrakis(ethynyl)borate salts (**117**).⁷¹ The formation of **117** which could be isolated in 90% yield by hexane precipitation is shown in Scheme I-18. Several other aliphatic and aromatic terminal alkynes could be borylated through similar means. These tetrakis(ethynyl)borate salts were demonstrated to be useful for C-C bond forming reactions such as the allylic substitution of tri-*O*-acetyl-D-glucal to form **118** (Scheme I-18, bottom). PMP could also be recovered in an 83% yield from the resulting $[\text{PMP-H}][\text{BF}_4]$ salt via treatment with aqueous sodium hydroxide followed by extraction and vacuum distillation.



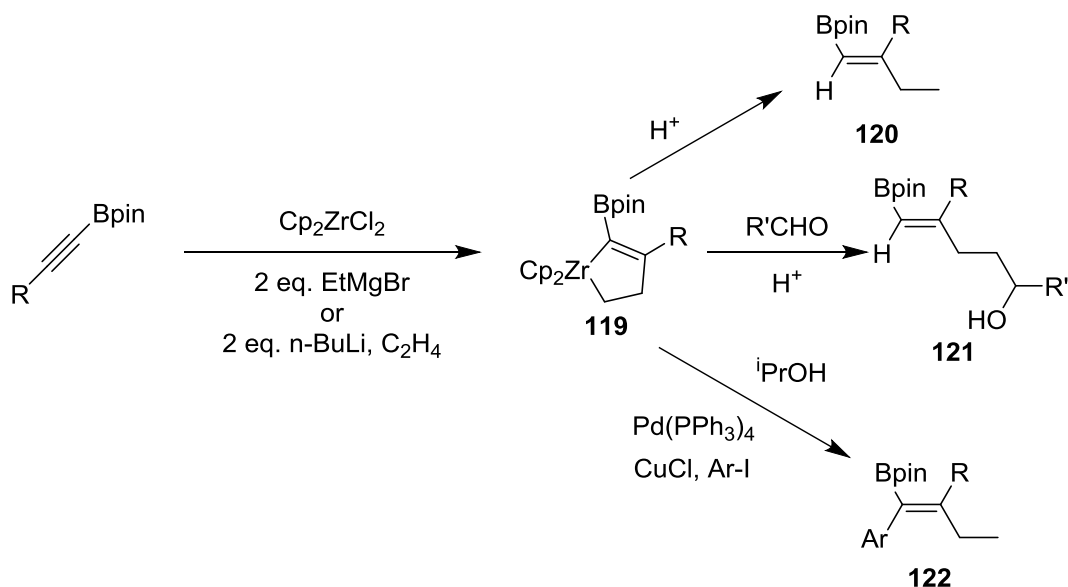
Scheme I-18. Formation of tetraalkynylborate salts from the PMP-BF₃ adduct.

1.3 Applications of Alkynylboronates

1.3.1 Synthesis of Multisubstituted Olefins

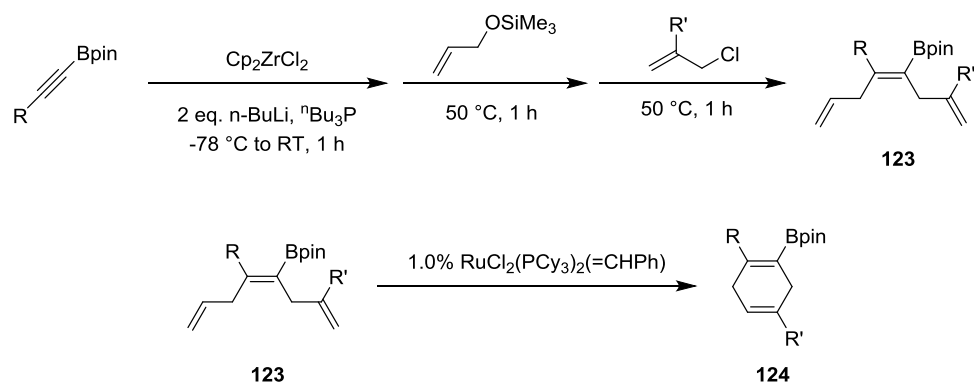
The production of multisubstituted olefins from alkynylboronates mediated by zirconacenes started with the Srebnik group,⁷² and the Nishihara group continued this work.⁷³⁻⁷⁵ When zirconocene dichloride is treated with a base and an alkyne in the presence of an olefin, a zirconacyclopentene is formed. If an alkynylboronate is used for the alkyne, the zirconacyclopentene will contain a C(sp²)-B bond (**119**). This five-membered ring can subsequently be protonolyzed to form a trisubstituted olefin **120**,⁷² or it can undergo further reactivity such as insertion of an aldehyde **121** (Scheme I-19).⁷² The Nishihara group also showed that the zirconacyclopentene can be directly used in palladium-catalyzed coupling reactions to form tetrasubstituted olefins containing boron substituents, as shown in Scheme I-19 where the zirconacyclopentene is coupled with an

aryl iodide to yield **122**.⁷³ These zirconacyclopentenes were also capable of undergoing similar Pd-catalyzed coupling with iodomethane and were also shown to undergo iodolysis to form iodine-substituted alkenylboronic esters.⁷⁴



Scheme I-19. Reactions of alkynylboronates with zirconocene to make multisubstituted olefins.

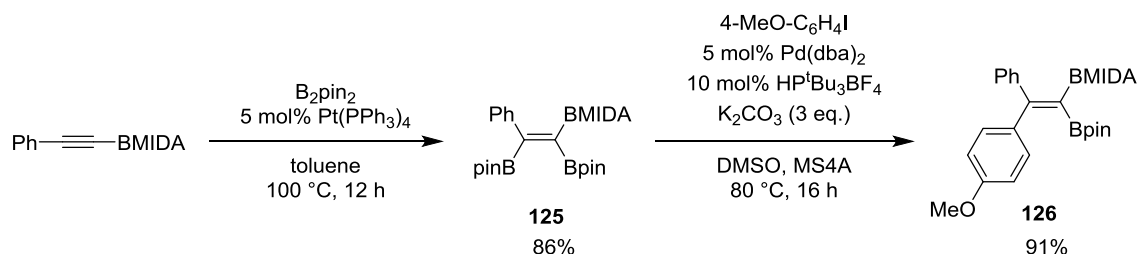
The most recent development with zirconocene-mediated functionalization of an alkynylboronate was performed by the Nishihara group and showcases a double allylation of an alkynylboronate to yield **123**, which can then undergo ring-closing metathesis with a ruthenium catalyst to form a borylated cyclohexadiene (**124**) (Scheme I-20).⁷⁵ These products were shown to be suitable substrates for Suzuki coupling.



Scheme I-20. Zirconium-mediated double allylation of an alkynylboronate and subsequent ring-closing olefin metathesis to yield borylated cyclohexadiene.

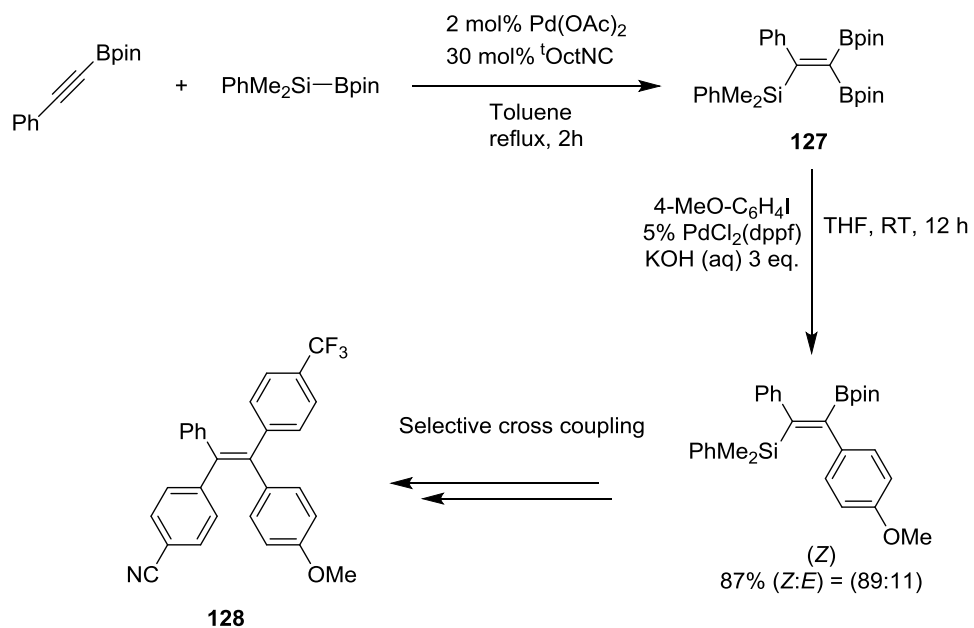
The disadvantage of synthesizing multisubstituted olefins through zirconocene mediated processes is that a stoichiometric amount of Cp_2ZrCl_2 is required. Another popular method of accessing multisubstituted olefins is adding a main group intraelement or interelement compound across an alkyne followed by cross-coupling reactions.⁷⁶ Diboron reagents such as bis(pinacolato)diboron (B_2pin_2) have been reported to add across the triple bond of terminal alkynes and internal alkynes.⁷⁷ Alkynylboronates bearing pinacolboronate termini were initially subjected to diboration using B_2pin_2 and a platinum catalyst.⁷⁸ This reaction would yield a triborylalkene with three pinacolboronate substituents. This presents problems for stepwise coupling reactions to occur selectively at the nonequivalent C-B linkages. To provide better differentiation of the three C-B bonds, the Nishihara group used alkynyl MIDA boronates in a platinum-catalyzed diboration to form **125** (Scheme I-21).⁷⁹ Subsequent Suzuki coupling is selective for the C-B bond trans to the BMIDA and will yield **126**, which can then undergo further Suzuki coupling to make a tetrasubstituted olefin. The MIDA group can also be removed

from the boron in near quantitative yields by treating the species with pinacol in the presence of excess NaHCO_3 in methanol at 45 °C. This method is complimentary to using asymmetric diboron reagents such as (pin)B-B(dan) with platinum catalysts to diborylate alkynes.⁵⁹



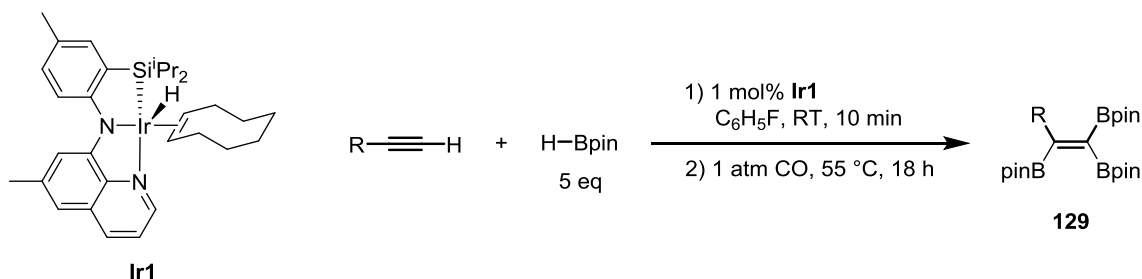
Scheme I-21. Diboration of alkynyl MIDA boronates and subsequent selective Suzuki coupling.

Another synthesis that tailors toward selective stepwise cross coupling can be performed through the palladium-catalyzed silaboration of alkynylboronates to yield a 1-aryl-1-silyl-2,2-diborylethylene (**127**). These reagents can be treated with different cross coupling conditions to selectively yield a tetraarylethene (**128**) (Scheme I-22).^{80,81}



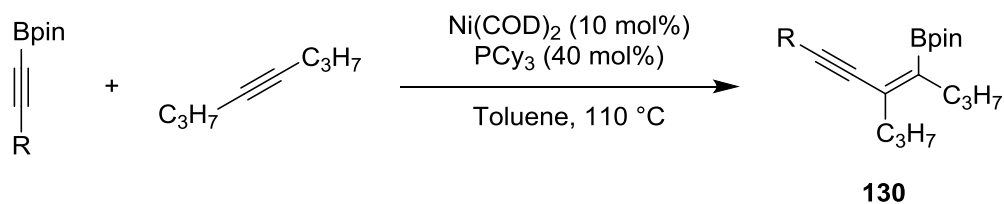
Scheme I-22. Silylboration of an alkynylboronate and subsequent selective cross coupling reactions to form a tetraarylethene.

The Ozerov group also performed a one-pot C-H borylation of terminal alkynes and subsequent dehydrogenative diboration of the resulting alkynylboronates with the (SiNN)Ir catalyst and HBpin as a borane source (Scheme I-23).⁸² This system was optimized to give good yields of triborylalkenes (**129**) under an atmosphere of CO in fluorobenzene.



Scheme I-23. Ir1-catalyzed DHBTA and dehydrogenative diboration of terminal alkynes.

The alkynylboronate itself can be added across the triple bond of an alkyne using nickel catalysts. This reaction forms conjugated enynes bearing a C(sp²)-Bpin moiety (**130**) (Scheme I-24).⁸³ This reaction is similar to alkyne dimerization in that it adds the terminal C-B bond across the triple bond of another alkyne to form a conjugated enyne.

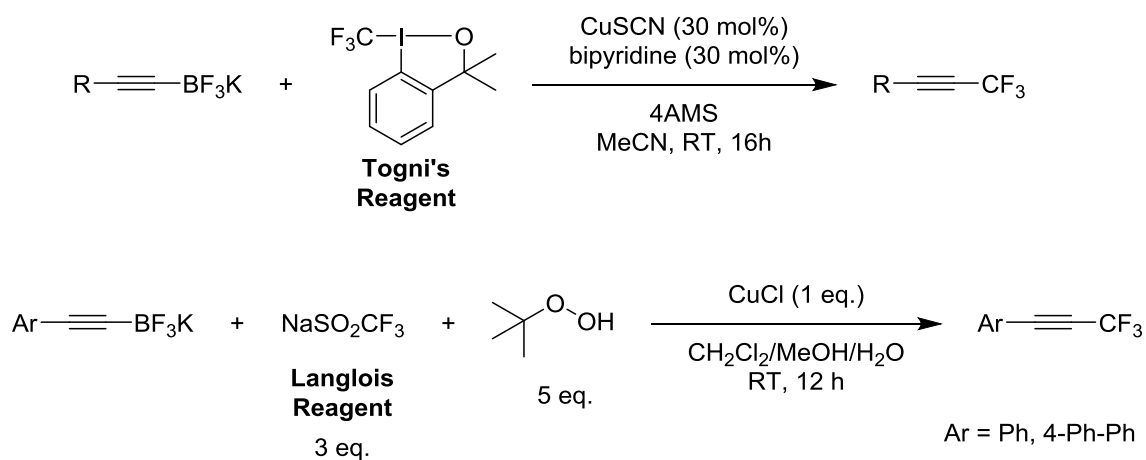


Scheme I-24. Nickel-catalyzed carboboration of an internal alkyne with an alkynylboronate.

1.3.2 Applications in C-C Coupling Chemistry

Various organoboron reagents have been used to incorporate trifluoromethyl groups into molecules.⁸⁴ Methods have been developed to directly trifluoromethylate terminal alkynes;⁸⁵ however, there are limitations to these systems that have been overcome with the use of alkynyltrifluoroborate salts. Work by the Weng group has

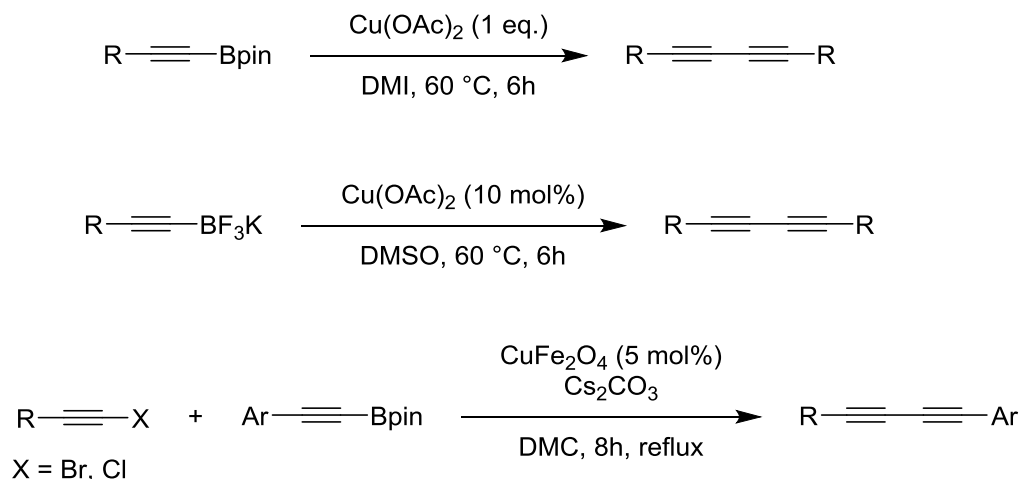
focused on developing a method of synthesizing trifluoromethylated acetylenes using Togni's reagent (Scheme I-25, top).⁸⁶ The Molander group included alkynyltrifluoroborate salts in their studies performing trifluoromethylation using the Langlois reagent with *tert*-butyl hydroperoxide (Scheme I-25, bottom).⁸⁷



Scheme I-25. Trifluoromethylation of alkynyl trifluoroborate salts.

Alkynylboron compounds have also shown to be efficient synthons for 1,3-diyne through homocoupling procedures. Copper-mediated homocoupling of alkynylboronates has been accomplished to synthesize 1,3-butadiynes. The first report of this chemistry used alkynylboronates and required stoichiometric amounts of copper salt and 1,3-dimethyl-2-imidazolidinone (DMI) as a solvent (Scheme I-26, top).⁸⁸ This system was improved by switching to the more nucleophilic alkynyltrifluoroborate species, which was capable of undergoing homocoupling with catalytic amounts of copper in dimethyl sulfoxide (DMSO) (Scheme I-26, middle).⁸⁹ Unsymmetrical 1,3-

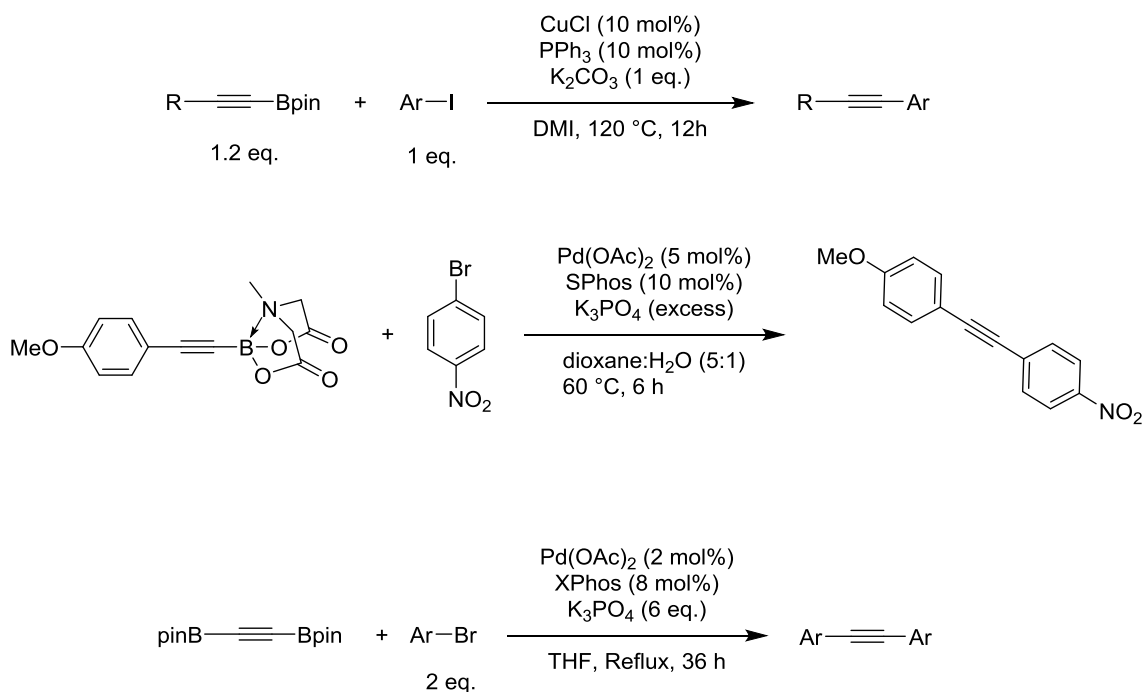
diynes have more recently been synthesized through the cross coupling of alkynylbromides and alkynylboronic esters using CuFe_2O_4 nanoparticles in dimethyl carbonate (DMC) (Scheme I-26, bottom).⁹⁰



Scheme I-26. Synthesis of 1,3-diynes from alkynylboron compounds.

Alkynylboronates also provide a convenient building block for asymmetric diarylacetylenes. Although diarylacetylenes are traditionally synthesized via the coupling of an arylacetylene with an aryl halide through palladium-catalyzed Sonagashira coupling,⁹¹ alkynylboronates offer routes to these desirable products without the requirement of expensive palladium. This process has been accomplished by the Nishihara group using catalytic copper in DMI at 120 °C (Scheme I-27, top).⁹² Borylated ethyne has also been exploited as a convenient building block for diarylacetylenes. As shown in Scheme I-8, ethynyl MIDA boronate can undergo Sonagashira coupling to access an arylethynyl MIDA boronate, and this species can

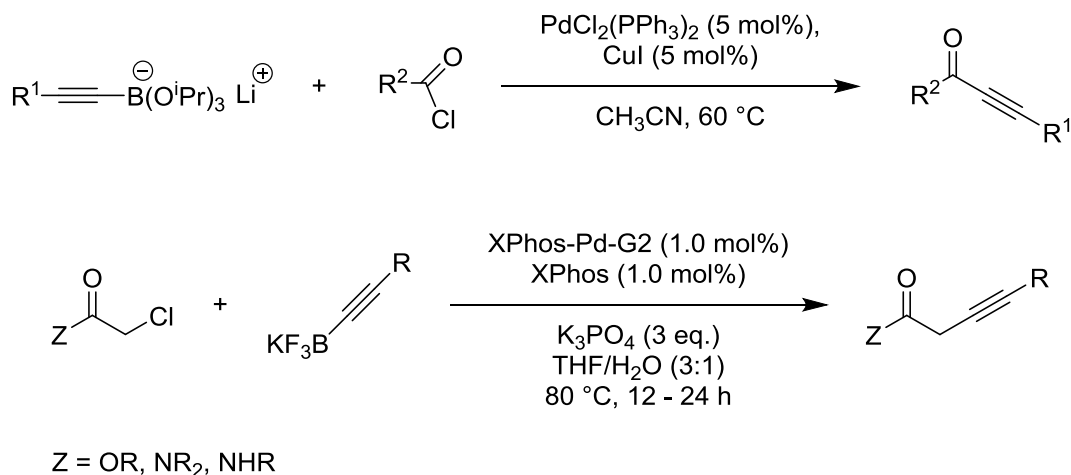
undergo slow release of the corresponding boronic acid under slightly basic conditions, which can undergo Suzuki coupling with another haloarene.⁵¹ The Rivard group has also used diborylated acetylene as a C₂ building block to make symmetric diarylacetylenes through Suzuki coupling (Scheme I-27).⁹³



Scheme I-27. Synthesis of diarylacetylenes from alkynylboron reagents.

While C(sp²)- and C(sp³)-boron reagents are typically the favored substrates for palladium-catalyzed Suzuki coupling, there are applications of alkynylboronates in Suzuki coupling to access valuable organic molecules. For instance, Oh et al. showed that lithium alkynylboronates can be used in Suzuki coupling for the formation of 1,3-dynes (Scheme I-28, top).⁹⁴ In a similar vein as Oh's work on the Suzuki coupling of

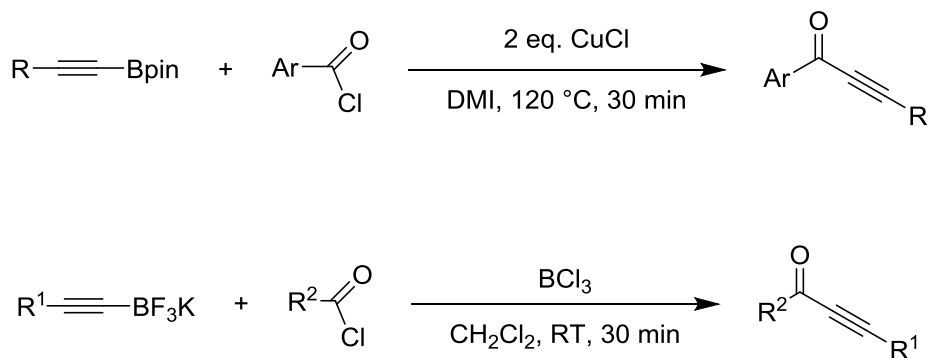
alkynylborates with acid chlorides, the Molander group used Suzuki coupling with 2-chloroacetates and 2-chloroacetamides for the synthesis of amides and esters (Scheme I-28, bottom).⁹⁵



Scheme I-28. Suzuki coupling of alkynylboron reagents with acid chlorides and 2-chloroacetates and 2-chloroacetamides.

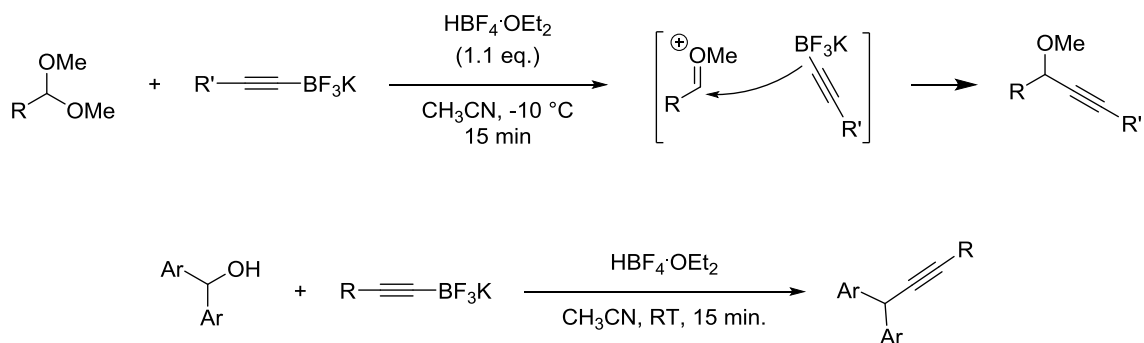
In the interest of accessing ynones without the use of palladium, the Nishihara group investigated the copper mediated⁹⁶ coupling of alkynylboronic esters to acid chlorides (Scheme I-29, top). While copper-mediated processes have better functional group tolerance (such as tolerance for 4-methylchloro substituents on arylbenzoyl chlorides), the reaction did require the use of toxic DMI as a solvent and high reaction temperatures. Most recently, the formation of ynones from alkynyltrifluoroborates and acid chlorides in the absence of transition metals has recently been developed using BCl_3 as a Lewis acid to promote the reaction (Scheme I-29, bottom).⁹⁷ Bolshon's work on the Lewis acid mediated synthesis of ynones most likely occurs via the formation of an

alkynyldihaloborane species formed from Lewis acid abstraction of one of the fluorines on boron. These intermediates are extremely reactive and limit the functional group tolerance of the system.



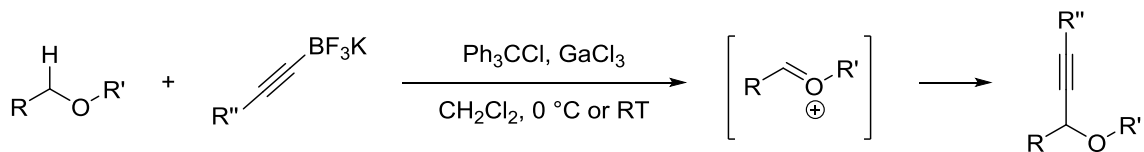
Scheme I-29. Copper-mediated coupling of alkynylboronates with acid chlorides, and boron trichloride-assisted coupling of alkynyltrifluoroborate salts with acid chlorides.

The Bolshon group followed up on this work by using a Bronsted acid catalyzed approach to the alkylation of acetals and ketals to make propargyl ethers.⁹⁸ Mechanistic studies performed during this investigation suggest that the reaction takes place via a direct addition of the nucleophilic trifluoroborate salt to an oxycarbenium ion without the formation of a dihaloborane (Scheme I-30, top). This system had functional group tolerance for aromatic aldehydes and ketones, which would likely not tolerate a dihaloborane intermediate. This Bronsted acid-catalyzed procedure could be extended to the reaction of trifluoroborate salts with benzhydryl alcohols to make secondary alkylacetylenes (Scheme I-30, bottom).⁹⁹



Scheme I-30. Bronsted acid catalyzed formation of propargyl ethers and secondary alkynylacetylenes from alkynyltrifluoroborate salts.

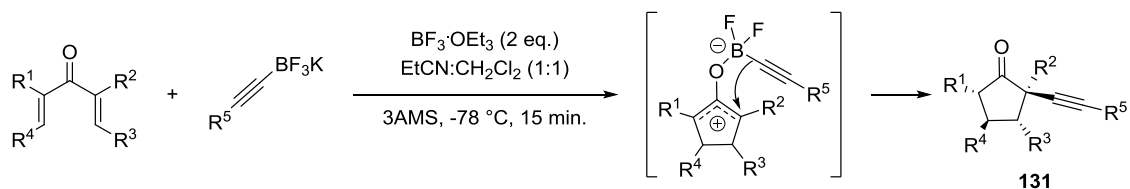
Potassium alkynyltrifluoroborates were shown to be efficient nucleophiles for the trityl ion mediated C-H alkylation of ethers (Scheme I-31).¹⁰⁰ Mechanistic studies performed by the Liu group on this system suggested that the trityl cation abstracted a hydride from the ether to form an oxycarbenium ion that underwent nucleophilic attack by the alkynyltrifluoroborate.



Scheme I-31. Trityl ion mediated C-H alkylation of ethers with alkynyltrifluoroborate salts.

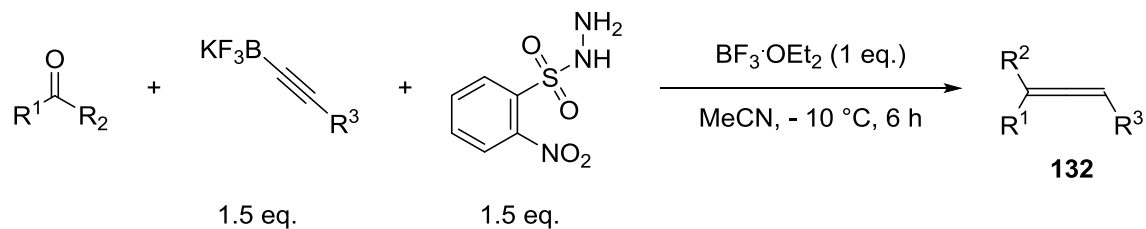
The treatment of trifluoroborate salts with a Lewis acid generates a difluoroborane species that is incredibly reactive. Alkynyltrifluoroborate salts treated with a Lewis acid, such as boron trifluoride etherate, have been used to trap Nazarov

reaction intermediates to form substituted α -alkynylated cyclopentanones (**131**) (Scheme I-32).¹⁰¹



Scheme I-32. Potassium alkynyltrifluoroborates as σ -nucleophiles in an interrupted Nazarov reaction.

The nucleophilicity of trifluoroalkynylborates was exploited in a reaction with hydrazones generated during a Petasis reaction (Scheme I-33). Due to the use of an alkynyl nucleophile, the reaction yielded allenes (**132**) instead of a typical amine product.¹⁰²



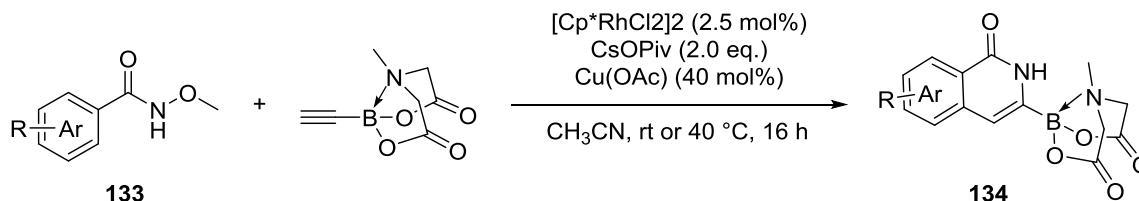
Scheme I-33. Synthesis of allenes from alkynyl trifluoroborate salts in a Petasis reaction.

1.3.3 Synthesis of Cyclic Compounds Containing Pendant C-B Bonds

One of the most attractive uses for alkynylboronates is to use them in cycloaddition reactions that produce cyclic products with pendent C-B bonds. These

methods provide access to cyclic compounds that would be difficult to borylate through traditional means.

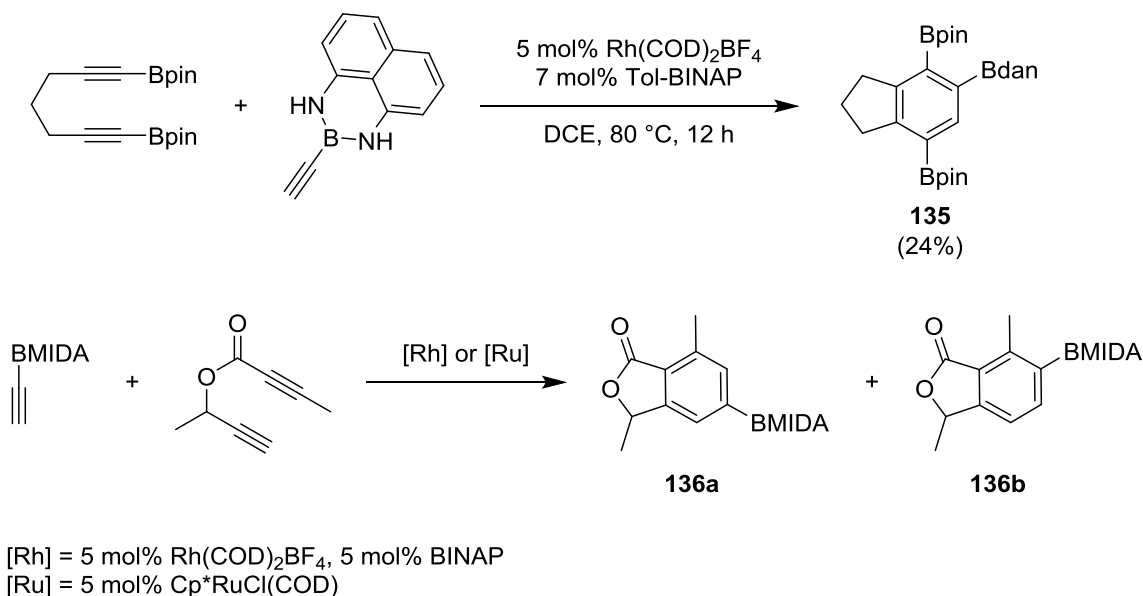
Using pentamethylcyclopentadienylrhodium (III) chloride dimer as a catalyst the Glorius group was able to C-H activate *N*-(pivaloyloxy)benzamides (**133**) and couple them with ethynyl MIDA boronate (Scheme I-34).¹⁰³ This process yielded borylated isoquinilones (**134**), and the Glorius group was also able to synthesize isoquinolines, indoles, and pyrroles using different coupling partners.



Scheme I-34. Rhodium catalyzed C-H activation and annulation with ethynyl MIDA boronate to synthesize borylated heterocyclic compounds.

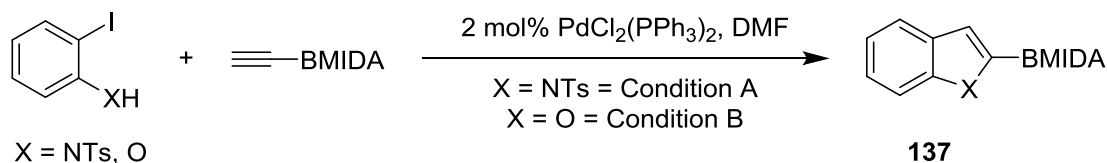
[2+2+2] Cyclization reactions with alkynes are useful routes to synthesizing multisubstituted arenes. The use of alkynylboronates in [2+2+2] reactions has been accomplished by the Gandon group who have used cobalt-mediated cyclizations with alkynylboronates to form fused arylboronic esters¹⁰⁴ and cyclohexadienes^{105,106} The Gandon group most recently used rhodium- and cobalt-catalyzed [2+2+2] cycloadditions of alkynylboronates to form multiborylated arenes (**135**), which could undergo selective Suzuki coupling in order to synthesize a series of oligoaryls (Scheme I-35, top).¹⁰⁷ Ethynyl MIDA boronate was recently been incorporated into this family of reactions by

Melnes and coworkers with the use of rhodium and ruthenium catalysts to make borylated bicyclic compounds (**136a,b**) (Scheme I-35, bottom).¹⁰⁸



Scheme I-35. (Top) [2+2+2] cycloaddition with an alkynylboronate and a borylated 1,6-diyne, (Bottom) [2+2+2] cycloaddition with ethynyl MIDA boronate.

Ethynyl MIDA boronate has also recently been used in a one pot catalytic synthesis of bicyclic heterocycles bearing a BMIDA substituent (**137**) (Scheme I-36).¹⁰⁹



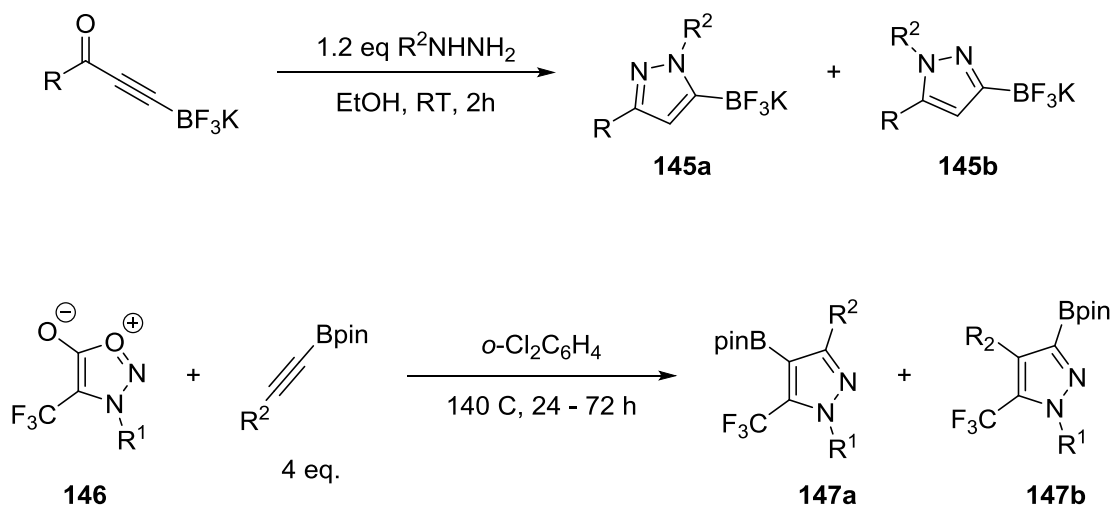
Condition A: 10 mol% CuI, 30 mol% Cu(OAc)₂, 1 eq. K₃PO₄, 30-55 °C
 Condition B: 6 mol% CuI, 10 mol% Cu(OAc)₂, 1.5 eq. K₂CO₃, RT - 60 °C

Scheme I-36. Synthesis of borylated bicyclic heterocycles from ethynyl MIDA boronates and 2-iodoanilines/phenols.

Despite the lack of catalytic activity, Group 4 metallocenes have been investigated as ways of coupling borylated alkynes into arenes. The Rosenthal group has studied the reactivity of diborylacetylene with titanocenes and zirconocenes.^{110,111} While no catalytic reactions have been reported for titanocenes or zirconocenes with alkynylboronates, the Rosenthal group has demonstrated that a zirconacycle containing two units of diborylacetylene (**138**) can undergo a reaction with (PPh₃)₂NiCl₂ and another alkyne to form a hexasubstituted arene (**139**) (Scheme I-37, top). Isolation of this compound from the reaction mixture was very difficult; however, excellent selectivity for the arene was observed.

The Rivard group, in their studies on conjugated polymers, used the formation of borylated zirconacyclopentenes (**140**) to make main group element-containing bis(borylated) bicyclic compounds (**141**) via transmetallation to a main group element. These compounds could undergo Suzuki coupling with bisiodoarenes to form conjugated polymers (**142**) (Scheme I-37, bottom).¹¹²

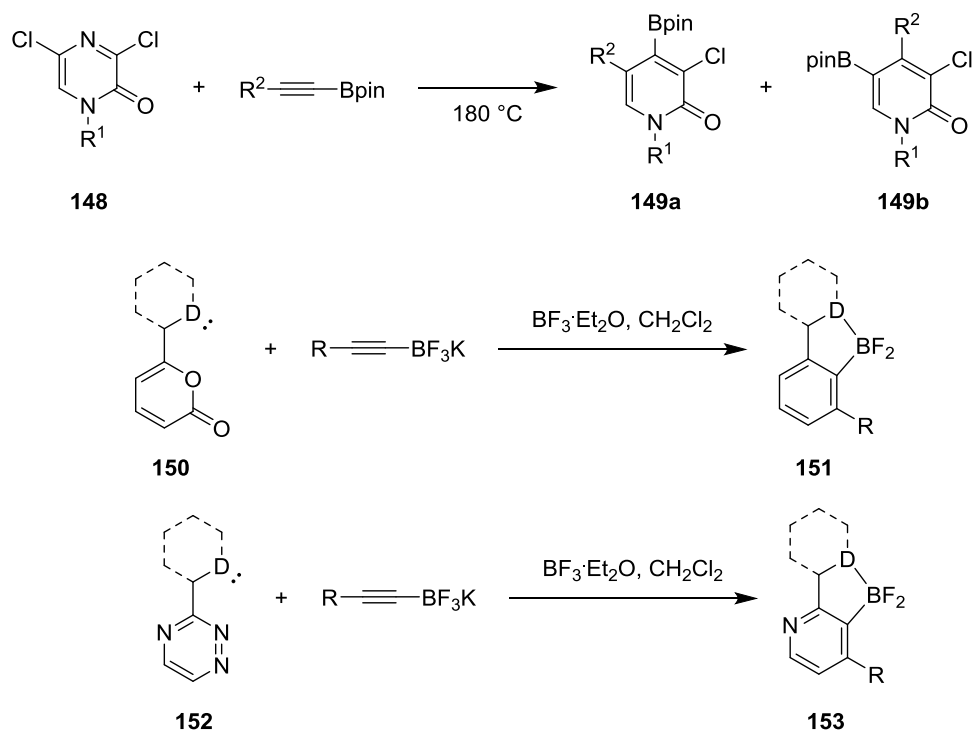
heterocyclic cores is the pyrazole ring (**145**), which they have accessed through the nucleophilic cyclization of borylated ynones with hydrazines (Scheme I-39, top).¹¹⁵ This methodology was recently paired with the selective halogenation of the C4 position on the pyrazole ring to allow for the synthesis of fully functionalized pyrazoles.¹¹⁶ The Harrity group has also accessed trifluoromethylated pyrazoles (**147**) through the cycloaddition between alkynes and 4-fluoromethylsydnones (**146**) (Scheme I-39, bottom).¹¹⁷



Scheme I-39. Cycloaddition reactions with alkynylboron compounds to form pyrazoles.

The Harrity group also used alkynylboronates in [4+2] cycloaddition reactions with 2-pyrazinones (**148**) to make 2-pyridinones (**149**) (Scheme I-40, top).¹¹⁸ While these published works on the synthesis of pyrazoles and 2-pyridinones can form mixtures of regioisomers, the Harrity group has also used the Lewis acidic properties of alkynylboron reagents to do directed cycloadditions to substrates that contain Lewis

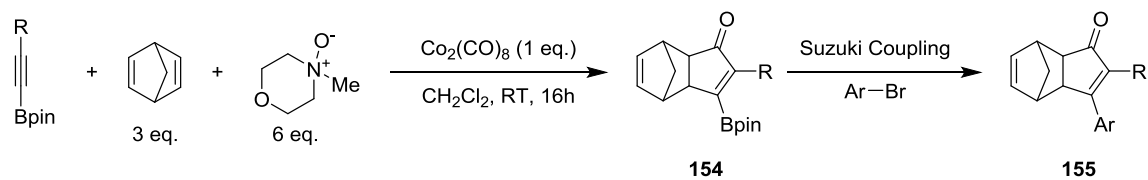
basic heteroatoms. This strategy was successfully used for the cyclization of potassium trifluoroalkynylborate salts with 2-pyrones (**150**) to make borylated arenes (**151**) (Scheme I-40, middle).¹¹⁹ It was also employed for the synthesis of substituted pyridines (**153**) from triazines (**152**) (Scheme I-40, bottom).¹²⁰



Scheme I-40. Cycloaddition reaction of alkynylboronates with 2-pyrazinones and the directed cycloadditions of potassium alkynyltrifluoroborate salts with 2-pyrones and triazines.

Alkynylboronates were used as biased internal alkynes for a regioselective intermolecular Pauson Khand reaction (Scheme I-41).¹²¹ It was discovered that cobalt-mediated PKR with norbornadiene and alkynylboronates yielded cyclopentenones with the boron moiety at the β -position of the ring (**154**). However, this reaction did require

the use of 6 equivalents of *N*-methylmorpholine *N*-oxide. These borylated cyclopentenones provided a versatile route to the regioselective synthesis of α,β -substituted cyclopentenones via a subsequent Suzuki coupling step (**155**).



Scheme I-41. Cobalt-mediated Pauson Khand reaction of alkynylboronates and norbornadiene.

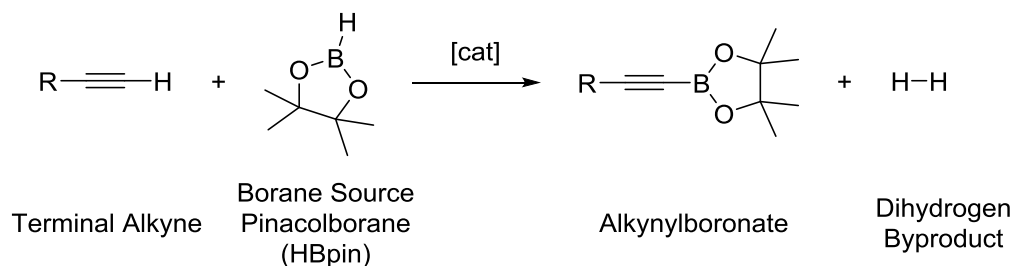
CHAPTER II
PINCER-LIGATED PALLADIUM CATALYZED DEHYDROGENATIVE
BORYLATION OF TERMINAL ALKYNES*

2.1 Introduction

The dehydrogenative formation of carbon-boron bonds directly from carbon-hydrogen bonds is one of the most attractive methods of transition metal-catalyzed C-H functionalization due to the utility of the resulting organoboronate reagent.¹¹ Significant progress has been achieved with iridium and rhodium catalysts, especially in borylation of aromatic C-H bonds.^{16,17,23,122} Group 10 metal catalysts have featured less prominently in the studies of C-H borylation. Palladium is responsible for most of these examples such as the borylation of olefins,¹²³⁻¹²⁵ isoindoles,¹²⁶ phenylpyridines,¹²⁷ and benzylic arms of alkylbenzenes.³⁴ Nickel has recently made its first appearance as a dehydrogenative C-H borylation catalyst with the borylation of arenes and indoles.¹²⁸ Platinum is rarely mentioned in the field of dehydrogenative borylation, but has been shown to catalyze the dehydrogenative borylation of olefins with borane clusters.¹²³

Our group recently introduced dehydrogenative borylation of terminal alkynes (DHBTA), a new type of a C-H borylation reaction that produces alkynylboronates (Scheme II-1).

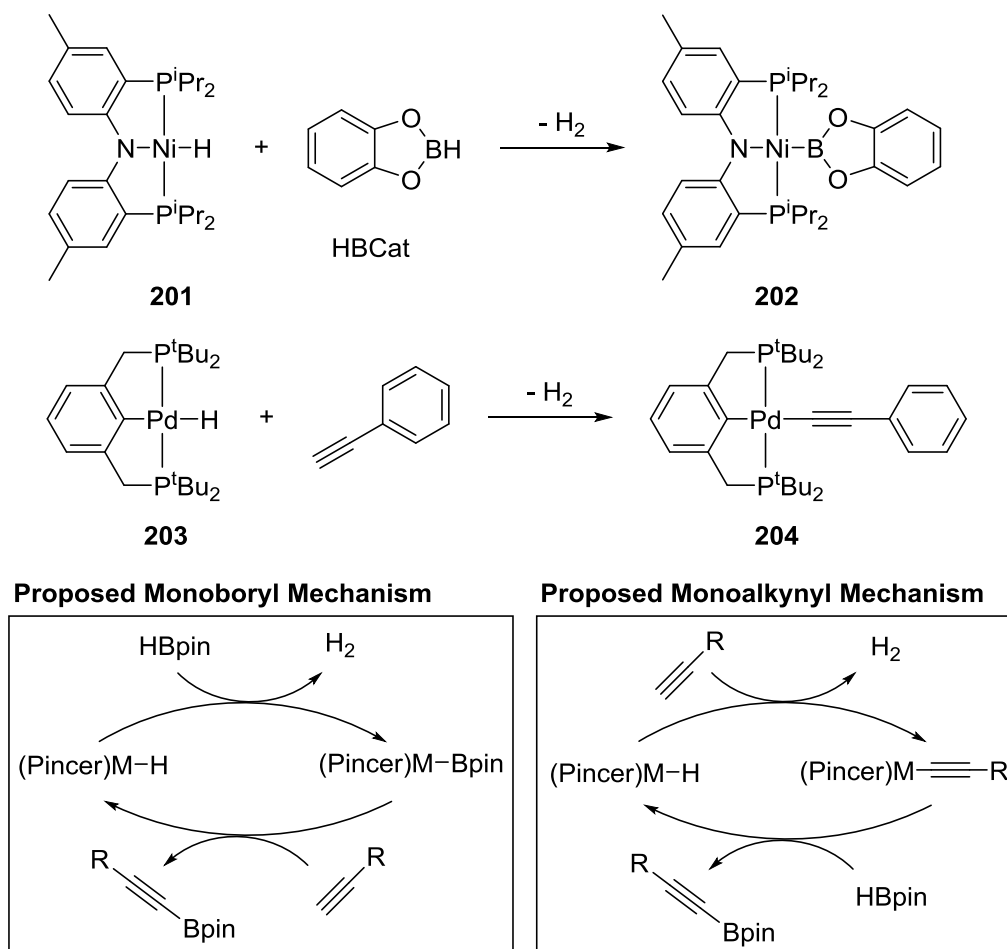
* Partially reproduced by permission of the Chinese Chemical Society (CCS), Peking University (PKU), and the Royal Society of Chemistry. From "Catalytic dehydrogenative borylation of terminal alkynes by POCOP-supported palladium complexes." Pell, C J.; Ozerov, O. V. *Inorg. Chem. Front.* **2015**, 2, 720. DOI: 10.1039/c5qi00074b



Scheme II-1. General reaction scheme for the dehydrogenative borylation of terminal alkynes (DHBTA).

Alkynylboronates are widely applicable in organic synthesis and their use has recently been reviewed.⁴³ In the original report on DHBTA, we utilized an iridium catalyst supported by a SiNN-type ligand,³⁷ and later improved on it through the use of other pincer ligands.⁵⁶ A slower DHBTA catalysis with a similar scope was reported by Tsuchimoto et al. using $Zn(OTf)_2$ /pyridine.⁵⁸ Interestingly, SiNN complexes of Rh¹²⁹ and the non-pincer Ir catalysts that excel at aromatic C-H borylation do not catalyze DHBTA. In the search for alternative DHBTA catalysts outside of group 9, we sought to examine pincer complexes of group 10 metals. We surmised that pincer-ligated group 10 metal hydrides should be appropriate for entry into potential DHBTA catalysis, especially since they have been shown to dehydrogenatively form metal alkynyl and metal boryl species. For instance, Mindiola showed that **201** can react with catecholborane to form metal boryl species **202**, and Wendt has shown that **203** can react with phenylacetylene to form **204** (Scheme II-2, top).¹³⁰⁻¹³³ These species could be potential intermediates in DHBTA if an alkyne could react with a metal boryl, such as compound **202** to reform the metal hydride and produce an alkynylboronate as outlined

in the proposed monoboryl mechanism in Scheme II-2. Alternatively, we imagined that a borane source could react with a metal alkynyl species, such as **204**, to reform the metal hydride and an equivalent of the alkynylboronate as shown in the proposed monoalkynyl mechanism shown in Scheme II-2.

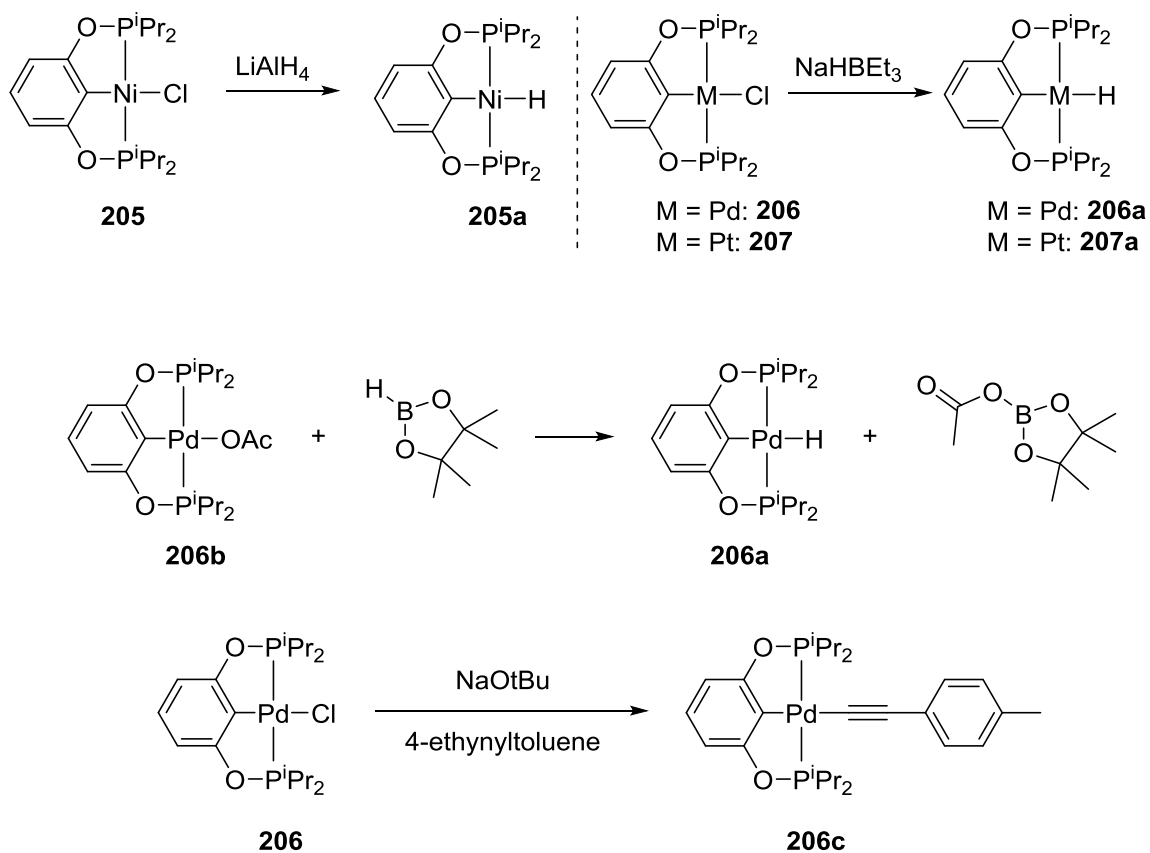


Scheme II-2. Examples of the dehydrogenative formation of pincer-ligated group 10 metal boryl and alkynyl species from the corresponding metal hydride and the proposed mechanisms for pincer-ligated group 10 metal DHBTA.

We chose to initially focus on the aryl/bisphosphinite ligand family^{134,135} because of its simple synthesis and the relative ease with which we can vary the size of the phosphine substituents.

2.2 Results and Discussion

2.2.1 Synthesis of Group 10 DHBTA Catalysts



Scheme II-3. Synthesis of (POCOP)M-H complexes and **206c**.

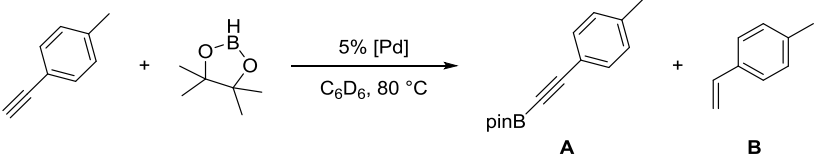
Compound **205a** was synthesized by a literature procedure¹³⁶ by treating **205** with lithium aluminum hydride (Scheme II-3, top left). The synthesis of **206a** using lithium aluminum hydride was low yielding and not reproducible as was the Guan group's procedure, which used lithium triethylborohydride at -78 °C.¹³³ Using sodium triethylborohydride gave better results for synthesizing **206a** and **207a**; however, the palladium species was still isolated in low yield (23%) and was difficult to purify (Scheme II-3, top right). Fortunately, it was found that the easily synthesized palladium acetate species (**206b**)¹³⁷ could exchange an acetate group for the hydride of HBpin to form **206a** *in situ* within seconds (Scheme II-3, middle). **206c**, a proposed catalytic intermediate, could be synthesized by treating **206** with 2 eq. of NaO^tBu in toluene in the presence of 4-ethynyltoluene (Scheme II-3, bottom). **206c** was also observed when **206b** was treated with 1 eq. of 4-ethynyltoluene, which resulted in the formation of acetic acid and a 3:2 equilibrium mixture of compounds **206b**:**206c**. When this equilibrium mixture was treated with 1 eq. HBpin, acetic acid was converted to AcOBpin and **206c** was the resulting product.

2.2.2 Catalytic DHBTA Activity with Group 10 Metal (POCOP) Complexes

To test the catalytic potential of the (POCOP) group 10 metal hydrides, 5 mol% of **205a**, **206a**, and **207a** were dissolved in C₆D₆ and treated with 4-ethynyltoluene and pinacolborane (HBpin) at 80 °C for 1 day (Table II-1). The reaction with **205a** (entry 1) gave a complex catalytic mixture of products containing olefinic signals as seen by ¹H NMR spectroscopy due to the ability of terminal alkynes to insert into the nickel-hydride bond,¹³⁸ while **207a** yielded about 5% of the hydroboration product, (E)-2-pinacolboryl-

1-(4-methylphenyl) ethylene (entry 2). **206a** did act as a DHBTA catalyst, converting 40% of the alkyne into the alkynylboronate (**A**). However there was an almost equal amount of 4-methylstyrene (**B**) produced from the semihydrogenation of 4-ethynyltoluene (entry 3).

Table II-1. DHBTA catalyst screening with (POCOP)M complexes (M = Ni, Pd, Pt).

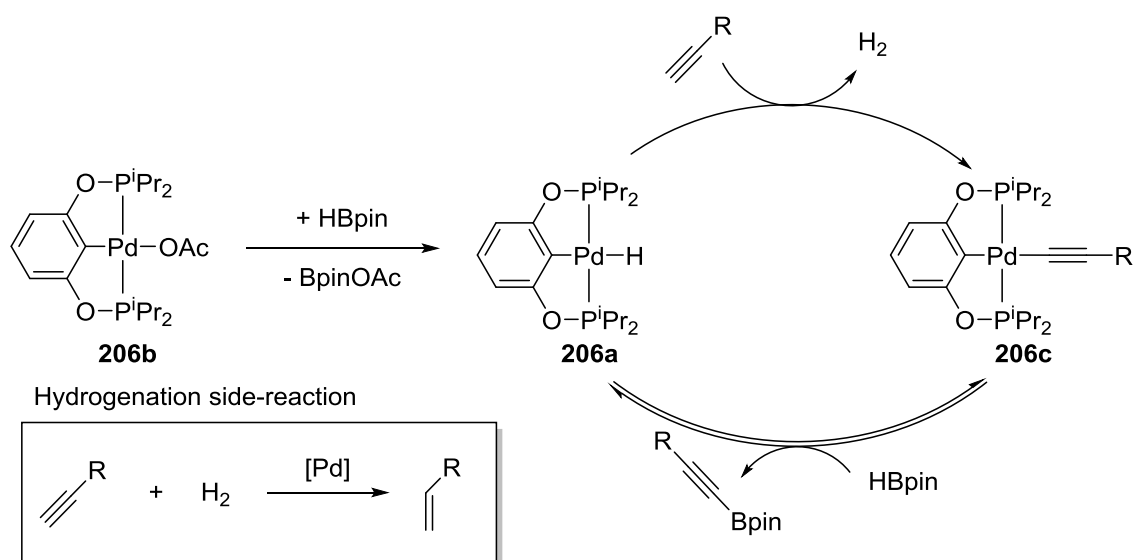
				
Entry #	[Pd]	A ^a	B ^{a,b}	Time
1	205a ^c	<5%	7%	1 d
2	207a ^d	0%	<5%	1 d
3	206a	40%	39%	1 d
4	206b	44%	49%	1 d
5	206c	45%	42%	1 d

All reactions performed at 80 °C in C₆D₆ with 0.34 mmol alkyne, 0.34 mmol HBpin, and 5% catalyst loading. ^a Yields were determined by ¹H NMR integration versus an internal standard (1,4-Dioxane). ^b Reactions that produced significant amounts of **B** also showed trace production of 4-ethyltoluene. ^c Many intractable products observed containing olefinic resonances. ^d 5% E)-2-pinacolboryl-1-(4-methylphenyl) ethylene was observed by ¹H NMR spectroscopy.

The use of **206a**, **206b**, or **206c** as precatalysts was observed to lead to essentially the same results in the catalytic borylation of 4-ethynyltoluene (entries 3, 4, and 5), indicating that all three allowed equal access to the catalytically active species. Since AcOBpin was not detrimental to catalysis and because **206b** was easiest to make and store, it is the most practical choice of precatalyst.

Scheme II-4 shows the catalytic cycle we propose for (POCOP)Pd catalyzed DHBTA. It entails the reaction of **206a** with the terminal alkyne to evolve H₂ and produce **206c**, which would then react with HBpin to release the alkynylboronate product and regenerate **206a**. **206c** was the sole product detectable by ³¹P{¹H} NMR spectroscopy until the end of the catalytic reactions using compounds **206a**, **206b**, and **206c**; and it appears to be the resting state of the catalyst. Stoichiometric experiments are also consistent with the mechanistic proposal. Reaction of **206a** with 1 eq. of 4-ethynyltoluene led to a clean conversion to **206c** within minutes. The Guan laboratory recently reported¹³³ that the addition of 1 eq. of phenylacetylene to **206a** led to 7% alkyne insertion products in addition to formation of the palladium alkynyl as quantified by ³¹P{¹H} NMR integration. In our hands, 4-ethynyltoluene was not seen to insert into the Pd-H bond under stoichiometric conditions at room temperature. Treatment of **206c** with 5 eq. of pinacolborane resulted in 50% conversion to **206a** after 5 h at 80 °C, with concomitant formation of **A**.^{*} This reaction is reversible; when **206a** was thermalized with 1 eq. of **A** at 80 °C for 3 h, analysis by ³¹P{¹H} NMR spectroscopy showed 16% conversion to **206c**. An alternative mechanistic pathway might involve intermediacy of (POCOP)Pd-Bpin, however, we have no evidence of its formation in catalytic reactions or in stoichiometric reactions of **206a** or **206c** with HBpin.

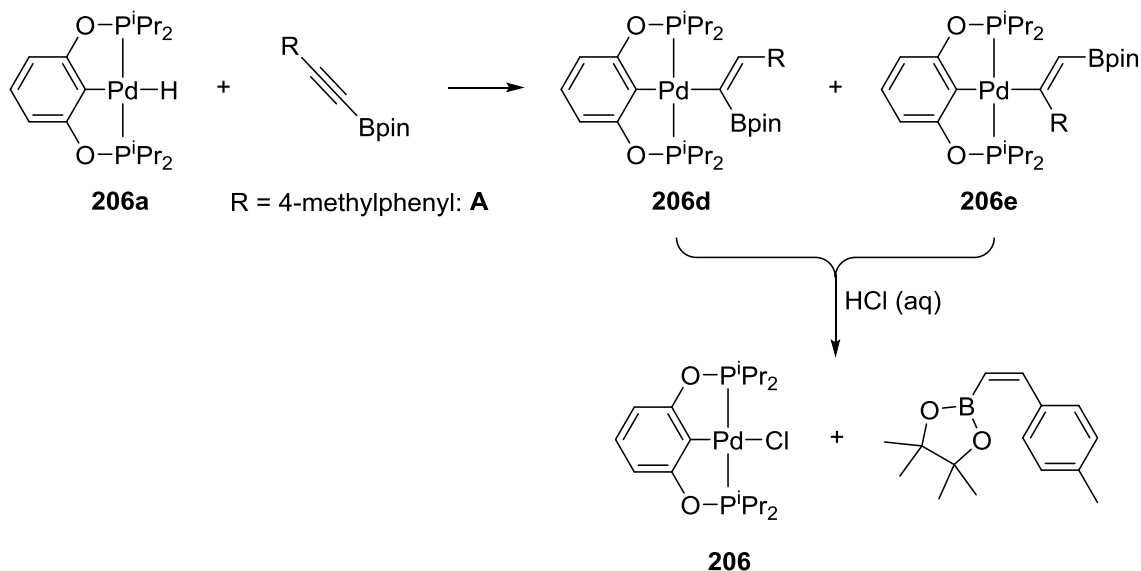
* Alkynylboronate insertion products (**206d** and **206e** shown in Scheme II-5) were formed upon further heating of this mixture.



Scheme II-4. Proposed mechanism for palladium-catalyzed DHBTA .

The equilibrium between **206c**/HBpin and **206a**/**A** is eventually disturbed by the irreversible insertion of the alkynylboronate into the palladium hydride bond. When **206a** was treated with 1 eq. of **A** and heated for 4 days at 80 °C, **206d** and **206e** were formed and accounted for 71% of the reaction mixture as judged by $^{31}\text{P}\{^1\text{H}\}$ NMR integration (Scheme II-5). Treating this mixture with concentrated HCl converted all of the (POCOP)Pd compounds to **206**, and (*Z*)-2-pinacolboronyl-1-(4-methylphenyl) ethylene was observed by ^1H NMR spectroscopy, consistent with the proposed isomeric structures for **206d** and **206e**. Under catalytic conditions, the insertion of the **A** is much slower than the rate of DHBTA and we have not observed formation of any alkenyl products in catalytic reactions with **206a**, **206b**, **206c** until the reaction is nearly complete and the concentration of alkyne in solution is low enough to allow **206a** to start

accumulating. However, insertion of alkynes into the Pd-H bond may be responsible for the ultimate demise of the catalyst.



Scheme II-5. Insertion of an alkyneboronate into **206a**'s Pd-H bond and the protonolysis of **206d** and **206e**.

Catalytic 4-ethynyltoluene DHBTA reactions with **206a**, **206b**, or **206c** precatalysts inevitably produce comparable quantities of the semihydrogenation product (4-methylstyrene), presumably by using the H_2 formed as a byproduct of DHBTA. The Guan group reported that **206a** functions as an alkyne semihydrogenation catalyst, but ostensibly through generation of Pd(0) nanoparticles as the hydrogenation catalysis was inhibited by elemental mercury.¹³³ Many pincer-ligated palladium complexes have been shown to leach soluble Pd(0) into solution.¹³⁹⁻¹⁴³ Over the course of the reaction, (POCOP)Pd-catalyzed DHBTA reaction mixtures developed a red color

associated with palladium nanoparticles in solution.^{140,144} Introduction of elemental mercury inhibited the hydrogenation of the terminal alkynes in DHBTA mixtures, and >95% of the terminal alkyne was converted to **A** (Table II-2, entry 6). A photograph comparing the colors of two DHBTA reactions, one with mercury and one without, can be seen in Figure II-1. It was also determined that the rate of DHBTA was not affected by the presence of mercury. After 1 day, parallel reactions catalyzed by **206a** with and without mercury (entries 6 and 3, respectively) had both converted about 40% of the terminal alkyne to **A**. We were intrigued by the possible use of gallium as an alternative, less toxic liquid metal trap for palladium nanoparticles, but it proved completely ineffective at stopping hydrogenation (entry 7 and 8).



Figure II-1. Photograph of J. Young tubes for entries 3, Table II-1 (right) and 6, Table II-2 (left) after 1 day. A drop of Mercury can be seen in the left tube. The right tube has changed to a red/orange color indicating the presence of Pd nanoparticles.

Hydrogenation of the alkyne could also be mitigated by the addition of PMe_3 , PPh_3 , or P(OMe)_3 (entries 9-13). PPh_3 and PMe_3 were similarly effective at 10%

loading. 10% P(OMe)₃ also inhibited hydrogenation, but suppressed the formation of **A**, as well (entry 13). Addition of 10% SⁱPr₂ (entry 14) or of a large excess of poly(4-vinylpyridine)¹⁴⁰ (entry 15) had no effect on the reaction.

Table II-2. The effect of additives on Pd-catalyzed DHBTA of 4-ethynyltoluene.

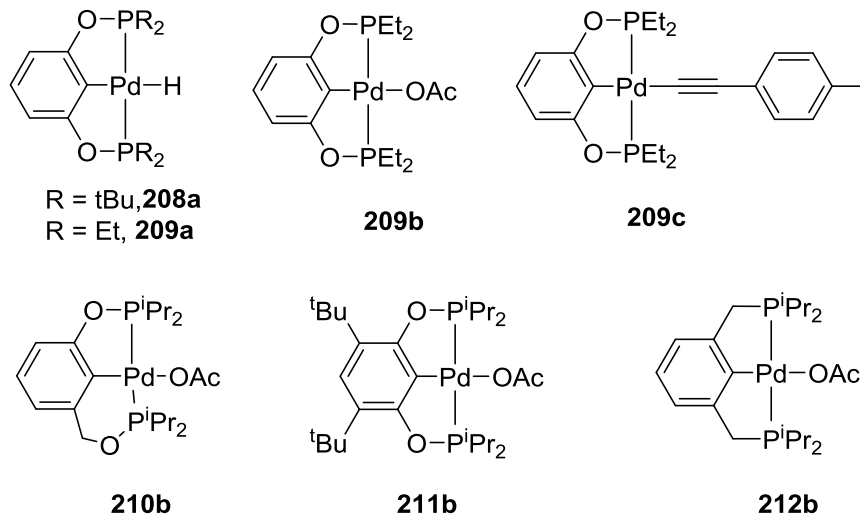
#	[Pd]	A ^a	B ^{a,b}	Time	Additives
6	206a	>95%	<5%	6 d	0.45 mmol Hg
7	206b	53%	43%	1 d	1.12 mmol Ga
8	206b	49%	51%	1 d	5.45 mmol Ga
9	206a	63%	35%	2 d	0.017 mmol PPh ₃
10	206a	87%	<5%	3 d	0.034 mmol PPh ₃
11	206b	85%	<5%	3 d	0.034 mmol PPh ₃
12	206b	88%	6%	3 d	0.034 mmol PMe ₃
13	206b	46%	<5%	4 d	0.034 mmol P(OMe) ₃
14	206b	45%	48%	1 d	0.034 mmol S ⁱ Pr ₂
15	206b	44%	43%	1 d	150 eq. PVPy

All reactions performed at 80 °C in C₆D₆ with 0.34 mmol alkyne, 0.34 mmol HBpin, and 5% catalyst loading. ^a Yields were determined by ¹H NMR integration versus an internal standard (1,4-Dioxane). ^b Reactions that produced significant amounts of **B** also showed trace production of 4-ethyltoluene.

2.2.3 Ligand Screening and Catalyst Optimization

We prepared Pd complexes supported by several other (PCP)- and POCOP-type pincer ligands to test as catalysts and to compare them to **206b**. Complexes **208a**, **209b**, **210b**, **211b**, **212b** were synthesized according to literature procedures and precedent and

were used as precatalysts (Scheme II-6).^{133,137,145} **209c** was synthesized through the same method as complex **206c**.

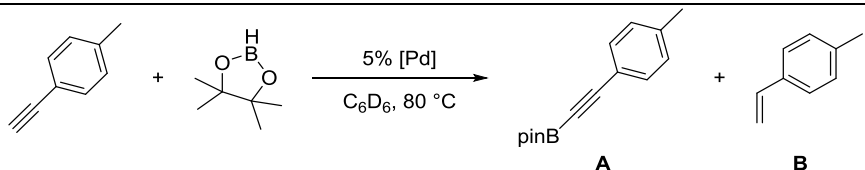


Scheme II-6. Additional PCP-type pincer-ligated palladium DHBTA precatalysts.

Our catalogue of different palladium catalysts were tested for DHBTA at 5 mol% loading with 4-ethynyltoluene and pinacolborane. It was discovered that the relative rate of alkyne consumption is greatly dependent on the size of the substituents on the phosphine arms. The bulkier **208a** only produced trace amounts of alkynylboronate (Table II-3, entry 16), while the less sterically imposing **209b** was capable of consuming all of the alkyne substrate within 2 h (entry 17), and **209c** was also found to be an analogous precatalyst (entry 18). Similar to **206b**, phosphine additives and mercury were able to inhibit the semihydrogenation reaction with **209b** (entries 19-22). Higher concentrations of HBpin were also examined using **209b**, but did not prove to be any more beneficial than 1 equivalent (see section 2.4.4 for further discussion). **210b** did not

perform nearly as well as the resorcinol-based pincer ligands (entry 23), and **211b** performed similarly to the unsubstituted **206b** (entry 24). **212b** gave a nearly identical distribution of **A** and semihydrogenated product, but required a much longer reaction time of three days (Entry 25) possibly resulting from the slightly bulkier nature of the ligand compared to POCOP.¹⁴⁶ The longevity of **209b** was investigated using mercury as a hydrogenation inhibitor by using 0.5 mol% catalyst loading for the borylation of 4-ethynyltoluene (entry 26). The catalysis ceased after 1 day and 38% conversion to **A**, which accounted for about 75 turnovers. Control reactions using Pd₂(DBA)₃ and Pd(COD)Cl₂ as catalysts did not show any formation of alkynylboronate.

Table II-3. DHBTA with different (pincer)Pd catalysts.

					
#	[Pd]	A ^a	B ^{a,b}	Time	Additives
16	208a	2%	10%	3 d	X
17	209b	40%	37%	2 h	X
18	209c	36%	27%	2 h	X
19	209b	91%	<5%	5 h	0.45 mmol Hg
20	209b	85%	<5%	1 d	0.034 mmol PPh ₃
21	209b	64% (32%)	8%	1 d	0.034 mmol PMe ₃
22	209b	<5%	-	1 d	0.034 mmol P(OMe) ₃
23	210b	7%	13%	1 d	X
24	211b	49%	43%	1 d	X
25	212b	43%	48%	3 d	X
26	209b ^c	38%	<5%	1 d	0.45 mmol Hg
All reactions performed at 80 °C in C ₆ D ₆ with 0.34 mmol alkyne, 0.34 mmol HBpin, and 5% catalyst loading. ^a Yields were determined by ¹ H NMR integration versus an internal standard (1,4-Dioxane). ^b Reactions that produced significant amounts of B also showed trace production of 4-ethyltoluene. ^c 1.7 μmol of 5b used.					

209a could not be isolated due to its inherent instability. Attempts to synthesize it through the same means of obtaining **206a** did not prove successful, and attempts to treat **209b** with HBpin resulted in the immediate formation of dihydrogen and a rapid color change from a clear solution to dark brown signifying decomposition of the palladium complex. However, analysis of catalytic mixtures with **209b** by $^{31}\text{P}\{^1\text{H}\}$ NMR spectroscopy showed the presence of **209c** under catalytic conditions, and stoichiometric reactions treating **209c** with HBpin did lead to the production of **A**.

It was also hypothesized that (POCOP)Pd species could perform hydrogenolysis of bis(pinacolato)diboron. The B-B cleavage of diboron reagents with dihydrogen has been reported by Marder et. al. with heterogeneous group 10 metal catalysts.¹⁴⁷ B_2Pin_2 would have been a beneficial hydrogen acceptor in the DHBTA of terminal alkynes because the hydrogenolysis product (HBpin) is a reagent in the reaction. However, when B_2Pin_2 was treated with 5 mol% **206a** and heated at 80 °C for 24 h under an atmosphere of H_2 , no pinacolborane was observed by ^1H NMR spectroscopy.

2.2.4 Substrate Scope

The substrate scope of our system was briefly examined using **206b** and **209b** as catalysts and is outlined in Table II-4. **209b** gave better results than **206b** in DHBTA of 4-ethynyltoluene (entries 11 and 20) and ethynyltrimethylsilane (entries 27 and 28), but fared less well in DHBTA of 1-hexyne (entries 29 and 30).

Propargyl-functionalized alkynes had been problematic with the original iridium system³⁷ and also proved to be difficult for our palladium systems. **209b** was not at all effective at DHBTA with substrates featuring heteroatoms at the propargyl position

(entries 32, 33, and 36), while **206b** resulted in some formation of DHBTA products (entries 31, 33, and 35). However, side reactions dominated in all cases. Phenyl propargyl ether was susceptible to hydrogenation and C-O bond cleavage to form PhOBpin, while trimethyl silyl propargyl ether was mostly susceptible to C-O bond cleavage which resulted in the formation of Me₃Si-O-Bpin. Propyne and propylene were also detected by ¹H NMR spectroscopy in reaction mixtures.

Table II-4. DHBTA with various alkynes.

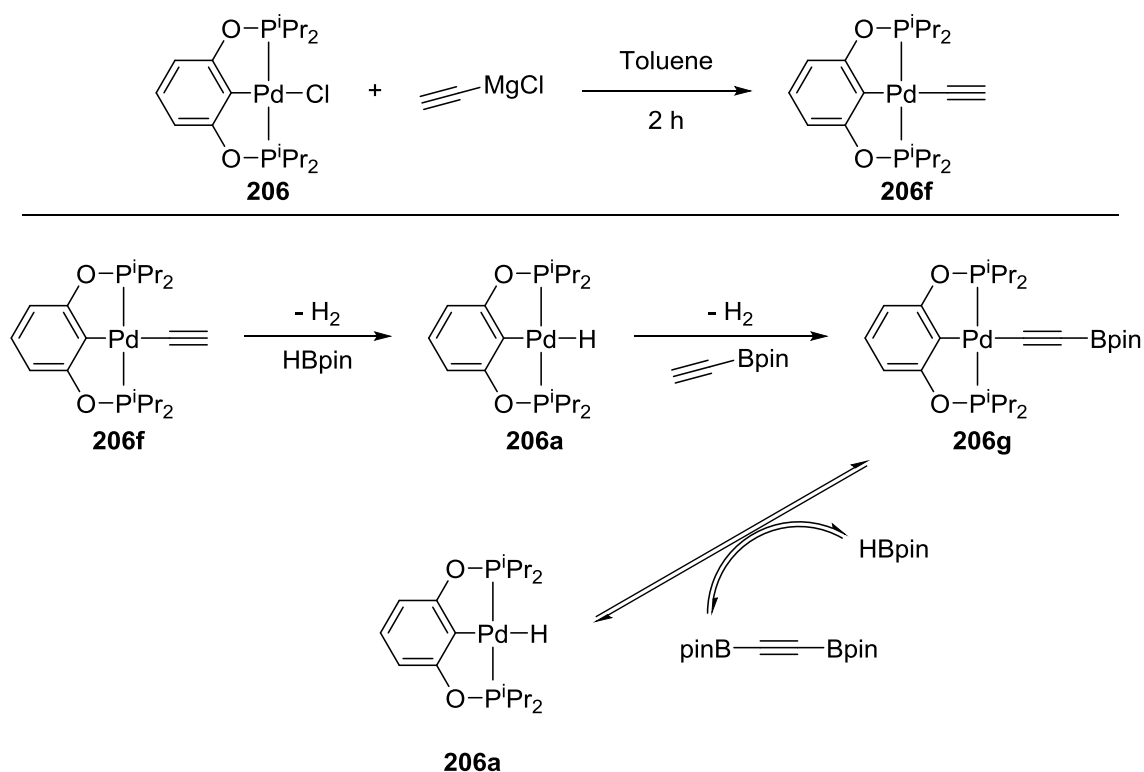
#	[Pd]	R	C ^a	D ^a	Other
27	209b	Me ₃ Si	80%	4%	16% SM ^b
28	206b	Me ₃ Si	11%	-	85% SM
29	209b	ⁿ Bu	<5%	11%	85% SM
30	206b	ⁿ Bu	84% (58%)	<5%	12% SM
31	206b	Me ₃ SiOCH ₂	50%	<5%	8% Me ₃ SiOBpin
32	209b	Me ₃ SiOCH ₂	-	-	90% Me ₃ SiOBpin
33	206b	PhOCH ₂	20%	19%	15% PhOBpin
34	209b	PhOCH ₂	-	-	95% PhOBpin
35	206b	PhSCH ₂	5%	-	77% SM
36	209b	PhSCH ₂	-	-	80% SM

All reactions performed for 1 day at 80 °C in C₆D₆ with 0.34 mmol alkyne, 0.34 mmol HBpin, 0.034 mmol PPh₃, 5% catalyst loading. ^a Yields were determined by ¹H NMR integration versus an internal standard (1,4-dioxane). ^b SM = starting material.

2.2.5 Attempts to Diborylate Acetylene

It has been an interest of ours to perform DHBTA on acetylene, the simplest alkyne, in order to make diborylated acetylene. However acetylene is unstable in its pure

form and is often handled as a solution in acetone.¹⁴⁸ Acetylene can also be obtained through the hydrolysis of calcium carbide; however, the exothermic and wet nature of this reaction produces water vapor. Since our borane source is extremely sensitive to moisture, attempts to perform DHBTA with wet acetylene were not successful.



Scheme II-7. Synthesis of **206f** and subsequent reaction with HBpin.

We were able to synthesize the catalytic intermediate for the DHBTA of acetylene by treating **206** with ethynyl magnesium grignard. This reaction produced **206f**, which could be recrystallized from pentane in a 71% yield as white needle-shaped crystals.

In an attempt to form diborylacetylene, we reacted **206f** with 2 eq. of HBpin and heated the reaction at 80 °C for 96 hours. Due to the reversible nature of the reaction that forms an alkynylboronate from a palladium alkynyl, very little diborylacetylene was observed. Instead there was a mixture of three dominant products that could be monitored by $^{31}\text{P}\{^1\text{H}\}$ NMR. The starting material, **206f**, was seen to decrease in concentration as a new product was formed, which is presumed to be **206g**. **206a** was observed to maintain a steady concentration of about 10% of the mixture throughout the reaction. The progress of the reaction as monitored by $^{31}\text{P}\{^1\text{H}\}$ NMR is shown in Figure II-2.

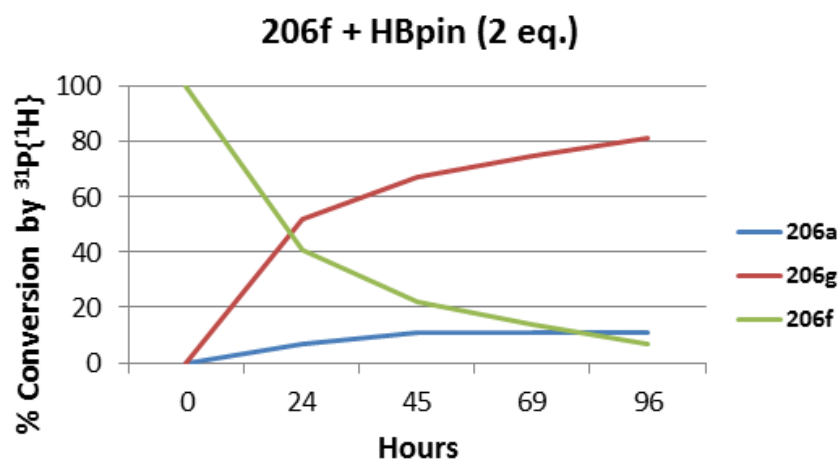


Figure II-2. Reaction mixture concentrations resulting from the treatment of **206f** with 2 eq. of pinacolborane.

In order to characterize **206g**, **206f** was treated with 1 eq. of pinacolborane and heated for 90 h at 80 °C. Analysis of the reaction mixture by $^{31}\text{P}\{^1\text{H}\}$ NMR spectroscopy

showed 78% conversion **206g**. The product was precipitated from a pentane solution at -35 °C as a white solid in >90% purity. The ^1H NMR spectrum showed a singlet at 1.09 ppm, which integrated to 12 protons with respect to the POCOP ligand. The $^{13}\text{C}\{^1\text{H}\}$ and $^{11}\text{B}\{^1\text{H}\}$ NMR spectra also corroborated the assignment of this product as **206g**.

2.3 Conclusions

In conclusion, we have shown that palladium can perform dehydrogenative borylation of terminal alkynes. This expands the realm of substrates that palladium can borylate and also shows that DHBTA can be performed by other pincer-ligated metals that behave differently from the original (SiNN)Ir catalyst.

This palladium system is limited by the propensity for pincer-ligated palladium complexes to leach palladium(0) into solution, which can then perform hydrogenation of the terminal alkyne. However, hydrogenation can be prevented with the addition of phosphines to the reaction mixture. The system also suffers from the reversible nature of the product forming step, which leads to longer reaction times and incomplete conversions. This work also shows the ability of pincer-ligated Pd-X compounds to perform metathesis reactions to couple its X-substituent with another reagent.

2.4 Experimental

2.4.1 General Considerations

Unless otherwise specified, all manipulations were performed under an argon atmosphere using standard Schlenk line or glove box techniques. Toluene, THF, pentane, and isooctane were dried and deoxygenated (by purging) using a solvent

purification system and stored over molecular sieves in an Ar-filled glove box. C₆D₆ was dried over and distilled from NaK/Ph₂CO/18-crown-6 and stored over molecular sieves in an Ar-filled glove box. 1,4-Dioxane, CH₂Cl₂, and CDCl₃ were dried with CaH₂ and vacuum transferred to be stored over molecular sieves in an Ar-filled glove box. NMR spectra were recorded on a Varian NMRS 500 (¹H NMR, 499.686 MHz; ¹³C NMR, 125.659 MHz; ³¹P NMR, 202.298 MHz) and Varian Inova 400 (¹¹B NMR, 128.185 MHz) spectrometer. Chemical shifts are reported in δ (ppm). For ¹H and ¹³C NMR spectra, the residual solvent peak was used as an internal reference. ³¹P NMR spectra were referenced externally using 85% H₃PO₄ to δ = 0 ppm. For ¹¹B NMR, spectra were referenced externally to δ = 0 ppm by using BF₃·Et₂O. Elemental analyses were performed by CALI Labs, Inc. (Parsippany, NJ). **206**,¹⁴⁹ **206b**,¹³⁷ **207**,¹⁵⁰ **208a**,¹³³ (4,6-ditertbutylPOCOP)PdCl (**211b**),¹⁵¹ and **210b**¹³⁷ were synthesized according to literature procedures.

2.4.2 Synthesis and Characterization

Synthesis of (POCOP^{iPr})PdH (206a). In a Schlenk flask, **206**¹⁴⁹ (362 mg, 0.750 mmol) was dissolved in pyridine and treated with NaBEt₃H (750 μL, 1.0 M solution in toluene). The reaction was stirred for 1 h at room temperature. The volatiles were removed and the resulting solid was dissolved in toluene and passed through a pad of Celite. The volatiles were removed, and the resulting yellow solid was dissolved in minimum of Et₂O and places in a -35 °C freezer. The resulting light yellow crystals were dissolved in Et₂O and placed back into a -35 °C freezer to be recrystallized again. The

resulting yellow crystals were washed with cold pentane and dried under vacuum (77 mg, 23%). The spectral data matched that reported in the literature.¹³³

Synthesis of (POCOP^{iPr})Pd(-C≡C-*p*-C₆H₄Me) (206c). In a Schlenk flask, **206**¹⁴⁹ (227 mg, 0.47 mmol) was dissolved in toluene and treated with NaO^tBu (68 mg, 0.705 mmol) and 4-ethynyltoluene (60 μL, 0.47 mmol). The reaction was stirred overnight and the volatiles removed under vacuum in the morning. The product was extracted with pentane and filtered through a plug of silica and Celite to be recrystallized from pentane at -35 °C to yield beige crystals (180 mg, 68%). ³¹P{¹H} NMR (C₆D₆): δ 193.0 (s); ¹H NMR (C₆D₆): δ 7.59 (d, 2H, *J* = 8.0 Hz, Ar-*H*), 6.97 (d, 2H, *J* = 8.0 Hz, Ar-*H*), 6.93 (t, 1H, *J* = 8.0 Hz, POCOP-*H*), 6.77 (d, 2H, *J* = 8.0 Hz, Ar-*H*), 2.18 (m, 4H, PCHMe₂), 2.07 (s, 3H, Ar-Me), 1.30 (m, 12H, PCHMe₂), 1.11 (apparent q (dvt), 12H, *J* = 7 Hz, PCHMe₂). ¹³C{¹H}(C₆D₆): δ 167.0 (t, *J* = 6.7 Hz, Ar-OP), 138.4 (t, *J* = 4.7 Hz, Ar-Pd), 134.4 (s), 131.3 (s), 129.1 (s), 128.8 (s), 127.2 (s), 119.2 (s, C≡C-tolyl), 108.6 (t, *J*_{C-P} = 17.9 Hz, Pd-C≡C-tolyl), 105.7 (t, *J*_{C-P} = 7.2 Hz, (POCOP)Ar-*H*), 29.5 (t, *J*_{C-P} = 12.1 Hz, PCHMe₂), 21.3 (s, Ar-Me), 17.8 (t, *J*_{C-P} = 3.8 Hz, PCHMe₂), 17.0 (s, PCHMe₂). Elem. Anal. Found (Calculated) for C₂₇H₃₈O₂P₂Pd: C, 57.71 (57.61); H, 6.83 (6.80).

Synthesis of (POCOP^{iPr})PtH (207a). **207** (250 mg, 0.437 mmol) was dissolved in THF and treated with NaHBET₃ (480 μL, 1.0 M toluene) and left to stir for 10 minutes. The volatiles were removed and the product was extracted with pentane and filtered through Celite. The volatiles were removed and the resulting solid was dissolved in a minimum amount of pentane and placed in a -35 °C freezer to recrystallize. **207a** was isolated as a white solid (102 mg, 43% yield). ³¹P{¹H} NMR (C₆D₆): δ 190.5 (s, *J*_{P-Pt} =

3002 Hz); ^1H NMR (C_6D_6): δ 7.04 (m, 1H, Ar-H), 6.49 (m, 2H, Ar-H), 2.13 (m, 4H, PCHMe_2), 1.12 (dvt, $J = 9$ Hz, $J = 7$ Hz, 12H, PCHMe_2), 1.07 (apparent q (dvt), $J = 7$ Hz, 12H, PCHMe_2), 1.01 (t, $J_{\text{H-P}} = 17$ Hz, $J_{\text{H-Pt}} = 444$ Hz, 1H, Pt-H); $^{13}\text{C}\{^1\text{H}\}$ NMR (C_6D_6): δ 165.3 (t, $J_{\text{C-P}} = 6.4$ Hz, $J_{\text{C-Pt}} = 33$ Hz, Ar-OP), 144.3 (t, $J_{\text{C-P}} = 6.0$ Hz, $J_{\text{C-Pt}} = 467$ Hz, Ar-Pt), 127.6 (s, Ar-H), 105.0 (t, $J_{\text{C-P}} = 6.0$ Hz, Ar-H), 30.3 (t, $J_{\text{C-P}} = 17$ Hz, $J_{\text{C-Pt}} = 58.5$ Hz, P- CHMe_2), 18.7 (vt, $J_{\text{C-P}} = 3.9$ Hz, $J_{\text{C-Pt}} = 19.0$ Hz, PCHMe), 17.2 (s, $J_{\text{C-Pt}} = 24.7$ Hz, PCHMe_2).

Synthesis of (POCOP^{Et}). In a Schlenk flask, resorcinol (443 mg, 4.015 mmol) was dissolved in THF and treated with triethylamine (1.22 grams, 12.1 mmol). Diethylchlorophosphine (1.00 gram, 8.03 mmol) was added dropwise and the solution was left to stir overnight at room temperature. The volatiles were removed under vacuum, and the product was extracted with pentane and filtered through Celite. The volatiles were removed under vacuum to leave a clear oil that was determined to be >95% pure by ^1H NMR spectroscopy and could be used in further reactions (1.04 g, 90% yield). $^{31}\text{P}\{^1\text{H}\}$ NMR (C_6D_6): δ 138.7 (s); ^1H NMR (C_6D_6): δ 7.26 (m, 1H, Ar-H), 7.01 (t, 1H, $J = 8.0$ Hz, Ar-H), 6.88 (m, 2H, Ar-H), 1.58 (m, 4H, PCH_2Me), 1.36 (m, 4H, PCH_2Me), 0.99 (dt, 12H, $J_{\text{H-P}} = 14.5$ Hz, $J_{\text{H-H}} = 7.5$ Hz, PCH_2Me); $^{13}\text{C}\{^1\text{H}\}$ (C_6D_6): δ 160.1 (d, $J_{\text{C-P}} = 8.2$ Hz, Ar-OP), 130.2 (s, Ar-H), 112.5 (d, $J_{\text{C-P}} = 11.2$ Hz, Ar-H), 109.7 (t, $J_{\text{C-P}} = 11.2$ Hz, Ar-H), 25.4 (d, $J_{\text{C-P}} = 18.6$ Hz, PCH_2), 8.0 (d, $J_{\text{C-P}} = 13.2$, PCH_2Me).

(POCOP^{Et})PdCl (209). In a Schlenk flask, (POCOP^{Et}) (380 mg, 1.33 mmol) was refluxed in toluene with Pd(COD)Cl₂ (379 mg, 1.33 mmol) overnight. The volatiles were removed from the reaction mixture, which was then dissolved in dichloromethane and

passed through a pad of silica and Celite. The volatiles were removed under vacuum and the resulting solid was washed with diethyl ether and pentane to yield a white solid (438 mg, 77% Yield). $^{31}\text{P}\{^1\text{H}\}$ NMR (C_6D_6): 177.8 (s); ^1H NMR (C_6D_6): δ 6.86 (t, 1H, $J = 8.5$ Hz, *Ar-H*), 6.67 (d, 2H, $J = 8.0$ Hz, *Ar-H*), 1.76 (m, 4H, PCH_2Me), 1.67 (m, 4H, PCH_2Me), 1.08 (m, 12H, PCH_2Me); $^{13}\text{C}\{^1\text{H}\}$ NMR (CDCl_3): δ 165.5 (t, $J_{\text{C-P}} = 7.0$ Hz, *Ar-OP*), 129.8 (t, $J_{\text{C-P}} = 3.0$ Hz, *Ar-Pd*), 128.4 (s, *Ar-H*), 106.3 (t, $J_{\text{C-P}} = 8$ Hz, *Ar-H*), 24.0 (t, $J_{\text{C-P}} = 13$ Hz, PCH_2Me), 7.6 (s, PCH_2Me).

(POCOP^{Et})Pd(OAc) (209b). **209** (185 mg, 0.433 mmol) was dissolved in toluene in a culture tube and treated with AgOAc (80 mg, 0.476 mmol) and stirred overnight in the dark. The solution was filtered through a plug of silica and Celite and the volatiles were removed under vacuum. The product was recrystallized from pentane to yield a white crystalline solid (137 mg, 70%). $^{31}\text{P}\{^1\text{H}\}$ NMR (C_6D_6): δ 172.6 (s); ^1H NMR (C_6D_6): δ 6.90 (m, 1H, *Ar-H*), 6.68 (d, 2H, $J = 8.0$ Hz, *Ar-H*), 2.26 (s, OAc), 2.14 (m, 4H, PCH_2Me), 1.84 (m, 4H, PCH_2Me), 1.12 (m, 12H, PCH_2Me); $^{13}\text{C}\{^1\text{H}\}$ NMR (C_6D_6): δ 175.0 (t, $J_{\text{C-P}} = 2.3$ Hz, OAc), 166.7 (t, $J_{\text{C-P}} = 7.1$ Hz, *Ar-OP*), 129.0 (s, *Ar-Pd* signal not present (obscured by C_6D_6), 106.1 (s), 25.4 (t, $J_{\text{C-P}} = 14.5$ Hz, PCH_2Me), 22.3 (s, OAc), 8.4 (s, PCH_2Me). Elem. Anal. Found (Calculated) for $\text{C}_{16}\text{H}_{26}\text{O}_4\text{P}_2\text{Pd}$: C, 42.59 (42.63); H, 5.89 (5.81).

Synthesis of (POCOP^{Et})Pd(C \equiv C-*p*-C₆H₄Me) (209c). In a Schlenk flask, **209** (111 mg, 0.26 mmol) was dissolved in toluene and was treated with NaO^tBu (37 mg, 0.39 mmol), and 4-ethynyltoluene (33 ml, 0.26 mmol). The reaction was stirred overnight and the volatiles were removed under vacuum. The product was extracted in

benzene and filtered through Celite. The volatiles were removed and the product was recrystallized from pentane in a -35 °C freezer (94 mg, 71%). $^{31}\text{P}\{^1\text{H}\}$ NMR (C_6D_6): δ 179.5 (s); ^1H (C_6D_6): δ 7.63 (d, $J = 8.0$ Hz, 2H, Ar-*H*), 6.96 (d, $J = 8.0$ Hz, 2H, Ar-*H*), 6.95 (t, $J = 8.0$ Hz, 1H, Ar-*H*), 6.78 (d, $J = 8.0$ Hz, 2H, Ar-*H*), 2.06 (s, 3H, Ar-*Me*), 1.81 (m, 8H, $\text{P}(\text{CH}_2\text{Me})_2$), 1.12 (app. pent. (overlapping tvt), $J = 7.5$ Hz, 12H, $\text{P}(\text{CH}_2\text{CH}_3)_2$); $^{13}\text{C}\{^1\text{H}\}$ NMR (C_6D_6): δ 166.2 (t, $J_{\text{C-P}} = 7.3$ Hz, Ar-OP), 139.1 (t, $J_{\text{C-P}} = 5.2$, Ar), 134.5 (s), 131.4 (s), 129.1 (s), 128.4 (s), 127.0 (s), 117.0 (s, $\text{C}\equiv\text{C}$ -tolyl), 109.2 (t, $J_{\text{C-P}} = 18.1$ Hz, $\text{C}\equiv\text{C}$ -tol), 106.1 (t, $J_{\text{C-P}} = 18.1$ Hz, Ar), 24.7 (t, $J_{\text{C-P}} = 13.5$ Hz, PCH_2Me), 21.3 (s, Ar-*Me*), 8.0 (s, PCH_2Me). Elem. Anal. Found (Calculated) for $\text{C}_{23}\text{H}_{30}\text{O}_2\text{P}_2\text{Pd}$: C, 54.29 (54.50); H, 5.79 (5.97).

Synthesis of (4,6-ditertbutylPOCOP)Pd(OAc) (211b). In a culture tube, (4,6-ditertbutylPOCOP)PdCl (**211**)¹⁵¹ (155 mg, 0.26 mmol) was dissolved in toluene and treated with Ag(OAc) (48 mg, 0.29 mmol) and stirred overnight. The reaction mixture was passed through a pad of silica and Celite and stripped down. The product was recrystallized from isooctane as white crystals (72 mg, 44% yield). $^{31}\text{P}\{^1\text{H}\}$ NMR (C_6D_6): δ 185.1 (s); ^1H NMR (C_6D_6): δ 7.26 (s, 1H, Ar-*H*), 2.40 (m, 4H, $\text{P}(\text{CHMe}_2)_2$), 2.28 (s, 3H, OAc), 1.46 (s, 18H, ArCMe₃), 1.30 (apparent q (dvt), 12H, $J = 9.0$ Hz, PCHMe_2), 1.16 (apparent q (dvt), 12H, $J = 7.0$ Hz, PCHMe_2); $^{13}\text{C}\{^1\text{H}\}$ NMR (C_6D_6): δ 174.8 (s, OAc), 162.7 (t, $J_{\text{C-P}} = 6.2$ Hz, Ar-OP), 130.9 (t, $J_{\text{C-P}} = 4.2$ Hz, Ar-Pd), 127.4 (t, $J_{\text{C-P}} = 5.9$ Hz, Ar-^tBu), 123.3 (s, Ar-*H*), 34.8 (s, Ar-CMe₃), 30.4 (s, OAc), 29.8 (t, $J_{\text{C-P}} = 12.0$ Hz, PCHMe_2), 17.9 (t, $J_{\text{C-P}} = 3.8$ Hz, PCHMe_2), 17.3 (s, ArCMe₃). Elem. Anal. Found (Calculated) for $\text{C}_{28}\text{H}_{50}\text{O}_4\text{P}_2\text{Pd}$: C, 54.24 (54.32); H, 8.06 (8.14).

Synthesis of PhOBpin¹⁵². In a J. Young tube, phenol (32 mg, 0.34 mmol) was dissolved in C₆D₆ and treated with pinacolborane (49 μL, 0.34 mmol). Hydrogen gas was produced immediately upon mixing. Analysis by ¹H NMR spectroscopy showed that the reaction was completed within minutes. The reaction mixture was transferred to a flask, and the volatiles were removed under vacuum to yield a fine white powder (54 mg, 72%). ¹H NMR (C₆D₆): 7.22 (d, *J* = 8 Hz, 2H), 7.06 (m, 2H), 6.83 (t, *J* = 7.5 Hz, 1H), 1.01 (s, 12H); ¹³C{¹H} NMR (C₆D₆): 154.4, 129.6, 123.3, 120.1, 83.3, 24.6; ¹¹B{¹H} NMR (C₆D₆): 21.9 (s).

Synthesis of (POCOP^{iPr})Pd(C≡CH) (206f). In a teflon screw-top flask, (POCOP^{iPr})PdCl (**209**) (300 mg, 0.621 mmol) was dissolved in toluene and treated with ethynylmagnesium chloride (1.5 mL of 0.5 M in THF, 0.75 mmol). The reaction was stirred for 2 h at room temperature and filtered through a pad of silica and Celite. The product was recrystallized from pentane at -35 °C to form off-white needle-like crystals (209 mg, 71% yield). ³¹P{¹H} NMR (C₆D₆): δ 193.0 (s); ¹H NMR (C₆D₆): 6.92 (t, 1H, *J* = 7.5 Hz, *Ar-H*), 6.76 (d, 2H, *J* = 8 Hz, *Ar-H*), 2.78 (s, 1H, C≡CH), 2.18 (m, 4H, PCHMe₂), 1.29 (apparent q (dvt), 12H, *J* = 8.5 Hz, PCHMe₂), 1.10 (apparent q (dvt), 12H, *J* = 7 Hz, PCHMe₂); ¹³C{¹H} (C₆D₆): δ 167.0 (t, *J*_{C-P} = 6.7 Hz, *Ar-OP*), 138.2 (t, *J*_{C-P} = 4.8 Hz, *Ar-Pd*), 128.8 (s, *Ar-H*), 105.7 (t, *J*_{C-P} = 7.2 Hz, *Ar-H*), 103.7 (s, Pd-C≡CH), 102.0 (t, *J*_{C-P} = 17.3 Hz, Pd-C≡CH), 29.4 (t, *J*_{C-P} = 12.1 Hz, PCHMe₂), 17.8 (t, *J*_{C-P} = 3.8 Hz, PCHMe₂), 17.0 (s, PCHMe₂). Elem. Anal. Found (Calculated) for C₂₀H₃₂O₂P₂Pd: C, 51.06 (50.80); H, 7.04 (6.82).

Characterization of (POCOP)PdCCBpin (206g). 206f (44 mg, 0.093 mmol) was treated with pinacolborane (14 μ L, 0.096 mmol) in a J. Young tube. The mixture was then heated for 90 h at 80 °C. Analysis of the reaction mixture by $^{31}\text{P}\{^1\text{H}\}$ NMR spectroscopy showed 78% conversion to **206g** (193.6 ppm, s) the remaining phosphorus containing species were **206a** (8%) and unreacted **206f** (14%). The reaction mixture was filtered through Celite and the volatiles were removed under vacuum. The resulting whitish solid was dissolved in pentane and recrystallized at -35 °C and washed with cold pentane. The resulting white solid contained 93% of a product resonating at 193.6 ppm, and 7% unreacted **206f**. $^{31}\text{P}\{^1\text{H}\}$ NMR (C_6D_6): δ 193.6 (s); ^1H NMR (C_6D_6): 6.90 (t, 1H, $J = 7.5$ Hz, POCOP), 6.73 (d, 2H, $J = 8$ Hz, POCOP), 2.10 (m, 4H, PCHMe_2), 1.25 (apparent q (dvt), 12H, $J = 9$ Hz, PCHMe_2), 1.09 (s, 12H, Bpin), 1.03 (apparent q (dvt), 12H, $J = 7$ Hz, PCHMe_2); $^{13}\text{C}\{^1\text{H}\}$ NMR (C_6D_6): 167.1 (t, $J_{\text{C-P}} = 6.7$ Hz, Ar-OP), 138.1 (t, $J_{\text{C-P}} = 4.8$ Hz, Ar-Pd), 128.9 (s, Ar-H), 105.7 (t, $J_{\text{C-P}} = 7.1$ Hz, Ar-H), 82.3 (s, Bpin), 29.3 (t, $J_{\text{C-P}} = 12.2$ Hz, PCHMe_2), 25.1 (s, Bpin), 17.8 (t, $J_{\text{C-P}} = 3.7$ Hz, PCHMe_2), 16.8 (s, PCHMe_2); $^{11}\text{B}\{^1\text{H}\}$ NMR (C_6D_6): 22.6.

2.4.3 Stoichiometric Reactions

Treatment of 206a with 4-ethynyltoluene. 206a (15 mg, 0.033 mmol) was dissolved and treated with 4-ethynyltoluene (4 μ L, 0.033 mmol). Analysis by ^1H and $^{31}\text{P}\{^1\text{H}\}$ NMR spectroscopy <15 minutes after the addition of 4-ethynyltoluene showed complete conversion to **206c** by $^{31}\text{P}\{^1\text{H}\}$ NMR spectroscopy and ^1H NMR spectroscopy showed the evolution of H_2 .

Treatment of 206b with pinacolborane. **206b** (35 mg, 0.069 mmol) was dissolved in C₆D₆ and treated with pinacolborane (10 μL, 0.069 mmol), which immediately made the solution turn from clear to a light yellow. Analysis by ¹H and ³¹P{¹H} NMR spectroscopy <15 minutes after the addition of pinacolborane showed 100% conversion to **206a** and the appearance of two new singlets at 1.597 ppm (3H) and 1.025 ppm (12H) showing the formation of pinBOAc.

Treatment of 206b with 4-ethynyltoluene. **206b** (40 mg, 0.079 mmol) was treated with 4-ethynyltoluene (10 μL, 0.079 mmol). Within 23 h at room temperature, a 3:2 **206b:206c** equilibrium was established as seen by ³¹P{¹H} NMR spectroscopy. ¹H NMR spectroscopy shows the formation of acetic acid from the characteristic broad singlet at 13.25 ppm. Addition of 1 equivalent of pinacolborane (11.5 μL, 0.079 mmol) consumed the acetic acid and gave immediate production of PinBOAc and **206a**, which subsequently reacted with free alkyne resulting in >98% conversion to **206c** by ³¹P{¹H} NMR spectroscopy.

Treatment of 206c with pinacolborane. **206c** (15 mg, 0.027 mmol) was dissolved in C₆D₆ and treated with pinacolborane (20 μL, 0.14 mmol) and heated at 80 °C. After 5 h, the reaction showed ~50% conversion to **206a** by ³¹P{¹H} NMR spectroscopy, and ¹H NMR spectroscopy showed formation of **A**. However, further heating of the reaction mixture led to the formation of other products visible by ³¹P{¹H} NMR spectroscopy at 198.5 (s), 185.1 (s), 183.6 (s) ppm.

Treatment of 2a with 4-Me-C₆H₄-C≡C-Bpin (A). **206a** (14 mg, 0.031 mmol) was dissolved in C₆D₆ and treated with **A** (8 mg, 0.03 mmol) and heated at 80 °C. After

3 h, the sample was analyzed by $^{31}\text{P}\{^1\text{H}\}$ NMR spectroscopy, which showed 16% conversion to **206c**, pinacolborane was also visible by ^1H NMR spectroscopy. After 6 h at 80 °C, $^{31}\text{P}\{^1\text{H}\}$ NMR analysis showed 23% conversion to **206c** and 8% formation of a product at 185.1 ppm. Heating the sample for 4 days at 80 °C showed a distribution of 8% **206a**, 21% **206c**, and 71% accounting for compounds **206d** and **206e** (62% 185.1 ppm, and 9% 183.6 ppm) by $^{31}\text{P}\{^1\text{H}\}$ NMR integration. Analysis of the mixtures by ^1H NMR spectroscopy showed two new singlets presumed to be olefinic protons at 7.39 ppm and 6.42 ppm. After HCl (50 μL , 37%) was added to the J. Young tube, analysis by $^{31}\text{P}\{^1\text{H}\}$ NMR spectroscopy showed complete conversion of phosphorus-containing compounds to **206**. The volatiles were removed under vacuum and the products extracted with diethyl ether. The ether solution was dried over magnesium sulfate, decanted, and the volatiles were removed under vacuum. The resulting solid was dissolved in CDCl_3 , and ^1H NMR spectroscopy showed the presence of (Z)-(4-methylstyryl)Bpin.¹⁵³

Treatment of 209b with 4-ethynyltoluene. **209b** (36 mg, 0.079 mmol) was dissolved in C_6D_6 and treated with 4-ethynyltoluene (10 μL , 0.079 mmol). Within 30 minutes at room temperature, the reaction mixture reached an equilibrium mixture of 15:85 **209c:209b**, observed by $^{31}\text{P}\{^1\text{H}\}$ NMR spectroscopy. ^1H NMR spectroscopy showed that free acetic acid was present in the reaction mixture. **209b** has been shifted in the $^{31}\text{P}\{^1\text{H}\}$ NMR spectrum to 173.3 ppm due to an interaction with free acetic acid in solution. Further treatment with pinacolborane forms a black solution and decomposition of the palladium complex.

Treatment of 209b with acetic acid. **209b** (9 mg, 0.02 mmol) was dissolved in C₆D₆ and treated with acetic acid (1 μL, 0.02 mmol). Analysis of mixture by ³¹P{¹H} NMR spectroscopy showed a downfield shift of the signal for **209b** to 174.2 ppm.

Treatment of 209b with pinacolborane. **209b** (25 mg, 0.055 mmol) was dissolved in C₆D₆ and treated with pinacolborane (8 μL, 0.552 mmol). Upon mixing, the solution formed bubbles and quickly turned from clear to orange, red, and finally a dark brown. ¹H NMR spectroscopy showed the formation of dihydrogen, and **209b** was observed to be the major identifiable complex by ³¹P{¹H} NMR spectroscopy. The reaction mixture was filtered through silica and Celite and the volatiles were removed under vacuum to produce a brown solid, which contained **209b** and other unidentifiable decomposition products.

Treatment of (POCOP^{Et})PdCl (209) with NaHBET₃. **209** (30 mg, 0.070 mmol) was dissolved in C₆D₆ and treated with NaHBET₃ (77 μL, 1.0 M solution in toluene). The reaction mixture turned bright orange and quickly turned to red and finally brown with black precipitate. Analysis by ³¹P{¹H} NMR spectroscopy showed several products.

Treatment of 209c with pinacolborane. **209c** (27 mg, 0.053 mmol) was dissolved in C₆D₆ and treated with pinacolborane (8 μL, 0.055 mmol). After 1 day at room temperature, there was a 20% conversion of the pinacolborane to **A**, and the solution turned from a clear yellow to brown. Dihydrogen was also detected by ¹H NMR spectroscopy. ³¹P{¹H} NMR spectroscopy showed only the presence of **209c**.

Attempts to Hydrogenate Bis(pinacolato)diboron. Bis(pinacolato)diboron (86 mg, 0.34 mmol) was dissolved in C₆D₆ with **206a** (8 mg, 0.02 mmol) in a J. Young tube.

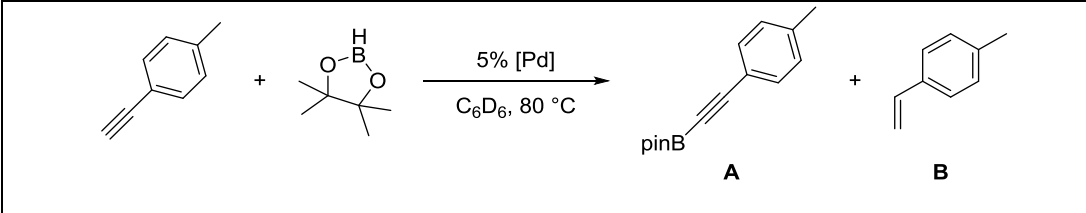
The headspace was removed, and filled with an atmosphere of H₂. The reaction was heated at 80 °C for 24 h with no apparent formation of pinacolborane.

Treatment of 206f with pinacolborane. 206f (24 mg, 0.051 mmol) in a J. Young tube was dissolved in C₆D₆ and treated with pinacolborane (15 μL, 0.10 mmol). 1,4-dioxane was added to the reaction mixture to act as an internal standard. The reaction mixtures were heated at 80 °C and monitored by ¹H and ³¹P{¹H} NMR spectroscopy for 96 h at approximately 24 h intervals. Only about a 10% conversion of pinacolborane to diborylacetylene was observed by ¹H NMR. ³¹P{¹H} NMR spectroscopy was used to show the conversion of 206f to the 206g and 206a.

2.4.4 Catalytic Reactions

General Procedure for Catalytic Reactions. A stock solution of the desired catalyst was used to deliver 0.017 mmol of catalyst in C₆D₆. 1,4-dioxane (100 μL of 0.035 mmol stock solution in C₆D₆), pinacolborane (49 μL, 0.34 mmol), and 4-ethynyltoluene (43 μL, 0.34 mmol) were added to the J. Young tube. The reaction was then heated at 80 °C until completion. In addition to the hydrogenation of 4-ethynyltoluene to 4-methylstyrene, there was trace production of 4-ethyltoluene in reactions where hydrogenation was significant.

Table II-5. Comprehensive list of all DHBTA reactions of 4-ethynyltoluene with different (POCOP)Pd catalysts and various additives.



#	[Pd]	A ^a	B ^{a,b}	Time	Additives
1	205a ^c	<5%	7%	1 d	X
2	207a ^d	0%	<5%	1 d	X
3	206a	40%	39%	1 d	X
4	206b	44%	49%	1 d	X
5	206c	45%	42%	1 d	X
6	206a	>95%	<5%	6 d	0.45 mmol Hg
7	206b	53%	43%	1 d	1.12 mmol Ga
8	206b	49%	51%	1 d	5.45 mmol Ga
9	206a	63%	35%	2 d	0.017 mmol PPh ₃
10	206a	87%	<5%	3 d	0.034 mmol PPh ₃
11	206b	85%	<5%	3 d	0.034 mmol PPh ₃
12	206b	88%	6%	3 d	0.034 mmol PMe ₃
13	206b	46%	<5%	4 d	0.034 mmol P(OMe) ₃
14	206b	45%	48%	1 d	0.034 mmol S'Pr ₂
15	206b	44%	43%	1 d	150 eq. PVPy
16	208a	2%	10%	3 d	X
17	209b	40%	37%	2 h	X
18	209c	36%	27%	2 h	X
19	209b	91%	<5%	5 h	0.45 mmol Hg
20	209b	85%	<5%	1 d	0.034 mmol PPh ₃
21	209b	64% (32%)	8%	1 d	0.034 mmol PMe ₃
22	209b	<5%	-	1 d	0.034 mmol P(OMe) ₃
23	210b	7%	13%	1 d	X
24	211b	49%	43%	1 d	X
25	212b	43%	48%	3 d	X
26	209b ^e	38%	<5%	1 d	0.45 mmol Hg

All reactions performed at 80 °C in C₆D₆ with 0.34 mmol alkyne, 0.34 mmol HBpin, and 5% catalyst loading. ^a Yields were determined by ¹H NMR integration versus an internal standard (1,4-Dioxane). ^b Reactions that produced significant amounts of **B** also showed trace production of 4-ethyltoluene. ^c Many intractable products observed containing olefinic resonances. ^d 5% (E)-(4-methylstyryl)Bpin was observed by ¹H NMR spectroscopy. ^e 1.7 μmol of **209b** used.

Catalysis with (POCOP^{iPr})NiH (205a). **205a** (0.017 mmol) was dissolved in C₆D₆ in a J. Young tube and 1,4-dioxane (100 μL of 0.035 mmol stock solution in C₆D₆), pinacolborane (49 μL, 0.34 mmol), and 4-ethynyltoluene (43 μL, 0.34 mmol) were added. The reaction was heated at 80 °C for 1 day. Analysis by ¹H NMR spectroscopy showed complete consumption of 4-ethynyltoluene and a complex mixture of compounds with olefinic signals. However, 83% of the pinacolborane was still present at the end of the reaction time.

Catalysis with (POCOP^{iPr})PtH (207a). **207a** (0.017 mmol) was dissolved in C₆D₆ in a J. Young tube and 1,4-dioxane (100 μL of 0.035 mmol stock solution in C₆D₆), pinacolborane (49 μL, 0.34 mmol), and 4-ethynyltoluene (43 μL, 0.34 mmol) were added. The reaction was heated at 80 °C for 1 day. Analysis by ³¹P{¹H} NMR spectroscopy showed that 5% of 4-ethynyltoluene was converted to (E)-(4-methylstyryl)Bpin, which was identified by ¹H NMR spectroscopy and comparison to the reported ¹H NMR spectral data.¹⁵⁴

NMR analysis of catalytic mixtures with 209b. Approximately 10 min. after mixing **209b** (5%, 0.017 mmol) with 4-ethynyltoluene, pinacolborane, and a dioxane standard, the sample was monitored by ¹H and ³¹P{¹H}NMR spectroscopy. PinBOAc and dihydrogen were visible by ¹H NMR spectroscopy, and **209c** was observed by ³¹P{¹H} NMR spectroscopy.

Elemental Mercury as an Additive. Mercury was capable of drastically inhibiting the hydrogenation reaction, and allowed for nearly complete conversion of the terminal alkyne to the alkynylboronate and hydrogen. Monitoring the reaction with

mercury (Entry 6) showed that after 1 day at 80 °C the reaction with mercury as an additive had undergone 37% conversion to the alkynylboronate. The control reaction (Entry 3) showed complete consumption of the terminal alkyne at this time with a 40% conversion to the alkynylboronate.

Turnover tests for 209b. A stock solution of the desired catalyst was used to deliver 0.0017 mmol of **209b** in C₆D₆. 1,4-dioxane (100 μL of 0.035 mmol stock solution in C₆D₆), pinacolborane (49 μL, 0.34 mmol), and 4-ethynyltoluene (43 μL, 0.34 mmol) were added to the J. Young tube along with the desired amount of mercury or triphenylphosphine. The reaction was then heated at 80 °C until completion.

Table II-6. Turnover test for **209b**.

Entry	A	4-Methylstyrene	Time	Additives
1	39%	41%	2 d	x
2	45%	43%	4 d	0.0017 mmol PPh ₃
3	37%	38%	5 d	0.0034 mmol PPh ₃
4	25%	24%	2 d	0.017 mmol PPh ₃
5	38%	2%	1 d	0.45 mmol Hg

When 0.0034 mmol of triphenylphosphine was used in entry 3, there was a significant inhibition of 4-methylstyrene production for the first 24 h, but hydrogenation did occur beyond the first day.

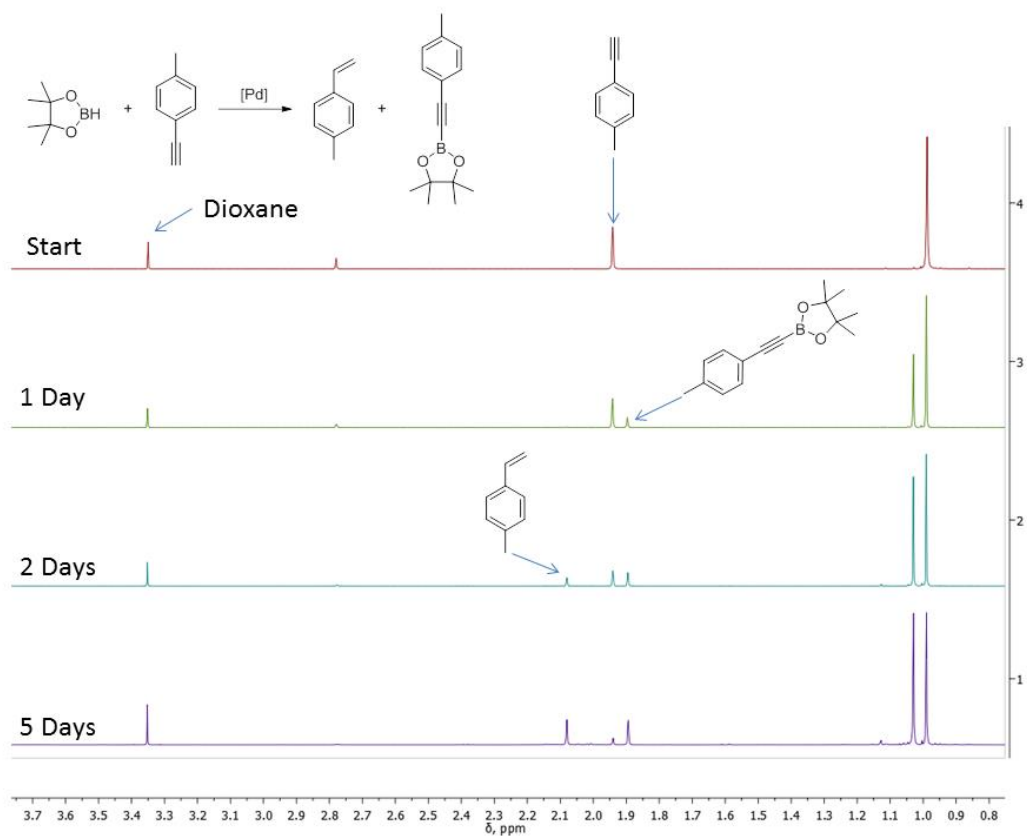


Figure II-3. Stacked ^1H NMR spectra from Table II-6, entry 3. 4-methylstyrene is not produced until after day 1.

209b Turnover test with mercury (Table II-6, Entry 5). When mercury was used as an additive the reaction was heated for 1 day at 80 °C. Palladium black had precipitated out on the sides of the J. Young tube, the solution was a pale clear yellow color, and no reactivity was seen after this point. 38% of the starting alkyne had been converted to **A** and there were trace amounts of 4-methylstyrene and trace amounts of 4-ethyltoluene. The catalyst was seen to perform about 76 turn overs.

Higher HBpin : Alkyne ratios. A stock solution of the desired catalyst was used to deliver 0.017 mmol of **209b** in C_6D_6 . 1,4-dioxane (100 μL of 0.035 mmol stock

solution in C₆D₆), pinacolborane (49 μL, 0.34 mmol), (54 μL, 0.37 mmol), (74 μL, 0.51 mmol), triphenylphosphine (0.034 mmol), and 4-ethynyltoluene (43 μL, 0.34 mmol) were added to the J. Young tube. The reaction was then heated at 80 °C until completion.

Table II-7. Higher HBpin:Alkyne Ratios

HBpin: alkyne	4 Hours @ 80 °C			1 Day @ 80 °C		
	SM	A	B	SM	A	B
1:1	7%	6%	84%	<2%	7%	88%
1.1 : 1	13%	6%	81%	3%	7%	92%
1.5 : 1	14%	5%	81%	5%	7%	87%

Control reaction with Pd(COD)Cl₂. In a J. Young tube, Pd(COD)Cl₂ (5 mg, 0.0175 mmol) was dissolved in C₆D₆ with 4-ethynyltoluene (43 μL, 0.34 mmol) and pinacolborane (49 μL, 0.34 mmol). The reaction mixture was heated for 24 h at 80 °C. Analysis by ¹H NMR spectroscopy showed no visible production of **A** or 4-methylstyrene.

Control reactions with Pd₂(DBA)₃ and triphenylphosphine. In a J. Young tube, Pd₂(DBA)₃ (8 mg, 0.0087 mmol) was treated with PPh₃ (9 mg, 0.034 mmol), 4-ethynyltoluene (43 μL, 0.34 mmol) and pinacolborane (49 μL, 0.34 mmol) in C₆D₆. The reaction mixture was heated for 24 h at 80 °C. Analysis of the reaction mixture by ¹H NMR spectroscopy shows >90% of the starting alkyne remains, and there was no visible production of **A**.

Control reaction with Pd₂(DBA)₃. In a J. Young tube, Pd₂(DBA)₃ (8 mg, 0.0087 mmol) was dissolved in C₆D₆ and treated with 4-ethynyltoluene (43 μL, 0.34 mmol) and pinacolborane (49 μL, 0.34 mmol). The reaction mixture was heated for 24 h

at 80 °C. Analysis of the reaction mixture by ^1H NMR spectroscopy shows that >90% of the pinacolborane remains. Broad signals at around 7.00 ppm and 2.00 ppm suggest that the alkyne has been converted to polymeric and oligomeric products.

2.4.5 Characterization of Alkynylboronates

Alkynylboronates were characterized *in situ* by ^1H NMR spectroscopy and compared to literature data.³⁷

4-Me-C₆H₄-C≡C-Bpin (A): ^1H NMR (500 MHz, C₆D₆): δ 7.34 (d, $J = 7.5$ Hz, 2H), 6.65 (d, $J = 7.5$ Hz, 2H), 1.87 (s, 3H, Ar-CH₃), 1.02 (s, 12H, -CH₃ on Bpin).

n-Bu-C≡C-Bpin: ^1H NMR (500 MHz, C₆D₆): δ 1.95 (t, $J = 7$ Hz, 2H), 1.21 (m, 4H), 0.99 (s, 12H, -CH₃ on Bpin), 0.66 (t, $J = 7$ Hz, 3H).

Me₃Si-C≡C-Bpin: ^1H NMR (500 MHz, C₆D₆): δ 0.94 (s, 12H, -CH₃ on Bpin), 0.06 (s, 9H, -CH₃ on Me₃Si).

Me₃SiO-CH₂-C≡C-Bpin: ^1H NMR (500 MHz, C₆D₆): δ 4.07 (s, 2H, O-CH₂-C≡C), 0.97 (s, 12H, -CH₃), 0.07 (s, 9H, -CH₃ on Me₃Si). ^{11}B NMR (128 MHz, C₆D₆): δ 24.0.

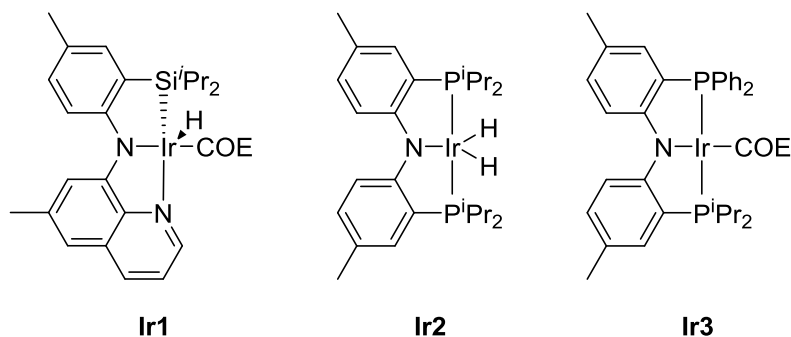
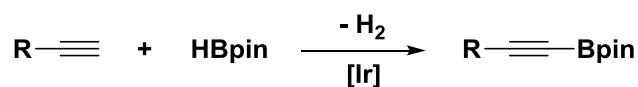
PhO-CH₂-C≡C-Bpin: Selected data for PhO-CH₂-C≡C-Bpin: ^1H NMR (500 MHz, C₆D₆): δ 4.22 (s, 2H, O-CH₂-C≡C), 0.93 (s, 12H, -CH₃ on Bpin); ^{11}B NMR (128 MHz, C₆D₆): δ 23.7. Selected NMR data for PhO-CH₂-C≡CH: ^1H NMR (500 MHz, C₆D₆): δ 4.19 (d, $J = 2$ Hz, 2H, O-CH₂-C≡C).

Me₃Si-O-Bpin: ^1H NMR (500 MHz, C₆D₆): δ 1.04 (s, 12H, -CH₃ on Bpin), 0.19 (s, 9H, -CH₃ on Me₃Si); ^{11}B NMR (128 MHz, C₆D₆): δ 20.8.¹⁵⁵

CHAPTER III
DEHYDROGENATIVE BORYLATION OF 1,6-ENYNES AND 1,6-DIYNES AND
SUBSEQUENT REDUCTIVE CYCLIZATION

3.1 Introduction

Organoboronic esters have proven to be versatile building blocks that can undergo a number of transformations.¹¹ Most notably they are used as substrates in Suzuki coupling,^{8,156} but numerous transformations can be performed with these compounds to access a number of functionalities.²³ Due to the versatility of organoboronic esters, new methodologies for incorporating C-B bonds into molecules are of great interest. Our group has been focused on developing the dehydrogenative borylation of terminal alkynes (DHBTA) using pincer-ligated iridium^{37,56} and palladium catalysts.⁵⁷ Other catalysts for the dehydrogenative borylation of terminal alkynes have recently been reported by Tsuchimoto⁵⁸ and Bertrand.⁶⁰ Our second generation Ir catalysts **Ir2** and **Ir3** (Scheme III-1) have shown remarkable reactivity and substrate scope, and **Ir3** has outperformed our first generation DHBTA catalyst **Ir1**. These complexes have allowed us to explore more sophisticated substrates such as 1,6-enynes and 1,6-diynes.

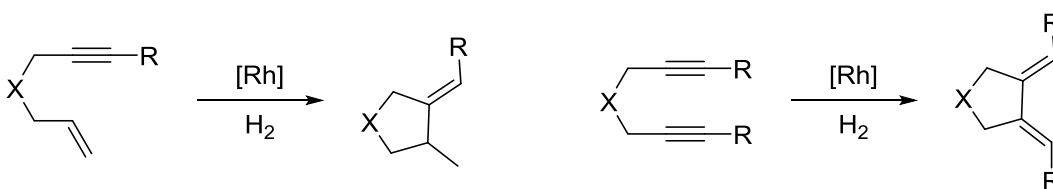


Scheme III-1. DHBTA and Ir DHBTA catalysts

The use of 1,6-ynes and 1,6-diynes in cyclization reactions is a well-developed area of chemistry,¹⁵⁷ but there are only a few reports of reactions using the borylated substrates. The benefit of using alkynylboronates in cyclization reactions is that the resulting cyclic compound will have a versatile C-B linkage preinstalled. This benefit has prompted other chemists to pursue cyclizations with alkynylboronates. For instance, Renaud et al. showed that borylated 1,6-enynes could undergo enyne metathesis using ruthenium catalysts.¹¹³ The Gandon group has also conducted cobalt-mediated [2+2+2] cycloadditions with alkynylboronates and borylated α,ω -diynes.^{104,105} Borylated monoynes however, are more frequently used in cyclization reactions.⁴³ The Gandon group used rhodium-catalyzed [2+2+2] cycloadditions of alkynylboronates followed by selective Suzuki coupling in order to synthesize a series of oligoaryls.¹⁰⁷ The Harrity group has also used numerous cyclization reactions with alkynylboronates to synthesize borylated cyclic compounds such as pyrazoles,¹¹⁶ pyridones,^{118,158} arenes,¹¹⁹ and a

number of other cyclic compounds.¹¹⁴ Recently alkynylboronates have also been used as substrates for regioselective Pauson-Khand reactions.¹²¹ The alkynylboron reagents used in these reactions were all synthesized via the use of a stoichiometric organometallic base and anhydrous acidic work up developed by Brown.⁴⁵ For a more in depth discussion about cyclization reactions with alkynylboronates refer to section 1.3.3.

For the work described in this chapter, we were inspired by the work of the Krische group¹⁵⁹ to investigate the use of cationic rhodium catalysts to perform reductive cyclization with borylated 1,6-enynes and 1,6-diynes. This reaction uses dihydrogen as a terminal reductant to form a five-membered exocyclic alkene from a 1,6-enyne or a five-membered exocyclic diene from a 1,6-diyne (Scheme III-2). Reductive cyclization is a useful way of synthesizing five-membered rings, and has been used in the total synthesis of daphnane diterpene orthoesters¹⁶⁰ and lucentamycin A.¹⁶¹

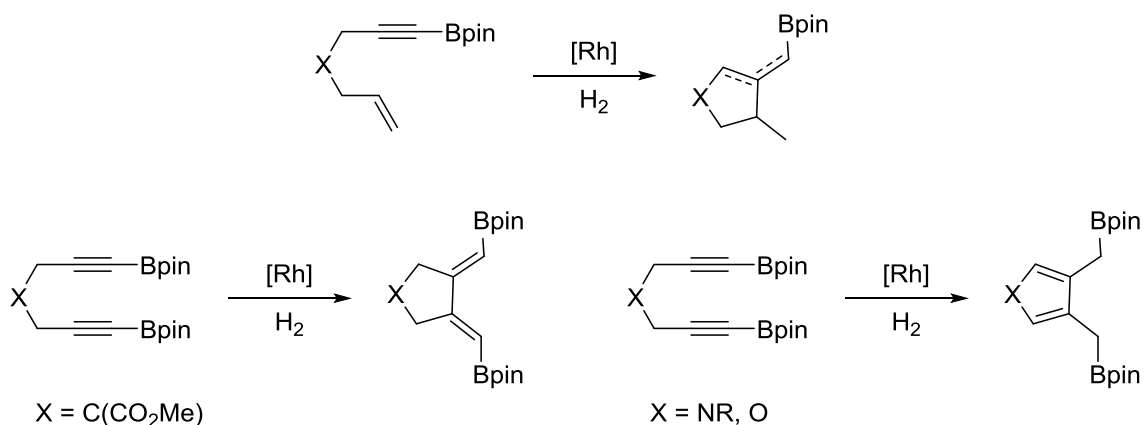


Scheme III-2. Rhodium-catalyzed reductive cyclization of 1,6-enynes and 1,6-diynes as first described by the Krische group.

The benefit of extending this reaction to use alkynylboronates is that the resulting five-membered ring will form with a C_{sp2}-B preinstalled and ready for further functionalization. Alternatively, boranes can be used as a reductant in cyclization reactions with 1,6-enynes and 1,6-diynes to synthesize cyclic compounds with C-B

bonds. Enynes have been shown to undergo borylative cyclization reactions such as the palladium-catalyzed borylative cyclization to exocyclic alkenylboronates,¹⁶² or the rhodium catalyzed hydroborylation-cyclization reactions to form exocyclic alkenylboronates.¹⁶³ Recently the Lu group has also used cobalt catalysts to perform hydroboration/cyclization of 1,6-enynes.¹⁶⁴ In addition to using dihydrogen or boranes as reductants, other reducing agents such as silanes¹⁶⁵ and aldehydes¹⁶⁶ have been used.

Herein, we describe a method of borylating 1,6-enynes and 1,6-diynes through DHBTA, and using these products in reductive cyclization with cationic rhodium complexes (Scheme III-3). In our experience, Borylated 1,6-enynes would undergo reductive cyclization and then experience an olefin isomerization, which usually resulted in a mixture of endocyclic alkenes and exocyclic alkenes. Borylated 1,6-diynes could also undergo a similar isomerization, and borylated 1,6-diynes with amine linkers were shown to form 3,4-bis(methylpinacolborane)-substituted pyrroles. By combining DHBTA with reductive cyclization, we have developed an atom economical method of developing pyrroles with C-B bonds preinstalled. Pyrroles in general are valuable target molecules due to their presence in pharmaceuticals,¹⁶⁷ their ubiquity in all branches of chemistry, and the attention that is devoted to developing new synthetic routes.^{168,169}



Scheme III-3. Reductive cyclization with borylated 1,6-enynes and 1,6-diynes.

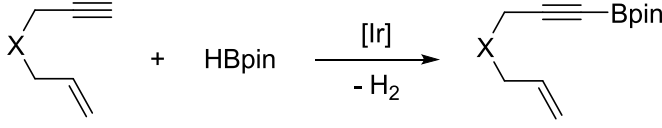
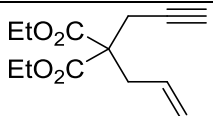
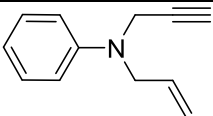
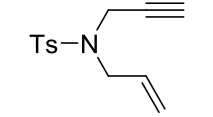
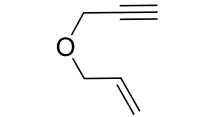
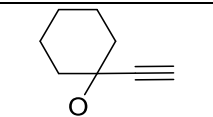
3.2 Results and Discussion

3.2.1 DHBTA of 1,6-Enynes

We have previously shown that **Ir3** is capable of borylating *N*-allyl-*N*-propargyl toluenesulfonamide, and dimethyl 2-allyl-2-propargylmalonate at 0.1% catalyst loading using 2 eq. of pinacolborane (HBpin).⁵⁶ We have expanded this substrate scope by investigating 1,6-enynes tethered by amines and ethers and investigated their reactivity with 1.1 eq of HBpin. **Ir3** performed well with all of the substrates using 0.1 mol% catalyst loading. Diethyl 2-allyl-2-propargylmalonate (**301**) could be borylated within 1 h at 60 °C using 1.1 eq. of HBpin (entry 1, Table III-1); however, substrates containing heteroatoms at the propargylic position required slightly more forcing conditions.

Aniline-tethered **302** (entry 2-4) and toluenesulfonamide-tethered **303** (entries 5 and 6) required reaction times longer than 1 h. It is also noticeable that these substrates experienced even longer reaction times with lower yields when only 1.1 eq. of HBpin

Table III-1. DHBTA of 1,6-enynes.

						
301 - 305			301B - 305B			
Entry	Substrate	Catalyst	Eq. HBpin	Time	Temp	40nB N = 1-5
1	 301	0.1% Ir3	1.1	1 h	60 °C	95% (81%*)
2	 302	0.1% Ir3	1.1	24 h	60 °C	83%
3		0.1% Ir3	2.0	4 h	60 °C	94% (>94%*)
4		1.0% Ir2	2.0	3 h	RT	96%
5	 303	0.1% Ir3	2.0	5 h	60 °C	(82%)
6		0.1% Ir3	1.1	5 h	60 °C	(66%)
7	 304	0.1 % Ir3	2.0	24 h	60 °C	93%
8		1.0% Ir2	2.0	3.5 h	RT	94%
9		0.1% Ir2	2.0	5 h	60 °C	89% (>89%*)
10		0.1% Ir2	1.1	7 h	60 °C	81%
11	 305	0.1% Ir3	2.0	1h	60 °C	97%
12		0.1% Ir3	1.1	1 h	60 °C	93%(>93%*)

* Product was isolated as an oil and judged to be >95% pure by ¹H NMR spectroscopy. Isolated yields are in parenthesis.

was used. Allyl propargyl ether (**304**) experienced longer reaction times of 24 h in catalytic reactions with 0.1 mol% of **Ir3** (entry 7), and was more efficiently borylated with catalyst **Ir2** (entries 7-10). Again, decreased yields and longer reaction times were observed using 1.1 eq. of HBpin (entry 10). Similar to our previous results borylating

propargyl ethers,³⁷ crowding the propargylic ether with alkyl substituents allowed for the reaction to proceed faster and with higher yields than the unsubstituted ether. This was shown as **305** could be borylated in 1 h at 60 °C with 0.1 mol% of **Ir3** (entry 11), and was effectively borylated using 1.1 eq. of HBpin (entries 12). All of the borylated enynes except for **303B** were oils. Due to the instability of alkynylboronates to silica gel, column chromatography was not an option for purification. However, due to the low catalyst loading and high yielding nature of the reactions, the alkynylboronates were isolated with no further purification after removing the volatiles from the reaction mixture and filtering through Celite to remove insoluble material. The products were observed to be >95% pure by ¹H NMR spectroscopy and were used in subsequent reactions. Preparative scale DHBTA was performed on a 5.0 mmol scale.

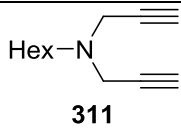
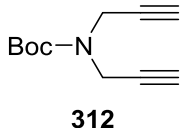
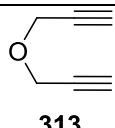
3.2.2 DHBTA of 1,6-Diynes

In our previous work with Ir DHBTA catalysts we have had success borylating 1,7-octadiyne.³⁷ In this work, we have attempted to borylate several 1,6-diynes tethered by various groups such as a malonate, ether, amines, carbamate, and toluenesulfonamide. Table III-2 shows our results for the borylation of various 1,6-diynes.

Table III-2. DHBTA of 1,6-diynes

R = H = 306 - 313 R = Me = 308Me, 309Me			R = H = 306B - 313B R = Me = 308MeB, 309MeB			306B₂ - 313B₂		
#	Substrate	Catalyst	Eq. HBpin	Time	Temp	% Conv.	B	B ₂
1	 306	0.1% Ir3	4.0	1 h	60 °C	>95%	0%	>95%
2		0.1% Ir3	2.2	1 h	60 °C	>95%	0%	>95% (81%)
3	 307	0.1% Ir3	4.0	1 h	60 °C	>95%	0%	>95%
4		0.1% Ir3	2.2	1 h	60 °C	>95%	0%	>95% (83%)
5	 308	0.1% Ir3	4.0	6 h	60 °C	15%	10%	<5%
6		1.0% Ir3	4.0	24 h	RT	>95%	0%	18%
7		1.0% Ir1	4.0	0.5 h	RT	16%	10%	6%
8		1.0% Ir1	4.0	9 h	60 °C	66%	16%	7%
9		1.0% Ir2	4.0	1 h	60 °C	>95%	0%	46% (20%)
10		1.0% Ir2	4.0	20 h	RT	>95%	0%	48%
11	 308Me	1.0% Ir3	4.0	1 h	RT	>95%	78% (65%)	N/A
12		0.1% Ir3	4.0	43 h	60 °C	91%	51%	N/A
13		1.0% Ir3	4.0	1 h	60 °C	>95%	60%	N/A
14	 309	0.1% Ir3	4.0	6 h	60 °C	>95%	0%	78% (70%)
15	 309Me	0.1% Ir3	4.0	26 h	60 °C	26%	16%	5%
16		1.0% Ir3	4.0	1 h	60 °C	>95%	0%	92% (>92%) #
17	 310	0.1% Ir3	4.0	51 h	60 °C	>95%	0%	86%
18		1.0% Ir3	4.0	1 h	60 C	>95%	0%	89% (73%)

Table III-2. Continued

#	Substrate	Catalyst	Eq. HBpin	Time	Temp	% Conv.	B	B ₂
19	 311	0.1% Ir3	4.0	29 h	60 °C	<5%	0%	0%
20		1.0% Ir3	4.0	1 h	60 °C	>95%	0%	92% (78%)
21	 312	0.1% Ir3	4.0	20h	60 °C	49%	23%	5%
22		1.0% Ir3	4.0	1 h	60 °C	>95%	0%	62% (54%)
23	 313	0.1% Ir3	4.0	96 h	60 °C	>95%	0%	75%
24		1.0% Ir3	4.0	48 h	RT	>95%	0%	81% (45%)
25		1.0% Ir3	4.0	3 h	60 °C	88%	23%	64%
26		1.0% Ir3	4.0	21 h	60 °C	86%	23%	29%
27		0.1% Ir2	4.0	3.5 h	60 °C	68%*	46%	11%
28		1.0% Ir2	4.0	21 h	60 °C	92%	14%	28%
*no further conversion to alkynylboronate was observed. # Product was isolated as an oil of >90% purity with no further purification.								

Dimethyl dipropargyl malonate (**306**) was very effectively borylated under the traditional procedure of 2 eq. of HBpin for every unit of terminal alkyne at 0.1 mol% catalyst loading (entry 1, Table III-2). It also proved to be a well behaved substrate when only 1.1 eq of HBpin per alkynyl C-H was used, and **306B₂** could be isolated in an 81% yield (entry 2). 1,6-Heptadiyne (**307**) could also undergo >95% conversion to **307B₂** with either 2 or 1.1 eq of HBpin per alkynyl C-H at the same conditions and could be isolated in an 83% yield (Entry 3 and 4).

Similar to the enynes, substrates with heteroatoms at the propargylic site required slightly more forcing conditions. DHBTA of **308** did not proceed as smoothly as **303**, it's 1,6-enyne counterpart. Using **Ir3** at a 0.1 mol% catalyst loading and heating the

reaction at 60 °C for 6 h (entry 5) gave poor conversion from **308**, and only trace production of **308B₂** was observed. Performing the reaction with 1.0 mol% catalyst loading at room temperature (Entry 6) consumed most of **308** but gave poor yields of the **308B₂**. **Ir1** was also tested as a catalyst, but was shown to perform worse than the (PNP)Ir catalysts (Entries 7 and 8). The best results were obtained using 1.0 mol% **Ir2** as a catalyst, which provided 46% conversion to **308B₂** with a mixture of other unidentified products (entries 9 and 10). Despite this mixture of products, pure **308B₂** could be isolated in a 20% yield through recrystallization from dichloromethane and pentane.

Replacing an acetylenic proton with a methyl by using **308Me** gave markedly different results. Using a 1.0 mol% catalyst loading of **Ir3** for 1 h at room temperature gave a 78% conversion to the **308MeB**, which could be isolated through recrystallization in a 65% yield (Entry 11). **308Me** gave lower yields of the alkynylboronate in reactions that were performed at 60 °C (entries 12 and 13). We were also able to efficiently diborylate **309** using 0.1 mol% catalyst loading of **Ir3** at 60 °C to obtain a 70% recrystallized yield of **309B₂** (entry 14). **309Me** was also tested as a substrate, and low yields of **309MeB** were obtained using 0.1 mol% **Ir3** (entry 15), but **309Me** was efficiently borylated within an hour upon increasing the catalyst loading to 1.0 mol% (entry 16). This could be due to impurities in the substrate that shut down the catalyst when it is present in such small concentrations.

With the notion that different types of nitrogenous propargyl linkers in 1,6-diynes had a major effect on their suitability as DHBTA substrates, we sought to investigate different bis(propargyl) amines. *N,N*-dipropargyl benzylamine (**310**) could be borylated

with 0.1 mol% of **Ir3**, but the reaction required 51 h at 60 °C (entry 17). The substrate could be more efficiently borylated within 1 h when the catalyst loading was increased to 1.0 mol%, and **310B₂** could be isolated in a 73% yield (entry 18). This extended reaction time could result from an increased donor-ability of the benzylamine or from trace impurities that disrupt the catalyst at low concentrations. We expect a similar reasons for why *N,N*-dipropargyl hexylamine (**311**) showed no reactivity when treated with 0.1 mol% of **Ir3** over a period of 29 h (entry 19). Once again, the substrate could be borylated within 1 h at 60 °C when the catalyst loading was increased to 1.0 mol%, and **311B₂** could be isolated in a 78% yield (entry 20).

Tert-butyl *N,N*-dipropargyl carbamate (**312**) was investigated to see if Boc-protected amines could withstand DHBTA. The borylation of this substrate proved to be more difficult than the electron-rich amines, and we witnessed low yields and long reaction times similar to reactions with **309**. At 0.1 mol% of **Ir3**, the reaction only gave trace production of **312B₂** (entry 21). Upon increasing the catalyst loading to 1.0 mol%, the **12** could be consumed in 1 h at 60 °C, but there was only a 62% conversion to **312B₂** (entry 22). Luckily, **312B₂** was easily recrystallized from cold pentane in an isolated yield of 54%.

Ether tethered diynes, much like other propargyl ether substrates, were troublesome for our (PNP)Ir catalysts. Bispropargyl ether (**313**) could be diborylated with appreciable conversions to **313B₂** using **Ir3** at 0.1 mol% catalyst loading, but the reaction required 96 h to reach 75% conversion to **313B₂** (Entry 23). The reaction time could be cut in half by using 1.0 mol% **Ir3** to achieve a conversion of 81% to **313B₂**

(Entry 24). These conditions were used to obtain **313B₂** in a 45% yield via recrystallization from cold pentane. Using a 1.0 mol% catalyst loading of **Ir3** at 60 °C eventually lead to a decomposition of the **313B₂** that had formed during the course of the reaction (Entry 25 and 26). Unlike the case of allyl propargyl ether (**304**), catalyst **Ir2** did not perform better than **Ir3** (entries 27 and 28).

In general, it was observed that the central linker of the 1,6-diyne chain will dictate whether the substrate will undergo facile DHBTA. Alkane chains present the easiest substrates to borylate (substrates **306** and **307**), while amines and ethers are more difficult. In the case of a toluenesulfanamide linker, it should be noted that **308**, the substrate with two terminal Csp-H bonds, performed much worse than the other toluenesulfonamides (**303** and **308Me**). The toluenesulfonamides with only one Csp-H bond could undergo DHBTA much more cleanly and, in the case of the enyne, with higher turn overs.

3.2.3 Reductive Cyclization of 1,6-Enynes

Due to the ease of isolation and purification through recrystallization, **303B**⁵⁶ was chosen as an initial substrate to screen conditions for the reductive cyclization of borylated 1,6-enynes. Traditionally, these reactions are preformed using a cationic rhodium precatalyst such as Rh(COD)₂OTf or Rh(COD)₂BF₄ with a bisphosphine ligand.¹⁵⁹ We favored racemic BINAP as a ligand, and due to its limited solubility we prepared (BINAP)Rh(COD)OTf and (BINAP)Rh(COD)BF₄ as precatalysts that could be conveniently kept in stock solutions.

Table III-3. Reductive cyclization of **303B**.

Entry	Catalyst	Volume	303Bc-exo	303Bc-endo
1	3% (BINAP)Rh(COD)OTf	1.25 mL	81%	7%
2	3% (BINAP)Rh(COD)BF ₄	1.25 mL	9%	75%
3	5% (BINAP)Rh(COD)OTf	1.25 mL	42%	37%
4	5% (BINAP)Rh(COD)BF ₄	1.25 mL	60%	30%
5	5% (BINAP)Rh(COD)OTf	5 mL	51%	32%
6	5% (BINAP)Rh(COD)BF ₄	5 mL	64%	19%
7	5% (BINAP)Rh(COD)BF ₄	0.50 mL ^a	28%	32%
8	3% (BINAP)Rh(COD)OTf	0.50 mL ^a	9%	41%
9	3% (BINAP)Rh(COD)BF ₄	0.50 mL ^a	7%	59%
10	5% Rh(COD) ₂ OTf	1.25 mL	-	- ^b
11	5% dippf / 5% Rh(COD) ₂ OTf	1.25 mL	0%	0% ^c
12	5% dppf / 5% Rh(COD) ₂ OTf	1.25 mL	-	- ^d
13	5% dppp / 5% Rh(COD)OTf	1.25 mL	7%	0% ^e

^a Intermolecular [2+2+2] product formed. ^b 90% Starting Material. ^c >98% conversion to *N*-propyl-*N*-(3-pinacolborylpropyl) toluenesulfonamide (**303B-H₆**), isolated in 60% yield. ^d 62% conversion to **303B-H₆**. ^e 65% Starting material, 24% bisolefin.

Using 3 mol% (BINAP)Rh(COD)OTf in 1.25 mL of CH₂Cl₂ and an atmosphere of dihydrogen for 2 h, gave 81% conversion to the expected exocyclic alkene, **303Bc-exo** (entry 1). However, when 3% (BINAP)Rh(COD)BF₄ was used under the same conditions, the exocyclic alkene was a minor product and another similar product was observed in 75% yield (Entry 2). This product was later determined to be a structural isomer of the exocyclic alkene, where the olefin had undergone a 1,3-hydride shift to

form **303Bc-endo**. **303Bc-endo** can be distinguished from **303Bc-exo** by ^1H NMR spectroscopy. The most characteristic difference in the molecules' ^1H NMR spectra are the signals for the $\text{C}_{\text{sp}^2}\text{-H}$ resonance. In the **303Bc-exo**, this proton is farther upfield (5.18 ppm) since it is removed from the electron-withdrawing toluenesulfonamide, while **303Bc-endo** has an olefinic proton adjacent to nitrogen, which forces the resonance more downfield (6.11 ppm). The diastereotopic CH_2 resonances are also much more upfield in the **303Bc-endo** (1.59 and 1.43 ppm) compared to the **303Bc-exo**'s pair of diastereotopic protons in the pyrrolidine ring (4.16 and 3.97 ppm). Comparing the $^{11}\text{B}\{^1\text{H}\}$ NMR spectra of the two molecules also distinguishes **303Bc-exo** as an alkenylboronate (29.3 ppm) and the **303Bc-endo** as an alkylboronate (32.5 ppm).*

From these results, we tried to optimize the catalytic system into two pathways that would either favor the endocyclic or exocyclic alkene for preparative scale synthesis. However, selectivity was not translated upon scaling the reaction up to 1.0 mmol using either rhodium catalyst. We set out on determining what was responsible for the selectivity between the two isomers. We discovered that selectivity was hard to reproduce in the reductive cyclization of **303B**. For instance, 5% catalyst loading of (BINAP)Rh(COD)OTf or (BINAP)Rh(COD)BF₄ with a reaction volume of 1.25 mL, did not reproduce the selectivity observed at a 3 mol% catalyst loading (Entries 3 and 4). Performing the reactions at 5 mol% catalyst loading in 5 mL of solvent (Entries 5 and 6) gave a similar product distribution as entries 3 and 4. Entries 7, 8, and 9 were performed

* A ^1H - ^{13}C HSQC NMR spectrum was also obtained to help determine the structure of **303Bc-endo**.

in 0.5 mL of solvent and showed a decreased production of either reductive cyclization product and the formation of a [2+2+2] cyclization product (discussed below).

We observed that a supporting ligand is necessary because 5 mol% Rh(COD)₂OTf alone under an atmosphere of H₂ did not produce any reductive cyclization products and 90% of the starting material was still observable (entry 10). 5 mol% bis(diisopropylphosphino)ferrocene with 5 mol% Rh(COD)OTf gave full conversion to the fully hydrogenated product, which was isolated in a 60% yield (entry 11). Using bis(diphenylphosphino)ferrocene as a ligand provided a lower conversion to the fully hydrogenated product (entry 12), and bis(diphenylphosphino)propane yielded a mixture of products including a trace amount of the exocyclic alkene, a diene, and starting material (entry 13).

In most of the reports about reductive cyclizations^{159,161,163-166,170-177} and cycloisomerizations^{178,179} of 1,6-enynes, 2,3-unsaturated heterocycles have not been observed and exocyclic alkenes are reliably produced. However, (NHC)Pt complexes have been reported to catalyze the reductive cyclization of 1,6-enynes to yield 3,4-unsaturated five-membered cyclic compounds.¹⁸⁰ Olefin rearrangement has been observed in Rh-catalyzed enyne cycloisomerizations previously such as the isomerization from a 1,4-diene to a conjugated 1,3-diene observed by the Zhang group; however both isomers were exocyclic alkenes.¹⁸¹ This isomerization was also not observed when the Lin group used (BINAP)Rh-based metal organic frameworks for the same reaction.¹⁷⁰

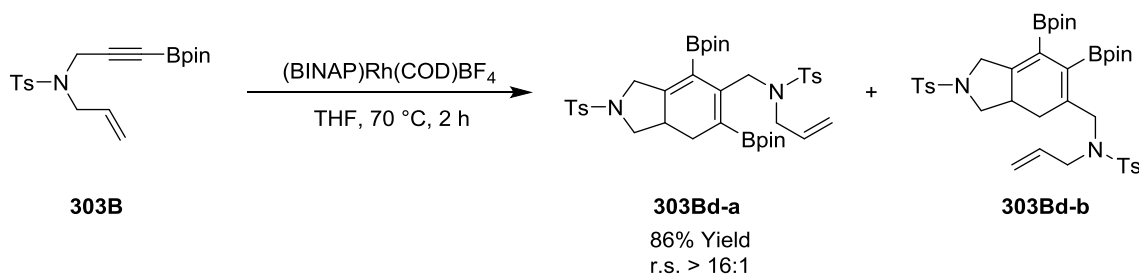
There have been reports of 1,6-enynes undergoing a series of Sonagashira, Heck, and cyclization reactions to form five-membered exocyclic dienes that proceed to isomerize to form furans at 80 °C in the presence of palladium catalysts.¹⁸² Furans have also been selectively formed from allyl propargyl ethers during cycloisomerization reactions using bisphosphine-ligated cationic rhodium catalysts at 100 °C.¹⁸³ In the study of [2+2+2] cycloaddition between toluenesulfonamide-linked 1,6-enynes containing monosubstituted olefins and electron-deficient ketones at 80 °C, the Tanaka group observed the formation of pyrroles as side products to the desired dihydropyran product.¹⁸⁴ While these isomerizations are similar to what we observe in our reactions (exocyclic alkene rearranging to an endocyclic alkene) all of the reactions cited here require heat and form aromatic products. The formation of **303Bc-endo** in our reactions occurs at room temperature and the product is not stabilized by aromaticity.

We were interested in whether this isomerization was occurring during catalysis or was occurring after the reaction had finished. Pure **303Bc-exo** was isolated on a 0.5 mmol scale using 3 mol% (BINAP)Rh(COD)OTf followed by column chromatography. When **303Bc-exo** was treated with 3 mol% (BINAP)Rh(COD)OTf and thermolized at 75 °C for 1 h, analysis by ¹¹B{¹H} NMR spectroscopy showed >90% conversion to **303Bc-endo**. However, heat and the rhodium catalyst were necessary for the isomerization to occur. When **303Bc-exo** was treated with 5 mol% of (BINAP)Rh(COD)OTf in CD₂Cl₂ for 20 h at room temperature, no isomerization was observed. Even vigorously stirring the reaction mixture under an atmosphere of H₂ in a flask led to no isomerization to

303Bc-endo after 24 hours at room temperature. Thermolysis of **303Bc-exo** at 75 °C with no rhodium catalyst in dichloroethane showed no isomerization to **303Bc-endo**.

We tried to apply thermally induced isomerization in order to selectively synthesize **303Bc-endo**. In this reaction **303B** was treated with 3 mol% (BINAP)Rh(COD)OTf and stirred under 1 atm of H₂ for 2 hours. At this time, the reaction vessel was moved to a 70 °C oil bath and heated for 1 h. Upon removing the volatiles, it was discovered that **303Bc-exo** was the dominant product and **303Bc-endo** was barely present.

In reactions with higher concentrations of enyne, thus a lower relative concentration of H₂ in solution (entries 7-9), we discovered that a [2+2+2] cyclization reaction to form a tetrahydroindene structure was favored. By performing the reaction in THF at 70 °C in the absence of dihydrogen, we were able to selectively form the [2+2+2] product (Scheme III-4). This reaction exhibited a high degree of regioselectivity, furnishing isomers **303Bd-a** and **303Bd-b** in at least a 16:1 ratio. Isomer **303Bd-a** could be isolated in an 86% recrystallized yield, and was further characterized by ¹H-¹³C two dimensional NMR spectroscopy to verify the assignment. We hypothesized that isomer **303Bd-a** is preferred due to the steric bulk of the pinacolboryl group. In other carbocyclizations of 1,6-enynes and asymmetric alkynes, regioselectivity has been observed with alkynes possessing bulky substituents, and there is a tendency for products to be formed with the bulkier substituents at 1,3 positions instead of 1,2 positions of a six-membered ring.¹⁸⁵



Scheme III-4. Rh-catalyzed [2+2+2] cycloaddition of **303B**.

In order to study the exocyclic versus endocyclic alkene product distributions resulting from the reductive cyclization of borylated 1,6-enynes we decided to investigate other substrates. **301B** gave good conversion to the exocyclic alkene isomer, **301Bc-exo**, whether (BINAP)Rh(COD)OTf or (BINAP)Rh(COD)BF₄ was used (entries 1 and 2,). This selectivity is also translated when the reaction is scaled up to a 2 mmol scale and the product could be isolated in a 67% yield.

302B did not fit the same patterns observed for the previous substrates. Using 3% (BINAP)Rh(COD)OTf as a catalyst, **302B** gave an 81% yield of the endocyclic alkene, **302Bc-endo** (entry 3). Attempts to scale up this reaction to isolate **302Bc-endo** led to a mixture of intractable products. However, 3% (BINAP)Rh(COD)BF₄ gave a mixture of **302Bc-exo** and **302Bc-endo** (entry 4). Using 3% (BINAP)Rh(COD)OTf with 2 eq. of 2,6-lutidine shifted the preference to about a 1:1 distribution of **302Bc-exo** and **302Bc-endo**, but 18% starting material was still observed (entry 5). We also investigated using (BINAP)Rh(COD)BARF₂₀ as a catalyst, which converted 50% of the starting material to a 1:1 product distribution of **302Bc-exo** and **302Bc-endo** (entry 6). However, performing the reaction in THF lead to a 69% yield of the **302Bc-endo** (entry 7).

Table III-4. Reductive cyclization of various borylated 1,6-enynes.

301B - 405B		301 - 305Bc-exo	301 - 305Bc-endo		
#	Substrate	Catalyst / Additive/ Time	Bc-exo	Bc-endo	
1	 301B	3% (BINAP)Rh(COD)OTf	95% (67%)	0%	
2		3% (BINAP)Rh(COD)BF ₄	86%	0%	
3	 302B	3% (BINAP)Rh(COD)OTf		81%	
4		3% (BINAP)Rh(COD)BF ₄	22%	59%	
5		3% (BINAP)Rh(COD)OTf 0.2 mmol (2,6-lutidine)	32% ^c	37%	
6		3% (BINAP)Rh(COD)BArF ₂₀	26% ^d	27%	
7		3% (BINAP)Rh(COD)BArF ₂₀ ^e		69%	
8	 304B	3% (BINAP)Rh(COD)OTf	2% ^a	11%	
9		3% (BIPHEP)/3% Rh(COD) ₂ OTf		57%	
10		3% (BIPHEP)/3% Rh(COD) ₂ BF ₄		59%	
11		5% (BIPHEP)/Rh(COD) ₂ BF ₄		56%	
12		3% (BIPHEP)/Rh(COD) ₂ BF ₄ 0.2 mmol (2,6-lutidine)	2h	38% ^b	7%
13		3% (BIPHEP)/Rh(COD) ₂ BF ₄ 0.2 mmol (2,6-lutidine)	8h	42%	22%
14		3% (BIPHEP)/Rh(COD) ₂ BF ₄ 0.2 mmol (2,6-lutidine)	18h	18%	40%
15	 305B	3% (BINAP)Rh(COD)OTf	97% (70%)	0%	

All reactions, unless otherwise specified, were performed at room temperature for 2 h with a total volume of 1.25 mL of CH₂Cl₂. ^a Many other products observed. ^b 26% starting material remains. ^c 18% starting material remains. ^d 25% starting material remains. ^e Reaction performed in THF.

304B showed little to no reactivity when BINAP was used as a ligand (entry 8). It has been observed in previous reductive cyclization publications that allyl propargyl ethers benefit from using BIPHEP as a ligand instead of BINAP.¹⁵⁹ Upon using a mixture of 3 mol% BIPHEP and 3 mol% Rh(COD)₂OTf, the **304Bc-endo** dominated the mixture of products with a 57% yield (entry 9). Similar results were observed when 3 mol% of Rh(COD)₂BF₄ was used in place of the rhodium triflate (entry 6). Increasing the loading of ligand and catalyst did not result in an increased yield of the product (entry 11). Alkylboronic esters are sensitive to hydrolysis, so chromatography was not available to isolate the product of this reaction. Attempts to isolate **304Bc-endo** as the potassium trifluoroborate salt through recrystallization were met with an intractable mixture of products.

Entries 12, 13, and 14 show the reductive cyclization of **304B** with 2 eq. of 2,6-lutidine added at different reaction times. After stopping the reaction at 2 h shows that the presence of an added base changes the distribution of the endo and exocyclic isomers but also decreases the rate of the reaction (entry 12). If the reaction runs for 8 h, the starting material is consumed and there is about a 2:1 preference for the **304Bc-exo** over **304Bc-endo** (entry 13). However, when the reaction runs for 18 h it results in a decrease in the amount of **304Bc-exo** and an overall increase in the amount of **304Bc-endo** (entry 14). This could be indicative of an isomerization from the exocyclic alkene to the endo under reaction conditions.

Due to the absence of propargyl C-H bonds, **305B** could undergo reductive cyclization with no risk of isomerization to an endocyclic product and gave nearly a

quantitative conversion to the exocyclic alkene and can be isolated in a 70% yield (entry 15).

A similar trend in the substrate dictating the preferred isomer in rhodium-catalyzed reductive cyclizations has been reported by Ojima et. al. in their study on the silylcarbocyclization of 1,6-diynes.¹⁸⁶ They observed that the C-4 position of the 1,6-diyne greatly affects the product distribution: 1-2-hydrosilylation is favored for diynes with heteroatoms at the C-4 position while 1,4-hydrosilylation was favored by diynes with C(CO₂Et)₂ at the C-4 position. This is a similarity to our system favoring exocyclic alkenes as products for the malonate tethered enynes. It is possible that the rhodium catalyst in our reductive cyclization reactions needs to activate the propargyl sp³ C-H bond for the isomerization to occur, and the C-H bonds adjacent to heteroatoms are more reactive than those surrounded by carbons.¹⁸⁷

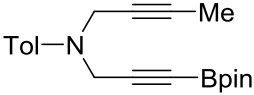
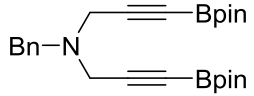
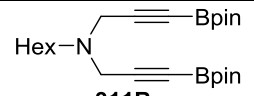
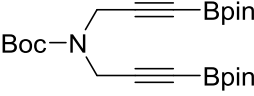
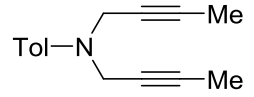
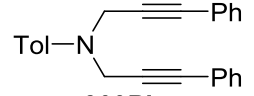
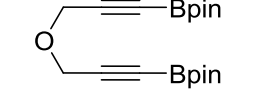
3.2.4 Reductive Cyclization of 1,6-Diynes

Due to the unreliable results of reductive cyclization using borylated 1,6-enynes, we sought to investigate the use of borylated 1,6-diynes in the analogous reaction. Traditionally, reductive cyclization of 1,6-diynes would yield a compound with a 1,2-dialkylidene cyclopentane skeleton.¹⁵⁹ However, with borylated, amine-tethered diynes an olefin isomerization was observed to occur yielding pyrroles in place of 3,4-dialkylidene pyrrolidines. We also observed that amine-tethered diynes that do not contain the alkynylboronate moiety were also susceptible to isomerization after reductive cyclization. The pyrrole products were identified by characteristic signals in their ¹H, ¹³C, and ¹¹B{¹H} NMR spectra.

Table III-5. Reductive cyclization of borylated 1,6-diynes.

#	Substrate	Catalyst	Diene	Pyrrole/ Furan
<p> 306 - 313B₂, 308MeB, 309MeB, 309Me₂, 309Ph₂ </p> <p> 306B₂c-exo, 308MeBc-exo, 309Me₂c-exo, 309Ph₂c-exo </p> <p> 308 - 412B₂c-pyr, 313B₂c-fur, 309Me₂c-pyr, 309Ph₂c-pyr </p>				
1	<p>306B₂</p>	3% (BINAP)Rh(COD)OTf	75% (70%)	0%
2	<p>307B₂</p>	3% (BINAP)Rh(COD)OTf	26%	
3		3% (BINAP)Rh(COD)BF ₄	13%	
4		3% BIPHEP / 3% Rh(COD) ₂ OTf	21%	
5	<p>308B₂</p>	3% (BINAP)Rh(COD)OTf	0%	77% (66%)
6	<p>309B₂</p>	3% (BINAP)Rh(COD)OTf	0%	93% (85%)
7		3% (BINAP)Rh(COD)BF ₄	0%	44% ^a
8	<p>308MeB</p>	3% (BINAP)Rh(COD)OTf	57% (9%)	0%
9		3% (BINAP)Rh(COD)OTf ^c	61%	0%
10		3% (BINAP)Rh(COD)OTf ^d	0%	61% (56%)

Table III-5. Continued

#	Substrate	Catalyst	Diene	Pyrrole/ Furan
11	 309MeB	3% (BINAP)Rh(COD)OTf	0%	65% (66%)
12	 310B2	3% (BINAP)Rh(COD)OTf	0%	40% ^a
13		5% (BINAP)Rh(COD)OTf ^b	0%	86% (85%)
14	 311B2	5% (BINAP)Rh(COD)OTf ^b	0%	83% (82%)
15	 312B2	3% (BINAP)Rh(COD)OTf	0%	75% (73%)
16	 309Me2	3% (BINAP)Rh(COD)OTf	17%	62%
17		3% (BINAP)Rh(COD)OTf ^d	0%	77% (77%)
18	 309Ph2	3% (BINAP)Rh(COD)OTf	39%	54%
19		3% (BINAP)Rh(COD)OTf ^d	0%	84% (65%)
20	 313B2	3% (BINAP)Rh(COD)OTf	0%	62% (59%)

^a Significant amount of starting material remaining. ^b Reaction lasted 4 h. ^c Reaction performed in 3.00 mL of CH₂Cl₂. ^d 2 hours at room temperature followed by 1.5 h at 60°C.

306B₂ behaved as a traditional substrate and yielded an exocyclic diene when 3 mol% (BINAP)Rh(COD)OTf was used for reductive cyclization, and **306B₂c-exo** was isolated through recrystallization in a 70% yield (Entry 1, Table III-5). **307B₂** was

resistant to reductive cyclization yielding only the semihydrogenation 1,6-enyne (**307B₂-H₂**) (entries 2-4).

308B₂ formed a pyrrole product **308B₂c-pyr** when treated with 3 mol% (BINAP)Rh(COD)OTf, and no exocyclic product was observed (entry 5). **308B₂c-pyr** could be isolated in 66% yield. **309B₂** also formed a pyrrole, **309B₂c-pyr**, after reductive cyclization and no exocyclic diene was observed in the reaction mixture when 3 mol% (BINAP)Rh(COD)OTf was used as a catalyst (entry 6). The analogous (BINAP)Rh(COD)BF₄ catalyst showed lower conversion to **309B₂c-pyr** and also produced no observable amount of the exocyclic alkene (entry 7). This observation led us to use 3 mol% (BINAP)Rh(COD)OTf as the default catalyst. **309B₂c-pyr** could be recrystallized in an 85% isolated yield.

308MeB however did not yield a pyrrole product and instead formed the exocyclic diene under reductive cyclization conditions (**308MeBc-exo**) (Entry 8 and 9). This substrate was also susceptible to [2+2+2] cycloadditions due to the small steric profile of the but-2-ynyl moiety. Attempts to discourage this side reaction by using a larger reaction volume did not deliver a significantly higher conversion to the exocyclic diene (entry 9). If the reaction were performed at room temperature for 2h and then transferred to a 60 °C oil bath, it was observed that **308MeBc-exo** would isomerize to **308MeBc-pyr** (entry 10). This product could be isolated in a 56% yield. When **309MeB** was used as a substrate for reductive cyclization, we observed that even at room temperature, only **309MeBc-pyr** was produced, and could be isolated in a 66% yield (entry 11).

Pyrroles were reliably formed from **310B₂** (entry 12 and 13) and **311B₂** (entry 14). However, low product yields were observed under the default conditions and a significant amount of starting material was observed by ¹H NMR spectroscopy. We attribute this to the higher coordinating ability of trialkylamines, which slows down the cyclization reaction by competing with the alkyne substituent for coordination sites on rhodium. Increasing the catalyst loading to 5 mol% and running the reaction for 4 hours led to a full consumption of the starting material. Products **310B₂c-pyr** and **311B₂c-pyr** could be isolated in 85% and 82% yields, respectively (entries 13 and 14).

312B₂ also formed a pyrrole (**312B₂c-pyr**) under reductive cyclization conditions. **312B₂c-pyr** could be isolated in a 73% yield (entry 15).

We were intrigued by **308MeB**'s unique ability amongst this class of substrates to form an exocyclic diene instead of a pyrrole in reactions that occurred at room temperature. Although the substrate has a 2-butynyl substituent as well as a 3-pinacolborylpropynyl moiety, it is unlikely that the 2-butynyl substituent was solely responsible for this outcome because **309MeB** resulted in a pyrrole product during reductive cyclization. This again leads us to believe that the central linker is responsible for dictating the resulting isomer.

In Krische's original report on the reductive cyclization of 1,6-diyne, the only amine-tethered diyne that was used was *N,N*-di(2-butynyl)toluenesulfonamide.^{159a} This reaction resulted in the formation of a 3,4-dialkylidene pyrrolidine. There are similarities between this substrate and **308MeB**, which was the only one of our borylated diynes that resulted in a pyrrolidine. Both substrates contain a toluenesulfonamide linker and both

have at least one but-2-ynyl substituent. Observing this, we hypothesized that amines with weak donor substituents, such as a tosyl group, have a deficiency of electrons on the nitrogen lone pair, and can resist isomerization to the aromatic pyrrole product. We wondered if pinacolboryl substituents were necessary for this isomerization to pyrroles, so we investigated substrates that contained a toluidine linker and internal alkynes as substituents.

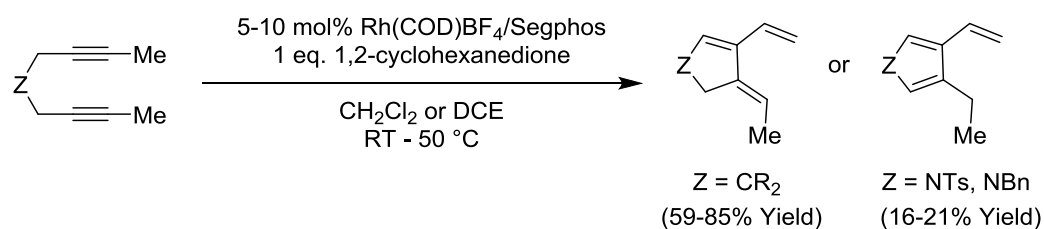
During reductive cyclization **309Me₂** was observed to give a mixture of products, favoring the pyrrole (**309Me₂c-pyr**) in a ratio of 3.65 over the exocyclic diene (**309Me₂c-exo**) (entry 16). **309Ph₂** gave a mixture of products favoring the pyrrole (**309Ph₂c-pyr**) in a ratio of 1.38 over the exocyclic diene (**309Me₂c-exo**) (entry 18). This shows that the alkynylboron substituent is not necessary for a pyrrole to be produced during reductive cyclization; however, the alkynylboronic ester moiety on the analogous toluidine-tethered diynes did ensure that the pyrrole product was exclusively produced at room temperature. The substrates that form a mixture of the 3,4-dialkylidene pyrrolidine and pyrrole compounds could be forced to isomerize to exclusively the pyrrole by thermalizing the reaction mixture at 60 °C for 1.5 h after the completion of 2 h at room temperature (entries 17 and 19).

In addition to the formation of pyrroles from *N,N*-dipropargylamines, **313B₂** was observed to undergo reductive cyclization to form a furan product (**313B₂c-fur**) instead of the 3,4-dialkylidenetetrahydrofuran (entry 20).

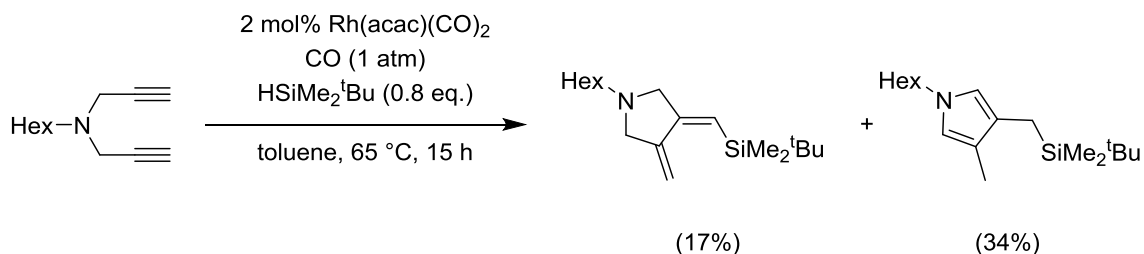
There have been previous examples of pyrroles being synthesized through inter- and intramolecular cyclizations of *N*-propargylamines, but only a few reports using *N,N*-

dipropargylamines.¹⁸⁸ A closely related report to the chemistry described here is the use of 1,6-diynes in the rhodium-catalyzed cycloisomerization reaction to form cyclic trienes and vinylpyrroles (Scheme III-5).¹⁸⁹ This method resulted in the formation of cyclic trienes for alkyl chain 1,6-diynes and vinylpyrroles for amine-tethered diynes (albeit in low yields). This method also required methyl substituents on the alkyne to allow for β -hydride elimination.

Tanaka



Ojima



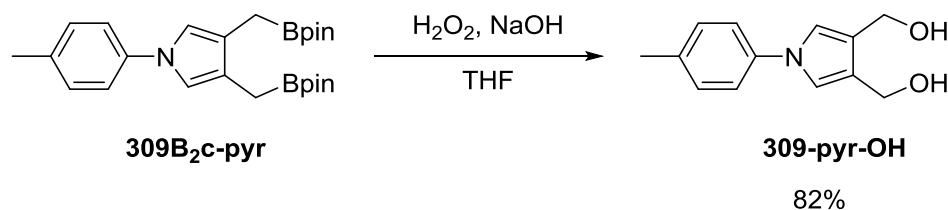
Scheme III-5. Reported synthesis of pyrroles from *N,N*-dipropargylamines.

In their work on the silylcarbocyclization of 1,6-diynes catalyzed by Rh(acac)(CO)₂, the Ojima group observed that with a deficiency of silane they could observe hexyl dipropargylamine form a pyrrole product under catalytic conditions (Scheme III-5).¹⁸⁶ However, under standard catalytic conditions using 4 eq. of silane the

pyrrole product was never observed. They supposed that the pyrrole was an aromatized isomer of their exocyclic diene intermediate, and that during normal catalytic conditions the silane was able to hydrosilylate the exocyclic alkene and prevent isomerization to the pyrrole. The Yoshimatsu group has also shown that sulfanyl-1,6-diynes can undergo transition metal-free reductive cyclization/isomerization to form pyrroles using sodium borohydride; however, this reaction requires the presence of organosulfanyl substituents on the alkyne.¹⁹⁰ Both of these rhodium-catalyzed reactions required elevated temperatures, while the pyrrole products we obtain from the reductive cyclization of borylated diynes occurs at room temperature.

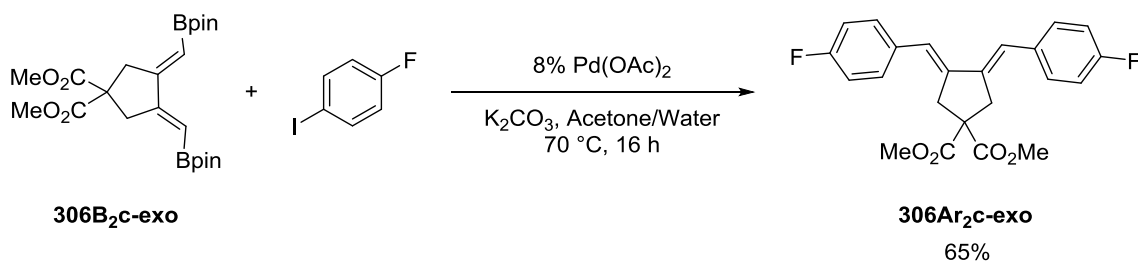
3.2.5 Subsequent Reactions of Reductive Cyclization Products

To showcase the utility of the products resulting from reductive cyclization, we have performed reactions on the resulting five-membered cyclic compounds. **309B₂c-pyr** could be efficiently oxidized with hydrogen peroxide in the presence of a base to give **309-pyr-OH** (Scheme III-6). *N*-aryl-3,4-bis(hydroxymethyl)pyrroles have been used as intermediates in the synthesis of compounds that possess antineoplastic activity.¹⁹¹



Scheme III-6. Oxidation of **309B₂c-pyr** to form a 3,4-bis(hydroxymethyl)pyrrole

Our borylated exocyclic alkenes were successful candidates for Suzuki-Miyaura coupling. To illustrate this, we arylated **306B₂c-exo** to form **306Ar₂c-exo** using a catalytic amount of Pd(OAc)₂ and para-fluoroiodobenzene (Scheme III-7).



Scheme III-7. Suzuki coupling of **306B₂c-exo** with 4-fluoroiodobenzene.

3.3 Conclusions

We have expanded the substrate scope of Ir-catalyzed DHBTA to include a number of 1,6-enynes and 1,6-diynes. These species are capable of undergoing rhodium-catalyzed reductive cyclization. However the pinacolboryl substituent seems to promote an alkene isomerization with heteroatom-tethered enynes and diynes. This double bond isomerization was difficult to gain control of with 1,6-enynes, and these reactions usually resulted in a mixture of products. However, the reductive cyclization of 1,6-diynes was a well-behaved reaction, and a number of amine-tethered borylated 1,6-diynes were found to undergo reductive cyclization to form pyrroles. Investigating reductive cyclization using amine-derived 1,6-diynes led to the discovery that the absence of boryl substituents can lead to a mixture of pyrrolidine and pyrrole products,

but thermolysis of the reaction after reductive cyclization has completed will isomerize the pyrrolidines to pyrroles.

3.4 Experimental

3.4.1 General Considerations

Unless otherwise specified, all manipulations were performed under an argon atmosphere using standard Schlenk or glovebox techniques. Toluene, THF, diethyl ether, pentane, and isooctane were dried and deoxygenated (by purging) using a solvent purification system and stored over molecular sieves in an Ar-filled glovebox. 1,4-dioxane, Dichloromethane, and 1,2-dichloroethane were dried with and then vacuum transferred from CaH₂ and stored over molecular sieves in an Ar-filled glovebox. C₆D₆ was dried over and distilled from NaK/Ph₂CO/18-crown-6 and stored over molecular sieves in an Ar-filled glovebox. NMR spectra were recorded on a Varian NMRS 500 (¹H NMR, 499.686 MHz; ¹³C NMR, 125.659 MHz; ³¹P NMR, 202.298 MHz) spectrometer. Chemical shifts are reported in δ (ppm). For ¹H and ¹³C NMR spectra, the residual solvent peak was used as an internal reference. CDCl₃ was referenced to 77.16 ppm for ¹³C NMR spectra and 7.26 ppm for ¹H NMR spectra. C₆D₆ was referenced to 128.06 for ¹³C NMR spectra and 7.15 ppm for ¹H NMR spectra. ¹¹B NMR spectra were referenced externally using neat BF₃OEt₂ at $\delta = 0$ ppm, ³¹P{¹H} NMR spectra were referenced externally using 85% H₃PO₄ at $\delta = 0$ ppm, and ¹⁹F NMR spectra were referenced externally using 1.0 M CF₃CO₂H in CDCl₃ at $\delta = -78.5$ ppm.

Propargyl allyl ether (**304**),¹⁹² 1-(allyloxy)-1-ethynylcyclohexane (**305**),¹⁹³ diethyl 2-allyl-2-propargylmalonate (**301**),¹⁷¹ *N*-allyl-*N*-propargylaniline (**302**),¹⁹⁴ bispropargyl ether (**313**),¹⁹⁵ *N,N*-bispropargyl toluenesulfonamide (**308**),¹⁹⁶ *N*-(but-2-yn-1-yl)-*N*-propargyl toluenesulfonamide (**308Me**),¹⁹⁷ dimethyl dipropargylmalonate (**306**),¹⁹⁸ *N,N*-bispropargyltoluidine (**309**),¹⁹⁹ *N*-propargyl toluidine,²⁰⁰ and *N-tert*-butoxycarbonyl-dipropargylamine (**312**)²⁰¹ were prepared by methods described in the literature. *N*-allyl-*N*-(3-pinacolborylprop-2-yn-1-yl) toluenesulfonamide (**303B**) was prepared using previously described DHBTA techniques.⁵⁶ Pinacolborane was purchased from Sigma-Aldrich in the Sure/Seal form.

In the ¹³C{¹H} NMR spectra of organic product, carbon atoms attached to boron were not usually observed due to low intensity.

3.4.2 DHBTA of 1,6-Enynes and 1,6-Diynes

3.4.2.1 Synthesis and Characterization of Borylated 1,6-Enynes

The desired catalyst was added to a J. Young tube in a stock solution:

0.1% **Ir3** = 100 μ L of 0.001 M solution in C₆D₆

1.0% **Ir3** = 100 μ L of 0.01 M solution in C₆D₆

1.0% **Ir2** = 100 μ L of 0.01 M solution in C₆D₆

C₆D₆ (170 μ L) diluted the catalyst, and pinacolborane (29 μ L, 0.20 mmol) was added. Finally the enyne (200 μ L, 0.5 M enyne / 0.175 M 1,4-dioxane) was added to the solution dropwise. The reaction was monitored by ¹H NMR spectroscopy integration versus the 1,4-dioxane internal standard.

2-allyl-2-(3-pinacolborylprop-2-yn-1-yl) diethyl malonate (301B). In an Ar-filled glovebox, **Ir3** (4 mg, 0.006 mmol) was dissolved in 6 mL of toluene. Pinacolborane (761 μ L, 5.2 mmol), was added and the solution was stirred for three minutes at room temperature. Diethyl 2-allyl-2-propynylmalonate (**301**) (1.19 g, 5.0 mmol) was dissolved in 3 mL of toluene and added to the reaction mixture dropwise. The reaction was heated at 60 °C for 1.5 h, and then the volatiles were removed under vacuum. The product was redissolved in toluene and passed through a pad of Celite. Analysis by ^1H NMR spectroscopy determined that the product was >95% pure, and the product was used in later reactions with no further purification. (Yield: 1.47 g, 81% judged to be >95% pure by ^1H NMR spectroscopy). ^1H NMR (500 MHz, C_6D_6): δ 5.65 (ddt, $J = 17$ Hz, 10 Hz, 7.5 Hz, 1H, $\text{CH}=\text{CH}_2$), 5.15 (ddt, $J = 16.5$ Hz, 2 Hz, 0.5 Hz, 1H, $\text{CH}=\text{CH}_a\text{H}_b$), 4.95 (ddt, $J = 10$ Hz, 2 Hz, 1 Hz, 1H, $\text{CH}=\text{CH}_a\text{H}_b$), 3.91 (q, $J = 7$ Hz, 4 H, CO_2CH_2), 3.1 (s, CH_2CCB), 3.09 (dt, $J = 7.5$ Hz, 1 Hz, $\text{CH}_2\text{CH}=\text{CH}_2$), 0.94 (s, 12 H, *Me* on *Bpin*), 0.87 (t, $J = 7$ Hz, OCH_2CH_3); $^{13}\text{C}\{^1\text{H}\}$ NMR (126 MHz, C_6D_6): δ 169.5 (s, $\text{C}=\text{O}$), 132.3 (s, $\text{CH}=\text{CH}_2$), 119.9 (s, $\text{CH}=\text{CH}_2$), 98.7 (bs, $\text{C}\equiv\text{C}-\text{B}$), 83.9 (s, *Bpin*), 61.6 (s, $\text{C}(\text{CO}_2\text{Et})_2$), 57.0 (CO_2CH_2), 37.1 (s, CH_2), 24.7 (s, *Me* on *Bpin*), 24.2 (s, CH_2), 14.0 (CH_2CH_3). $^{11}\text{B}\{^1\text{H}\}$ NMR (128.2 MHz, C_6D_6): δ 23.8 (s). Unit Mass (ESI) m/z : $[\text{M} + \text{Na}]^+$ calcd for $\text{C}_{19}\text{H}_{29}\text{BO}_6$ 387.19; Found 387.30.

***N*-allyl-*N*-(3-pinacolborylprop-2-yn-1-yl) aniline (302B).** In an argon filled glovebox, **Ir3** (4 mg, 0.006 mmol) was dissolved in 6 mL of toluene. Pinacolborane (1.45 mL, 10.0 mmol) was added to the solution and stirred for three minutes. *N*-allyl-*N*-propargylaniline (**302**) (856 mg, 5.0 mmol) was dissolved in 3 mL of toluene and added

to the solution dropwise. The reaction was heated at 60 °C for 4 h, and then the volatiles were removed under vacuum. The product was extracted with pentane and filtered through Celite. The volatiles were removed under vacuum to yield an amber oil judged to be >95% pure by ^1H NMR spectroscopy. The product was used in later reactions with no further purification. (Yield: 1.48 g, >94% judged to be >95% pure by ^1H NMR spectroscopy). ^1H NMR (500 MHz, C_6D_6): δ 7.12 (m, 2H, Ar-*H*), 6.75 (d, $J = 7.5$ Hz, 2H, Ar-*H*), 6.74 (m, 1H, Ar-*H*), 5.56 (ddt, $J = 17$ Hz, $J = 10$ Hz, $J = 5.5$ Hz, 1H, CH=CH₂), 5.02 (ddt, $J = 17$ Hz, $J = 4$ Hz, $J = 2$ Hz, 1H, CH=CHH), 4.91 (ddt, $J = 10.5$ Hz, $J = 4$ Hz, $J = 2$ Hz, 1H, CH=CHH), 3.70 (s, 2H, CH₂CCB), 3.63 (dt, $J = 5$ Hz, $J = 1.5$ Hz, CH₂CH=CH₂), 0.93 (s, 12H, *Me* on Bpin); $^{13}\text{C}\{^1\text{H}\}$ (126 MHz, C_6D_6): δ 148.8 (s, Ar-N), 134.4 (s, CH=CH₂), 129.4 (s, Ar), 118.4 (s, Ar), 116.4 (s, CH=CH₂), 114.5 (s, Ar), 99.6 (s, C \equiv C-B), 84.0 (s, Bpin), 53.7 (s, N-CH₂), 40.4 (s, N-CH₂), 24.7 (s, *Me* on Bpin); $^{11}\text{B}\{^1\text{H}\}$ NMR (128.2 MHz, C_6D_6): δ 24.0.

Allyl 3-pinacolborylprop-2-yn-1-yl ether (304B). In an argon filled glovebox, **Ir3** (4 mg, 0.006 mmol) was dissolved in 6 mL of toluene. Pinacolborane (1.45 mL, 10.0 mmol) was added to the solution and stirred for three minutes. Propargyl allyl ether (**304**) (481 mg, 5.0 mmol) was dissolved in 3 mL of toluene and added to the solution dropwise. The reaction was heated at 60 °C for 5 h, and then the volatiles were removed under vacuum. The product was extracted with pentane and filtered through Celite. The volatiles were removed to yield a light orange oil (1.07 grams, >89% yield, judged to be >95% pure by ^1H NMR spectroscopy). ^1H NMR (500 MHz, C_6D_6): δ 5.66 (ddt, $J = 17$ Hz, $J = 10.5$ Hz, $J = 5.5$ Hz, CH=CH₂), 5.12 (ddt (app. dq), $J = 17.5$ Hz, $J = 2$ Hz, 1H,

CH=CH_aH_b), 4.94 (ddt, $J = 10.5$ Hz, $J = 2$ Hz, $J = 1$ Hz, 1H, CH=CH_aH_b), 3.86 (s, 2H, CH₂CCB), 3.84 (dt, $J = 5.5$ Hz, $J = 1.5$ Hz, 2H, CH₂CH=CH₂), 0.97 (s, 12H, Me on Bpin); ¹³C{¹H} NMR (126 MHz, C₆D₆): δ 134.5 (s, CH=CH₂), 117.0 (s, CH=CH₂), 99.3 (bs, C≡C-B), 84.1 (s, Bpin), 70.5 (s, CH₂), 57.6 (s, CH₂), 24.7 (s, Me on Bpin); ¹¹B{¹H} NMR (128.2 MHz, C₆D₆): δ 23.9 (s). Unit Mass (ESI) m/z: [M + Na]⁺ calcd for C₁₂H₁₉BO₃ 245.13; Found 245.11.

1-(allyloxy)-1-(2-pinacolborylethynyl) cyclohexane (305B). In an argon filled glovebox, **Ir3** (4 mg, 0.006 mmol) was dissolved in 6 mL of toluene. Pinacolborane (0.798 mL, 5.5 mmol) was added to the solution and stirred for three minutes. 1-allyloxy-1-ethynylcyclohexane (**305**) (481 mg, 5.0 mmol) was dissolved in 3 mL of toluene and added to the solution dropwise. The reaction was heated at 60 °C for 1 h, and then the volatiles were removed under vacuum. The product was extracted with pentane and filtered through Celite. The volatiles were removed to yield a light yellow oil (1.45 grams, >93% yield judged to be >95% pure by ¹H NMR spectroscopy). ¹H NMR (500 MHz, C₆D₆): δ 5.91 (ddt, $J = 17$ Hz, $J = 10.5$ Hz, $J = 5$ Hz, 1H, CH=CH₂), 5.26 (overlapping ddt (apparent q), $J = 17.5$ Hz, $J = 2$ Hz, 1H, CH=CHH), 4.99 (ddt, $J = 10.5$ Hz, $J = 2$ Hz, $J = 1.5$ Hz, 1H, CH=CHH), 4.18 (overlapping ddd (apparent dt), $J = 5$ Hz, $J = 1.5$ Hz, 2H, OCH₂), 1.90 (m, 2H, Cy), 1.65 (m, 2H, Cy), 1.50 (m, 2H, Cy), 1.22 (m, 1H, Cy), 1.07 (m, 1H, Cy), 0.97 (s, 12H, Me on Bpin); ¹³C{¹H} NMR (126 MHz, C₆D₆): δ 136.2 (s, CH=CH₂), 115.4 (CH=CH₂), 104.7 (bs, C≡C-B), 84.0 (s, Bpin), 73.9 (s, C_{quart}), 64.9 (s, CH₂), 37.2 (s, Cy), 25.7 (s, Cy), 24.7 (s, Me on Bpin), 22.8 (s, Cy);

$^{11}\text{B}\{^1\text{H}\}$ NMR (128.2 MHz, C_6D_6): δ 24.2. Unit Mass (ESI) m/z : $[\text{M} + \text{H}]^+$ Calcd for $\text{C}_{17}\text{H}_{27}\text{BO}_3$ 291.21; Found 291.07.

3.4.2.2 Synthesis and Characterization of 1,6-Diynes

Synthesis of *N*-(2-butyn-1-yl)-*N*-(propargyl) toluidine (309Me). *N*-propargyl toluidine (997 mg, 6.9 mmol) was dissolved in THF and treated with K_2CO_3 (3.81 g, 27.6 mmol). The reaction mixture was treated with 1-bromo-2-butyne (0.906 mL, 10.35 mmol). The reaction was refluxed overnight. The volatiles were removed and treated with a saturated solution of NaHCO_3 . The product was extracted with ethyl acetate and dried over MgSO_4 . The solution was filtered through Celite, and the volatiles were removed. The product was extracted with diethyl ether and filtered through silica and Celite. The volatiles were removed to yield a brown oil (1.17 grams, 86% yield). ^1H NMR (500 MHz, CDCl_3): δ 7.09 (d, $J = 9$ Hz, 2H, Ar-*H*), 6.89 (s, $J = 9$ Hz, 2H, Ar-*H*), 4.09 (d, $J = 2.5$ Hz, 2H, NCH_2), 4.01 (q, $J = 2.5$ Hz, NCH_2CCMe), 2.27 (s, 3H, Ar-*Me*), 2.21 (t, $J = 2.5$ Hz, CCH), 1.81 (t, $J = 2.5$ Hz, CCMe); $^{13}\text{C}\{^1\text{H}\}$ NMR (126 MHz, CDCl_3): δ 146.2 (s, Ar-*N*), 129.8 (s, Ar-*H*), 129.4 (s, Ar-*Me*), 116.6 (s, Ar-*H*), 80.6 (s, Csp), 79.7 (s, Csp), 74.6 (s, Csp), 72.5 (s, Csp), 41.2 (s, NCH_2), 40.8 (s, NCH_2), 20.6 (s, Ar-*Me*).

Synthesis of *N,N*-dipropargyl benzylamine (310). Benzylamine (1.1 mL, 10 mmol) was dissolved in THF and treated with anhydrous K_2CO_3 (5.53 g, 40.0 mmol). Propargyl bromide (2.6 mL, 80% wt/toluene, 23 mmol) was added to the solution. The reaction was stirred at 35 °C for 24 h. At this point, the volatiles were removed under vacuum and a saturated solution of NaHCO_3 was added to the resulting cakey solid. The

product was extracted with CH_2Cl_2 and filtered through a plug of silica and celite. The volatiles were removed and the resulting oil was dissolved in Et_2O , dried with MgSO_4 and filtered through a plug of Celite. The volatiles were removed to yield a brown oil that matched the ^1H NMR of the previously reported compound (1.09 grams, 60% yield).²⁰²

Synthesis of *N,N*-dipropargyl hexylamine (311). Hexylamine (1.3 mL, 10 mmol) was dissolved in THF and treated with anhydrous K_2CO_3 (5.53 g, 40.0 mmol). Propargyl bromide (2.6 mL, 80% wt/toluene, 23 mmol) was added to the solution. The reaction was stirred at room temperature for 3 days. The volatiles were removed under vacuum and diethyl ether was added to the resulting solid. To the ether solution, a saturated solution of NaHCO_3 was added to and the mixture was vigorously stirred for 30 min. The organic layer was separated and dried with MgSO_4 before being filtered through a pad of silica and Celite. The volatiles were removed to yield a yellow-brown oil (1.0 g, 57% Yield). ^1H NMR (500 MHz, C_6D_6): δ 3.33 (d, $J = 2.5$ Hz, 4H, $\text{N-CH}_2\text{C}\equiv\text{CH}$), 2.41 (t, $J = 7.5$ Hz, 2H, N-CH_2), 1.84 (t, $J = 2.5$ Hz, 2H, $\text{N-CH}_2\text{C}\equiv\text{CH}$), 1.31 (m, 2H, Hex), 1.86 (m, 6H, Hex), 0.85 (t, $J = 7$ Hz, 3H, Hex); $^{13}\text{C}\{^1\text{H}\}$ NMR (126 MHz, CDCl_3): δ 79.0 (s), 72.9 (s), 53.1 (s), 42.2 (s), 31.8 (s), 27.5 (s), 27.1 (s), 22.7 (s), 15.2 (s).

Synthesis of *N,N*-bis(2-butyn-1-yl) toluidine (309Me₂). Toluidine (800 mg, 7.47 mmol) was dissolved in CH_3CN and treated with K_2CO_3 (5.16 g, 37.3 mmol). 1-bromo-2-butyne (1.6 mL, 18.3 mmol) was added to the reaction and it was refluxed overnight. The volatiles were removed in the morning and the resulting solid was treated

with NaHCO₃ (aq). The product was extracted with Ethyl acetate. The organic layers were dried with MgSO₄ and then filtered through a pad of Celite and silica. The volatiles were removed to yield a brown oil, which was dissolved in pentane and filtered through a plug of silica and Celite. The volatiles were removed to yield a light yellow solid (1.24 g, 79% yield). ¹H NMR (500 MHz, CDCl₃): δ 7.08 (d, *J* = 8.5 Hz, 2H, Ar-*H*), 6.89 (d, *J* = 8.5 Hz, 2H, Ar-*H*), 4.01 (q, *J* = 2 Hz, 4H, NCH₂CCMe), 2.27 (s, 3H, Ar-*Me*), 1.80 (t, *J* = 2 Hz, 6H, CH₂CCMe); ¹³C{¹H} NMR (126 MHz, CDCl₃): δ 146.5 (s, Ar-N), 129.7 (s, Ar-*H*), 128.9 (s, Ar-*Me*), 116.5 (s, Ar-*H*), 80.2 (s, Csp), 74.8 (s, Csp), 41.1 (s, N-CH₂), 20.6 (s, Ar-*Me*), 3.8 (s, CC-*Me*). Unit Mass (ESI) *m/z*: [2(M) - H]⁺ calcd for C₁₅H₁₇N 421.26; found 421.09.

Synthesis of *N,N*-bis(3-phenylprop-2-yn-1-yl) toluidine (309Ph₂). In a screw-top vial, (PPh₃)₄Pd (58 mg, 0.05 mmol), CuI (19 mg, 0.10 mmol), and iodobenzene (1.2 mL, 10.8 mmol) were dissolved in THF. *N,N*-bispropargyl toluidine (**309**) (916 mg, 5.0 mmol) and triethylamine (4.2 mL, 30.1 mmol) were added to the reaction mixture. The progression of the reaction was monitored by ¹H NMR spectroscopy, and after 48 h at room temperature **9** was observed to be completely consumed. The reaction was quenched with aqueous ammonium chloride, and the product was extracted with diethyl ether. The organic fractions were dried of magnesium sulfate and filtered through a pad of Celite and silica. The compound was purified by column chromatography (1:10 EA:hexane). The product was isolated as a light yellow solid (531 mg, 32% yield). ¹H NMR (500 MHz, CDCl₃): δ 7.39 (m, 4H, Ar-*H*), 7.27 (m, 6H, Ar-*H*), 7.12 (d, *J* = 8 Hz, 2H, Ar-*H*), 7.01 (d, *J* = 8 Hz, Ar-*H*), 4.36 (s, 4H, N-CH₂), 2.29 (s, 3H, Ar-*Me*); ¹³C{¹H}

NMR (126 MHz, CDCl₃): δ 146.2 (s, *Ar-N*), 131.9 (s, *Ar-H*), 129.8 (s, *Ar-H*), 129.3 (s, *Ar-Me*), 128.29 (s, *Ar-H*), 128.22 (s, *Ar-H*), 123.1 (s, *Ar-C*), 116.7 (s, *Ar-H*), 85.3 (s, C_{sp}), 84.7 (s, C_{sp}), 41.9 (s, N-CH₂), 20.6 (s, *Ar-Me*). Unit Mass (ESI) m/z: [M + H]⁺ calcd for C₂₅H₂₁N 336.17; Found 336.23.

3.4.2.3 Synthesis and Characterization of Borylated 1,6-Diynes

The desired catalyst was added to a J. Young tube in a stock solution:

0.1% **Ir3** = 100 μ L of 0.001 M solution in C₆D₆

1.0% **Ir3** = 100 μ L of 0.01 M solution in C₆D₆

1.0% **Ir2** = 100 μ L of 0.01 M solution in C₆D₆

1.0% **Ir1** = 100 μ L of 0.01 M solution in C₆D₆

C₆D₆ (170 μ L) diluted the catalyst, and pinacolborane (29 μ L, 0.20 mmol (4.0 eq)/ 16 μ L, 0.11 mmol (2.2 eq.)) was added. Finally the diyne (200 μ L, 0.25 M diyne / 0.175 M 1,4-dioxane)/(200 μ L, 0.5 M substituted diyne / 0.175 M 1,4-dioxane) was added to the solution dropwise.

Dimethyl 2,2-di(3-pinacolborylprop-2-yn-1-yl)malonate (306B₂). In an Ar-filled glovebox, **Ir3** (7 mg, 0.01 mmol) was dissolved in 5 mL of toluene with pinacolborane (1.52 mL, 10.5 mmol) in a 100 mL Teflon screw-top flask. **306** (1.04 g, 5.0 mmol) was dissolved in 5 mL of toluene and added to the mixture dropwise over a period of two minutes. The reaction mixture was heated for 1 h at 60 °C and then the volatiles were removed under vacuum. The solid was redissolved in toluene and filtered through a pad of Celite. The volatiles were removed and the resulting solid was recrystallized from dichloromethane layered with pentane to yield a beige solid (1.87 g,

81% yield). ^1H NMR (500 MHz, C_6D_6): δ 3.28 (s, 4H, CH_2), 3.22 (s, 6H, *Me*), 0.93 (s, 12H, *Me* on Bpin); ^1H NMR (500 MHz, C_6D_6): δ 3.75 (s, 6H, *Me*), 3.09 (s, 4H, CH_2), 1.25 (s, 24H, *Me* on Bpin). $^{13}\text{C}\{^1\text{H}\}$ (126 MHz, CDCl_3): δ 168.7 (s, $\text{C}=\text{O}$), 97.7 (s, $\text{C}(\text{sp})$), 84.3 (s, Bpin), 56.3 (s, $\text{C}_{\text{quat.}}$), 53.3 (s, *OMe*), 24.7 (s, *Me* on Bpin), 23.8 (s, CH_2); $^{11}\text{B}\{^1\text{H}\}$ NMR (128.2 MHz, CDCl_3): δ 23.5. Unit Mass (ESI) m/z $[\text{M} + \text{H}]^+$ calcd. for $\text{C}_{23}\text{H}_{35}\text{B}_2\text{O}_8$ 461.25; Found 461.25.

1,7-bis(pinacolboryl)hepta-1,6-diyne (307B₂). In a Teflon-screwtop flask, **Ir3** (8 mg, 0.01 mmol) was dissolved in 10 mL of toluene with pinacolborane (1.6 mL, 11 mmol). 1,6-heptadiyne (**307**) (522 μL , 5.0 mmol) was added dropwise to the solution. The reaction mixture was taken out of the glovebox and heated at 60 °C for 1 h. The volatiles were removed under vacuum and the product was extracted with diethyl ether and filtered through a pad of Celite. The volatiles were removed and the resulting solid was washed with cold pentane to yield a white solid (1.43 g, 83% yield). ^1H NMR (500 MHz, C_6D_6): δ 1.95 (t, $J = 7$ Hz, 2H, CH_2), 1.31 (pent, $J = 7$ Hz, 4H, CH_2), 0.99 (s, 24H, *Me* on Bpin); $^{13}\text{C}\{^1\text{H}\}$ NMR: δ 103.2 (s), 83.7 (s), 27.0 (s), 24.7 (s), 18.6 (s); $^{11}\text{B}\{^1\text{H}\}$ NMR (128.2 MHz, C_6D_6): δ 23.9. Unit Mass (ESI) m/z : $[\text{M} + \text{Na}]^+$ Calcd for $\text{C}_{19}\text{H}_{30}\text{B}_2\text{O}_4$ 367.22; Found 367.28.

***N,N*-bis(3-pinacolborylprop-2-yn-1-yl) toluenesulfonamide (308B₂)**. **Ir2** (62 mg, 0.1 mmol) was dissolved in 10 mL of toluene in a 100 mL Teflon screw-top flask. HBpin (2.9 mL, 20 mmol) was added to the reaction mixture. **308** (1.24 g, 5.0 mmol) was dissolved in 5 mL of toluene and added to the reaction mixture, and the flask was heated at 60 °C for 1 h. The volatiles were removed and the resulting cakey solid was

dissolved in CH₂Cl₂ and filtered through a pad of Celite. The volatiles were removed and triturated with pentane. The resulting solid was dissolved in a minimum amount of CH₂Cl₂ and layered with pentane and placed in a -35 °C freezer. A yellow solid precipitated overnight. This solid was collected and redissolved in CH₂Cl₂, layered with pentane, and placed in a -35 °C freezer. The product was isolated as white crystals (492 mg, 20% yield). ¹H NMR (500 MHz, C₆D₆): δ 7.58 (d, *J* = 8.5 Hz, 2H, Ar-*H*), 6.83 (d, *J* = 8 Hz, Ar-*H*), 4.02 (s, 4H, NCH₂CCBpin), 1.90 (s, 3H, Ar-*Me*), 0.93 (s, 24H, *Me* on Bpin); ¹³C{¹H} NMR (126 MHz, C₆D₆): δ 143.2 (s), 136.0 (s), 129.7 (s, Ar-*H*), 128.4 (s, Ar-*H*), 95.3 (br. s, C≡C-Bpin), 84.0 (s, Bpin), 37.1 (s, NCH₂), 24.6 (s, *Me* on Bpin), 21.4 (s, Ar-*Me*); ¹¹B{¹H} NMR (128.2 MHz, CDCl₃): δ 23.4 (s). Unit Mass (ESI) *m/z* [M + Na]⁺ calcd. for C₂₅H₃₅B₂NO₆S 522.23; Found 522.28.

***N*-(but-2-yn-1-yl)-*N*-(3-pinacolborylprop-2-yn-1-yl) toluenesulfonamide (308MeB).** In an Ar-filled glovebox, **Ir3** (40 mg, 0.05 mmol) was dissolved in 5 mL of toluene. Pinacolborane (1.45 mL, 10 mmol) was added. **308Me** (1.31 g, 5.0 mmol) was dissolved in 5 mL of toluene and added to the reaction dropwise over a period of two minutes. The reaction was stirred at room temperature for 1 h and the volatiles were removed under vacuum. The resulting solid was dissolved in dichloromethane and filtered through Celite. The volatiles were removed and the product was recrystallized from dichloromethane and pentane to yield a beige solid (1.26 g, 65% yield). ¹H NMR (500 MHz, CDCl₃): δ 7.71 (d, *J* = 8 Hz, 2H, Ar-*H*), 7.29 (d, *J* = 8 Hz, 2H Ar-*H*), 4.18 (s, 2H, N-CH₂), 4.09 (q, *J* = 2.5 Hz, 2H, N-CH₂), 2.41 (s, 3H, Ar-*Me*), 1.63 (t, *J* = 2.5 Hz, 3H, C≡C-*Me*), 1.24 (s, 12H, *Me* on Bpin); ¹³C{¹H} NMR (126 MHz, CDCl₃): δ 143.7

(s), 135.3 (s), 129.5 (s, *Ar-H*), 128.1 (s, *Ar-H*), 95.3 (br. s, C≡C-Bpin), 84.4 (s), 82.2 (s), 71.4 (s), 37.0 (s), 36.9 (s), 24.7 (s), 21.6 (s), 3.47 (s); $^{11}\text{B}\{^1\text{H}\}$ NMR (128.2 MHz, CDCl_3): δ 23.3 (s). HRMS (ESI-TOF) m/z : $[\text{M} + \text{Na}]^+$ Calcd. for $\text{C}_{20}\text{H}_{26}\text{BNO}_4\text{S}$ 410.1568; Found 410.1551.

***N,N*-di(3-pinacolborylprop-2-yn-1-yl) toluidine (309B₂)**. In a 100 mL teflon-screwtop flask, **Ir3** (8 mg, 0.010 mmol) was dissolved in 5 mL of toluene and pinacolborane (2.90 mL, 20 mmol) was added to the solution. **309** (916 mg, 5.0 mmol) was dissolved in 3 mL of toluene and the alkyne was added dropwise. The reaction vessel was removed from the glovebox and placed in a 60 °C oilbath overnight. The volatiles were removed in the morning and the product was extracted with THF and filtered through Celite. The volatiles were removed and washed with pentane. The product was recrystallized from THF to yield a beige solid (1.52g, 70% yield). ^1H NMR (500 MHz, C_6D_6): δ 6.82 (d, $J = 8.5$ Hz, 2H, *Ar-H*), 6.68 (d, $J = 8.5$ Hz, 2H, *Ar-H*), 3.85 (s, 4H, CH_2), 2.05 (s, 3H, *Ar-Me*), 0.94 (s, 24H, *Me* on Bpin); $^{13}\text{C}\{^1\text{H}\}$ NMR (C_6D_6 , 126 MHz): δ 146.3 (s), 129.9 (s), 129.0 (s), 116.7 (s), 99.0 (br. s), 83.9 (s), 41.3 (s), 24.7 (s), 20.5 (s); $^{11}\text{B}\{^1\text{H}\}$ NMR (128.2 MHz, C_6D_6): δ 24.0. Unit mass (ESI) m/z : $[\text{M} + \text{H}]^+$ calcd for $\text{C}_{25}\text{H}_{36}\text{B}_2\text{NO}_4$ 436.28; Found 436.37.

***N*-(but-2-yn-1-yl)-*N*-(3-pinacolborylprop-2-yn-1-yl) toluidine (309MeB)**. To a 100 ml Teflon-screw top flask was added **Ir3** (40 mg, 0.05 mmol), which was dissolved in 5 mL of toluene. HBpin (1.45 mL, 10 mmol) was added to the solution. **309Me** (986 mg, 5.0 mmol) was dissolved in 5 ml of toluene and added to the reaction mixture dropwise. The reaction was placed in a 60 °C oil bath for 1 h. The volatiles were

removed and the product was extracted with pentane and filtered through a pad of Celite. The volatiles were removed to yield a brown oil observed to be >90% pure based on ^1H NMR spectroscopy (1.70 grams, >92% yield). ^1H NMR (500 MHz, C_6D_6): δ 6.91 (d, $J = 9$ Hz, 2H, Ar-*H*), 6.80 (d, $J = 9$ Hz, 2H, Ar-*H*), 3.97 (s, 2H, CH_2 , $\text{NCH}_2\text{CCBpin}$), 3.93 (q, $J = 2$ Hz, 2H, NCH_2CCMe), 2.09 (s, 3H, Ar-*Me*), 1.40 (t, $J = 2$ Hz, 3H, CCMe), 0.94 (s, 12H, *Me* on Bpin); $^{13}\text{C}\{^1\text{H}\}$ (126 MHz, C_6D_6): δ 146.6 (s, Ar-N), 129.9 (s, Ar-H), 128.7 (s, Ar-*Me*), 116.6 (s, Ar-H), 99.4 (br. s, $\text{C}\equiv\text{CBpin}$), 83.9 (s, Bpin), 80.3 (s, $\text{C}\equiv\text{C}$), 75.2 (s, $\text{C}\equiv\text{C}$), 41.4 (s, NCH_2), 41.1 (s, NCH_2), 24.7 (s, *Me* on Bpin), 20.5 (s, Ar-*Me*), 3.3 (s, $\text{C}\equiv\text{CMe}$); $^{11}\text{B}\{^1\text{H}\}$ NMR (128.2 MHz, C_6D_6): δ 23.4. Unit Mass (ESI) m/z $[\text{M} + \text{H}]^+$ calcd. for $\text{C}_{20}\text{H}_{26}\text{BNO}_2$ 324.21; Found 324.27.

***N,N*-di(3-pinacolborylprop-2-yn-1-yl) benzylamine (310B₂)**. In a 100 mL Teflon screw-top flask, **Ir3** (80 mg, 0.10 mmol) was dissolved in 5 mL of toluene with pinacolborane (2.9 mL, 20 mmol). **310** (916 mg, 5.0 mmol) was dissolved in 5 mL toluene and added dropwise to the solution. The reaction mixture was heated at 60 °C for 1 hour, and then the volatiles were removed under vacuum. The resulting solid was rinsed with pentane, and the volatiles were removed. The resulting solid was dissolved in THF and filtered through a pad of Celite. The volatiles were removed and the resulting solid was washed with pentane before being recrystallized from diethyl ether in a -35 °C freezer to yield a beige solid (1.59 g, 73% yield). ^1H NMR (500 MHz, C_6D_6): δ 7.19 (d, $J = 7.5$ Hz, 2H, Ar-*H*), 7.02 (m, 3H, overlapping Ar-*H* signals), 3.50 (s, 2H, PhCH_2N), 3.30 (s, 4H, NCH_2CCB), 0.98 (s, 24H, *Me* on Bpin); $^{13}\text{C}\{^1\text{H}\}$ NMR (C_6D_6 , 126 MHz): δ 138.4 (s), 129.3 (s), 128.6 (s), 127.4 (s), 98.8 (br. s), 83.2 (s), 57.4 (s), 42.7 (s), 24.7 (s);

$^{11}\text{B}\{^1\text{H}\}$ NMR (128.2 MHz, C_6D_6): δ 24.4. Unit mass (ESI) m/z : $[\text{M} + \text{H}]^+$ calcd for $\text{C}_{25}\text{H}_{36}\text{B}_2\text{NO}_4$ 436.28; Found 436.40.

***N,N*-di(3-pinacolborylprop-2-yn-1-yl) hexylamine (311B₂)**. In a 100 mL Teflon-screwtop flask, **Ir3** (80 mg, 0.10 mmol) was dissolved in 5 mL of toluene with pinacolborane (2.90 mL, 20 mmol). A solution of **311** (886 mg, 5.0 mmol) in 5 mL of toluene was added dropwise to the reaction mixture. The reaction was heated at 60 °C for 1 h. The volatile were removed under vacuum and the product was washed with cold pentane and collected on a frit as a white solid (1.70 g, 79% yield). ^1H NMR (500 MHz, C_6D_6): δ 3.35 (s, 4H, N- CH_2), 2.39 (t, $J = 7.5$ Hz, 2H, N- CH_2), 1.20 (m, 2H, CH_2), 1.17 (m, 2H, CH_2), 1.08 (m, 4H, CH_2), 0.97 (s, 24H, *Me* on Bpin), 0.83 (t, $J = 7.5$ Hz, 3H, CH_3); $^{13}\text{C}\{^1\text{H}\}$ NMR (C_6D_6 , 126 MHz): δ 99.1 (s, $\text{C}\equiv\text{CBpin}$), 83.9 (s, Bpin), 53.1 (s, N- CH_2), 43.1 (s, N- CH_2), 32.0 (s, *Hex*), 27.7 (s, *Hex*), 27.1 (s, *Hex*), 24.7 (s, *Me* on Bpin), 23.0 (s, *Hex*), 14.3 (s, *Hex*); $^{11}\text{B}\{^1\text{H}\}$ NMR (126 MHz, C_6D_6): δ 23.9. Unit mass (ESI) m/z : $[\text{M} + \text{Na}]^+$ calcd for $\text{C}_{24}\text{H}_{41}\text{B}_2\text{NO}_4$ 452.31; Found 453.45.

***N,N*-di(3-pinacolborylprop-2-yn-1-yl) *tert*-butyl carbamate (312B₂)**. In a 100 mL Teflon-screwtop flask, **Ir3** (31 mg, 0.003 mmol) was dissolved in 5 mL of toluene and treated with HBpin (2.23 mL, 15.4 mmol). A solution of **312** (740 mg, 3.85 mmol) in 5 mL of toluene was added to the reaction mixture dropwise. The reaction was heated at 60 °C for 1 h. The volatiles were removed under vacuum, and the product was extracted with pentane and filtered through a pad of Celite. The volatiles were removed under vacuum, and the resulting solid was dissolved in pentane and placed in a -35 °C freezer to recrystallize as a yellow solid (926 mg, 54% yield). ^1H NMR (500 MHz,

C_6D_6): δ 4.20 (br. s, 2H, NCH_2), 4.01 (br. s, 2H, NCH_2), 1.29 (s, 9H, CMe_3), 0.95 (s, 24H, *Me* on Bpin); $^{13}C\{^1H\}$ (C_6D_6 , 126 MHz) NMR: δ 153.9 (s, NCO_2), 98.3 (br. s, $C\equiv CBpin$), 84.0 (s, *Bpin*), 80.6 (2, CMe_3), 36.1 (br. s, NCH_2), 35.8 (br. s, NCH_2), 28.1 (s, CMe_3), 24.7 (s, *Me* on Bpin); $^{11}B\{^1H\}$ NMR (126 MHz, C_6D_6): δ 23.9. Unit Mass (ESI) m/z : $[M + Na]^+$ Calcd for $C_{23}H_{37}B_2NO_6$ 468.27; Found 468.34.

Bis(3-pinacolborylprop-2-yn-1-yl) ether (313B₂). **Ir3** (80 mg, 0.10 mmol) was dissolved in 5 mL of toluene in a 100 mL Teflon screw-top flask. Pinacolborane (2.9 mL, 20 mmol) was added to the mixture. **313** (515 μ L, 5.0 mmol) was dissolved in 5 mL of toluene and added to the reaction mixture dropwise. The reaction vessel was left at room temperature for 48 h. The volatiles were removed and the resulting cakey solid was extracted with diethyl ether and filtered through Celite. The product was isolated as a light yellow solid after being recrystallized from cold pentane (771 mg, 45% yield). 1H NMR (500 MHz, C_6D_6): δ 3.97 (s, 4H, OCH_2), 0.97 (s, 24H, *Me* on Bpin); $^{13}C\{^1H\}$ (C_6D_6 , 126 MHz) NMR: δ 98.2 (br. s, $C\equiv CBpin$), 84.1 (s, *Bpin*), 56.7 (s, OCH_2), 24.7 (s, *Me* on Bpin); $^{11}B\{^1H\}$ NMR (128.2 MHz, C_6D_6): δ 23.9 (s).

3.4.3 Synthesis of Reductive Cyclization Catalysts

Synthesis of racemic (BINAP)Rh(COD)BF₄. A Schlenk flask was charged with racemic BINAP (107 mg, 0.172 mmol) and $Rh(COD)_2BF_4$ (70 mg, 0.172 mmol) and dissolved in CH_2Cl_2 . The solution was stirred for 2 h and then the volatiles were removed under vacuum. The resulting solid was then rinsed with pentane, and then filtered through a pad of Celite in CH_2Cl_2 . The product was then recrystallized from

CH₂Cl₂ and pentane in a -35 °C freezer (148 mg, 94% yield). The spectral data matched that recorded in the literature.²⁰³

Synthesis of racemic (BINAP)Rh(COD)OTf. A Schlenk flask was charged with racemic BINAP (107 mg, 0.172 mmol) and Rh(COD)₂OTf (80.5 mg, 0.172 mmol) and dissolved in CH₂Cl₂. The solution was stirred for 2 h and then the volatiles were removed under vacuum. The resulting solid was then rinsed with pentane, and then filtered through a pad of Celite in CH₂Cl₂. The product was then recrystallized from CH₂Cl₂ and pentane in a -35 °C freezer (157 mg, 93% yield). The spectral data matched that recorded in the literature.²⁰³

3.4.4 Reductive Cyclization of Borylated 1,6-Enynes

3.4.4.1 General Procedure for Catalyst Screening

303B (38 mg, 0.10 mmol) was added to a 25 mL Teflon-capped screw-top flask and dissolved in the desired amount of CH₂Cl₂ to achieve the target volume. (BINAP)Rh(COD)OTf or (BINAP)Rh(COD)BF₄ (3% Loading = 0.003 mmol, 150 μL of a 0.02 M solution in CH₂Cl₂ / 5% Loading = 0.005 mmol, 250 μL of a 0.02 M solution in CH₂Cl₂) was added to the solution. When a rhodium precatalyst was used with a ligand to make the catalyst *in situ*, Rh(COD)₂OTf or Rh(COD)₂BF₄ (0.003 mmol, 150 μL of a 0.02 M solution in CH₂Cl₂ / 5% Loading = 0.005 mmol, 250 μL of a 0.02 M solution in CH₂Cl₂) and ligand (3% Loading = 0.003 mmol, 150 μL of a 0.02 M in CH₂Cl₂ / 5% = 0.005 mmol, 250 μL of a 0.02 M in CH₂Cl₂) were added to the flask separately and mixed together. The reaction vessel was degassed using the freeze-pump-thaw method

and refilled with an atmosphere of H₂. The reaction was then stirred at room temperature for 2 h. The volatiles were removed and 0.600 mL of a 0.063 M solution of 1,4-dioxane in CDCl₃ was used to extract the reaction mixture to a J. Young tube. ¹H NMR integration versus the 1,4-dioxane internal standard was used to determine the yield of the product. The integration was compared to an equimolar amount of the substrate in another 0.600 mL aliquot of the same 1,4-dioxane solution.

Stock solutions

0.02 M (BINAP)Rh(COD)OTf = 20 mg/1mL CH₂Cl₂

0.02 M (BINAP)Rh(COD)BF₄ = 36.8/2mL CH₂Cl₂

0.02 M Rh(COD)₂OTf = 19mg/2 mL CH₂Cl₂

0.02 M Rh(COD)₂BF₄ = 16mg/2 mL CH₂Cl₂

0.02 M dippf = 17 mg/2 mL CH₂Cl₂

0.02 M dppf = 22.2 mg/2 mL CH₂Cl₂

3.4.4.2 General Procedure for Substrate Screening

The substrate (500 μL, 0.2 M solution in CH₂Cl₂, 0.1 mmol) was added to a 25 mL Teflon screw-top flask and diluted with CH₂Cl₂ to achieve the desired final volume. The rhodium catalyst (BINAP)Rh(COD)OTf or (BINAP)Rh(COD)BF₄ (3% Loading = 0.003 mmol, 150 μL of a 0.02 M solution in CH₂Cl₂ / 5% Loading = 0.005 mmol, 250 μL of a 0.02 M solution in CH₂Cl₂) was added to the solution. When a rhodium precatalyst was used with a ligand to make the catalyst *in situ*, rhodium precatalyst (0.003 mmol, 150 μL of a 0.02 M solution in CH₂Cl₂ / 5% Loading = 0.005 mmol, 250 μL of a 0.02 M solution in CH₂Cl₂) and ligand (3% Loading = 0.003 mmol, 150 μL of a

0.02 M in CH₂Cl₂ / 5% = 0.005 mmol, 250 μL of a 0.02 M in CH₂Cl₂). The reaction vessel was degassed using the freeze-pump-thaw method and refilled with an atmosphere of H₂. The reaction was then stirred at room temperature for 2 h. The volatiles were removed and 0.600 mL of a 0.063 M solution of 1,4-dioxane in CDCl₃ was used to extract the reaction mixture to a J. Young tube. ¹H NMR integration versus the 1,4-dioxane internal standard was used to determine the yield of the product. The integration was compared to an equimolar amount of the substrate in another 0.600 mL aliquot of the same 1,4-dioxane solution.

3.4.4.3 Synthesis and Characterization of Organic Products

***N*-propyl-*N*-(3-pinacolborylprop-1-yl) toluenesulfonamide (303B-H₆).**

Prepared via general procedure for catalyst screening with 5% dippf / 5% Rh(COD)₂OTf and **303B**. Volatiles were removed under vacuum and the resulting solid was dissolved in toluene. The solution was filtered through Celite and silica, and the volatiles were removed to yield a clear light yellow oil (23 mg, 60% yield). ¹H NMR (500 MHz, CDCl₃): δ 7.69 (d, *J* = 8 Hz, 2H, Ar-*H*), 7.28 (d, *J* = 8 Hz, 2H, Ar-*H*), 3.08 (t, *J* = 8 Hz, 2H, N-CH₂), 3.07 (t, *J* = 8 Hz, 2H, N-CH₂), 2.42 (s, 3H, Ar-*Me*), 1.63 (pent, *J* = 8 Hz, CH₂), 1.56 (sext, *J* = 7.5 Hz, CH₂), 1.24 (s, 12H, *Me* on Bpin), 0.87 (t, *J* = 7.5 Hz, 3H, CH₃), 0.73 (t, *J* = 8 Hz, 2H, CH₂-B). ¹³C{¹H} NMR (75.4 MHz, CDCl₃): δ 142.9 (Ar-S), 137.5 (Ar-*Me*), 129.6 (s, Ar-*H*), 127.3 (s, Ar-*H*), 83.3 (s, Bpin), 50.2 (s, N-CH₂), 50.0 (s, N-CH₂), 25.0 (s, *Me* on Bpin), 23.3 (s), 22.0 (s), 21.6 (s), 11.3 (s). CH₂-Bpin not observed. ¹¹B{¹H} NMR (128 MHz, CDCl₃): δ 33.4.

(Z)-3-pinacolborylmethylidene-4-methyl-1-tosylpyrrolidine (303Bc-exo).

BINAP (10 mg, 0.015 mmol) was mixed with Rh(COD)₂OTf (7 mg, 0.015 mmol) in 1.25 mL of CH₂Cl₂ in a 50 mL Teflon screw-top flask. **303B** (188 mg, 0.5 mmol) was dissolved in 5.0 mL of CH₂Cl₂ and was added to the reaction mixture. The reaction was degassed using the freeze-pump-thaw technique and refilled with 1 atm of H₂. The reaction was stirred for 2 h at room temperature for 2 h. The volatiles were removed and the product was extracted with CH₂Cl₂ and filtered through Celite. The product was purified by Purified by column chromatography with 1:3 EA: Hexanes to yield a white powder (126 mg, 67% yield). ¹H NMR (500 MHz, CDCl₃): δ 7.71 (d, *J* = 8 Hz, 2H, Ar-*H*), 7.31 (d, *J* = 8 Hz, 2H, Ar-*H*), 5.18 (dt, *J* = 4.5 Hz, *J* = 2 Hz, C=CH-Bpin), 4.16 (dd, *J* = 16.5 Hz, *J* = 2 Hz, 1H, N-CH_aH_b-C(sp²)), 3.97 (dt, *J* = 16.5 Hz, *J* = 2 Hz, 1H, N-CH_aH_b-C(sp²)), 3.55 (dd, *J* = 8.5 Hz, *J* = 7 Hz, 1H, N-CH_aH_b-C(sp³)), 2.66 (m, 1H, CHMe), 2.63 (dd (apparent t), *J* = 8.5 Hz, 1H, N-CH_aH_b-C(sp³)), 2.42 (s, 3H, Ar-Me), 1.24 (s, 6H, Me on Bpin), 1.23 (s, 6H, Me on Bpin), 1.02 (d, *J* = 6.5 Hz, 3H, CH-Me). ¹³C{¹H} NMR (126 MHz, CDCl₃): δ 165.2 (s, C=C-Bpin), 143.6 (s, Ar), 132.8 (s, Ar), 129.7 (s, Ar), 127.9 (s, Ar), 109.0 (b, C=C-Bpin), 83.3 (s, C_{quart}, Bpin), 54.4 (s, CH₂), 52.7 (s, CH₂), 39.8 (s, C-Me), 25.0 (s, Me, Bpin), 24.9 (s, Me, Bpin), 21.6 (s, Me), 16.0 (s, Me). ¹¹B{¹H} NMR (128.2 MHz, CDCl₃): δ 29.3. Unit Mass (ESI) *m/z*: [M + H]⁺ Calcd for C₁₉H₂₉BNO₄S 378.19; Found 378.22.

Attempt to synthesize 303Bc-exo on 1.00 mmol scale. BINAP (19 mg, 0.03 mmol) was mixed with Rh(COD)₂OTf (14 mg, 0.03 mmol) in 7.5 mL of CH₂Cl₂ in a 100 mL Teflon screw-top flask. **303B** (375 mg, 1.00 mmol) was dissolved in 5 mL of

CH₂Cl₂ and added to the reaction mixture to make a concentration of 0.08 M. The flask was degassed using the freeze-pump-thaw technique and refilled with an atmosphere of dihydrogen. The reaction was stirred for 2 h at room temperature and the volatiles were removed under vacuum. Analysis of the reaction mixture by ¹H NMR spectroscopy showed that **303Bc-endo** was the major product and **303Bc-exo** was present in only trace amounts. Attempts to purify the product with column chromatography resulted in the decomposition of the alkylboronate on silica. Crude **303Bc-endo** was characterized by ¹H, ¹³C{¹H}, ¹¹B{¹H}, and ¹H-¹³C HSQC NMR spectroscopy.

3-methyl-4-(pinacolborylmethyl)-1-tosyl-2,3-dihydro-1H-pyrrole (303Bc-endo). ¹H (500 MHz, CDCl₃): δ 7.65 (d, *J* = 8.5 Hz, 2H, *Ar-H*), 7.29 (d, *J* = 8 Hz, 2H, *Ar-H*), 6.11 (dt (apparent q), *J* = 1.5 Hz, *J* = 1.5 Hz, 1H, *N-CH*), 3.62 (dd, *J* = 10.5 Hz, *J* = 10 Hz, 1H, *N-CH_aH_b*), 2.96 (dd, *J* = 10.5 Hz, *J* = 7 Hz, 1H, *N-CH_aH_b*), 2.67 (m, 1H, *CH-Me*), 2.41 (s, 3H, *Ar-Me*), 1.59 (d, *J* = 17 Hz, 1H, *CH_aH_b-Bpin*), 1.43 (d, *J* = 17.5 Hz, 1H, *CH_aH_b-Bpin*), 1.221 (s, 6H, *Me* on Bpin), 1.215 (s, 6H, *Me* on Bpin), 0.78 (d, *J* = 7 Hz, 3H, *CH-Me*). ¹³C{¹H} (100 Mhz, CDCl₃): δ 143.5 (s, *Ar-Me*), 133.1 (*Ar-S*), 129.6 (s, *Ar-H*), 128.0 (s, *Ar-H*), 124.0 (s, *N-CH*), 83.4 (s, *Bpin*), 55.1 (s, *N-CH₂*), 40.6 (s, *CH-Me*), 24.9 (s, *Me* on Bpin), 21.7 (s, *Ar-Me*), 18.3 (s, *CH-Me*), 9.4 (observed through cross peak with HSQC, *CH₂-Bpin*). ¹¹B{¹H} NMR (128.2 MHz, CDCl₃): δ 32.5.

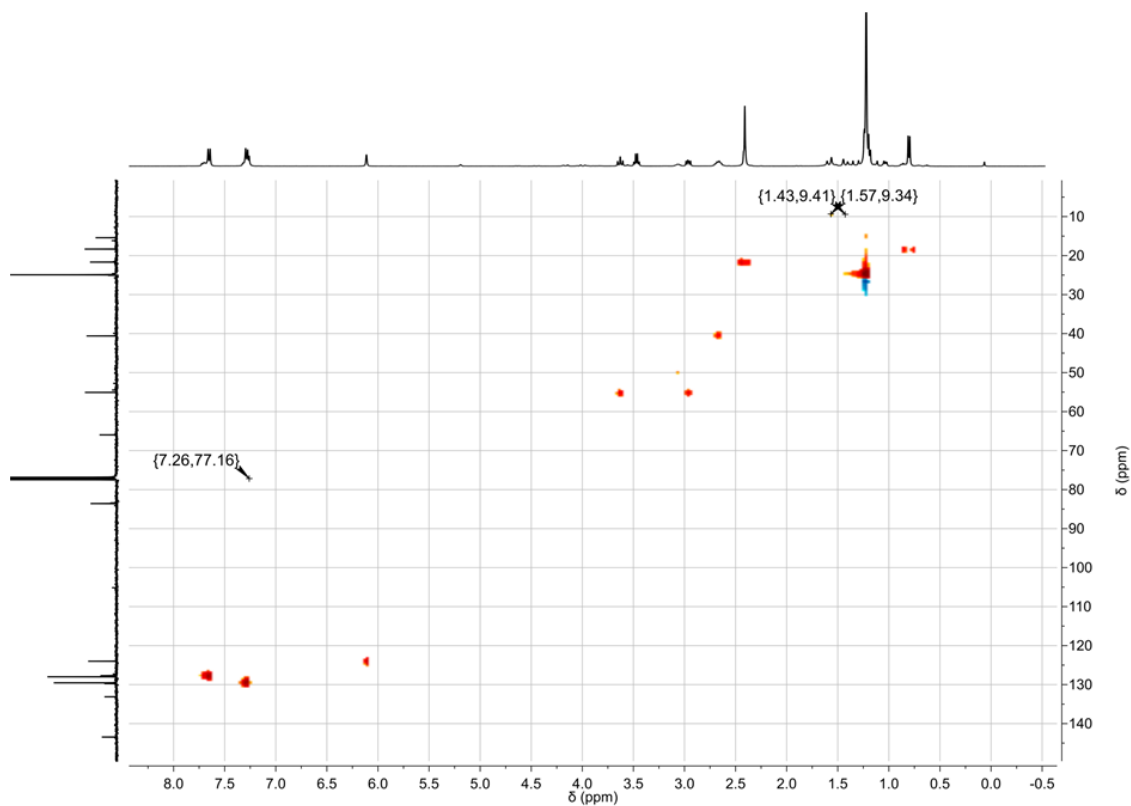


Figure III-1. ^1H - ^{13}C HSQC NMR spectrum of crude **303Bc-endo** in CDCl_3 . Resonances for residual pentane are visible at 0.88 and 1.27 ppm. Cross peak for CH_2 -Bpin ^1H - ^{13}C correlations highlighted at (1.43,9.41) and (1.57,9.34).

Attempt to synthesize 303Bc-endo via thermally induced isomerization. 3B

(38 mg, 0.10 mmol) was dissolved in 1.1 ml of 1,2-dichloroethane in a 25 mL Teflon screw-top flask and treated with (BINAP)Rh(COD)OTf (150 μL of a 0.02 M solution in CH_2Cl_2 , 0.003 mmol). The reaction vessel was degassed and filled with 1 atm of H_2 . The mixture was stirred for 2 h at room temperature, and then transferred to a 70 $^\circ\text{C}$ oil bath for 1 h. The volatiles were removed from the reaction and redissolved in a $\text{CDCl}_3/1,4$ -

dioxane solution. ^1H NMR integration versus the 1,4-dioxane internal standard showed a 88% yield of **3Bc-exo** and only trace amounts of the desired product.

Diethyl (E)-3-methyl-4-(pinacolborylmethylene)cyclopentane-1,1-dicarboxylate (301Bc-exo). BINAP (37 mg, 0.06 mmol) was mixed with $\text{Rh}(\text{COD})_2\text{OTf}$ (28 mg, 0.06 mmol) in 20 mL of CH_2Cl_2 in a 100 mL Teflon screw-top flask. **301B** (729 mg, 2 mmol) was dissolved in 5 mL of CH_2Cl_2 and added to the reaction mixture. The flask was degassed using the freeze-pump-thaw technique and refilled with an atmosphere of H_2 . The reaction was stirred at RT for 2 h. The volatiles were removed and the product was purified by auto column chromatography with 1:5 EA: Hexanes to yield a clear oil (455 mg, 62% yield). ^1H NMR (500 MHz, CDCl_3): δ 5.17 (dt apparent q, $J = 2.5$ Hz, 1H, =CH), 4.17 (q, $J = 7$ Hz, 2H, OCH_2), 4.17 (q, $J = 7.5$ Hz, 2H, OCH_2), 3.34 (dt, $J = 18.5$ Hz, $J = 1.5$ Hz, 1H, CH_aH_b - C(sp 2)), 3.15 (dt, $J = 18.5$ Hz, $J = 2.5$ Hz, 1H, CH_aH_b - C(sp 2)), 2.57 (m, 2H, overlapping signals, CH_aH_b and CHMe), 1.70 (dd, $J = 12$ Hz, $J = 11$ Hz, 1 H, CH_aH_b), 1.239 (s, 6H, *Me* on Bpin), 1.236 (s, 6H, *Me* on Bpin), 1.23 (m, 6H, overlapping OCH_2Me signals), 1.08 (d, $J = 6.5$ Hz, 3H, CHMe). $^{13}\text{C}\{^1\text{H}\}$ NMR (126 MHz, CDCl_3): δ 172.2 (s, C=O), 172.1 (s, C=O), 170.4 (s, C=CBpin), 108.5 (bs, C=CBpin), 82.9 (s, Bpin), 61.53 (s, OCH_2), 61.52 (s, OCH_2), 58.5 (s, $\text{C}_{\text{quart.}}$), 41.5 (s), 40.9 (s), 40.1 (s), 25.01 (s, *Me* on Bpin), 24.97 (s, *Me* on Bpin), 17.8 (s, CHMe), 14.2 (s, *Me*), 14.2 (s, *Me*). $^{11}\text{B}\{^1\text{H}\}$ NMR (128.2 MHz, CDCl_3): δ 29.9. Unit Mass (ESI) m/z : $[\text{M} + \text{H}]^+$ Calcd for $\text{C}_{19}\text{H}_{32}\text{BO}_6$ 367.23; Found 367.24.

(Z)-4,4,5,5-tetramethyl-2-((3-methyl-1-oxaspiro[4.5]decan-4-ylidene)methyl)-1,3,2-dioxaborolane (305Bc-exo). BINAP (37 mg, 0.06 mmol) was mixed with

Rh(COD)₂OTf (28 mg, 0.06 mmol) in 20 mL of CH₂Cl₂ in a 100 mL Teflon screw-top flask. **305B** (584 mg, 2 mmol) was dissolved in 5 mL of CH₂Cl₂ and added the reaction mixture. The flask was degassed using the freeze-pump-thaw technique and was refilled with an atmosphere of H₂. The reaction was stirred for 2 h at RT. The volatiles were then removed and the product was extracted with pentane and filtered through Celite. The product was purified by auto column with 1:15 EA:Hexanes to yield a clear oil (410 mg, Yield 70%). ¹H NMR (500 MHz, CDCl₃): δ 5.16 (d, *J* = 2.5 Hz, 1H, =CH), 3.97 (dd, *J* = 8.5 Hz, *J* = 7.5 Hz, 1H, CH_aH_b), 3.31 (dd (apparent t), *J* = 9 Hz, 1H, CH_aH_b), 2.73 (m, 1H, C-H), 2.10 (m, 1H, Cy), 1.95 (m, 1H, Cy), 1.28 (s, 12H, Me on Bpin), 1.05 (d, *J* = 7 Hz, 3H, CH-Me); ¹³C{¹H} NMR (100 MHz, CDCl₃): δ 176.5 (s, C_{sp}²), 84.8 (s, C_{quart.}), 83.4 (s, C_{quart.} Bpin), 70.7 (s, O-CH₂), 42.2 (s, CHMe), 35.1 (s, Cy), 33.7 (s, Cy), 25.3 (s, Cy), 25.1 (s, Me on Bpin), 25.0 (s, Me on Bpin), 23.0 (s, Cy), 22.9 (s, Cy), 16.4 (s, Me); ¹¹B{¹H} NMR (128.2 MHz, CDCl₃): δ 29.7. Unit Mass (ESI) *m/z*: [M + H]⁺ Calcd for C₁₇H₂₉BO₃ 293.23; Found 293.12.

4-(pinacolborylmethyl)-3-methyl-2,3-dihydrofuran (304Bc-endo). Observed *in situ* ¹H NMR (500 MHz, CDCl₃): δ 6.12 (dt (apparent q), *J* = 2 Hz, *J* = 1.5 Hz, 1H, O-CH=C), 4.38 (dd, *J* = 10 Hz, *J* = 9 Hz, 1H, OCH_aH_b), 3.76 (dd, *J* = 8.5 Hz, 8 Hz, 1H, OCH_aH_b), 2.86 (m, 1H, CH-Me), 1.59 (d, *J* = 17 Hz, 1H, CH_aH_bBpin), 1.44 (d, *J* = 17 Hz, 1H, CH_aH_bBpin), 1.24 (s, 12H, Me on Bpin), 1.04 (d, *J* = 6.5 Hz, 3H, CHMe).

(Z)-3-(pinacolborylmethylene)-4-methyltetrahydrofuran (304Bc-exo). Observed *in situ* ¹H NMR (500 MHz, CDCl₃): δ 5.24 (dt (apparent q), *J* = 2.5 Hz, *J* = 2 Hz, 1H, =CH-Bpin), 4.57 (dd, *J* = 15.5 Hz, *J* = 2 Hz, 1H, OCH_aH_b), 4.45 (dd, *J* = 15.5

Hz, $J = 2.5$ Hz, 1H, OCH_aH_b), 4.05 (m, 1H, $\text{OCH}_a\text{H}_b\text{-CHMe}$), 3.30 (dd (apparent t), $J = 8$ Hz, 1H, $\text{OCH}_a\text{H}_b\text{-CHMe}$), 2.69 (m, 1H, CHMe), 1.25 (s, 6H, *Me* on Bpin), 1.22 (s, 6H, *Me* on Bpin), 1.07 (d, $J = 7$ Hz, 3H, CHMe).

3-methyl-1-phenyl-4-(pinacolborylmethyl)-2,3-dihydro-1H-pyrrole (302Bc-endo). Observed *in situ* ^1H NMR (500 MHz, CDCl_3): δ 7.20 (dd, $J = 8.5$ Hz, $J = 7$ Hz, 2H, Ar-*H*), 6.66 (t, $J = 7$ Hz, 1H, Ar-*H*), 6.63 (d, $J = 8$ Hz, 2H, Ar-*H*), 6.47 (dt (apparent q), $J = 1.5$ Hz, $J = 1.5$ Hz, 1H, N- $\text{CH}=\text{C}$), 3.83 (dd (apparent t), $J = 10$ Hz, $J = 10$ Hz, 1H, NCH_aH_b), 3.16 (dd, $J = 10$ Hz, $J = 7$ Hz, 1H, NCH_aH_b), 2.99 (m, 1H, CHMe), 1.76 (d, $J = 17$ Hz, 1H, $\text{CH}_a\text{H}_b\text{Bpin}$), 1.63 (d, $J = 17$ Hz, 1H, $\text{NCH}_a\text{H}_b\text{Bpin}$), 1.28 (s, 12H, *Me* on Bpin), 1.13 (d, $J = 7$ Hz, CHMe).

(Z)-3-methyl-1-phenyl-4-(pinacolborlylmethylene)pyrrolidine (302Bc-exo). Observed *in situ* ^1H NMR (500 MHz, CDCl_3): δ (selected signals reported) 5.32 (dt (apparent q), $J = 2.5$ Hz, $J = 2.5$ Hz, 1H, $\text{C}=\text{CH-Bpin}$), 4.24 (dd, $J = 16.5$ Hz, $J = 1.5$ Hz, 1H, $\text{NCH}_a\text{H}_b\text{-C}=\text{}$), 4.13 (ddd, $J = 16.5$ Hz, $J = 2$ Hz, $J = 2$ Hz, 1H, $\text{NCH}_a\text{H}_b\text{-C}=\text{}$), 3.65 (dd (apparent t), $J = 9$ Hz, $J = 9$ Hz, 1H, $\text{NCH}_a\text{H}_b\text{-CH}$), 2.85 (dd (apparent t), $J = 8.5$ Hz, $J = 8.5$ Hz, 1H, $\text{NCH}_a\text{H}_b\text{-CH}$), 1.12 (d, $J = 7$ Hz, 3H, CHMe).

3.4.5 Synthesis and Characterization of [2+2+2] Cyclization Product

Synthesis of 302Bd-a. BINAP (37 mg, 0.06 mmol) was mixed with $\text{Rh}(\text{COD})\text{-}_2\text{BF}_4$ (24 mg, 0.06 mmol) in 25 mL THF in a 50 mL Teflon screw-top flask. **302B** (750 mg, 2.0 mmol) was added to the reaction mixture. The reaction mixture was heated for 2 h at 70 °C. After this time, the volatiles were removed under vacuum and the resulting cakey solid was dissolved in toluene and treated with 1 atm of CO to precipitate the

cationic rhodium catalyst. The solution was filtered through a pad of Celite. The volatiles were removed and the product was recrystallized from a concentrated solution of dichloromethane layered with pentane to yield an off-white powder (642 mg, 86% yield). The structure was determined to be the regioisomer with the pinacolboryl substituents on C₄ and C₆ by a ¹H-¹³C HMBC experiment in C₆D₆. ¹H NMR (500 MHz, CDCl₃): δ 7.70 (d, *J* = 8.5 Hz, 2H, Ar-*H*), 7.68 (d, *J* = 8 Hz, 2H, Ar-*H*), 7.31 (d, *J* = 8 Hz, 2H, Ar-*H*), 7.27 (d, *J* = 8 Hz, 2H, Ar-*H*), 5.38 (ddt, *J* = 17 Hz, *J* = 10.5 Hz, *J* = 6 Hz, 1H, CHCH=CH₂), 4.87 (dd, *J* = 17.5 Hz, *J* = 1 Hz, 1H, CHCH=CH_aH_b), 4.76 (dd, *J* = 10 Hz, *J* = 1 Hz, 1H, CHCH=CH_aH_b), 4.66 (dd, *J* = 12.5 Hz, *J* = 2.5 Hz, 1H, NCH_aH_bC=CBpin), 4.44 (d, *J* = 18 Hz, 1H, off ring NCH_aH_b), 4.24 (d, *J* = 12.5 Hz, 1H, NCH_aH_bC=CBpin), 3.92 (d, *J* = 18 Hz, 1H, off ring NCH_aCH_b), 3.82 (t, *J* = 8.5 Hz, 1H, NCH_aH_bCH), 3.47 (dd, *J* = 16.5 Hz, *J* = 6.5 Hz, 1H, NCH_aH_bCH=CH₂), 3.39 (dd, *J* = 16.5 Hz, *J* = 6.5 Hz, 1H, NCH_aH_bCH=CH₂), 2.62 (t, *J* = 9 Hz, 1H, NCH_aH_bCH), 2.410 (s, 6H, Ar-*Me*), 2.406 (s, 6H, Ar-*Me*), 2.36 (overlapping m, 2H, CH-CH_aH_b-Bpin), 1.54 (m, 1H, CH), 1.36 (s, 6H, *Me* on Bpin), 1.303 (s, 6H, *Me* on Bpin), 1.12 (s, 6H, *Me* on Bpin), 1.05 (s, 6H, *Me* on Bpin). Assignments assisted with the aid of ¹H-¹H COSY and ¹H-¹³C HSQC. ¹H NMR (400.13 MHz, C₆D₆): δ 7.77 (d, *J* = 8 Hz, 2H, Ar-*H*), 7.74 (d, *J* = 8 Hz, 2H, Ar-*H*), 6.82 (d, *J* = 8 Hz, 2H, Ar-*H*), 6.77 (d, *J* = 8 Hz, 2H, Ar-*H*), 5.66 (ddt, *J* = 17 Hz, *J* = 11 Hz, *J* = 7 Hz, 1H, CH₂CH=CH₂), 5.18 (dd, *J* = 12 Hz, *J* = 3 Hz, 1H, off ring CH_aH_bNTs), 4.89 (ddt, *J* = 17 Hz, *J* = 2 Hz, *J* = 1 Hz, 1H, CH=CH_aH_b), 4.83 (dd, *J* = 18 Hz, 1H, NCH_aH_b-C=CBpin), 4.69 (ddt, *J* = 10 Hz, *J* = 2 Hz, *J* = 2 Hz, 1H, CH=CH_aH_b), 4.48 (d, *J* = 12 Hz, 1H, off ring CH_aH_bNTs), 4.37 (dd, *J* = 18 Hz, *J* = 2 Hz,

1H, NCH_aH_b-C=CBpin), 3.76 (dd, *J* = 10 Hz, *J* = 8 Hz, 1H, NCH_aH_b-CH), 3.70 (ddt, *J* = 17 Hz, *J* = 6 Hz, *J* = 2 Hz, 1H, NCH_aH_bCH=CH₂), 3.63 (ddt, *J* = 16 Hz, *J* = 6 Hz, *J* = 2 Hz, 1H, NCH_aH_bCH=CH₂), 2.59 (dd (apparent t), *J* = 10 Hz, 1H, NCH_aH_b-CH), 2.39 (dd, *J* = 17 Hz, *J* = 7 Hz, 1H, C₇H_aH_b), 2.15 (m, 1H, C₈H), 1.96 (s, 3H, Ar-Me), 1.87 (s, 3H, Ar-Me), 1.30 (s, 6H, Me on Bpin), 1.29 (overlapped m, 1H, C₇H_aH_b), 1.24 (s, 6H, Me on Bpin), 0.91 (s, 6H, Me on Bpin), 0.86 (s, 6H, Me on Bpin). ¹³C{¹H} NMR (100.69 MHz, C₆D₆): δ 159.5 (s, C₃), 149.0 (s, C₅), 143.0 (s, Ar-Me), 142.4 (s, Ar-Me), 137.1 (s, Ar-S), 135.1 (s, Ar-S), 135.0 (s, NCH₂CH=CH₂), 129.7 (s, Ar-H), 129.4 (s, Ar-H), 128.5 (s, Ar-H), 128.2 (s, Ar-H), 116.4 (s, CH=CH₂), 84.2 (s, Me on Bpin), 83.2 (s, Me on Bpin), 54.1 (s, C₉), 53.2 (s, C₂), 51.1 (s, C₅-CH₂), 49.9 (NCH₂CH=CH₂), 38.8 (s, C₈), 29.4 (s, C₇), 25.9 (s, Me on Bpin), 24.8 (s, Me on Bpin), 24.7 (s, Me on Bpin), 24.6 (s, Me on Bpin), 21.1 (overlapping s, 2x C, Ar-Me). C₄ and C₆ were not observed due to their proximity to Boron. ¹H-¹³C HSQC and ¹H-¹³C HMBC was used to assign peaks. ¹¹B{¹H} NMR (128.2 MHz, CDCl₃): δ 30.6. Unit Mass (ESI) m/z: [M + Na]⁺ calcd for C₃₈H₅₂B₂N₂O₈S₂ 773.32; Found 773.49.

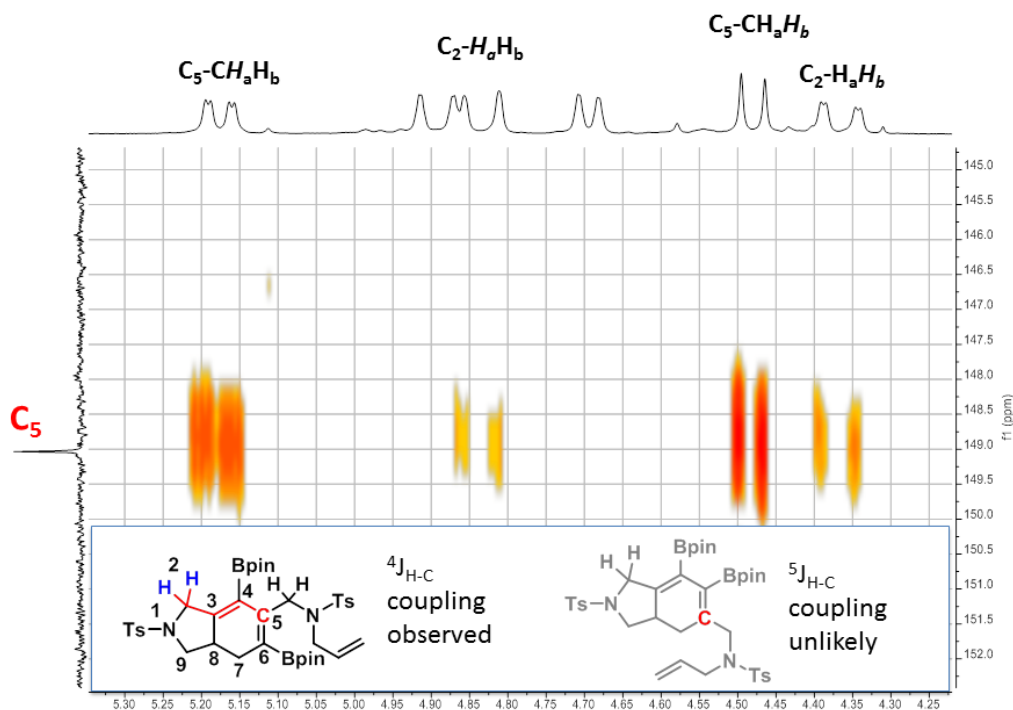


Figure III-2. ^1H - ^{13}C HMBC spectrum of **302Bd-a** indicating the correlation between the proton on C_2 with C_5 .

3.4.6 Reductive Cyclization of Borylated 1,6-Diynes

3.4.6.1 General Procedure for Substrate Screening

The substrate (500 μL , 0.2 M solution in CH_2Cl_2 , 0.1 mmol) was added to a 25 mL Teflon screw-top flask and diluted with CH_2Cl_2 to achieve the desired final volume. The rhodium catalyst (BINAP)Rh(COD)OTf or (BINAP)Rh(COD)BF₄ (3% Loading = 0.003 mmol, 150 μL of a 0.02 M solution in CH_2Cl_2 / 5% Loading = 0.005 mmol, 250 μL of a 0.02 M solution in CH_2Cl_2) was added to the solution. When Rh(COD)₂OTf was

used with a ligand to make the catalyst *in situ*, Rh(COD)₂OTf (0.003 mmol, 150 μL of a 0.02 M solution in CH₂Cl₂) and BIPHEP (3% Loading = 0.003 mmol, 150 μL of a 0.02 M in CH₂Cl₂). The reaction vessel was degassed using the freeze-pump-thaw method and refilled with an atmosphere of H₂. The reaction was then stirred at room temperature for 2 h or 4 h. If the application of heat were necessary, the reaction flask was moved to a 60 °C oil bath for 1.5 h. The volatiles were then removed and 0.600 mL of a 0.063 M solution of 1,4-dioxane in CDCl₃ was used to extract the reaction mixture to a J. Young tube. ¹H NMR integration versus the 1,4-dioxane internal standard was used to determine the yield of the product. The integration was compared to an equimolar amount of the substrate in another 0.600 mL aliquot of the same 1,4-dioxane solution.

3.4.6.2 Synthesis and Characterization of Organic Products

(3E,4E)-3,4-bis(pinacolborylmethylene)cyclopentane-1,1-dicarboxylate

(306B₂c-exo). (BINAP)Rh(COD)OTf (59 mg, 0.06 mmol) was dissolved in 25 mL of CH₂Cl₂ in a 100 mL teflon screw-top flask. **306B₂** (920 mg, 2 mmol) was added to the reaction mixture. The vessel was degassed using the freeze-pump-thaw technique and filled with 1 atm of H₂. The reaction was stirred for 2 h and then the volatiles were removed under vacuum. The product was extracted with toluene and filtered through a pad of Celite. The volatiles were removed and the product was recrystallized from CH₂Cl₂ layered with pentane (647 mg, 70% yield). ¹H NMR (500 MHz, CDCl₃): δ 5.87 (t, *J* = 2 Hz, 2H, =CHBpin), 3.73 (s, 6H, CO₂Me), 3.31 (d, *J* = 2 Hz, 4H, CH₂), 1.26 (s, 24H, Bpin); ¹³C{¹H} NMR (126 MHz, CDCl₃): δ 172.3 (s, CO₂), 159.3 (C_{quat}=C), 109.7 (br. s, C=CBpin), 83.2 (s, Bpin), 57.8 (s, C_{quat}), 52.9 (s, OMe), 40.8 (CH₂), 25.0 (Me on

Bpin); $^{11}\text{B}\{^1\text{H}\}$ NMR (128.2 MHz, CDCl_3): δ 29.7. Unit Mass (ESI) m/z : $[\text{M} + \text{Na}]^+$
Calcd for $\text{C}_{23}\text{H}_{36}\text{B}_2\text{O}_8$ 485.25; Found 485.73.

3,4-bis(pinacolborylmethyl)-1-tosyl-1H-pyrrole (308B₂c-pyr). In a 50 mL Teflon screw-top flask, BINAP (15 mg, 0.024 mmol) and $\text{Rh}(\text{COD})_2\text{OTf}$ (11 mg, 0.024 mmol) was dissolved in 5 mL CH_2Cl_2 . **308B₂** (400 mg, 0.80 mmol) was dissolved in 5 mL of CH_2Cl_2 and was added to the reaction mixture. The vessel was degassed using the freeze-pump-thaw technique and filled with 1 atm of H_2 . The reaction was stirred for 2 h and then the volatiles were removed under vacuum. The resulting solid was dissolved in toluene and the headspace was removed and replaced with an atmosphere of CO. The cationic rhodium species precipitated from solution and the reaction mixture was filtered through a pad of Celite. The volatiles were removed and the product was extracted with pentane. The pentane solution containing the product was placed into a $-35\text{ }^\circ\text{C}$ freezer overnight, where a yellow oil precipitated. The pentane supernatant was poured off and the volatiles were removed. The product was isolated as a light yellow oil (264 mg, 66% yield). ^1H NMR (500 MHz, CDCl_3): δ 7.67 (d, $J = 8.5$ Hz, 2H, Ar-H), 7.22 (d, $J = 8$ Hz, 2H, Ar-H), 6.93 (s, 2H, pyrrole C-H), 2.37 (s, 3H, Ar-Me), 1.87 (s, 4H, CH_2Bpin), 1.22 (s, 12H, Me on Bpin); $^{13}\text{C}\{^1\text{H}\}$ NMR (126 MHz, CDCl_3): δ 144.10 (s, Ar-Me), 136.7 (s, Ar-S), 129.6 (s, Ar-H), 126.6 (s, Ar-H), 125.6 (s, Pyrrole C- CH_2), 118.0 (s, Pyrrole-H), 83.3 (s, BPin), 24.8 (s, Me on Bpin), 21.5 (s, Ar-Me), 8.1 (br. s, CH_2Bpin); $^{11}\text{B}\{^1\text{H}\}$ NMR (128.2 MHz, CDCl_3): δ 32.5. Unit Mass (ESI) m/z : $[\text{M} + \text{H}]^+$ Calcd for $\text{C}_{25}\text{H}_{37}\text{B}_2\text{NO}_6\text{S}$ 502.26; Found 502.31.

(**3Z**, **4Z**)-**3-ethylidene-4-(pinacolborylmethylene)-1-tosylpyrrolidine (308MeBc-exo)**. Rh(COD)₂OTf (28 mg, 0.06 mmol) and BINAP (37 mg, 0.06 mmol) was dissolved in 25 mL of CH₂Cl₂ and mixed for about 5 min. **308MeB** (775 mg, 2.0 mmol) was added to the reaction mixture. The headspace was removed and refilled with an atmosphere of dihydrogen. The reaction was then stirred at room temperature for 2 h at RT. The volatiles were removed under vacuum, and an atmosphere of carbon monoxide was added to the mixture to precipitate the cationic rhodium catalyst. The solution was filtered through Celite and the volatiles were removed. The product was isolated by autocolumn chromatography (1:3 EA: Hexane) and recrystallized from a solution of dichloromethane layered with pentane (39 mg, 9% yield). ¹H NMR (500 MHz, CDCl₃): δ 7.73 (d, *J* = 8 Hz, 2H, Ar-*H*), 7.32 (d, *J* = 8 Hz, 2H, Ar-*H*), 6.01 (qt, *J* = 7 Hz, *J* = 2.5 Hz, 1H, C=*CH*Me), 5.56 (t, *J* = 1 Hz, 1H, C=*CH*Bpin), 4.21 (d, *J* = 2.5 Hz, 2H, CH₂C=C(H)(Bpin)), 3.93 (m, 2H, CH₂C=C(H)(Me)), 2.41 (s, 3H, Ar-*Me*), 1.67 (d, *J* = 7.5 Hz, 3H, C=C(H)(*Me*)), 1.25 (s, 12H, *Me* on Bpin); ¹³C{¹H} NMR (126 MHz, CDCl₃): δ 155.0 (s, C=), 143.7 (s, C=), 135.7 (s, Ar-*Me*), 133.0 (s, Ar-*S*), 129.8 (s, Ar-*H*), 127.9 (s, Ar-*H*), 119.7 (=C(Me)(H)), 83.4 (s, Bpin), 53.9 (s, N-CH₂) 50.4 (s, N-CH₂), 24.9 (s, *Me* on Bpin), 21.7 (Ar-*Me*), 15.2 (s, C=*CMe*), =CHBpin could not be observed; ¹¹B{¹H} NMR (128.2 MHz, CDCl₃): δ 29.5. Unit Mass (ESI) *m/z*: [M + Na]⁺ Calcd for C₂₀H₂₈BNO₄S 412.17; Found 412.45.

3-ethyl-4-(pinacolborylmethyl)-1-(tosyl)-1*H*-pyrrole (308MeBc-pyr). In a 50 mL Teflon screw-top flask BINAP (20 mg, 0.032 mmol) and Rh(COD)₂OTf (15 mg, 0.032 mmol) was dissolved in 10 mL of CH₂Cl₂. **308MeB** (418 mg, 1.08 mmol) was

dissolved in 3.5 mL of CH₂Cl₂ and was added to the reaction mixture. The vessel was degassed using the freeze-pump-thaw technique and filled with 1 atm of H₂. The reaction was stirred for 2 h and then transferred to a 60 °C oil bath for 1.5 h. The flask was removed from the oil bath and the volatiles were removed under vacuum. The resulting sticky solid was dissolved in toluene and the headspace of the flask was removed and replaced with an atmosphere of CO. The cationic rhodium catalyst precipitated from solution and the solvent was filtered through a pad of Celite. The resulting sticky solid was dissolved in THF and layered with pentane and placed in a -35 °C freezer overnight. A yellow solid precipitated, and the supernatant was filtered through a pad of Celite and the volatiles were removed. The product was isolated from the supernatant as a light yellow oil (234 mg, 56% yield). The product ¹H NMR (500 MHz, CDCl₃): δ 7.69 (d, *J* = 8 Hz, 2H, Ar-*H*), 7.25 (d, *J* = 8 Hz, 2H, Ar-*H*), 6.94 (m, 1H, pyrrole C-*H*), 6.80 (m, 1H, pyrrole C-*H*), 2.38 (s, 3H, Ar-*Me*), 2.30 (dq, *J* = 7.5 Hz, *J* = 1.5 Hz, 2H, CH₂Me), 1.87 (s, 2H, CH₂Bpin), 1.23 (s, 12H, Me on Bpin), 1.12 (t, *J* = 7.5 Hz, 3H, CH₂Me); ¹³C{¹H} NMR (126 MHz, CDCl₃): δ 144.35 (s, Ar-*Me*), 132.0 (s, Ar-*S*), 129.8 (s, Ar-*H*), 126.8 (s, Ar-*H*), 124.7 (s, Pyrrole-CH₂Bpin), 118.3 (s, Pyrrole-*H*), 116.8 (s, Pyrrole-Et), 83.6 (s, Bpin), 24.9 (s, Me on Bpin), 21.7 (s, Ar-*Me*), 18.6 (s, CH₂Me), 13.3 (s, CH₂Me); ¹¹B{¹H} NMR (128.2 MHz, CDCl₃): δ 32.7. Unit Mass (ESI) *m/z*: [M + H]⁺ Calcd for C₂₀H₂₈BNO₄S 390.19; Found 390.23.

3,4-bis(pinacolboryl)methyl-1-(*p*-tolyl)-1*H*-pyrrole (309B₂c-pyr). In a 100 mL Teflon screw-top flask, Rh(COD)₂OTf (28 mg, 0.06 mmol) and BINAP (37 mg, 0.06 mmol) was dissolved in 25 mL of CH₂Cl₂. **309B₂** (870 mg, 2.0 mmol) was added to the

reaction mixture. The solution was degassed using the freeze-pump-thaw method and refilled with an atmosphere of dihydrogen. The reaction was stirred for 2 h at room temperature. The volatiles were removed and the product was redissolved in toluene. The solution was then treated with an atmosphere of CO, upon stirring for 15 min., the solution turned from red to yellow and a precipitate formed. The reaction was filtered through Celite and the volatiles were removed. The product was recrystallized from pentane in a -35 °C freezer to yield a light yellow solid (747 mg, 85% yield). ^1H NMR (500 MHz, CDCl_3): δ 7.21 (d, $J = 8.5$ Hz, 2H, Ar-*H*), 7.15 (d, $J = 8.5$ Hz, 2H, Ar-*H*), 6.90 (s, 2H, NC-*H*), 2.34 (s, 3H, Ar-*Me*), 2.05 (s, 4H, CH_2 -Bpin), 1.28 (2, 24H, *Me* on Bpin); $^{13}\text{C}\{^1\text{H}\}$ NMR (126 MHz, CDCl_3): δ 138.8 (s, $\text{C}_{\text{Ar-N}}$), 133.6 (s, C-*Me*), 129.8 (s, Ar-*H*), 120.6 (s, C- CH_2), 119.2 (s, Ar-*H*), 116.7 (s, pyrrole C-*H*), 83.1 (s, Bpin), 24.9 (*Me* on Bpin), 20.8 (Ar-*Me*), 8.2 (br. s, CH_2 -Bpin); $^{11}\text{B}\{^1\text{H}\}$ NMR (128.2 MHz, CDCl_3): δ 33.5. Unit mass (ESI) m/z : $[\text{M} + \text{Na}]^+$ calcd for $\text{C}_{25}\text{H}_{37}\text{B}_2\text{NO}_4$ 460.28; Found 460.34.

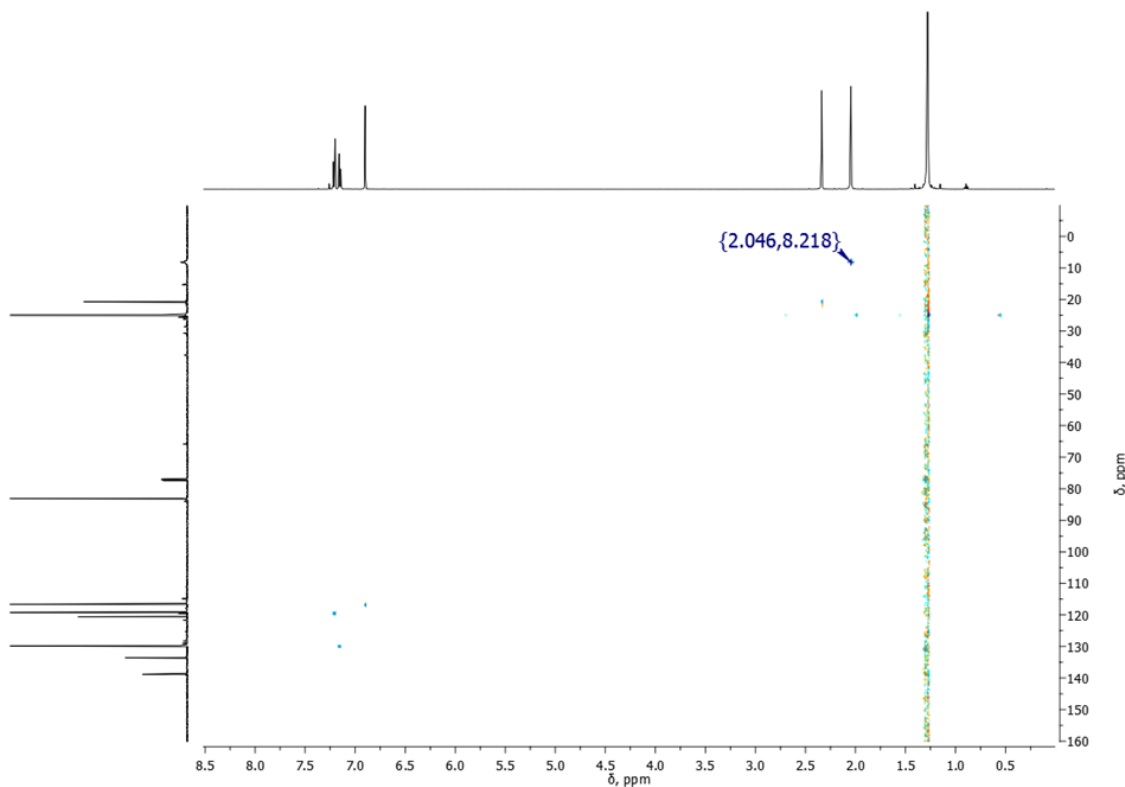


Figure III-3. ^1H - ^{13}C HSQC NMR spectrum of **309B₂c-pyr** in CDCl_3 . Crosspeak highlighted at (2.046,8.218) to show the ^1H - ^{13}C correlation between CH_2 -Bpin.

3-ethyl-4-(pinacolborylmethyl)-1-(*p*-tolyl)-1*H*-pyrrole (309MeBc-pyr). In a 100 mL Teflon screw-top flask, $\text{Rh}(\text{COD})_2\text{OTf}$ (28 mg, 0.06 mmol) and BINAP (37 mg, 0.06 mmol) was dissolved in 25 mL of CH_2Cl_2 . **309MeB** (646 mg, 2 mmol) was added to the reaction mixture. The solution was degassed using the freeze-pump-thaw method and refilled with an atmosphere of dihydrogen. The reaction was stirred for 2 h at room temperature. The volatiles were removed and the product was redissolved in diethyl ether. The reaction mixture was filtered through a pad of Celite, and the volatiles were removed. The product was extracted with cold pentane ($-35\text{ }^\circ\text{C}$) and filtered through a

plug of Celite, and the volatiles were removed to yield a yellow oil (431 mg, 66% yield). ^1H NMR (500 MHz, CDCl_3): δ 7.22 (d, $J = 8.5$ Hz, 2H, Ar-*H*), 7.16 (d, $J = 8.5$ Hz, 2H, Ar-*H*), 6.90 (m, 1H, pyr-*H*), 6.78 (m, 1H, pyr-*H*), 2.47 (dq, $J = 7.5$ Hz, $J = 1$ Hz, 2H, CH_2Me), 2.34 (s, 3H, Ar-*Me*), 2.05 (s, 2H, CH_2Bpin), 1.27 (s, 12H, *Me* on Bpin), 1.22 (t, $J = 7.5$ Hz, 3H, CH_2Me); $^{13}\text{C}\{^1\text{H}\}$ NMR (126 MHz, CDCl_3): δ 138.8 (s, Ar-N), 134.1 (s, Ar-*Me*), 130.0 (s, Ar-*H*), 127.6 (s, pyr- CH_2), 119.8 (s, Pyr- CH_2), 119.5 (s, Ar-*H*), 117.1 (s, pyr-*H*), 115.6 (s, pyr-*H*), 83.4 (s, Bpin), 25.0 (s, *Me* on Bpin), 20.9 (s, Ar-*Me*), 18.7 (s, CH_2), 14.4 (s, CH_3); $^{11}\text{B}\{^1\text{H}\}$ NMR (128.2 MHz, CDCl_3): δ 33.4. Unit Mass (ESI) m/z : $[\text{M} + \text{H}]^+$ Calcd for $\text{C}_{20}\text{H}_{28}\text{BNO}_2$ 326.22; Found 326.27.

3,4-bis(pinacolborylmethyl)-1-benzyl-1*H*-pyrrole (310B₂c-pyr). In a 100 mL Teflon screw-top flask, $\text{Rh}(\text{COD})_2\text{OTf}$ (47 mg, 0.10 mmol) and BINAP (62 mg, 0.10 mmol) was dissolved in 25 mL of CH_2Cl_2 . **310B₂** (870 mg, 2.0 mmol) was added the flask. The solution was degassed using the “freeze-pump-thaw” technique and the headspace was refilled with an atmosphere of dihydrogen. The reaction was stirred for 4 h at room temperature and the volatiles were removed under vacuum. The resulting solid was dissolved in a toluene and treated with 1 atm of carbon monoxide to precipitate the cationic rhodium catalyst. The solution was filtered through Celite and recrystallized from a solution in diethyl ether layered with pentane to yield (744 mg, 85% yield) of a yellow solid. ^1H NMR (500 MHz, CDCl_3): δ 7.29 (t, $J = 7.5$ Hz, 2H, Ar-*H*), 7.23 (t, $J = 7.5$ Hz, 1H, Ar-*H*), 7.10 (d, $J = 8$ Hz, 2H, Ar-*H*), 6.47 (s, 2H, pyrrole C-*H*), 4.92 (s, 2H, N- CH_2), 1.97 (s, 4H, CH_2Bpin), 1.23 (s, 24H, *Me* on Bpin); $^{13}\text{C}\{^1\text{H}\}$ (126 MHz, CDCl_3): δ 139.1 (s, Ar- CH_2N), 128.6 (s, Ar-*H*), 127.3 (s, Ar-*H*), 127.2 (s, Ar-*H*), 119.1 (s, pyrrole

C-H), 118.4 (s, pyrrole C-CH₂), 83.1 (s, Bpin), 53.2 (N-CH₂), 25.0 (s, Me on Bpin), CH₂-Bpin not observed. ¹¹B{¹H} NMR (128.2 MHz, CDCl₃): δ 33.4. Unit Mass (ESI) m/z [M + H]⁺ calcd. for C₂₅H₃₈B₂NO₄ 438.30; Found 438.46.

3,4-bis(pinacolborylmethyl)-1-hexyl-1H-pyrrole (311B₂c-pyr). In a 100 mL Teflon screw-top flask, Rh(COD)₂OTf (47 mg, 0.10 mmol) and BINAP (62 mg, 0.10 mmol) was dissolved in 25 mL of CH₂Cl₂. **311B₂** (870 mg, 2.0 mmol) was added the flask. The solution was degassed using the “freeze-pump-thaw” technique and the headspace was refilled with an atmosphere of dihydrogen. The reaction was stirred for 4 h at room temperature and the volatiles were removed under vacuum. The resulting solid was dissolved in a toluene and treated with 1 atm of carbon monoxide to precipitate the cationic rhodium catalyst. The volatiles were removed and the product was extracted with pentane and filtered through Celite to yield a yellow-brown oil (705 mg, 82% yield). ¹H NMR (500 MHz, CDCl₃): δ 6.43 (s, 2H, pyrrole C-H), 3.69 (t, *J* = 7 Hz, 2H, N-CH₂), 1.95 (s, 4H, CH₂Bpin), 1.69 (pent, *J* = 7.5 Hz, 2H, CH₂), 1.28 (m, 6H, Hex), 1.25 (s, 24H, Me on Bpin), 0.87 (t, *J* = 7 Hz, 3H, CH₃); ¹³C{¹H} (126 MHz, CDCl₃): δ 118.3 (s, Pyrrole C-N), 117.4 (s, Pyrrole C-CH₂), 83.0 (s, Bpin), 49.4 (s, CH₂N), 31.6 (s, Hex), 31.5 (s, Hex), 26.2 (s, Hex), 24.9 (s, Me on Bpin), 22.6 (s, Hex), 14.1 (s, Me on Bpin), 8.0 (br. s, CH₂Bpin); ¹¹B{¹H} NMR (128.2 MHz, CDCl₃): δ 33.4 (s). Unit Mass (ESI) m/z: [M + H]⁺ calcd. for C₂₄H₄₄B₂NO₄ 432.34; Found 432.43.

Tert-butyl 3,4-bis(pinacolborylmethyl)-1H-pyrrole-1-carboxylate (312B₂c-pyr). In a 100 mL Teflon screw-top flask, Rh(COD)₂OTf (23 mg, 0.05 mmol) and BINAP (30 mg, 0.05 mmol) was dissolved in 20 mL of dichloromethane. **312B₂** (714

mg, 1.6 mmol) was added the flask. The solution was degassed using the “freeze-pump-thaw” technique and the headspace was refilled with an atmosphere of dihydrogen. The reaction was stirred for 2 h at room temperature and the volatiles were removed under vacuum. The product was extracted with pentane and filtered through Celite. The volatiles were removed, and the resultant oil was dissolved in pentane and placed in a -35 °C freezer overnight. A brown precipitate formed, which was filtered off as the cold pentane solution was filtered through a pad of Celite to yield a yellow-brown oil (561 mg, 73% yield). ¹H NMR (500 MHz, CDCl₃): δ 7.00 (s, 2H, pyrrole C-H), 1.93 (s, 4H, Pyrrole-CH₂Bpin), 1.54 (s, 9H, CH₃), 1.26 (s, 24H, Me on Bpin); ¹³C{¹H} (126 MHz, CDCl₃): δ 149.1 (s, CO₂), 123.3 (s, pyr-H), 117.2 (s, pyr-C), 83.4 (s, Bpin), 82.3 (s, C-O), 28.2 (s, CMe₃), 25.0 (s, Me on Bpin), 8.4 (br. s, CH₂B); ¹¹B{¹H} NMR (128.2 MHz, CDCl₃): δ 33.4. Unit Mass (ESI) m/z: [M + H]⁺ calcd. for C₂₃H₃₉B₂NO₆ 448.30; Found 448.47.

3,4-bis(pinacolborylmethyl) furan (313B₂c-fur). In a 100 mL Teflon screw-top flask, BINAP (37 mg, 0.06 mmol) and Rh(COD)₂OTf (28 mg, 0.06 mmol) was dissolved in 20 mL of CH₂Cl₂. **313B₂** was dissolved in 5 mL of CH₂Cl₂ and was added to the reaction mixture. The reaction mixture was degassed the “freeze-pump-thaw” technique and the headspace was refilled with an atmosphere of dihydrogen. The reaction was stirred for 2 h at room temperature and the volatiles were removed under vacuum. The product was extracted with pentane and filtered through Celite. The resulting oil was dissolved in isooctane and placed in a -35 °C, a yellow solid precipitated from the solution. The cold solution was passed through a pad of Celite and

the volatile were removed under vacuum. The product was isolated as a clear oil (406 mg, 59% Yield). ^1H NMR (500 MHz, CDCl_3): δ 7.23 (s, 2H, furan-*H*), 1.89 (s, 4H, CH_2Bpin), 1.26 (s, 24H, *Me* on Bpin); $^{13}\text{C}\{^1\text{H}\}$ NMR (126 MHz, CDCl_3): δ 139.4 (s, furan *C-H*), 121.1 (s, furan *C-CH}_2*), 83.5 (s, Bpin), 25.0 (s, *Me* on Bpin); $^{11}\text{B}\{^1\text{H}\}$ NMR (128.2 MHz, CDCl_3): δ 33.3 (s). Unit Mass (ESI) *m/z*: [M + H]⁺ calcd. for $\text{C}_{18}\text{H}_{30}\text{B}_2\text{NO}_5$ 349.23; Found 349.29.

307B₂-H₂. Observed *in situ* ^1H NMR (500 MHz, CDCl_3): δ 6.35 (dt, *J* = 13.5 Hz, *J* = 8 Hz, 1H, =C(Bpin)*H*), 5.34 (dt, *J* = 13.5 Hz, 1 Hz, 1H, *CH=CH*(Bpin)), 2.45 (dq, *J* = 7.5 Hz, *J* = 1 Hz, 2H, CH_2), 2.24 (t, *J* = 7.5 Hz, 2H, CH_2), 1.61 (pent., *J* = 7 Hz, 2H, CH_2), 1.237 (s, 12H, *Me* on Bpin), 1.235 (s, 12H, *Me* on Bpin).

309Me₂c-exo. Observed *in situ* ^1H NMR (500 MHz, CDCl_3): δ 7.12 (d, *J* = 8.5 Hz, 2H, Ar-*H*), 6.61 (d, *J* = 8.5 Hz, 2H, Ar-*H*), 5.89 (m, 2H, =*CHMe*), 4.06 (s, 4H, NCH_2), 2.31 (s, 3H, Ar-*Me*), 1.79 (d, *J* = 7 Hz, 6H, =*CHMe*).

309Ph₂c-exo. Observed *in situ* ^1H NMR (500 MHz, CDCl_3): δ aromatic region overlaps with pyrrole isomer, 7.08 (t, *J* = 2.5 Hz, 2H, =*CHPh*), 6.71 (d, *J* = 9 Hz, 2H, Ar-*H*), 4.41 (d, *J* = 2.5 Hz, 4H, NCH_2), 2.33 (s, 3H, Ar-*Me*).

3,4-diethyl-1-tolyl-1*H*-pyrrole (309Me₂c-pyr). BINAP (37 mg, 0.06 mmol) and Rh(COD)₂OTf (28 mg, 0.06 mmol) were dissolved in 20 mL of CH_2Cl_2 in a 100 mL Teflon screw-top flask. **309Me₂** (422 mg, 2.0 mmol) was dissolved in 5 mL of CH_2Cl_2 and was added to the reaction mixture. The solution was degassed using the “freeze-pump-thaw” technique and the headspace was refilled with an atmosphere of dihydrogen. The reaction was stirred for 2 h at room temperature, and then the flask was

moved to a 55 °C oil bath for 1.5 hours. The volatiles were removed, and the product was extracted with diethyl ether. The volatiles were removed and the resulting brown oil was dissolved in pentane and stirred with silica gel for five minutes. The solution was then filtered through a plug of silica and Celite. The volatiles were removed to yield a clear oil (332 mg, 78% yield). ^1H NMR (500 MHz, CDCl_3): δ 7.25 (d, $J = 8$ Hz, 2H, Ar-*H*), 7.19 (d, $J = 8$ Hz, 2H, Ar-*H*), 6.82 (s, 2H, Ar-*H*), 2.51 (q, $J = 7.5$ Hz, 4H, CH_2Me), 2.36 (s, 3H, Ar-*Me*), 1.26 (t, $J = 7.5$ Hz, 6H, CH_2Me); $^{13}\text{C}\{^1\text{H}\}$ NMR (126 MHz, CDCl_3): δ 138.7 (s, Ar-*N*), 134.3 (s, Ar-*Me*), 130.0 (s, Ar-*H*), 126.9 (s, Ar-*Et*), 119.7 (s, Ar-*H*), 115.9 (s, Ar-*H*), 20.9 (s, Ar-*Me*), 18.7 (s, CH_2CH_3), 14.5 (s, CH_2CH_3). Unit Mass (ESI) m/z : $[\text{2M} + \text{H}]^+$ calcd. for $\text{C}_{15}\text{H}_{19}\text{N}$ 427.31; Found 427.32.

3,4-dibenzyl-1-(*p*-tolyl)-1*H*-pyrrole (309Ph₂c-pyr). In a 50 mL Teflon screw-top flask, BINAP (13 mg, 0.02 mmol) and $\text{Rh}(\text{COD})_2\text{OTf}$ (10 mg, 0.02 mmol) was dissolved in 5 mL of CH_2Cl_2 . **309Ph₂** (233 mg, 0.7 mmol) was dissolved in 3.75 mL of CH_2Cl_2 and was added to the solution. The solution was degassed using the “freeze-pump-thaw” technique and the headspace was refilled with an atmosphere of dihydrogen. The reaction was stirred for 2 h at room temperature, and then the flask was moved to a 60 °C oil bath for 1.5 hours. The volatiles were removed under vacuum and the product was extracted with a 5:1 mixture of toluene:pentane and filtered through a pad of silica and Celite. The product was isolated as a light yellow solid (153 mg, 65% Yield). ^1H NMR (500 MHz, CDCl_3): δ 7.24 (m, 4H, Ar-*H* overlapping signals), 7.19-7.09 (m, 10H, Ar-*H* overlapping signals), 6.69 (s, 2H, *pyrrole* C-*H*), 3.72 (s, 4H, CH_2Ph), 2.29 (s, 3H, Ar-*H*); $^{13}\text{C}\{^1\text{H}\}$ NMR (126 MHz, CDCl_3): δ 141.4 (s), 138.4 (s),

134.6 (s), 130.0 (s), 128.9 (s), 128.4 (s), 125.9 (s), 124.1 (s), 119.6 (s), 118.0 (s), 32.1 (s, CH₂Ph), 20.9 (s, Ar-Me). Unit Mass (ESI) m/z: [M + Na]⁺ calcd. for C₂₅H₂₃N 360.17; Found 360.20.

3.4.7 Additional Experiments

Treatment of 303Bc-exo with 5% (BINAP)Rh(COD)OTf and H₂. (BINAP)Rh(COD)OTf (100 μL of a 0.02 M solution in CH₂Cl₂, 0.002 mmol) was added to a J. Young tube. The volatiles were removed under vacuum and **303Bc-exo** (15 mg, 0.04 mmol) was added to the tube and dissolved in 500 μL of CD₂Cl₂. After 20 h, no isomerization had been observed. The headspace of the J. Young tube was removed under vacuum using the freeze-pump-thaw method. The atmosphere was then refilled with H₂, and no isomerization was observed after 17 h at room temperature. The mixture was transferred to a 25 mL screw top flask, which was degassed and refilled with an atmosphere of H₂. After stirring vigorously for 24 at room temperature, no isomerization was observed.

Thermolysis of 303Bc-pyr. 303Bc-exo (8 mg, 0.02 mmol) was added to a J. Young tube and dissolved in dichloroethane. The solution was heated at 75 °C overnight. Analysis by ¹¹B NMR spectroscopy showed only the starting material being present in solution. (BINAP)Rh(COD)OTf (32 μL, 0.02 M solution in CH₂Cl₂) was added to the J. Young tube. The vessel was degassed using the “freeze-pump-thaw” method, and was back-filled with an atmosphere of dihydrogen. The solution was heated at 75 °C for 1 hour and analysis by ¹¹B NMR spectroscopy showed >90% isomerization to the **303Bc-endo**. The volatiles were removed, and the resulting solid was dissolved in CDCl₃ for ¹H

NMR spectroscopy analysis, which confirmed that the starting material had been isomerized to the endocyclic alkene.

Synthesis of (1-(p-tolyl)-1H-pyrrole-3,4-diyl)dimethanol (309-pyr-OH). In a screw-top vial, **309B₂c-pyr** (100 mg, 0.23 mmol) was dissolved in about 2 mL of THF. Although the substrate was stored in an argon-filled glovebox, the reaction vial was taken out of the glovebox and the reaction was conducted with exposure to ambient atmosphere. The solution was cooled to 0 °C and NaOH (0.77 mL, 3 M solution in water, 10 eq.) was added followed by H₂O₂ (0.20 mL, 35 wt% solution in water). The ice bath was removed and the reaction was allowed to warm to room temperature and was stirred for 1 h. Water (2 mL) and Ethyl acetate (3 mL) were added to the reaction and the layers were separated. The aqueous layer was extracted with Ethyl acetate (2 x 5 mL), and all the organic layers were combined and dried over MgSO₄ and filtered through a pad of Celite. The volatiles were removed and the product was precipitated from dichloromethane layered with petroleum ether. The product precipitated out of solution and was washed with cold ether to yield a beige powder (41 mg, 82% yield). ¹H NMR (500 MHz, CDCl₃): δ 7.23 (d, *J* = 9 Hz, 2H, *Ar-H*), 7.21 (d, *J* = 9 Hz, 2H, *Ar-H*), 7.02 (s, 2H, *N-CH₂*), 4.66 (s, 4H, *CH₂-OH*), 2.54 (br. s, 2H, *OH*), 2.37 (s, 3H, *Ar-Me*); ¹³C{¹H} (126 MHz, CDCl₃): δ 138.1 (s, *Ar-N*), 135.8 (s, *Ar-Me*), 130.3 (s, *Ar-H*), 124.5 (s, *pyrrole-CH₂*), 120.5 (s, *Ar-H*), 119.1 (*pyrrole-H*), 57.4 (s, *CH₂OH*), 21.0 (s, *Ar-Me*). Unit Mass (ESI) *m/z*: [*M* + Na]⁺ calcd. for C₁₃H₁₅NO₂ 240.10; Found 240.04.

Synthesis of 306Ar₂c-exo. 306B₂c-exo (50 mg, 0.108 mmol) was dissolved in 2 mL of a 2:1 mixture of acetone and water with potassium carbonate (60 mg, 0.43 mmol),

$\text{Pd}(\text{OAc})_2$ (2 mg, 0.009 mmol), and 4-fluoroiodobenzene (37 μL , 0.32 mmol). The reaction mixture was heated overnight at 70 °C. The volatiles were removed and the product was extracted with dichloromethane and filtered through Celite and Silica. The volatiles were removed and the product was dissolved in dichloromethane and layered with hexane and recrystallized in the freezer. The product was isolated as yellow crystals (28 mg, 65% yield). ^1H NMR (500 MHz, CDCl_3): δ 7.36 (m, 4H, Ar-*H*), 7.06 (m, 4H, Ar-*H*), 6.93 (m, 2H, C=CH), 3.72 (s, 6H, CO_2Me), 3.34 (d, $J = 2$ Hz, 4H, CCH_2); $^{13}\text{C}\{^1\text{H}\}$ (126 MHz, CDCl_3): δ 171.7 (s, C=O), 161.8 (d, $J_{\text{CF}} = 252$ Hz, C-F), 139.1 (s, C=CH), 133.6 (d, $J = 3$ Hz, Ar-C), 130.6 (d, $J = 8$ Hz, Ar-H), 119.6 (s, C=CH), 115.5 (d, $J = 22$ Hz, Ar-H), 59.0 (s, CCO_2Me), 53.2 (s, CO_2Me), 39.0 (s, CH_2); ^{19}F NMR (470 MHz, CDCl_3): δ -115.2. Unit Mass (ESI) m/z : $[\text{M} + \text{Na}]^+$ calcd. for $\text{C}_{23}\text{H}_{20}\text{F}_2\text{O}_4$ 421.12; Found 421.25.

CHAPTER IV

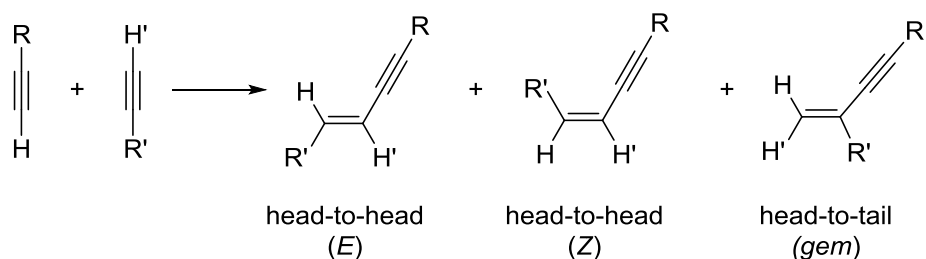
A SERIES OF PINCER-LIGATED RHODIUM COMPLEXES AS CATALYSTS FOR THE DIMERIZATION OF TERMINAL ALKYNES*

4.1 Introduction

Alkyne dimerization is a process in which a C_{sp}-H bond in a terminal alkyne is formally added across the C≡C bond in another molecule of alkyne. The products of alkyne dimerization, conjugated enynes, are versatile building blocks for a variety of organic transformations.²⁰⁴⁻²⁰⁷ This process is 100% atom-economical and requires a catalyst.²⁰⁸ The desired role for the catalyst is not limited to enabling a faster reaction, but formation of the desired product in a selective fashion. In principle, three isomers of a conjugated enyne arising from dimerization of a terminal alkyne are possible: *E*, *Z*, and *gem* (Scheme IV-1). In addition, terminal alkynes may undergo dimerization to a butatriene,³⁹ cyclotrimerization to arenes, or oligo- and polymerization to polyenes with various catalysts.^{41,209} Catalytic alkyne dimerization has been investigated using a number of transition metals,²¹¹⁻²¹⁸ main group elements,²¹⁹ and lanthanides.²²⁰ While some of these catalytic systems give mixtures of enyne and oligomeric products, several systems show excellent selectivity for a specific isomer. A recent NHC palladium (NHC = N-heterocyclic carbene) catalyst has achieved perfect regio- and stereoselectivity to form the *E*-enyne with a range of terminal alkynes possessing various functional

* Reprinted in part with permission from “A Series of Pincer-Ligated Rhodium Complexes for the Dimerization of Terminal Alkynes” by Pell, C. J.; Ozerov, O. V. *ACS Catal.* **2014**, *4*, 3470. Copyright 2014 by American Chemical Society. DOI: 10.1021/cs5009317

groups.^{216b} Palladium has also been used as a selective head-to-tail dimerization catalyst for a range of substituted alkynes when paired with a Brønsted acid.^{216c} Selective dimerization to form the *Z*-enyne has been primarily the specialty of ruthenium catalysts,^{213a,b} but lanthanide and zirconium complexes have also shown *Z*-selectivity.^{218,220}



Scheme IV-1. Alkyne dimerization.

In the domain of Rh-catalyzed alkyne dimerization, the frontier of cross dimerization is experiencing advancements. Miura's group was able to take advantage of sterically different terminal alkynes and a bulky Rh catalyst to selectively produce *E*-enyne with a high tolerance for functionalities.^{217a} More recently, the Xu group showed that a Rh phosphine system could effectively cross-dimerize arylacetylenes with propargylic alcohols, ethers, and amides.^{217e} Head-to-tail selective homodimerization has also been achieved by an NHC Rh catalyst.^{217c}

Several years ago, we reported that Rh complexes supported by diarylamido/bis(phosphine) PNP pincer ligands served as efficient catalysts for alkyne dimerization (Figure IV-1).²²¹ The more common member of this family, **401-Rh(H₂)**,

produced an unselective mixture of *E* and *gem* isomers, but the “tied” ^TPNP rhodium catalyst (**402-Rh(H₂)**) enabled selective production of predominantly isomer *E* for a rather broad selection of terminal alkynes.²²² The ^TPNP ligand requires multi-step synthesis and the reactions catalyzed by **402-Rh(H₂)** were not particularly fast, on the order of 10 TON/h at 100 °C. We surmised that there may be other, more easily accessible pincer ligands that could give rise to analogous Rh catalysts. To this end, we set out to prepare a series of (pincer)Rh complexes and test their prowess in alkyne dimerization.

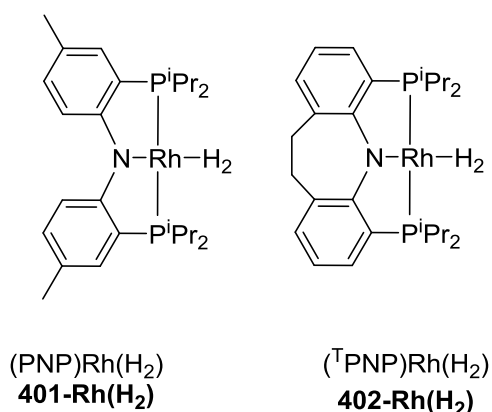
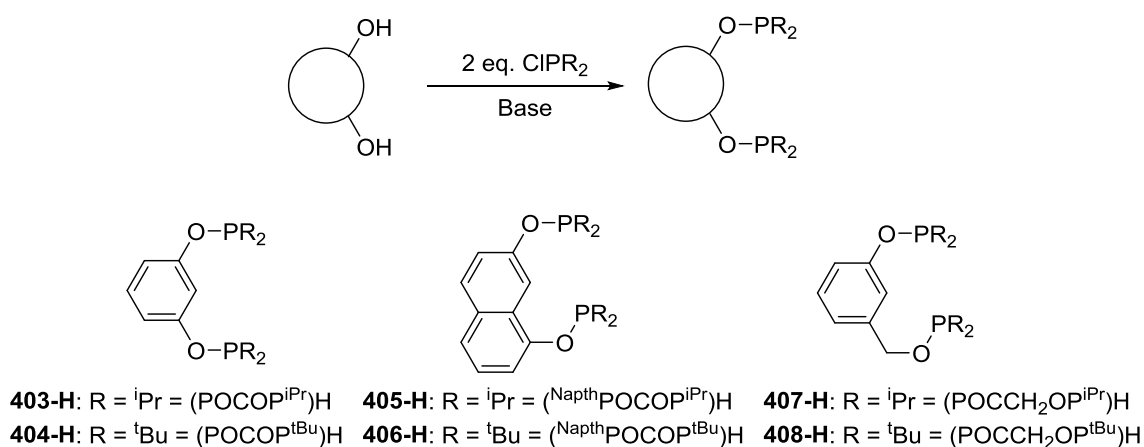


Figure IV-1. (PNP)Rh alkyne dimerization catalysts.

4.2 Results and Discussion

4.2.1 Synthesis of Pincer Ligands and Their Rh Complexes

We selected ligands **403-H** through **410-H** for our study. We primarily focused on aryl/bis(phosphine) ligands as they are most easily prepared, especially in the case of aryl/bis(phosphinite) variants (Scheme IV-2).



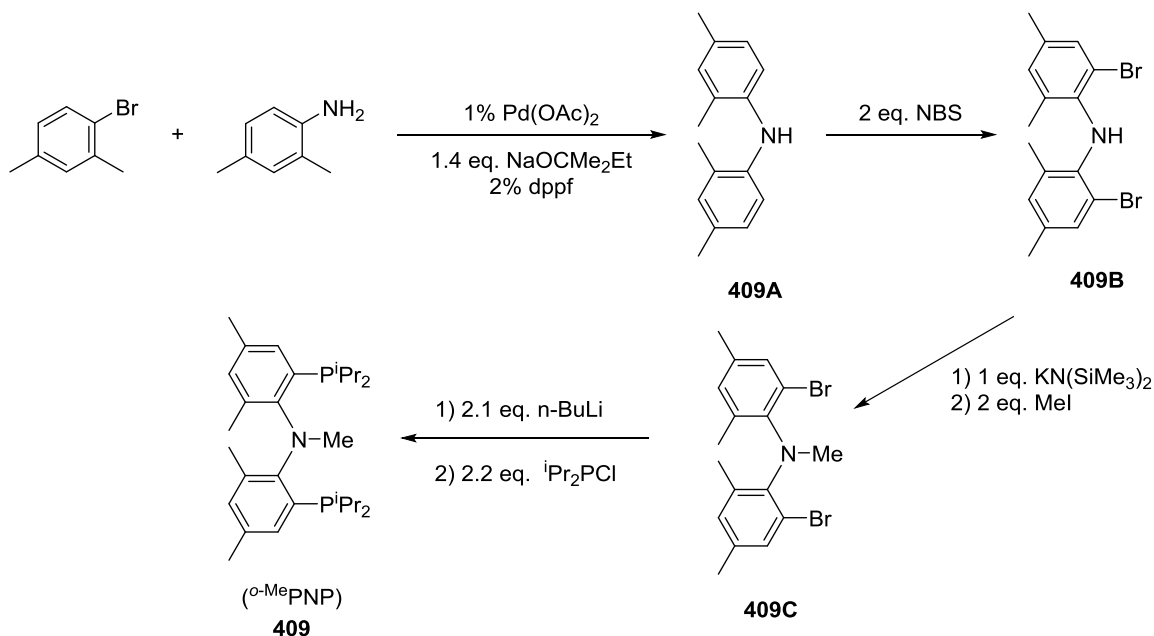
Scheme IV-2. Synthesis of bis(phosphinite) ligands.

Ligands, **403-H**,²²³ **404-H**,²²⁴ and **407-H**¹³⁷ have been previously reported and were synthesized as described in the literature (with some changes in the procedure for **407-H**). Ligands **405-H**, **406-H**, and **408-H** were prepared analogously from 1,7-naphthalenediol or 3-hydroxybenzyl alcohol, CIPR₂ (R = ⁱPr or ^tBu), and base. Ligands **403-H**, **405-H**, **407-H**, and **408-H** were obtained as oils of 95% or better purity as judged by ¹H NMR spectroscopy and were used as is for the synthesis of the Rh complexes. The aryl/bis(PR₃) ligands in this study differ by the size of the substituent on phosphorus, by the size of the pincer rings fused at the central M-C bond (5,5 vs 5,6), and by the difference in the electron richness of the backbone. The {[5,6]-PCP}⁻ ligands^{*,225} (**405-H**, **406-H**, **407-H**, and **408-H**) were intended to favor selectivity for the

* Using Fryzuk's notation for pincer ligands, {[5,6]-PCP}⁻ denotes a monoanionic, tridentate ligand that donates through two phosphorus and one carbon atom to form a five- and six-membered metallacycle.

E-enyne isomer by increasing the steric bulk around the active site of the metal, a strategy that has been used in several other systems.^{215,217a,221}

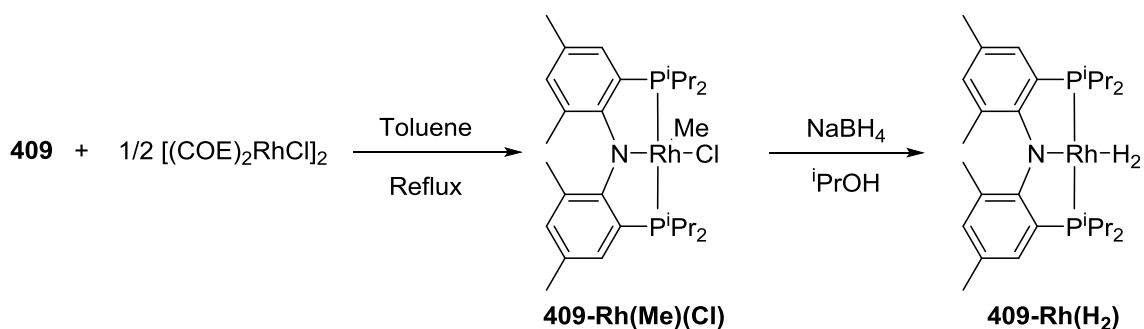
We also examined a new C_2 -symmetric PNP ligand **409**, which offered a variation on the diarylamido backbone (Scheme IV-3). Diarylamine **409A** was synthesized via Buchwald-Hartwig coupling²²⁶ of 2,4-dimethylaniline and 2,4-dimethylbromobenzene. Bromination of **409A** with *N*-bromosuccinimide yielded compound **409B**, which was *N*-methylated with $\text{KN}(\text{SiMe}_3)_2$ and iodomethane to give **409C**. Treatment of **409C** with *n*-butyllithium and ClP^iPr_2 yielded **409** as a white solid. Ligand **409** differs from **401** by possessing methyl groups *ortho* to the central nitrogen donor. This causes a high barrier to the rotation about the Ar-N bond and results in C_2 -symmetry on the NMR time scale as seen by the presence of two methine signals and four doublets of doublets for the P^iPr_2 methyls.²²⁷



Scheme IV-3. Synthesis of *Ortho*-methyl PNP (**409**).

The C_2 -symmetry of the ligand is reduced down to C_1 once the ligand is metalated with [(COE)₂RhCl]₂ (COE = cyclooctene) to form (^o-MePNP)Rh(Me)(Cl) (**409-Rh(Me)(Cl)**) (Scheme IV-4). This is evidenced by the appearance of eight signals for the PⁱPr₂ methyls by ¹H NMR. The ³¹P{¹H} NMR spectrum showed two different doublets of doublets and large coupling between the two inequivalent phosphorus donors, ²J_{PP} = 414 Hz. Reduction of **409-Rh(Me)(Cl)** with NaBH₄ in isopropanol yielded the Rh^I species **409-Rh(H₂)**, which showed atropisomeric C_2 -symmetry (Scheme IV-4). Complexes of ligand **409** differ from other atropisomeric pincer complexes to date due to the chirality being generated by a twist in the backbone of the ligand and the use of five-membered metallacycles. Previous atropisomeric pincer complexes rely on

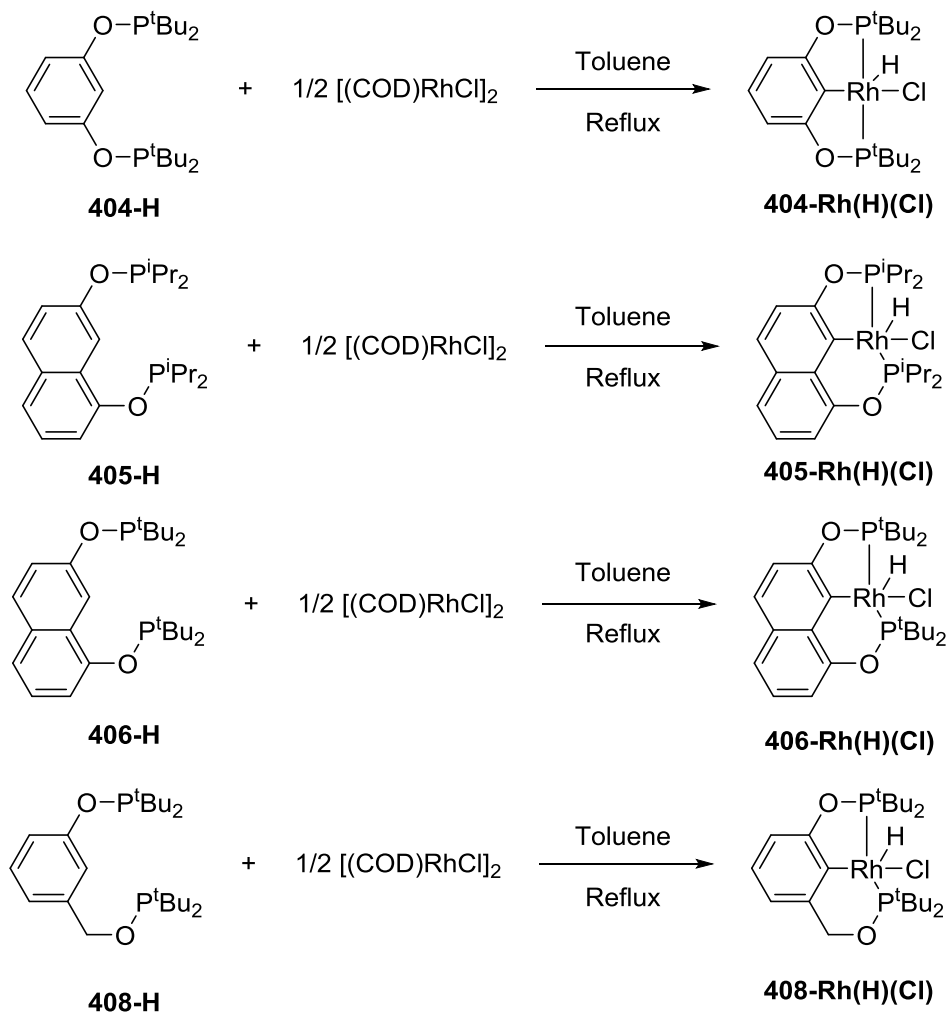
long pincer “arms” to establish six- or seven-membered metallacycles that twist the structure of the molecule out of planarity.²²⁸ The presence of five-membered metallacycles in complexes of **409** is notable because smaller metallacycles in atropisomeric compounds tend to lead to faster rates of atropisomerism that averages the two conformations.^{229,230} We also prepared **409-Rh(HD)** from which the J_{HD} value of 20 Hz was extracted. Using established²³¹ relationships between H-H distances and $J_{\text{H-D}}$ coupling, we conclude that **409-Rh(H₂)** is a “stretched” or “elongated” dihydrogen complex,²³² with a predicted H-H distance of 1.1 Å. This matches a previously synthesized PNP-based rhodium dihydrogen adduct.²²²



Scheme IV-4. Synthesis of rhodium complexes of the *Ortho*-methyl PNP ligand (**409**).

Installation of PCP/POCOP ligands into the coordination sphere of Rh is also most conveniently accomplished via reaction of the ligand precursor with [(COD)RhCl]₂. This reaction is ideally accompanied by loss of COD (= 1,5-cyclooctadiene) and insertion of Rh into the central C-H bond to give (pincer)Rh(H)(Cl).

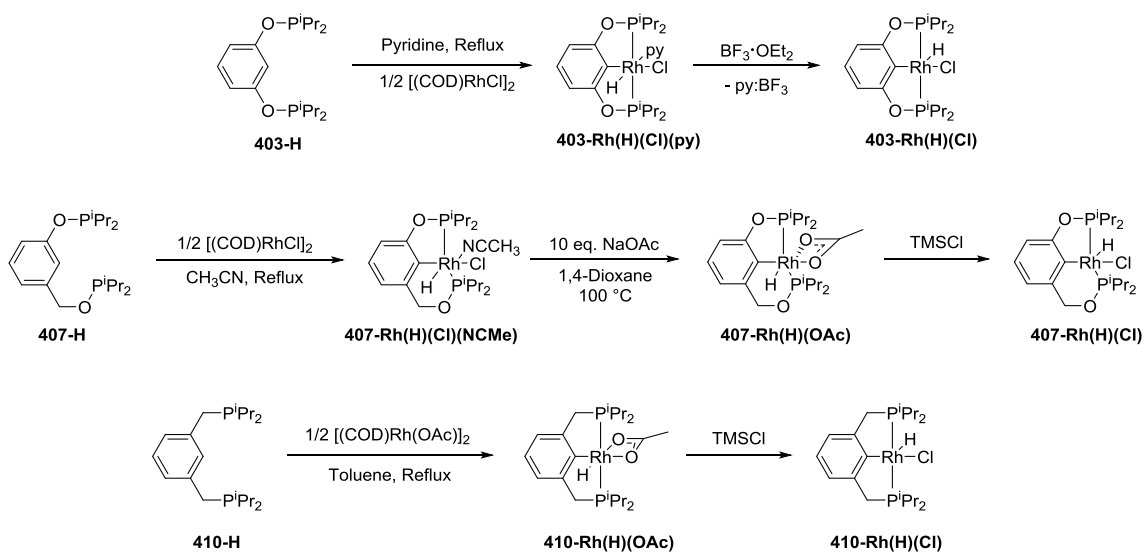
However, this reaction appeared to work cleanly only for the relatively sterically imposing POCOP ligands **404-H**, **405-H**, **406-H**, and **408-H** (Scheme IV-5).



Scheme IV-5. Direct metalation of (POCOP)-type pincer ligands with $[(\text{COD})\text{RhCl}]_2$.

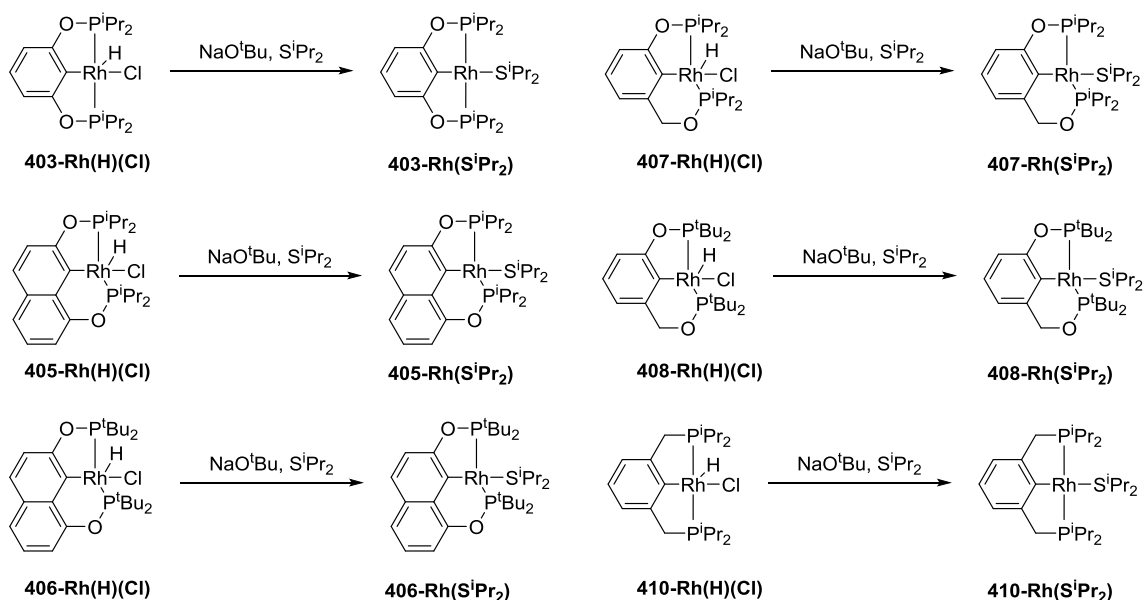
In other cases, the direct metalation of the ligand with $[(\text{COD})\text{RhCl}]_2$ was not clean. We previously described these issues in the synthesis of **403-Rh(H)(Cl)** where a second equivalent of free ligand can coordinate to rhodium, resulting in mixtures of six-

coordinate rhodium products.²³³ For **403-Rh(H)(Cl)**, the problem was solved via a two-step procedure, first preparing a pyridine adduct **403-Rh(H)(Cl)(py)** followed by abstraction of pyridine by BF₃. A similar approach was successful for the synthesis of **407-Rh(H)(Cl)** (Scheme IV-6). The reaction of **407-H** with [(COD)RhCl]₂ in acetonitrile cleanly gave the acetonitrile adduct **407-Rh(H)(Cl)(NCMe)**, which in reaction with excess NaOAc released the coordinated acetonitrile to produce **407-Rh(H)(OAc)**. Treatment of **407-Rh(H)(OAc)** with Me₃SiCl after removal of all of acetonitrile under vacuum resulted in the formation of **407-Rh(H)(Cl)**. In a yet another variation, six-coordinate **410-Rh(H)(OAc)** was prepared directly from **410-H**²³⁴ and [(COD)Rh(OAc)]₂ and metathesis with Me₃SiCl gave the corresponding five-coordinate hydrido-chloride complex **410-Rh(H)(Cl)** (Scheme IV-6). The five-coordinate complexes **n-Rh(H)(Cl)** (**n = 403-408, 410**) displayed a hydride resonance in the -24 to -27 ppm range in the ¹H NMR spectra. Complexes with inequivalent phosphorus donors showed strong phosphorus-phosphorus coupling in the ³¹P{¹H} NMR spectra, with ²J_{PP} values in the 400-430 Hz range.



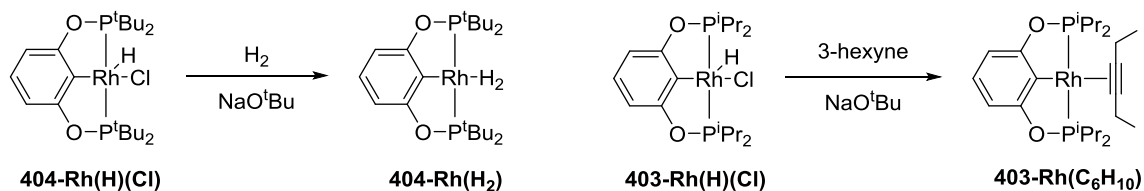
Scheme IV-6. Synthesis of Rh pincer complexes through six-coordinate intermediates.

The desired Rh^{I} precursors were made from complexes **n-Rh(H)(Cl)** (**n = 403, 405, 406, 407, 408, 410**) by treating them with NaO^tBu in the presence of diisopropyl sulfide, which led to clean formation of **n-Rh(S^iPr_2)** (**n = 403, 405, 406, 407, 408, 410**) (Scheme IV-7). We have previously used S^iPr_2 as a useful placeholder ligand in the chemistry of (PNP)Rh complexes: it forms isolable adducts with Rh^{I} , dissociates rather easily, and has no affinity for coordinating to Rh^{III} complexes.²³⁵ The Rh^{I} complexes possessed larger $^1J_{\text{Rh-P}}$ values compared to the Rh^{III} compounds described above, but lower $^2J_{\text{P-P}}$ values.



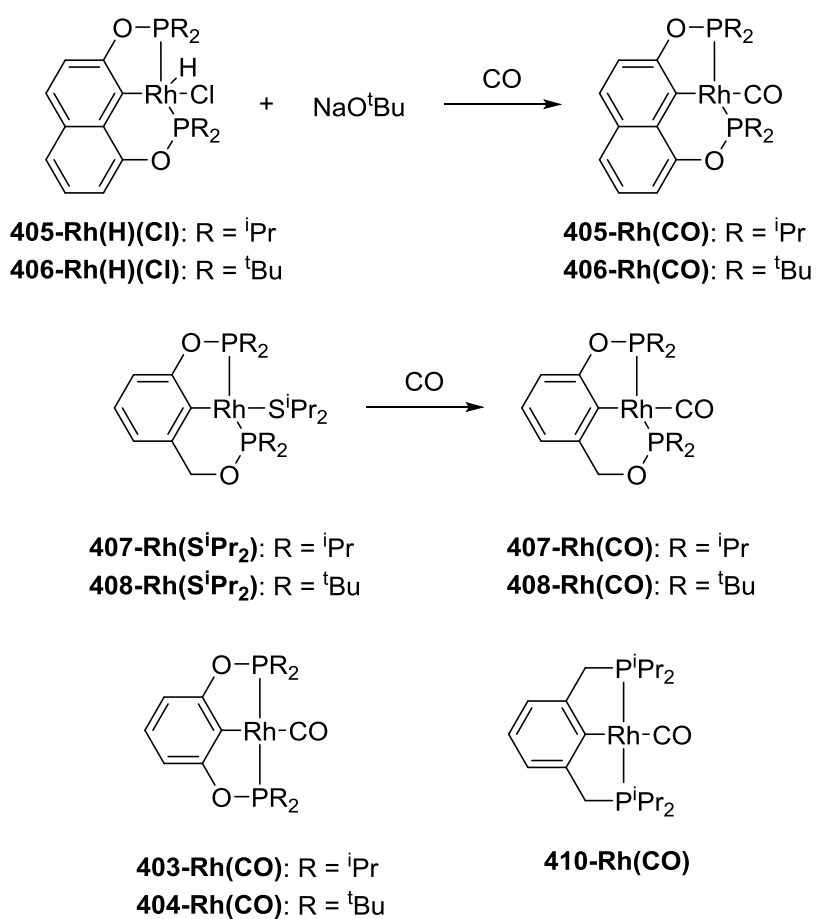
Scheme IV-7. Synthesis of Rh(I) diisopropylsulfide adducts.

We also prepared the 3-hexyne adduct **403-Rh(C₆H₁₀)** in an analogous fashion. For ligands **404-H**, dihydrogen complex **404-Rh(H₂)**²³⁶ was synthesized (Scheme IV-8). The PNP-ligated rhodium dihydrogen complex **409-Rh(H₂)** was synthesized as a precatalyst as well (Scheme IV-4).



Scheme IV-8. Synthesis of **404-Rh(H₂)** and **403-Rh(C₆H₁₀)**.

Treatment of **405-Rh(H)(Cl)** and **406-Rh(H)(Cl)** with NaO^tBu under an atmosphere of CO gave the corresponding (pincer)Rh(CO) complex (**405-Rh(CO)** and **406-Rh(CO)**), (Scheme IV-9). Pincer carbonyl complexes could also be obtained by treating the (pincer)Rh(SⁱPr₂) complexes (**407-Rh(SⁱPr₂)** and **408-Rh(SⁱPr₂)**) with an atmosphere of CO to form **407-Rh(CO)** and **408-Rh(CO)** (Scheme IV-9).



Scheme IV-9. Synthesis of Rh(I) pincer carbonyl complexes.

Complexes **n-Rh(CO)** (**n = 405-408**) were analyzed using IR spectroscopy and compared to the reported CO stretching frequencies of **403-Rh(CO)**,²³⁷ **404-Rh(CO)**,²³⁸ **410-Rh(CO)**²³⁷ to gauge the electron richness²³⁹ of the ligand backbone (Table IV-1). Not surprisingly, the bis(phosphinite) POCOP ligands showed lower electron donation to the metal center than the bis(phosphine) PCP ligand, due to the electron withdrawing ability of the oxygen atoms.

Table IV-1. Carbonyl stretching frequencies of PCP/POCOP rhodium carbonyl compounds .

Complex	IR ν_{CO} (cm^{-1})
(POCOP ^{iPr})Rh(CO) (403-Rh(CO))	1962
(POCOP ^{tBu})Rh(CO) (404-Rh(CO))	1961
(^{Naph} POCOP ^{iPr})Rh(CO) (405-Rh(CO))	1950
(POCCH ₂ OP ^{iPr})Rh(CO) (407-Rh(CO))	1948
(^{Naph} POCOP ^{tBu})Rh(CO) (406-Rh(CO))	1945
(POCCH ₂ OP ^{tBu})Rh(CO) (408-Rh(CO))	1943
(PCP ^{iPr})Rh(CO) (410-Rh(CO))	1941

4.2.2 Catalytic Alkyne Dimerization

We selected three alkynes for the screening of catalysts: ⁿBuC≡CH, Me₃SiC≡CH, and 4-MeC₆H₄C≡CH. These three substrates did not allow for the evaluation of the functional group tolerance of the catalysts, but they provided a reasonable sampling of steric and electronic differences in terminal alkynes. In this study, we were primarily

interested in gauging catalyst activity, longevity, and selectivity. All catalysts were introduced as either Rh^{I} diisopropyl sulfide adducts or as Rh^{I} dihydrogen adducts.

Table IV-2 details the results of our screening in reactions conducted at 80 °C with 1% catalyst loading. To more closely match the conditions used in our previous study,²²¹ we additionally conducted the dimerization of the three alkynes using 0.5% **403-Rh(SⁱPr₂)** at 100 °C, and found little difference with the selectivities observed with 1% **403-Rh(SⁱPr₂)** at 80 °C. We also conducted a comparison of **403-Rh(SⁱPr₂)** and **403-Rh(C₆H₁₀)** as catalysts in a separate pair of experiments, and found them giving the same conversion and isomer distribution within errors of measurement, thus confirming the irrelevance of the placeholder ligand L in **n-Rh(L)** compounds as catalysts

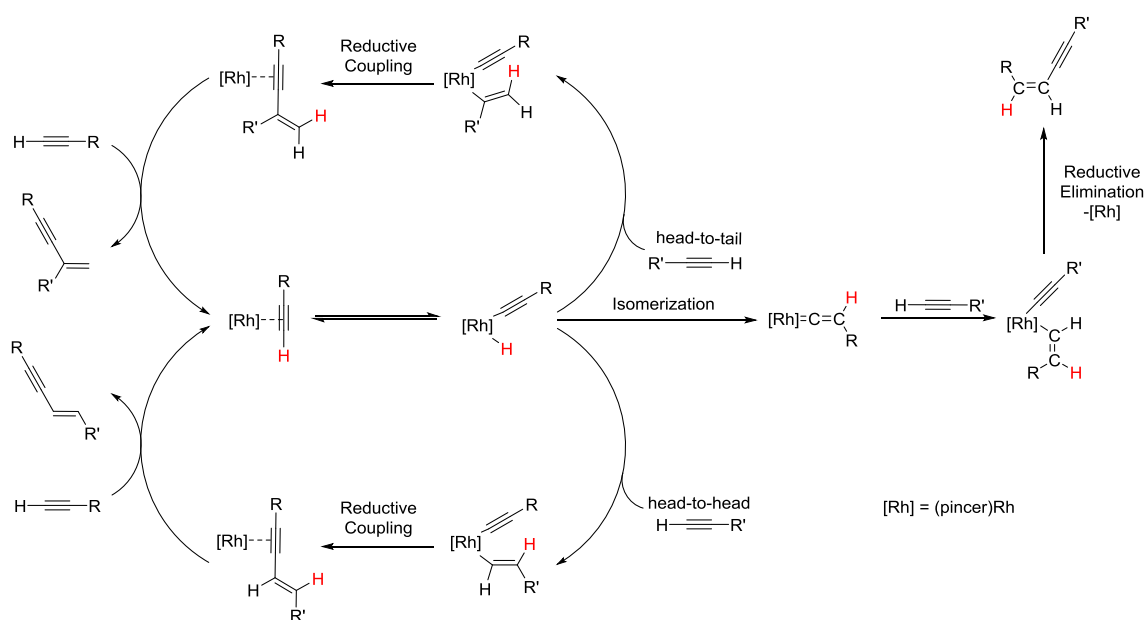
Table IV-2. Conversion of alkyne and the isomeric distribution of the produced enynes.

Substrate	[Rh] =	Time	Gem : E : Z : oligomers	% Conversion ^a
4-MeC ₆ H ₄ C≡CH	403-Rh(SⁱPr₂)	3 h	29 : 69 : 0 : 2	>97
ⁿ BuC≡CH	403-Rh(SⁱPr₂)	3 h	73: 19 : 0 : 8	97
Me ₃ SiC≡CH	403-Rh(SⁱPr₂)	3 h	63: 35 : 0 : 2	>97
4-MeC ₆ H ₄ C≡CH	404-Rh(H₂)	36 h	11: 73 : 0 : 16	83
ⁿ BuC≡CH	404-Rh(H₂)	36 h	84 : 16: 0 : 0	7

Table IV-2. Continued

Substrate	[Rh] =	Time	Gem : E : Z : oligomers	% Conversion ^a
Me ₃ SiC≡CH	404-Rh(H₂)	36 h	76 : 24 : 0 : 0	80
4-MeC ₆ H ₄ C≡CH	405-Rh(SⁱPr₂)	3 h	24 : 70 : 0 : 6	>97
ⁿ BuC≡CH	405-Rh(SⁱPr₂)	3 h	62 : 31 : 0 : 7	95
Me ₃ SiC≡CH	405-Rh(SⁱPr₂)	3 h	10 : 79 : 0 : 11	>97
4-MeC ₆ H ₄ C≡CH	406-Rh(SⁱPr₂)	36 h	11 : 46 : 0 : 43	5
ⁿ BuC≡CH	406-Rh(SⁱPr₂)	36 h	89 : 11 : 0 : 0	1
Me ₃ SiC≡CH	406-Rh(SⁱPr₂)	36 h	25 : 33 : 0 : 42	5
4-MeC ₆ H ₄ C≡CH	407-Rh(SⁱPr₂)	36 h	13 : 62 : 0 : 25	>97
ⁿ BuC≡CH	407-Rh(SⁱPr₂)	36 h	82 : 14 : 0 : 4	47
Me ₃ SiC≡CH	407-Rh(SⁱPr₂)	36 h	19 : 66 : 8 : 7	95
4-MeC ₆ H ₄ C≡CH	408-Rh(SⁱPr₂)	36 h	16 : 11 : 0 : 73	4
ⁿ BuC≡CH	408-Rh(SⁱPr₂)	36 h	74 : 26 : 0 : 0	3
Me ₃ SiC≡CH	408-Rh(SⁱPr₂)	36 h	15 : 60 : 0 : 25	22
4-MeC ₆ H ₄ C≡CH	409-Rh(H₂)	70 h	2 : 73 : 0 : 25	74
ⁿ BuC≡CH	409-Rh(H₂)	70 h	29 : 71 : 0 : 0	25
Me ₃ SiC≡CH	409-Rh(H₂)	70 h	17 : 53 : 0 : 30	45
4-MeC ₆ H ₄ C≡CH	410-Rh(SⁱPr₂)	36 h	22 : 56 : 0 : 22	94
ⁿ BuC≡CH	410-Rh(SⁱPr₂)	36 h	65 : 18 : 0 : 17	63
Me ₃ SiC≡CH	410-Rh(SⁱPr₂)	36 h	16 : 65 : 1 : 18	>97
^a Fraction of consumed alkyne by ¹ H NMR spectroscopy versus a 1,4-dioxane internal standard.				

The *Z* isomer was absent in all but two experiments with $\text{Me}_3\text{SiC}\equiv\text{CH}$ where it was produced in small amounts, possibly indicating the similarity in mechanism between PCP/POCOP and PNP-based catalysts (Scheme IV-10). The appearance of the *Z* isomer might be indicative of a competing vinylidene intermediate in the catalytic cycle that is accessible when using a strongly electron-donating terminal alkyne. It has been shown experimentally that ethynyltrimethylsilane can react with a nominally 14-electron Rh^{I} compound ($[\text{Rh}(\text{Cl})(\text{P}^i\text{Pr}_3)_2]_2$) to give a five-coordinate rhodium(III) hydridoalkynyl, which rearranges to the corresponding vinylidene isomer.²⁴⁰ This mechanism of coupling a vinylidene with an acetylide is a common motif found in *Z*-selective ruthenium alkyne dimerization catalysts^{213a,b} and was also considered by Goldman et al. in a study of alkyne dimerization by (pincer)Ir catalysts.²⁴¹



Scheme IV-10. Possible mechanism for alkyne dimerization.

The ratios of *gem*- vs *E*-isomers (Table IV-3) varied depending on the substrate and the supporting pincer ligand, but none of the catalysts screened in this study demonstrated high selectivity for either the *gem*- or the *E*-product. With 1-hexyne, the *gem*-isomer was typically preferred; with 4-ethynyltoluene, the *E*-isomer typically formed in greater quantity. However, no clear trend can be extracted from these results as far as analyzing the influence of the nature of the pincer ligand on selectivity. For example, there is no obvious correlation between ν_{CO} stretching frequencies of **n-Rh(CO)** (Table IV-1) and the rates of the dimerization reactions or selectivity. **409-Rh(H₂)** performed more similarly to **401-Rh(H₂)** than **402-Rh(H₂)**: sluggishly and not selectively. It would seem that catalyst **409-Rh(H₂)** had a high selectivity for forming the *E*-isomer over the *gem*-enyne for 4-ethynyltoluene, but by monitoring the reaction by ¹H NMR over the course of the 70 h reaction time, it was seen that the *gem* isomer was formed and reacts further to form oligomeric products, which is a known behavior of 1,3-diarylbutenyne.²⁴²

Table IV-3. Geminal/*E* enyne isomer ratios for dimerization catalysts.

	1-hexyne <i>Gem/E</i>	4-ethynyltoluene <i>Gem/E</i>	Ethynyltrimethylsilane <i>Gem/E</i>
403-Rh(SⁱPr₂)	3.8	0.42	1.8
404-Rh(H₂)	5.3	0.15	3.2
405-Rh(SⁱPr₂)	2.0	0.34	0.13
406-Rh(SⁱPr₂)	8.1	0.24	0.75
407-Rh(SⁱPr₂)	5.9	0.21	0.25
408-Rh(SⁱPr₂)	2.9	1.5	0.28
409-Rh(H₂)	0.4	0.03	0.32
410-Rh(SⁱPr₂)	3.6	0.39	0.25

With respect to the rates of reaction, (POCOP)- and (^{Napt}POCOP)-supported catalysts bearing PⁱPr₂ arms appeared to work the fastest, and faster than those reported with **402-Rh(H₂)**. Catalysts based on P^tBu₂-containing ligands **404**, **406**, and **408** operated much more slowly, presumably owing the prohibitive steric bulk of the four *tert*-butyl groups. In an effort to gauge the longevity of the catalyst, we have also performed dimerization of Me₃SiC≡CH using 0.005% of **403-Rh(SⁱPr₂)** at 100 °C, and observed >97% conversion to the dimerization products after 36 h, amounting to *ca.* 20,000 turnovers.

4.3 Conclusion

In summary, we have prepared a series of (pincer)Rh^I complexes for study as potential catalysts for alkyne dimerization to enynes. Some of the reported ligands and their Rh complexes are new. Our findings indicate that aryl/bis(phosphine/phosphinite) PCP or POCOP pincer ligands do result in Rh catalysts capable of alkyne dimerization. Similarly to the PNP-based catalysts reported previously, the PCP/POCOP systems produce little to no *Z*-enynes as products, possibly suggesting a common mechanism. PCP- and POCOP-based Rh compounds with PⁱPr₂ side arms are faster catalysts than the PNP-based Rh complexes. However, none of the compounds under study in this work displayed notable selectivity for either *E*- or *gem*-enyne isomer. While the isomeric ratios vary considerably as a function of the catalyst and the alkyne substrate, clear trends are not apparent.

4.4 Experimental

4.4.1 General Considerations

Unless otherwise specified, all manipulations were performed under an argon atmosphere using standard Schlenk line or glove box techniques. Toluene, THF, pentane, and isooctane were dried and deoxygenated (by purging) using a solvent purification system and stored over molecular sieves in an Ar-filled glove box. C₆D₆ was dried over and distilled from NaK/Ph₂CO/18-crown-6 and stored over molecular sieves in an Ar-filled glove box. Fluorobenzene and 1,4-dioxane were dried with and then distilled or vacuum transferred from CaH₂. Synthesis of **403-H**,²²³ **404-H**,²²⁴ **410-H**,²³⁴ **403-Rh(H)(Cl)**,²³³ **404-Rh(H₂)**,²³⁶ [(COD)RhCl]₂,²⁴³ [(COD)Rh(OAc)]₂,²⁴⁴ [(COE)₂RhCl]₂²⁴⁵ was accomplished according to literature procedures. **407-H** was synthesized by modification of a literature procedure.¹³⁷ NMR spectra were recorded on a Varian NMRS 500 (¹H NMR, 499.686 MHz; ¹³C NMR, 125.659 MHz; ³¹P NMR, 202.298 MHz) spectrometer. Chemical shifts are reported in δ (ppm). For ¹H and ¹³C NMR spectra, the residual solvent peak was used as an internal reference. ³¹P NMR spectra were referenced externally using 85% H₃PO₄ at δ 0 ppm. Alkynes and isopropyl sulfide were freeze-pumped-thawed to remove oxygen before entering the glovebox. Elemental analyses were performed by CALI Labs, Inc. (Parsippany, NJ).

4.4.2 Synthesis and Characterization

Synthesis of (POCOP)Rh(SⁱPr₂) (403-Rh(SⁱPr₂)). In a Schlenk flask, **403-Rh(H)(Cl)** (298 mg, 0.624 mmol) was dissolved in toluene and was treated with

NaO^tBu (148 mg, 1.54 mmol), and SⁱPr₂ (82.4 μL, 0.624 mmol). The reaction was stirred for 60 min at RT, the reaction was passed through a pad of Celite and the volatiles were removed by vacuum and recrystallized from pentane to give a brown-yellow solid (294 mg, 84% yield). ³¹P{¹H} NMR (C₆D₆): δ 184.8 (d, *J*_{Rh-P} = 174 Hz); ¹H NMR (C₆D₆): δ 6.99 (t, 1H, *Ar-H*, *J* = 7.5 Hz), 6.89 (d, 2H, *Ar-H*, *J* = 8.0 Hz), 2.70 (m, 2H, SCHMe₂), 2.20 (m, 4H, CHMe₂), 1.29 (apparent q (dvt), 12H, P(CHCH₃)₂, *J* = 7 Hz), 1.25 (apparent q (dvt), 12H, P(CHCH₃)₂, *J* = 7 Hz), 1.21 (d, 12H, S(CHCH₃)₂, *J* = 7 Hz); ¹³C{¹H} NMR (C₆D₆): δ 167.7 (t, *J*_{C-P} = 9 Hz, *Ar-OP*), 140.9 (dt, *J*_{Rh-C} = 35 Hz, *J*_{C-P} = 10 Hz, *Ar-Rh*), 124.7 (s, *Ar*), 103.8 (t, *J*_{C-P} = 7 Hz, *Ar-H*), 40.9 (s, SCHMe₂), 30.6 (dvt, *J*_{C-P} = 10 Hz, *J*_{Rh-C} = 2 Hz, PCHMe₂), 24.1 (s, SCHMe₂), 18.7 (t, *J*_{C-P} = 4 Hz, PCHMe₂), 17.6 (s, PCHMe₂). Elem. Anal. Found (Calculated) for C₂₄H₄₅O₂P₂RhS: C, 50.98 (51.24); H, 7.97 (8.06).

Synthesis of (POCOP)Rh(C₆H₁₀) (403-Rh(C₆H₁₀)). 403-Rh(H)(Cl) (150 mg, 0.312 mmol) was dissolved in toluene and treated with NaO^tBu (33 mg, 0.343 mmol) and 3-hexyne (39 μL, 0.343 mmol) and stirred for 2 h. The volatiles were removed under vacuum and the product was extracted with pentane and filtered through silica and Celite. The volatiles were removed under vacuum to yield a light orange solid judged to be >97% pure by ¹H NMR spectroscopy (85 mg, 52% yield). ³¹P{¹H} NMR (C₆D₆): δ 182.0 (d, *J*_{Rh-P} = 166 Hz); ¹H NMR (C₆D₆): δ 6.99 (t, 1H, *J* = 8 Hz, *Ar-H*), 6.93 (d, 2H, *J* = 8 Hz), 2.47 (q, 4H, *J* = 7.5 Hz, hexyne-CH₂), 2.03 (m, 4H, PCHMe₂), 1.24 (apparent q (dvt), 12H, P(CHCH₃)₂, *J* = 7 Hz), 1.16 (t, 6H, *J* = 7.5 Hz, hexyne-CH₃), 1.11 (apparent q (dvt), 12H, P(CHCH₃)₂, *J* = 7.5 Hz); ¹³C{¹H} NMR (C₆D₆): δ 168.7 (vt, *J*_{C-P} = 8.7 Hz,

Ar-OP), 143.3 (dvt, $J_{\text{Rh-C}} = 31.0$ Hz, $J_{\text{P-C}} = 9.2$ Hz, *Ar-Rh*), 127.3 (s, *Ar*), 104.2 (t, $J_{\text{C-P}} = 6.6$ Hz, *Ar-H*), 77.4 (d, $J_{\text{Rh-C}} = 6.8$ Hz, *Rh-(C≡C)*), 29.9 (dt, $J_{\text{C-P}} = 9.6$ Hz, $J_{\text{Rh-C}} = 2.1$ Hz, *PCHMe*₂), 20.8 (s, hexyne), 17.6 (t, $J_{\text{C-P}} = 4.5$ Hz, *PCHMe*₂), 17.5 (s, *PCHMe*₂), 16.0 (s, hexyne).

Synthesis of (^{Napt}POCOP)H (405-H). In a Teflon screw-top flask, 1,7-dihydroxynaphthalene (479 mg, 2.99 mmol) was dissolved in THF and *CIP*ⁱPr₂ (956 mg, 6.26 mmol) was added slowly while stirring. The solution turned from dark to light brown with the dropwise addition of NEt₃ (994 mg, 9.82 mmol). The reaction mixture was heated at 85 °C for 1.5 h. The mixture was then passed through Celite, and the volatiles were removed under vacuum to produce a thick brown oil that was determined to be >95% pure by ¹H NMR spectroscopy (926 mg, 79% yield). ³¹P{¹H} NMR (C₆D₆): δ 148.1 (s), 146.9 (s); ¹H NMR (C₆D₆): δ 8.41 (t, 1H, $J = 2.5$ Hz, *Ar-H*), 7.56 (t, 1H, $J = 2.5$ Hz, *Ar-H*), 7.53 (d, 1H, $J = 9.5$ Hz, *Ar-H*), 7.37 (m, 1H, *Ar-H*), 7.29 (d, 1H, $J = 8$ Hz, *Ar-H*), 7.15 (m, 1H, *Ar-H*), 1.83 (m, 4H, *P-CHMe*₂), 1.20 (m, 12H, CH(CH₃)₂), 1.01 (m, 12H, CH(CH₃)₂); ¹³C{¹H} NMR (C₆D₆): δ 157.6 (d, $J_{\text{C-P}} = 8$ Hz, *Ar-OP*), 154.9 (d, $J_{\text{C-P}} = 9$ Hz, *Ar-OP*), 131.4 (*Ar*), 129.8 (*Ar*), 124.2 (*Ar*), 121.3 (*Ar*), 121.1 (d, $J_{\text{C-P}} = 6$ Hz, *Ar*), 111.8 (*Ar*), 111.7 (*Ar*), 108.4 (d, $J_{\text{C-P}} = 16$ Hz, *Ar*), 28.7 (d, $J_{\text{C-P}} = 19$ Hz, 2 *CHMe*₂), 18.0 (d, $J_{\text{C-P}} = 15$ Hz, *CHMe*₂), 17.8 (d, $J_{\text{C-P}} = 15$ Hz, *CHMe*₂), 17.3 (d, $J_{\text{C-P}} = 5$ Hz, *CHMe*₂), 17.24 (d, $J_{\text{C-P}} = 5$ Hz, *CHMe*₂).

Synthesis of (^{Napt}POCOP)Rh(H)(Cl) (405-Rh(H)(Cl)). In a Teflon screw-top flask, **405-H** (209 mg, 0.533 mmol) and [(COD)RhCl]₂ (131 mg, 1.066 mmol) were dissolved in toluene and stirred overnight at 90 °C. The reaction mixture was passed

through silica and Celite, and the volatiles were removed under vacuum. The resulting red solid was dissolved in a minimum amount of toluene and layered with pentane. A red solid precipitated out of solution (215 mg, 76%). $^{31}\text{P}\{^1\text{H}\}$ (C_6D_6): δ 183.7 (dd, $J_{\text{P-P}} = 424$ Hz, $J_{\text{P-Rh}} = 111$ Hz), 164.4 (dd, $J_{\text{P-P}} = 418$ Hz, $J_{\text{P-Rh}} = 121$ Hz); ^1H NMR (C_6D_6): δ 7.38 (t, 2H, $J = 8.5$ Hz, Ar-H), 7.20 (d, 1H, $J = 9$ Hz, Ar-H), 7.11 (d, 1H, $J = 7.5$ Hz, Ar-H), 7.05 (t, 1H, $J = 8$ Hz, Ar-H), 2.75 (m, 1H, PCHMe₂), 2.64 (m, 1H, PCHMe₂), 2.46 (m, 1H, PCHMe₂), 2.21 (m, 1H, PCHMe₂), 1.35 (dd, 3H, $J_{\text{H-P}} = 17.5$ Hz, $J_{\text{H-H}} = 7.5$ Hz, PCH(CH₃)₂), 1.18 (m, 21H, PCH(CH₃)₂), -24.10 (apparent dt, 1H, $J_{\text{H-Rh}} = 45$ Hz, $J_{\text{H-P}} = 15$ Hz, Rh-H); $^{13}\text{C}\{^1\text{H}\}$ NMR (C_6D_6): δ 166.1 (m, Ar-OP), 154.7 (m, Ar-OP), 133.1 (s, Ar), 130.1 (d, $J = 9$ Hz, Ar), 128.4 (Ar), 125.4 (Ar), 123.4 (Ar), 123.1 (m, C-Rh) 115.5 (d, $J = 2.5$ Hz, Ar), 115.3 (d, $J_{\text{C-P}} = 13$ Hz, Ar), 29.8 (m, PCHMe₂), 29.5 (m, PCHMe₂) 29.0 (m, PCHMe₂), 28.17 (d, $J_{\text{C-P}} = 23$ Hz, PCHMe₂), 18.7 (d, $J_{\text{C-P}} = 4$ Hz, PCHMe₂), 18.3 (s, PCHMe₂), 18.0 (s, PCHMe₂), 17.7 (s, PCHMe₂), 17.6 (s, PCHMe₂), 17.1 (m, PCHMe₂), 16.4 (m, PCHMe₂), 16.1 (s, PCHMe₂). Elem. Anal. Found (Calculated) for C₂₂H₃₄ClO₂P₂Rh: C, 49.91 (49.78); H, 6.24 (6.46).

Synthesis of (^{Napt}POCOP^{iPr})Rh(S^{iPr}Pr₂) (405-Rh(S^{iPr}Pr₂)). In a Schlenk flask, **405-Rh(H)(Cl)** (180 mg, 0.339 mmol), NaO^tBu (56 mg, 0.509 mmol), and diisopropyl sulfide (100 μL , 0.688 mmol) were dissolved in toluene. The reaction mixture was stirred for 1 h at RT, and the volatiles were removed under vacuum. The resulting solid was washed with pentane and dissolved in benzene to be filtered over a pad of Celite. The volatiles were removed to yield a dark orange solid (73 mg, 35%). $^{31}\text{P}\{^1\text{H}\}$ NMR (C_6D_6): δ 181.6 (dd, $J_{\text{P-P}} = 362$ Hz, $J_{\text{P-Rh}} = 162$ Hz), 156.2 (dd, $J_{\text{P-P}} = 362$ Hz, $J_{\text{P-Rh}} = 172$

Hz); ^1H NMR (C_6D_6): δ 7.49 (m, 3H, Ar-H), 7.20 (d, $J = 10$ Hz, 1H, Ar-H), 7.15 (t, obscured by benzene peak, 1H, Ar-H), 2.71 (m, 2H, S(CHMe₂)₂), 2.40 (m, 2H, P(CHMe₂)₂), 2.22 (m, 2H, P(CHMe₂)₂), 1.30 (dd, 6H, $J = 7$ Hz, $J = 5$ Hz, PCH(CH₃)₂), 1.28 (dd, 6H, $J = 8$ Hz, $J = 4$ Hz, PCH(CH₃)₂), 1.27 (dd, 6H, $J = 7$ Hz, $J = 5$ Hz, PCH(CH₃)₂), 1.25 (dd, 6H, $J = 9$ Hz, $J = 5$ Hz, PCH(CH₃)₂), 1.21 (d, 12H, $J = 10$ Hz, S(CHMe₂)₂); $^{13}\text{C}\{^1\text{H}\}$ NMR (C_6D_6): δ 166.2 (d, $J_{\text{C-P}} = 16$ Hz, Ar-OP), 156.1 (d, $J_{\text{C-P}} = 3$ Hz, Ar-OP), 135.0 (br d, $J_{\text{C-Rh}} = 41$ Hz, Ar-Rh), 132.6 (Ar), 131.5 (d, $J = 12$ Hz, Ar), 126.6 (Ar), 123.7 (Ar), 122.2 (Ar), 114.3 (d, $J = 15$ Hz, Ar), 113.2 (d, $J = 5$ Hz, Ar), 37.6 (dd, $J = 13$ Hz, S(CHMe₂)₂), 31.0 (ddd, $J_{\text{C-P}} = 13$ Hz, $J = 5$ Hz, $J = 3$ Hz, P(CHMe₂)₂), 30.5 (ddd, $J_{\text{C-P}} = 19$ Hz, $J = 5$ Hz, $J = 3$ Hz, P(CHMe₂)₂), 24.9 (s, S(CHMe₂)₂), 19.2 (d, $J_{\text{C-P}} = 9$ Hz, P(CHMe₂)₂), 18.8 (d, $J_{\text{C-P}} = 6$ Hz, P(CHMe₂)₂), 17.8 (s, P(CHMe₂)₂), 17.6 (s, P(CHMe₂)₂). Elem. Anal. Found (Calculated) for C₂₈H₄₇O₂P₂RhS: C, 54.90 (54.81); H, 7.73 (7.69).

Synthesis of (^{Napt}POCOP^{iPr})Rh(CO) (405-Rh(CO)). In a Teflon screw-top flask, **405-Rh(H)(Cl)** (106 mg, 0.200 mmol) was dissolved in toluene and treated with NaO^tBu (30 mg, 0.312 mmol). The flask was then degassed, filled with CO, and stirred at RT for 2 h. The volatiles were removed and product was extracted with pentane and filtered through silica and Celite. The volatiles were removed and the product was recrystallized from hexamethyldisiloxane as yellow crystals in >98% purity as judged by ^1H NMR (64 mg, 62% yield). $^{31}\text{P}\{^1\text{H}\}$ NMR (C_6D_6): δ 199.3 (dd, $J_{\text{P-P}} = 318$ Hz, $J_{\text{P-Rh}} = 140$ Hz), 170.0 (dd, $J_{\text{P-P}} = 317$ Hz, $J_{\text{P-Rh}} = 147$ Hz); ^1H NMR (C_6D_6): δ 7.52 (dd, 1H, $J = 9$ Hz, $J = 2$ Hz), 8.5 (d, 2H, $J = 9$ Hz), 7.44 (dd, 1H, $J = 8$ Hz, 2 Hz), 7.20 (dd, 1H, $J = 8$

Hz, 2 Hz), 7.11 (dd, 1H, apparent t, 8 Hz), 2.13 (m, 4H, $CHMe_2$), 0.87 (dd, 6H, $J_{H-P} = 17.5$ Hz, $J = 7$ Hz, $PCH(Me)_2$), 0.86 (dd, 6H, $J_{H-P} = 18$ Hz, $J = 7$ Hz, $PCH(Me)_2$), 0.86 (dd, 6H, $J_{H-P} = 14.5$ Hz, 7 Hz, $PCH(Me)_2$), 0.85 (dd, 6H, $J_{H-P} = 14$ Hz, 7 Hz, $PCH(Me)_2$). $^{13}C\{^1H\}$ NMR (C_6D_6): δ 196.8 (ddd (apparent dt), $J_{Rh-C} = 56$ Hz, $J_{C-P} = 14$ Hz, $J_{C-P} = 14$ Hz, Rh-CO), 168.0 (dd, $J_{C-P} = 16$ Hz, $J_{C-Rh} = 3$ Hz, *Ar*-OP), 155.5 (dd (apparent t), $J_{C-P} = 2$ Hz, $J_{C-Rh} = 2$ Hz, *Ar*-OP), 137.8 (ddd, $J_{C-Rh} = 31$ Hz, $J_{C-P} = 13$ Hz, $J_{C-P} = 6$ Hz, *Ar*-Rh), 132.0 (m, *Ar*), 130.3 (s, *Ar*-H), 129.9 (d, $J = 12$ Hz, *Ar*), 124.9 (s, *Ar*-H), 122.7 (s, *Ar*-H), 114.9 (d, $J = 5$ Hz, *Ar*-H), 114.8 (d, $J = 5$ Hz, *Ar*-H), 114.8 (d, $J = 15$ Hz, *Ar*-H), 32.3 (ddd, $J_{C-P} = 24$ Hz, $J = 4$ Hz, $J = 2$ Hz, $P(CHMe_2)_2$), 30.4 (apparent dt (ddd), $J_{C-P} = 22$ Hz, $J = 3$ Hz, $P(CHMe_2)_2$), 18.6 (d, $J_{C-P} = 8$ Hz, $P(CHMe_2)_2$), 17.9 (d, $J_{C-P} = 7$ Hz, $P(CHMe_2)_2$), 17.6 (s, $P(CHMe_2)_2$), 17.5 (s, $P(CHMe_2)_2$). IR: 1950 cm^{-1} , ν_{CO} .

Synthesis of 1,7-bis(ditertbutylphosphinyl)naphthalenediol (406-H). In a culture tube, 1,7-dihydroxynaphthalene (78 mg, 0.487mmol) was dissolved in THF and NaH (36 mg, 1.5 mmol) was added slowly. The reaction mixture was refluxed for 4 h and passed through a pad of Celite with diethyl ether. The volatiles were removed under vacuum to give a brown solid determined by 1H NMR spectroscopy to be >95% pure (156 mg, 71%). $^{31}P\{^1H\}$ NMR (C_6D_6): δ 154.8 (s), 150.5 (s); 1H NMR (C_6D_6): 8.51 (s, 1H, *Ar*-H), 7.62 (m, 1H, *Ar*-H), 7.55 (d, 1H, $J = 9$ Hz, *Ar*-H), 7.35 (m, 1H, *Ar*-H), 7.29 (d, 1H, $J = 8$ Hz, *Ar*-H), 7.18 (d, 1H, $J = 8$ Hz, *Ar*-H), 1.19 (d, 36H, $C(CH_3)_3$, $J_{H-P} = 11$ Hz); $^{13}C\{^1H\}$ NMR (C_6D_6): δ 158.1 (d, $J_{C-P} = 10$ Hz, *Ar*-OP), 155.2 (d, $J_{C-P} = 9$ Hz, *Ar*-OP), 131.4 (*Ar*), 129.7 (*Ar*), 124.2 (*Ar*), 121.1 (d, $J_{C-P} = 6$ Hz, *Ar*), 120.9 (*Ar*), 111.3 (*Ar*), 111.2 (*Ar*), 108.4 (*Ar*, $J_{C-P} = 16$ Hz), 36.0 ($J_{C-P} = 16$ Hz, $PCMe_3$), 35.8 ($J_{C-P} = 15$

Hz, P(CMe₃)₂), 27.7 (d, $J_{C-P} = 2$ Hz, P(C(CH₃)₃), 27.6 (d, $J_{C-P} = 2$ Hz, P(C(CH₃)₃). HRMS (ESI+TOF) m/z : [M + H]⁺ Calcd. for C₂₆H₄₄O₂P₂ 449.2733; found 449.2728

Synthesis of (^{Napth}POCOP^{tBu})Rh(H)(Cl) (406-Rh(H)(Cl)). In a Teflon screw-top flask, **406-H** (64.4 mg, 0.144 mmol) and [(COD)Rh(Cl)]₂ (35.4 mg, 0.717 mmol) were dissolved in toluene and stirred overnight at 80 °C. The reaction mixture was filtered through Celite and the volatiles were removed under vacuum. The resulting solid recrystallized from diethyl ether at -35 °C to yield brown crystals judged to be >97% pure by ¹H NMR (78 mg, 92%). ³¹P{¹H} NMR (C₆D₆): δ 184.8 (dd, $J_{P-P} = 408$ Hz, $J_{P-Rh} = 115$ Hz), 166.5 (dd, $J_{P-P} = 406$ Hz, $J_{P-Rh} = 121$ Hz); ¹H NMR (C₆D₆): δ 7.40 (m, 2H, Ar-H), 7.21 (d, 2H, $J = 9$ Hz, Ar-H), 7.07 (m, 2H, Ar-H), 1.47 (d, 9H, $J_{H-P} = 14$ Hz, P(C(CH₃)₃), 1.42 (d, 9H, $J_{H-P} = 14$ Hz, P(C(CH₃)₃), 1.38 (d, 9H, $J_{H-P} = 15$ Hz, P(C(CH₃)₃), 1.35 (d, 9H, $J_{H-P} = 15$ Hz, P(C(CH₃)₃), -25.21 (ddd, 1H, $J_{H-Rh} = 46$ Hz, $J_{H-P} = 12$ Hz, $J_{H-P} = 12$ Hz); ¹³C{¹H} NMR (C₆D₆): δ 167.2 (dd, $J_{C-P} = 11$ Hz, $J_{C-Rh} = 4$ Hz, Ar-OP), 154.7 (dd, $J = 4$ Hz, $J = 3$ Hz, Ar-OP), 133.06 (Ar), 130.1 (d, $J = 8$ Hz, Ar), 125.2 (Ar), 123.3 (Ar), 115.47 (Ar), 115.43 (Ar), 115.37 (Ar), 115.27 (Ar), 43.0 (dd, $J_{C-P} = 8$ Hz, $J_{C-Rh} = 6$ Hz, P(CMe₃)₂), 41.4 (dd, $J_{C-P} = 9$ Hz, $J_{C-Rh} = 6$ Hz, P(CMe₃)₂), 40.4 (ddd, $J_{C-P} = 20$ Hz, $J = 5$ Hz, $J = 1$ Hz, P(CMe₃)₂), 38.6 (ddd, $J_{C-P} = 14$ Hz, $J = 5$ Hz, $J = 3$ Hz, P(CMe₃)₂), 28.9 (d, $J_{C-P} = 6$ Hz, P(CMe₃)₂), 28.8 (d, $J_{C-P} = 5$ Hz, P(CMe₃)₂), 28.7 (d, $J_{C-P} = 5$ Hz, P(CMe₃)₂), 28.1 (d, $J_{C-P} = 5$ Hz, P(CMe₃)₂).

Synthesis of (^{Nap^t}POCOP^{tBu})Rh(SⁱPr₂) (406-Rh(SⁱPr₂)). In a Schlenk flask, **406-Rh(H)(Cl)** (110 mg, 0.187 mmol), NaO^tBu (30 mg, 0.281 mmol), diisopropyl sulfide (55 μL, 0.374 mmol) were mixed in toluene and stirred for 3 h at RT. The

volatiles were removed under vacuum, and the resulting solid was dissolved in pentane and passed through Celite. The resulting brown solid was dissolved in a minimum of pentane and placed in a -35 °C freezer overnight to produce brown crystals (59 mg, 47% yield). $^{31}\text{P}\{^1\text{H}\}$ NMR (C_6D_6): δ 185.4 (dd, $J_{\text{P-P}} = 327$ Hz, $J_{\text{P-Rh}} = 168$ Hz), 163.2 (dd, $J_{\text{P-P}} = 323$ Hz, $J_{\text{P-Rh}} = 175$ Hz); ^1H NMR (C_6D_6): δ 7.41 (br s, 2H, Ar-H), 7.27 (br s, 1H, Ar-H), 7.15 (br s, 2H, Ar-H), 2.82 (m, 2H, S(CHMe₂)₂), 1.40 (d, 36H, $J_{\text{H-P}} = 6$ Hz, P(CMe₃)₂), 1.21 (d, 12H, $J_{\text{H-H}} = 4$ Hz, S(CHMe₂)₂); $^{13}\text{C}\{^1\text{H}\}$ NMR (C_6D_6): δ 166.8 (d, $J_{\text{C-P}} = 19$ Hz, Ar-OP), 156.1 (d, $J_{\text{C-P}} = 3$ Hz, Ar-OP), 132.8 (Ar), 131.6 (m, Ar-Rh), 126.3 (Ar), 124.1 (Ar), 122.2 (Ar), 114.4 (d, $J_{\text{C-P}} = 14$ Hz, Ar), 113.32 (Ar), 113.29 (Ar), 41.0 (m, S(CHMe₂)₂), 39.7 (m, P(CMe₃)₂), 38.2 (s, P(CMe₃)₂), 29.5 (d, $J_{\text{C-P}} = 9$ Hz, P(CMe₃)₂), 29.4 (d, $J = 8$ Hz, P(CMe₃)₂), 24.9 (s, S(CHMe₂)). Elem. Anal. Found (calculated) for C₃₂H₅₅O₂P₂RhS: C, 57.29 (57.48); H, 8.16 (8.29).

(^{Napt}POCOP^{tBu})Rh(CO) (406-Rh(CO)). In a 10 mL Teflon screw-top flask, **406-Rh(H)(Cl)** (50 mg, 0.085 mmol) was dissolved in toluene and treated with NaO^tBu (10 mg, 0.10 mmol). The flask was degassed and filled with CO and stirred overnight at RT. The volatiles were removed under vacuum and the product was extracted with pentane and filtered through silica and Celite. The volatiles were removed to produce a yellow powder judged to be >97% pure by ^1H NMR (30 mg, 61%). $^{31}\text{P}\{^1\text{H}\}$ NMR (C_6D_6): δ 207.1 (dd, $J_{\text{P-P}} = 306$ Hz, $J_{\text{P-Rh}} = 140$ Hz), 179.7 (dd, $J_{\text{P-P}} = 306$ Hz, $J_{\text{P-Rh}} = 147$ Hz); ^1H NMR (C_6D_6): δ 7.53 (dd, 1H, $J = 2$ Hz, $J = 9$ Hz), 7.44 (t, 2H, $J = 8$ Hz, Ar-H), 7.19 (dd, 1H, $J = 8$ Hz, $J = 2$ Hz, Ar-H), 7.13 (t, 2H, $J = 8$ Hz, Ar-H), 1.35 (d, 18H, $J_{\text{H-P}} = 7$ Hz, P(CMe₃)₂), 1.32 (d, 18H, $J_{\text{C-P}} = 7$ Hz, P(CMe₃)₂); $^{13}\text{C}\{^1\text{H}\}$ NMR (C_6D_6): δ 198.7

(ddd (apparent dt), $J_{C-Rh} = 57$ Hz, $J_{C-P} = 14$ Hz, Rh-CO), 168.9 (dd, $J_{C-P} = 15$ Hz, $J_{C-Rh} = 3$ Hz, Ar-OP), 156.4 (m, Ar-OP), 138.4 (ddd, $J_{C-Rh} = 33$ Hz, $J_{C-P} = 13$ Hz, $J_{C-P} = 6$ Hz, Ar-Rh), 132.0 (s, Ar), 130.2 (s, Ar-H), 129.3 (d, $J = 11$ Hz, Ar), 124.7 (s, Ar-H), 122.6 (s, Ar-H), 114.8 (d, $J = 15$ Hz, Ar-H), 114.5 (d, $J = 5$ Hz, Ar-H), 41.3 (ddd, $J_{C-P} = 17$ Hz, $J = 4$ Hz, $J = 2$ Hz, P(CMe₃)₂), 39.9 (apparent dt, $J_{C-P} = 15$ Hz, $J = 3$ Hz, P(CMe₃)₂), 28.6 (d, $J_{C-P} = 7$ Hz, P(CMe₃)₂), 28.3 (d, $J_{C-P} = 7$ Hz, P(CMe₃)₂). IR: 1945 cm⁻¹, ν_{CO} .

Synthesis of 1-(ⁱPr₂PO)-3-(ⁱPr₂POCH₂)(C₆H₄) (407-H).¹³⁷ To a solution of 3-hydroxybenzyl alcohol (0.508 g, 4.09 mmol) in THF, triethylamine (1.241 g, 12.3 mmol) was added dropwise while stirring. A solution of ClPⁱPr₂ (1.290 g, 8.18 mmol) in THF was added slowly while stirring. A precipitate formed immediately and the reaction was stirred overnight at RT. The reaction mixture was passed through a pad of Celite, and the solvent was removed under vacuum to produce a colorless oil determined to be >95% pure by ¹H NMR spectroscopy (1.236 g, 85%). ³¹P{¹H} NMR (C₆D₆): δ 155.2 (s), 147.6 (s); ¹H NMR (C₆D₆): δ 6.88 (d, 1H, $J = 8$ Hz, Ar-H); 6.79 (t, 1H, $J = 8$ Hz, Ar-H), 6.62 (d, 1H, Ar-H, $J = 8$ Hz, Ar-H), 4.43 (d, 2H, $J_{H-P} = 10$ Hz, CH₂OP), 1.47 (m, 2H, P(CHMe₂)₂), 1.37 (m, 2H, P(CHMe₂)₂), 0.85 (dd, 6H, $J_{H-P} = 10$ Hz, $J_{H-H} = 9$ Hz, PCH(CH₃)₂), 0.83 (dd, 6H, $J_{H-P} = 10$ Hz, $J_{H-H} = 9$ Hz, PCH(CH₃)₂), 0.69 (dd, 12H, $J_{H-P} = 15$ Hz, $J_{H-H} = 7$ Hz, PCH(CH₃)₂); ¹³C{¹H} NMR (C₆D₆): δ 160.0 (d, $J_{C-P} = 9$ Hz, Ar-OP), 141.9 (d, $J_{C-P} = 8$ Hz, Ar-CH₂OP), 129.6 (Ar-H), 120.9 (Ar-H), 118.0 (d, $J_{C-P} = 11$ Hz, Ar-H), 117.8 (d, $J_{C-P} = 11$ Hz, Ar-H), 74.4 (d, $J_{C-P} = 22$ Hz, CH₂OP), 28.7 (d, $J_{C-P} = 14$ Hz, P(CHMe₂)₂), 28.5 (d, $J_{C-P} = 14$ Hz, P(CHMe₂)₂), 18.2 (d, $J_{C-P} = 20$ Hz,

P(CHMe₂)₂), 17.8 (d, $J_{C-P} = 20$ Hz, P(CHMe₂)₂), 17.3 (d, $J_{C-P} = 9$ Hz, P(CHMe₂)₂), 17.2 (d, $J_{C-P} = 9$ Hz, P(CHMe₂)₂).

Synthesis of (POCCH₂OP^{iPr})Rh(H)(Cl)(NCCH₃) (407-Rh(H)(Cl)(NCMe)). In a Teflon screw-top flask, **407-H** (419 mg, 1.18 mmol) and [(COD)RhCl]₂ (299 mg, 0.59 mmol) were dissolved in acetonitrile and stirred overnight at 80 °C. The reaction mixture was passed through a pad of silica and Celite. The volatiles were removed under vacuum and the resulting solid was recrystallized from pentane to produce square yellow crystals judged to be >95% pure by ¹H NMR spectroscopy (520 mg, 97%) ³¹P{¹H} NMR (C₆D₆): δ 186.4 (dd, $J_{P-P} = 428$ Hz, $J_{P-Rh} = 119$ Hz), 153.9 (dd, $J_{P-P} = 416$ Hz, $J_{P-Rh} = 113$ Hz); ¹H NMR (C₆D₆): δ 6.96 (d, 1H, $J = 8$ Hz, Ar-H), 6.82 (t, 1H, $J = 8$ Hz, Ar-H), 6.62 (d, 1H, $J = 8$ Hz, Ar-H), 4.82 (m, 2H, CH₂OP), 3.09 (m, 1H, CHMe₂), 2.55 (m, 1H, CHMe₂), 2.49 (m, 1H, CHMe₂), 2.19 (m, 1H, CHMe₂), 1.62 (dd, 3H, CH(CH₃)₂, $J_{H-P} = 16$ Hz, $J_{H-H} = 7$ Hz), 1.57 (br m, 3H, CH(CH₃)₂), 1.39 (dd, 3H, CH(CH₃)₂, $J_{H-P} = 15$ Hz, $J_{H-H} = 7$ Hz), 1.31 (m, 6H, CH(CH₃)₂), 1.20 (m, 6H, CH(CH₃)₂), 0.82 (dd, 3H, CH(CH₃)₂, $J_{H-P} = 15$ Hz, $J_{H-H} = 7$ Hz), 0.52 (s, 3H, NCCH₃), -17.95 (br s, 1H, Rh-H); ¹³C{¹H} NMR (C₆D₆): δ 166.4 (d, $J_{C-P} = 13$ Hz, Ar-OP), 142.8 (d, $J_{C-P} = 9$ Hz, Ar-CH₂OP), 137.0 (m, Ar-Rh), 124.2 (Ar-H), 121.5 (Ar-H), 121.2 (NCCH₃), 111.5 (d, $J_{C-P} = 13$ Hz, Ar-H), 76.6 (s, CH₂OP), 31.6 (m, CHMe₂), 29.4 (s, CHMe₂), 29.1 (s, CHMe₂), 27.7 (s, CHMe₂), 18.6 (d, $J = 5$ Hz, CHMe₂), 18.5 (s, CHMe₂), 18.2 (s, CHMe₂), 18.0 (s, CHMe₂), 17.3 (d, $J = 3$ Hz, CHMe₂), 16.7 (d, $J = 6$ Hz, CHMe₂), 16.5 (d, $J = 9$ Hz, CHMe₂), 16.2 (s, CHMe₂), 1.2 (s, NCCH₃). Elem. Anal. Found (calculated) for C₂₁H₃₇ClNO₂P₂Rh: C, 47.07 (47.07); H, 6.98 (6.96).

Synthesis of (POCCH₂OP^{iPr})Rh(H)(Cl) (407-Rh(H)(Cl)). In a Teflon screw-top flask, **407-Rh(H)(Cl)(NCMe)** (261 mg, 0.483 mmol) was combined with sodium acetate (356 mg, 4.34 mmol) and dissolved in 1,4-dioxane. The reaction stirred overnight at 90 °C. The resulting orange solution was passed through a pad of Celite and the volatiles were removed under vacuum to produce **407-Rh(H)(OAc)** as an oily brown solid, which was characterized *in situ*. The brown solid was dissolved in toluene and trimethylsilyl chloride (100 μL, 0.788 mmol) was added. The reaction mixture was stirred for 1 h at RT and the volatiles were removed under vacuum. The oily orange solid produced was washed with hexamethyldisiloxane and redissolved in toluene to be passed through a plug of Celite. The volatiles were removed and the orange solid was dissolved in a minimum amount of toluene, layered with pentane, and then placed in a -35 °C freezer to produce an orange solid judged to be >95% pure by NMR spectroscopy (118 mg, 49%). ³¹P{¹H} NMR (C₆D₆): δ 186.7 (dd, *J*_{P-P} = 416 Hz, *J*_{P-Rh} = 118 Hz), 157.7 (dd, *J*_{P-P} = 416 Hz, *J*_{P-Rh} = 121 Hz); ¹H NMR (C₆D₆): δ 6.96 (d, 1H, *J* = 7 Hz, Ar-*H*), 6.86 (t, 1H, , *J* = 8 Hz, Ar-*H*), 6.47 (d, 1H, *J* = 7 Hz, Ar-*H*), 4.73 (dd, 1H, *J* = 17 Hz, *J* = 13 Hz, CH₂OP), 4.55 (dd, 1H, *J* = 17 Hz, *J* = 13 Hz, CH₂OP), 2.74 (m, 1H, PCHMe₂), 2.58 (m, 1H, PCHMe₂), 2.27 (m, 1H, PCHMe₂), 2.18 (m, 1H, PCHMe₂), 1.32 (dd, 3H, *J*_{H-P} = 17 Hz, *J*_{H-H} = 8 Hz, PCH(CH₃)₂), 1.28 (dd, 3H, *J*_{H-P} = 18 Hz, *J*_{H-H} = 8 Hz, PCH(CH₃)₂), 1.26 (dd, 3H, *J*_{H-P} = 17 Hz, *J*_{H-H} = 8 Hz, PCH(CH₃)₂), 1.20 (dd, 3H, *J*_{H-P} = 18 Hz, *J*_{H-H} = 7 Hz, PCH(CH₃)₂), 1.09 (dd, 3H, *J*_{H-P} = 17 Hz, *J*_{H-H} = 8 Hz, PCH(CH₃)₂), 1.07 (m, 6H, PCH(CH₃)₂), 1.05 (dd, 3H, *J*_{H-P} = 16 Hz, *J*_{H-H} = 7 Hz, PCH(CH₃)₂), -25.48 (br d, 1H, *J*_{H-Rh} = 45 Hz, Rh-*H*); ¹³C{¹H} NMR (C₆D₆): δ 168.7 (dd, *J*_{C-P} = 13 Hz, *J*_{C-Rh}

= 3.0 Hz, *Ar*-OP), 142.3 (d, $J = 8$ Hz, *Ar*-CH₂OP), 133.9 (ddd, $J_{C-Rh} = 29$ Hz, $J_{C-P} = 7$ Hz, $J_{C-P} = 5$ Hz, *Ar*-Rh), 125.6 (*Ar*-H), 121.8 (*Ar*-H), 112.4 (d, $J_{C-P} = 12$ Hz, *Ar*-H), 76.4 (d, $J_{C-P} = 2$ Hz, CH₂OP), 29.3 (m, PCHMe₂), 29.0 (m, PCHMe₂), 28.6 (m, PCHMe₂), 28.3 (m, PCHMe₂), 19.3 (d, $J_{C-P} = 4$ Hz, PCH(CH₃)₂), 18.3 (s, PCH(CH₃)₂), 18.2 (d, $J_{C-P} = 7$ Hz, PCH(CH₃)₂), 18.0 (d, $J_{C-P} = 5$ Hz, PCH(CH₃)₂), 17.9 (s, PCH(CH₃)₂), 17.1 (d, $J_{C-P} = 8$ Hz, PCH(CH₃)₂), 16.4 (apparent t (dd), $J = 2$ Hz, PCH(CH₃)₂), 16.1 (dd, $J = 4$ Hz, $J = 2$ Hz, PCH(CH₃)₂). Elem. Anal. Found (calculated) for C₁₉H₃₄ClO₂P₂Rh: C, 46.03 (46.12); H, 6.94 (6.93).

(POCCH₂OP^{iPr})Rh(H)(OAc) (407-Rh(H)(OAc)): ³¹P{¹H} NMR (C₆D₆): δ 187.1 (dd, $J_{P-P} = 416$ Hz, $J_{P-Rh} = 123$ Hz), 150.5 (dd, $J_{P-P} = 416$ Hz, $J_{P-Rh} = 119$ Hz); ¹H NMR (C₆D₆): δ 6.92 (d, 1H, $J = 8$ Hz, *Ar*-H), 6.80 (t, 1H, $J = 7$ Hz, *Ar*-H), 6.51 (d, 1H, $J = 8$ Hz, *Ar*-H), 5.01 (dd, 1H, $J_{H-P} = 8$ Hz, $J_{H-H} = 12$, CH₂OP), 4.65 (dd, 1H, $J_{H-P} = 29$ Hz, $J_{H-H} = 12$ Hz, CH₂OP), 2.38 (m, 1H, CHMe₂), 2.29 (m, 1H, CHMe₂), 2.21 (m, 1H, CHMe₂), 2.06 (m, 1H, CHMe₂), 1.93 (s, 3H, O₂CCH₃), 1.49 (dd, 3H, $J_{H-P} = 14$ Hz, $J_{H-H} = 8$ Hz, CH(CH₃)₂), 1.31 (dd, 3H, $J_{H-P} = 15$ Hz, $J_{H-H} = 8$ Hz, CH(CH₃)₂), 1.23 (dd, 3H, $J_{H-P} = 18$ Hz, $J_{H-H} = 7$ Hz, CH(CH₃)₂), 1.17 (dd, 3H, $J_{H-P} = 18$ Hz, $J_{H-H} = 7$ Hz, CH(CH₃)₂), 1.16 (dd, 3H, $J_{H-P} = 15$ Hz, $J_{H-H} = 8$ Hz, CH(CH₃)₂), 1.15 (dd, 3H, $J_{H-P} = 15$ Hz, $J_{H-H} = 8$ Hz, CH(CH₃)₂), 0.97 (dd, 3H, $J_{H-P} = 18$ Hz, $J_{H-H} = 7$ Hz, CH(CH₃)₂), 0.89 (dd, 3H, $J_{H-P} = 16$ Hz, $J_{H-H} = 8$ Hz, CH(CH₃)₂), -21.05 (ddd, $J_{H-Rh} = 27$ Hz, $J_{H-P} = 15$ Hz, $J_{H-P} = 12$ Hz, Rh-H); ¹³C{¹H} NMR (C₆D₆): δ 183.2 (s, O₂CCH₃), 167.6 (dd, $J_{C-P} = 13$ Hz, $J_{C-Rh} = 3$ Hz, *Ar*-OP), 142.2 (d, $J_{C-P} = 7$ Hz, *Ar*CH₂OP), 133.5 (br d, $J_{C-Rh} = 31$ Hz, *Ar*-Rh), 124.2 (*Ar*-H), 121.8 (*Ar*-H), 111.5 (d, $J = 11$ Hz, *Ar*-H), 76.6 (s, CH₂OP), 31.0

(apparent t (dd), $J = 10$ Hz, CHMe_2), 28.6 (ddd, $J_{\text{C-P}} = 26$ Hz, $J = 2$ Hz, $J = 2$ Hz, CHMe_2); 28.4 (apparent t (dd), $J = 10$ Hz, CHMe_2), 28.19 (apparent t (dd), $J = 3$ Hz, CHMe_2), 24.4 (s, O_2CCH_3), 18.2 (s, CHMe_2), 18.0 (d, $J_{\text{C-P}} = 3$ Hz, CHMe_2), 17.8 (s, CHMe_2), 17.4 (d, $J_{\text{C-P}} = 9$ Hz, CHMe_2), 16.9 (d, $J_{\text{C-P}} = 6$ Hz, CHMe_2), 16.5 (s, CHMe_2), 16.4 (dd, $J_{\text{C-P}} = 4$ Hz, $J_{\text{C-Rh}} = 1$ Hz, CHMe_2), 16.2 (d, $J_{\text{C-P}} = 10$ Hz, CHMe_2).

Synthesis of (POCCH₂OP^{iPr})Rh(SⁱPr₂) (407-Rh(SⁱPr₂)). In a Teflon screw-cap culture tube, **407-Rh(H)(Cl)** (118 mg, 0.238 mmol) was dissolved in toluene with NaO^tBu (40 mg, 0.363 mmol). Diisopropyl sulfide (50 μL , 0.344 mmol) was added and the mixture was stirred overnight at RT. The volatiles were removed under vacuum and the brown solid was dissolved in pentane and filtered through silica and Celite. The volatiles were removed under vacuum and the reaction mixture was dissolved in a minimum amount of diethyl ether and placed in a -35 °C freezer to precipitate the product as a reddish-brown solid. (16.3 mg, 46%). Although this material appears to be pure by NMR spectroscopy, we have been unable to obtain satisfactory elemental analysis data. ³¹P{¹H} NMR (C_6D_6): δ 186.7 (dd, $J_{\text{P-P}} = 345$ Hz, $J_{\text{P-Rh}} = 174$ Hz), 151.7 (dd, $J_{\text{P-P}} = 347$ Hz, $J_{\text{P-Rh}} = 176$ Hz); ¹H NMR (C_6D_6): δ 7.17 (d, 1H, $J = 8$ Hz, Ar-H), 6.96 (t, 1H, $J = 7$ Hz, Ar-H), 6.70 (d, 1H, $J = 8$ Hz, Ar-H), 4.92 (d, 2H, $J_{\text{H-P}} = 19$ Hz, CH_2OP), 2.77 (m, 2H, $\text{S}(\text{CHMe}_2)_2$), 2.23 (overlapping m, 4H, $\text{P}(\text{CHMe}_2)_2$), 1.30 (dd, 6H, $J_{\text{H-P}} = 16$ Hz, $J_{\text{H-H}} = 7$ Hz, $\text{P}(\text{CH}(\text{CH}_3)_2)_2$), 1.26 (d, 12H, $J_{\text{H-H}} = 7$ Hz, $\text{S}(\text{CH}(\text{CH}_3)_2)_2$), 1.25 (dd, 6H, $J_{\text{H-P}} = 12$ Hz, $J_{\text{H-H}} = 7$ Hz, $\text{P}(\text{CH}(\text{CH}_3)_2)_2$), 1.22 (dd, 6H, $J_{\text{H-P}} = 16$ Hz, $J_{\text{H-H}} = 7$ Hz, $\text{P}(\text{CH}(\text{CH}_3)_2)_2$), 1.08 (dd, 6H, $J_{\text{H-P}} = 12$ Hz, $J_{\text{H-H}} = 7$ Hz, $\text{P}(\text{CH}(\text{CH}_3)_2)_2$); ¹³C{¹H} NMR (C_6D_6): δ 168.33 (d, $J_{\text{C-P}} = 18$ Hz, Ar-OP), 146.38 (m, Ar-Rh), 144.38 (d,

$J_{C-P} = 13$ Hz, *Ar-OP*), 123.68 (*Ar-H*), 120.04 (*Ar-H*), 110.32 (d, $J_{C-P} = 14$ Hz, *Ar-H*), 78.50 (d, $J_{C-P} = 6$ Hz, CH_2OP), 41.95 (s, $S(CHMe_2)_2$), 37.60 (m (overlapping signals), $P(CHMe_2)_2$), 30.95 (m, $P(CHMe_2)_2$), 28.96 (dd, $J_{C-P} = 20$ Hz, $J_{C-Rh} = 3$ Hz, $P(CHMe_2)_2$), 24.49 (s, $S(CHMe_2)_2$), 19.05 (dd, $J_{C-P} = 9$ Hz, $J_{C-Rh} = 1$ Hz, $P(CH(CH_3)_2)$), 18.19 (dd, $J_{C-P} = 8$ Hz, $J_{C-Rh} = 3$ Hz, $P(CH(CH_3)_2)$), 17.81 (s, $P(CH(CH_3)_2)$), 17.42 (s, $P(CH(CH_3)_2)$).

Synthesis of $(POCCH_2OP^{iPr})Rh(CO)$ (407-Rh(CO)). In a Teflon capped 10 mL flask, **407-Rh(S^iPr_2)** (200 mg, 0.35 mmol) was dissolved in toluene and degassed. The flask was then filled with CO and stirred for 2 h at RT. The reaction mixture was then filtered through Celite and silica and the volatiles were removed under vacuum. The resulting yellow solid was then dissolved in pentane and placed in a -35 °C freezer to produce yellow crystals judged to be >97% pure by 1H NMR (97 mg, 57% yield). $^{31}P\{^1H\}$ NMR (C_6D_6): δ 202.0 (dd, $J_{P-P} = 310$ Hz, $J_{Rh-P} = 145$ Hz, *Ar-OP*), 166.3 (dd, $J_{P-P} = 310$ Hz, $J_{Rh-P} = 150$ Hz, *Ar-CH₂OP*); 1H NMR (C_6D_6): δ 7.16 (d, 1H, *Ar-H*, $J = 7.5$ Hz), 6.98 (t, 1H, *Ar-H*, $J = 7$ Hz), 6.62 (d, 1H, $J = 7$ Hz), 4.75 (d, 2H, CH_2OP , $J_{H-P} = 18$ Hz), 2.11 (m, 2H, $PCHMe_2$), 2.00 (m, 2H, $PCHMe_2$), 1.20 (dd, 6H, $PCH(Me)_2$, $J_{H-P} = 17.5$ Hz, $J_{H-H} = 7.5$ Hz), 1.15 (dd, 6H, $PCH(Me)_2$, $J_{H-P} = 14.5$ Hz, $J_{H-H} = 7$ Hz), 1.15 (dd, 6H, $PCH(Me)_2$, $J_{H-P} = 17.5$ Hz, $J_{H-H} = 7$ Hz), 1.07 (dd, 6H, $PCH(Me)_2$, $J_{H-P} = 13.5$ Hz, $J_{H-H} = 7$ Hz); $^{13}C\{^1H\}$ NMR (C_6D_6): δ 197.35 (ddd, $J_{Rh-C} = 56$ Hz, $J_{P-C} = 14$ Hz, $J_{P-C} = 13$ Hz, *Rh-CO*), 169.88 (dd, $J_{C-P} = 16$ Hz, $J_{C-Rh} = 3$ Hz, *Ar-OP*), 148.04 (ddd, $J_{Rh-C} = 29$ Hz, $J_{C-P} = 10$ Hz, $J_{C-P} = 9$ Hz, *C-Rh*), 143.02 (d, $J_{C-P} = 11$ Hz, *Ar-CH₂OP*), 127.51 (s, *Ar-H*), 120.35 (s, *Ar-H*), 111.37 (d, $J_{C-P} = 14$ Hz, *Ar-H*), 77.75 (t, $J_{C-P} = 3$ Hz, CH_2OP), 31.6 (ddd, $J_{C-P} = 26$ Hz, $J = 3$ Hz, $J = 2$ Hz, $PCHMe_2$), 30.69 (ddd, $J_{C-P} = 22$ Hz, $J = 4$ Hz, $J =$

3 Hz, PCHMe₂), 18.55 (d, J_{C-P} = 4 Hz, P(CHMe₂)₂), 18.48 (s, J_{C-P} = 5 Hz, P(CHMe₂)₂) 17.75 (s, P(CHMe₂), 17.50 (s, P(CHMe₂)). IR: 1948 cm⁻¹, ν_{CO} .

Synthesis of 1-(^tBu₂PO)-3-(^tBu₂POCH₂)(C₆H₄) (408-H). To a solution of 3-hydroxybenzyl alcohol (0.320 g, 2.64 mmol) in THF, sodium hydride (0.189 g, 7.71 mmol) was added slowly while stirring. The mixture was refluxed for 1 h, and a solution of ClP^tBu₂ (0.949 g, 5.25 mmol) in THF was added dropwise. The reaction was refluxed overnight. The volatiles were removed under vacuum and the residue was extracted with toluene and filtered through Celite. The solvent was removed under vacuum to give a colorless oil determined to be >95% pure by ¹H NMR spectroscopy (0.907 g, 2.20 mmol, 83%). ³¹P{¹H} NMR (C₆D₆): δ 164.6 (s), 153.2 (s); ¹H NMR (C₆D₆): δ 6.83 (d, 1H, J = 8 Hz, Ar-H) 6.80 (s, 1H, Ar-H), 6.74 (t, 1H, J = 8 Hz, Ar-H), 6.58 (d, 1H, J = 7 Hz, Ar-H), 4.42 (d, 2H, J = 8 Hz, CH₂OP), 0.78 (d, 18H, J_{H-P} = 12 Hz, PC(Me₃)₂), 0.76 (d, 18H, J_{H-P} = 12 Hz, PC(Me₃)₂); ¹³C{¹H} NMR (C₆D₆): δ 160.48 (d, J_{C-P} = 9 Hz, Ar-OP), 141.80 (d, J_{C-P} = 9 Hz, Ar-CH₂OP), 120.53 (s, Ar-H), 117.77 (d, J_{C-P} = 10 Hz, Ar-H), 117.54 (d, J_{C-P} = 11 Hz, Ar-H), 75.68 (d, J_{C-P} = 23 Hz, CH₂OP), 35.73 (d, J_{C-P} = 27 Hz, P(CMe₃)₂), 35.41 (d, J_{C-P} = 26 Hz, P(CMe₃)₂), 27.69 (d, J_{C-P} = 16 Hz, P(CMe₃)₂), 27.57 (d, J_{C-P} = 17 Hz, P(CMe₃)₂). HRMS (ESI+TOF) m/z: [M + H]⁺ Calcd. for C₂₃H₄₄O₂P₂ 413.2733; found 413.2750.

Synthesis of (POCCH₂OP^{tBu})Rh(H)(Cl) (408-Rh(H)(Cl)). In a Teflon screw-top flask, **408-H** (244 mg, 0.591 mmol) and [(COD)RhCl]₂ (146 mg, 0.296 mmol) were dissolved in toluene and heated at 90 °C for 18 h. The reaction mixture was passed through silica and Celite and recrystallized from toluene and pentane to produce

greenish-yellow crystals judged to be >97% pure by ^1H NMR spectroscopy (198 mg, 61%). $^{31}\text{P}\{^1\text{H}\}$ NMR (C_6D_6): δ 188.6 (dd, $J_{\text{P-P}} = 398$ Hz, $J_{\text{P-Rh}} = 117$ Hz), 161.7 (dd, $J_{\text{P-P}} = 398$ Hz, $J_{\text{P-Rh}} = 117$ Hz); ^1H NMR (C_6D_6): δ 6.97 (d, 1H, $J = 8$ Hz, Ar-H), 6.89 (t, 1H, $J = 7$ Hz, , Ar-H), 6.49 (d, 1H, $J = 7$ Hz, Ar-H), 4.73 (dd, 1H, $J_{\text{H-P}} = 16$ Hz, $J_{\text{H-H}} = 13$ Hz, CH_2OP), 4.57 (dd, 1H, $J_{\text{H-P}} = 17$ Hz, $J_{\text{H-H}} = 13$ Hz, CH_2OP), 1.41 (d, 9H, $J_{\text{H-P}} = 14$ Hz, $\text{PC}(\text{Me}_3)_2$), 1.40 (d, 9H, $J_{\text{H-P}} = 13$ Hz, $\text{PC}(\text{Me}_3)_2$), 1.39 (d, 9H, $J_{\text{H-P}} = 14$ Hz, $\text{PC}(\text{Me}_3)_2$), -26.84 (apparent dt, 1H, $J_{\text{H-Rh}} = 50$ Hz, $J_{\text{H-P}} = 12$ Hz); $^{13}\text{C}\{^1\text{H}\}$ NMR (C_6D_6): δ 169.7 (dd, $J_{\text{C-P}} = 12$ Hz, $J_{\text{C-Rh}} = 3$ Hz, Ar-OP), 142.1 (d, $J_{\text{C-P}} = 6$ Hz, Ar- CH_2OP), 134.2 (m, Ar-Rh), 125.7 (Ar-H), 121.5 (Ar-H), 112.2 (d, $J_{\text{C-P}} = 12$ Hz, Ar-H), 75.9 (d, $J_{\text{C-P}} = 3$ Hz, CH_2OP), 41.3 (dd, $J_{\text{C-P}} = 10$ Hz, $J_{\text{C-Rh}} = 6$ Hz, PCMe_3), 40.6 (dd, $J_{\text{C-P}} = 10$ Hz, $J_{\text{C-Rh}} = 7$ Hz, PCMe_3), 39.7 (ddd, $J_{\text{C-P}} = 18$ Hz, $J_{\text{C-Rh}} = 6$ Hz, $J_{\text{C-P}} = 2$ Hz, PCMe_3), 38.9 (ddd, $J_{\text{C-P}} = 13$ Hz, $J_{\text{C-Rh}} = 6$ Hz, $J_{\text{C-P}} = 3$ Hz, PCMe_3), 29.4 (d, $J_{\text{C-P}} = 5$ Hz, PCMe_3), 29.2 (d, $J_{\text{C-P}} = 5$ Hz, PCMe_3), 28.15 (d, $J_{\text{C-P}} = 5$ Hz, PCMe_3), 28.08 (d, $J_{\text{C-P}} = 5$ Hz, PCMe_3).

Synthesis of $(\text{POCCH}_2\text{OP}^{\text{tBu}})\text{Rh}(\text{S}^{\text{iPr}}_2)$ (408-Rh(S^{iPr}_2)). In a Teflon screw-cap vial, **408-Rh(H)(Cl)** (150 mg, 0.273 mmol), NaO^{tBu} (45 mg, 0.41 mmol), and diisopropylsulfide (80 μL , 0.546 mmol) were dissolved in toluene and stirred overnight at RT. The reaction mixture was passed through Celite, and then the volatiles were removed under vacuum yielding a brown solid, which was recrystallized from pentane (138 mg, 80%). $^{31}\text{P}\{^1\text{H}\}$ NMR (C_6D_6): δ 189.3 (dd, $J_{\text{P-P}} = 335$ Hz, $J_{\text{P-Rh}} = 184$ Hz), 160.9 (dd, $J_{\text{P-P}} = 331$ Hz, $J_{\text{P-Rh}} = 176$ Hz); ^1H NMR (C_6D_6): δ 6.96 (d, 1H, $J = 8$ Hz, Ar-H), 6.86 (t, 1H, $J = 8$ Hz, Ar-H), 6.63 (d, 1H, $J = 7$ Hz, Ar-H), 4.87 (d, 2H, $J_{\text{H-P}} = 19$ Hz, CH_2OP), 2.85 (m, 2H, $\text{S}(\text{CHMe}_2)_2$), 1.44 (d, 18H, $J_{\text{H-P}} = 12$ Hz, $\text{P}(\text{CMe}_3)_2$), 1.28 (d, 18H,

$J_{\text{H-P}} = 12$ Hz, $\text{P}(\text{CMe}_3)_2$), 1.29 (d, 12 H, $J = 7$ Hz, $\text{S}(\text{C}(\text{Me}_2)_2)_2$); $^{13}\text{C}\{^1\text{H}\}$ NMR (C_6D_6): δ 168.4 (d, $J_{\text{C-P}} = 15$ Hz, *Ar-OP*), 145.2 (m, *Ar-Rh*), 143.9 (d, $J_{\text{C-P}} = 9$ Hz, *Ar-CH}_2\text{OP}*), 123.1 (*Ar-H*), 120.0 (*Ar-H*), 110.2 (d, $J_{\text{C-P}} = 12$ Hz, *Ar-H*), 78.3 (d, $J_{\text{C-P}} = 5$ Hz, CH_2OP), 40.9 (s, $\text{S}(\text{CHMe}_2)_2$), 40.2 (m, $\text{PC}(\text{CH}_3)_3$), 39.8 (dd, $J_{\text{C-P}} = 10$ Hz, $J_{\text{C-Rh}} = 4$ Hz, $\text{PC}(\text{CH}_3)_3$), 37.6 (s, $\text{PC}(\text{CH}_3)_3$), 29.8 (d, $J_{\text{C-P}} = 8$ Hz, $\text{P}(\text{CMe}_3)_2$), 29.7 (d, $J_{\text{C-P}} = 8$ Hz, $\text{P}(\text{CMe}_3)_2$), 25.5 (s, $\text{S}(\text{CHMe}_2)_2$). Elem. Anal. Found (Calculated) for $\text{C}_{29}\text{H}_{55}\text{O}_2\text{P}_2\text{RhS}$: C, 55.09 (55.06); H, 8.57 (8.76); S, 4.93 (5.07).

Synthesis of $(\text{POCCH}_2\text{OP}^{\text{tBu}})\text{Rh}(\text{CO})$ (408-Rh(CO)). In a Teflon capped 10 mL flask, **408-Rh(S^{iPr}_2)** (65 mg, 0.104 mmol) was dissolved in toluene and degassed. The flask was then filled with CO and stirred for 2 h at RT. The reaction mixture was filtered through silica and Celite and the volatiles were removed under vacuum, resulting in a yellow solid judged to be >98% pure by ^1H NMR (34 mg, 61% yield). $^{31}\text{P}\{^1\text{H}\}$ NMR (C_6D_6): δ 210.6 (dd, $J_{\text{P-P}} = 300$ Hz, $J_{\text{P-Rh}} = 144$ Hz), 177.2 (dd, $J_{\text{P-P}} = 300$ Hz, $J_{\text{P-Rh}} = 150$ Hz); ^1H NMR (C_6D_6): δ 7.14 (d, 1H, $J = 8$ Hz, *Ar-H*), 6.99 (dt, 1H, $J = 8$ Hz, $J_{\text{H-P}} = 1$ Hz, 1H, *Ar-H*), 6.61 (d, 1H, $J = 8$ Hz, *Ar-H*), 4.78 (d, 2H, $J_{\text{C-P}} = 17$ Hz, CH_2OP), 1.33 (d, 18H, $J_{\text{C-P}} = 14$ Hz, $\text{P}(\text{CMe}_3)_2$), 1.30 (d, 18H, $J_{\text{C-P}} = 14$ Hz, $\text{P}(\text{CMe}_3)_2$); $^{13}\text{C}\{^1\text{H}\}$ NMR (C_6D_6): 199.2 (apparent dt (ddd), $J_{\text{C-Rh}} = 57$ Hz, $J_{\text{C-P}} = 14$ Hz, *Rh-CO*), 170.8 (dd, $J_{\text{C-P}} = 15$ Hz, $J_{\text{C-Rh}} = 3$ Hz, *Ar-OP*), 148.6 (apparent dt (ddd), $J_{\text{C-Rh}} = 29$ Hz, $J_{\text{C-P}} = 10$ Hz, *Ar-Rh*) 142.5 (d, $J_{\text{C-P}} = 10$ Hz, *Ar-CH}_2\text{OP}*), 127.3 (s, *Ar-H*), 120.0 (s, *Ar-H*), 111.2 (d, $J = 14$ Hz), 77.4 (dd, $J_{\text{C-P}} = 3$ Hz, $J_{\text{C-Rh}} = 1$ Hz, CH_2OP), 39.9 (m, contains both $\text{P}(\text{CMe}_3)_2$ signals), 28.9 (d, $J_{\text{C-P}} = 7$ Hz, $\text{P}(\text{CMe}_3)_2$), 28.7 (d, $J_{\text{C-P}} = 7$ Hz, $\text{P}(\text{CMe}_3)_2$). IR: 1943 cm^{-1} , ν_{CO} .

Synthesis of 2,2',4,4'-tetramethyldiphenylamine (409A). In a 250 mL Schlenk flask, 2,4-dimethylaniline (5.84 mL, 48 mmol), 2,4-dimethylbromobenzene (6.08 mL, 45 mmol), bis(diphenylphosphino)ferrocene (DPPF, 0.498 g, 0.90 mmol), Pd(OAc)₂ (0.100 g, 0.45 mmol Pd), and NaOCMe₂Et (7.06 g, 63 mmol) were refluxed in ca. 100 mL of toluene under argon. After 16 h, the mixture was filtered through silica and Celite and the filtrate was collected. All of the volatiles were removed under vacuum and a product judged to be >98% pure by ¹H NMR recrystallized from pentane. Yield: 7.51 g (74%). ¹H NMR (CDCl₃): δ 7.08 (s, 2H, Ar-H), 6.98 (d, 2H, *J* = 8 Hz, Ar-H), 6.90 (d, 2H, *J* = 8 Hz, Ar-H), 5.11 (br s, 1H, N-H), 2.36 (s, 6H, Ar-CH₃), 2.30 (s, 6H, Ar-CH₃); ¹³C{¹H} NMR (CDCl₃): δ 139.9 (s, N-Ar), 131.6 (s, Ar-H), 130.8 (s, Ar-Me), 127.76 (s, Ar-Me), 127.75 (s, Ar-H), 118.7 (s, Ar-H), 20.8 (s, Ar-Me), 17.9 (s, Ar-Me).

Synthesis of 2,2'-dibromo-4,4',6,6'-tetramethyldiphenylamine (409B). In a Schlenk flask under ambient atmosphere, **409A** (7.44 g, 33 mmol) was dissolved in dichloromethane. *N*-bromosuccinimide (11.75 g, 66 mmol) was added slowly and the reaction mixture was left to stir overnight at RT. The reaction mixture was then passed through Celite and the volatiles were removed by vacuum. The resulting brown solid was dissolved in pentane and filtered through silica and Celite. The volatiles were removed, and a white solid was obtained by recrystallizing the product from ethanol. The purity of product judged to be >97% by ¹H NMR spectroscopy. Yield: 8.91 g (70%). ¹H NMR (CDCl₃): δ 7.24 (s, 2H, Ar-H), 6.81 (s, 2H, Ar-H), 5.49 (br s, 1H, N-H), 2.42 (s, Ar-Me), 1.80 (s, Ar-Me); ¹³C{¹H} NMR (CDCl₃): δ 137.9 (s, Ar-N), 133.1, 132.1, 131.4, 131.0, 118.4 (s, Ar-Br), 20.5 (s, Ar-Me), 19.7 (s, Ar-Me).

Synthesis of *N*-methyl-2,2'-dibromo-4,4',6,6'-tetramethyldiphenylamine (409C). In a Schlenk flask, **409B** (1.26 g, 3.3 mmol) was dissolved in THF and treated with $\text{KN}(\text{SiMe}_3)_2$ (5 mL, 3.3 mmol, 0.66 M in toluene). The solution was stirred at RT for 2 h and iodomethane (410 μL , 6.6 mmol) was added. The solution was stirred overnight at RT and filtered through Celite and silica gel. The product was isolated as a yellow solid after recrystallizing from pentane. The purity of the product was judged to be >97% pure by ^1H NMR. Yield: 767 mg (58%). ^1H NMR (C_6D_6): δ 7.25 (s, 2H, Ar-*H*), 6.56 (s, 2H, Ar-*H*), 3.49 (s, 3H, N-*Me*), 1.98 (s, 6H, Ar-*Me*), 1.90 (s, 6H, Ar-*Me*). $^{13}\text{C}\{^1\text{H}\}$ NMR (C_6D_6): δ 143.6 (s, Ar-N), 137.0 (s, Ar), 134.3 (s, Ar), 133.9 (s, Ar), 132.6 (s, Ar), 121.2 (s, Ar-Br), 43.5 (s, NMe), 20.9 (s, Ar-*Me*), 20.1 (s, Ar-*Me*).

Synthesis of ($^o\text{-Me}$ PNP)Me (409). In a Schlenk flask, **409C** (752 mg, 1.89 mmol) was dissolved in Et_2O and *n*-BuLi (1.6 mL of 2.5M solution in hexanes, 4.0 mmol) was added slowly. The mixture was stirred for 2 h at RT and CIP^iPr_2 (635 mg, 4.16 mmol) was added slowly. The reaction was allowed to stir overnight and the volatiles were removed under vacuum. The dry solid was dissolved in toluene and passed through a pad of Celite. Pure product was recrystallized from Et_2O to form a white solid (418 mg, 45%). $^{31}\text{P}\{^1\text{H}\}$ NMR (C_6D_6): δ -2.28; ^1H NMR (C_6D_6): δ 7.10 (s, 2H, Ar-*H*), 6.85 (s, 2H, Ar-*H*), 3.58 (s, 3H, N-*Me*), 2.40 (s, 6H, Ar-*Me*), 2.18 (s, 6H, Ar-*Me*), 1.93 (m, 2H, $\text{P}(\text{CHMe}_2)_2$), 1.59 (m, 2H, $\text{P}(\text{CHMe}_2)_2$), 1.12 (dd, 6H, $J_{\text{H-P}} = 11$ Hz, $J_{\text{H-H}} = 7$ Hz, $\text{P}(\text{CHMe}_2)_2$), 1.11 (dd, 6H, $J_{\text{H-P}} = 13$ Hz, $J_{\text{H-H}} = 7$ Hz, $\text{P}(\text{CHMe}_2)_2$), 0.93 (dd, 6H, $J_{\text{H-P}} = 14$ Hz, $J_{\text{H-H}} = 7$ Hz, $\text{P}(\text{CHMe}_2)_2$), 0.87 (dd, 6H, $J_{\text{H-P}} = 12$ Hz, $J_{\text{H-H}} = 7$ Hz, $\text{P}(\text{CHMe}_2)_2$); $^{13}\text{C}\{^1\text{H}\}$ NMR (C_6D_6): δ 154.5 (m, Ar-N), 134.8 (m, Ar), 134.76 (s, Ar), 133.8 (m, Ar-P),

132.5 (s, Ar), 131.7 (s, Ar), 46.7 (m, N-Me), 25.6 (m, PCHMe₂), 25.4 (m, PCHMe₂), 23.8 (t, $J_{C-P} = 9$ Hz, PCHMe₂), 22.3 (t, $J_{C-P} = 10$ Hz, PCHMe₂), 21.2 (t, $J_{C-P} = 8$ Hz, PCHMe₂), 21.0 (t, $J_{C-P} = 8$ Hz, PCHMe₂), 20.7 (s, Ar-Me), 19.4 (t, $J_{C-P} = 7$ Hz, Ar-Me).
Elem. Anal. Found (Calculated) for C₂₉H₄₇NP₂: C, 73.75 (73.85); H, 10.15 (10.04).

Synthesis of (*o*-Me^oPNP)Rh(Me)(Cl) (409-Rh(Me)(Cl)). In a J. Young tube, **409** (104 mg, 0.22 mmol) and [Rh(COE)₂Cl] (79 mg, 0.11 mmol) were dissolved in C₆D₆ and the solution was heated at 70 °C for 18 h. The reaction mixture was filtered through Celite and silica and recrystallized from THF to produce a green solid judged to be >95% pure by ¹H NMR spectroscopy (44 mg, 33% yield). ³¹P{¹H} NMR (C₆D₆): δ 35.9 (dd, $J_{P-P} = 414$ Hz, $J_{P-Rh} = 111$ Hz), 29.3 (dd, $J_{P-P} = 415$ Hz, $J = 109$ Hz); ¹H NMR (C₆D₆): δ 6.84 (d, 1H, $J_{H-P} = 8$ Hz, Ar-H), 6.73 (d, 1H, $J_{H-P} = 6$ Hz, Ar-H), 6.66 (s, 1H, Ar-H), 2.89 (m, 1H, P(CHMe₂)₂), 2.46 (m, 3H, Rh-Me), 2.50-2.36 (m, 2H, overlapping P(CHMe₂)₂), 2.26 (m, 1H, P(CHMe₂)₂), 2.19 (s, 3H, Ar-Me), 2.16 (s, 3H, Ar-Me), 1.72 (s, 3H, Ar-Me), 1.62 (dd, 3H, $J_{H-P} = 15$ Hz, $J_{H-H} = 7$ Hz, P(CHMe₂)₂), 1.61 (s, 3H, Ar-Me), 1.38 (dd, 3H, $J_{H-P} = 15$ Hz, $J_{H-H} = 7$ Hz, P(CHMe₂)₂), 1.25 (dd, 3H, $J_{H-P} = 16$ Hz, $J_{H-H} = 7$ Hz, P(CHMe₂)₂), 1.20 (dd, 3H, $J_{H-P} = 16$ Hz, $J_{H-H} = 7$ Hz, P(CHMe₂)₂), 1.16 (dd, 3H, $J_{H-P} = 15$ Hz, $J_{H-H} = 7$ Hz, P(CHMe₂)₂), 1.11 (dd, 3H, $J_{H-P} = 14$ Hz, $J_{H-H} = 8$ Hz, P(CHMe₂)₂), 1.06 (dd, 3H, $J_{H-P} = 13$ Hz, $J_{H-H} = 7$ Hz, P(CHMe₂)₂), 1.57 (dd, 3H, $J_{H-P} = 13$ Hz, $J_{H-H} = 6$ Hz, P(CHMe₂)₂); ¹³C{¹H} NMR (C₆D₆): δ 162.5 (d, $J = 19$ Hz, Ar-N), 162.1 (d, $J = 19$ Hz, Ar-N), 135.3, 134.0, 129.8, 129.5, 129.3 (d, $J = 11$ Hz), 126.4 (d, $J = 7$ Hz), 126.3 (d, $J = 10$ Hz), 125.2 (d, $J = 7$ Hz), 123.4 (d, $J = 39$ Hz, Ar-P), 119.0 (d, $J = 39$ Hz, Ar-P), 27.3(m, PCHMe₂), 26.6 (m, PCHMe₂), 25.2 (m, PCHMe₂), 23.6 (m,

PCHMe₂), 21.7, 21.1, 20.94, 20.91, 20.7, 20.6, 19.3, 19.0 (d, $J = 4$ Hz), 18.8, 18.7 (d, $J = 4$ Hz), 18.3, 17.8, 2.8 (br d, $J_{C-Rh} = 29$ Hz, Rh-Me).

Synthesis of (*o*-MePNP)Rh(H₂) (409-Rh(H₂)). In a Schlenk flask (409-Rh(Me)(Cl)) (180 mg, 0.30 mmol) and NaBH₄ (30 mg, 0.79 mmol) was dissolved in degassed isopropanol and the reaction was stirred for 3 h at RT. The volatiles were removed and the resulting solid was dissolved in diethyl ether and passed through a pad of Celite and the volatiles were removed under vacuum. Orange crystals were formed (60 mg, 33%) by slow diffusion of pentane into a saturated toluene solution. ³¹P{¹H} NMR (C₆D₆): δ 58.4 (d, $J_{P-Rh} = 130$ Hz); ¹H NMR (C₆D₆): δ 6.79-6.77 (m, 4H, overlapping Ar-H), 2.23 (s, 6H, Ar-Me), 2.04 (m, 2H, P(CHMe₂)₂), 1.96 (m, 2H, P(CHMe₂)₂), 1.81 (s, 6H, Ar-Me), 1.41 (apparent q (dvt), 6H, $J = 8$ Hz, P(CHMe₂)₂), 1.11 (apparent q (dvt), 6H, $J = 7$ Hz, P(CHMe₂)₂), 0.99 (apparent q (dvt), 6H, $J = 8$ Hz, P(CHMe₂)₂), 0.93 (apparent q (dvt), 6H, $J = 8$ Hz, P(CHMe₂)₂), -13.4 (dvt, 2H, $J_{Rh-H} = 20$ Hz, $J_{P-H} = 9$ Hz, Rh-H₂); ¹³C{¹H} NMR (C₆D₆): δ 163.8 (dvt, $J_{C-P} = 12$ Hz, $J_{C-Rh} = 2$ Hz, Ar-N), 134.8 (s, Ar-H), 129.4 (s, Ar-H), 125.1 (dvt, $J_{C-P} = 5$ Hz, $J_{C-Rh} = 1$ Hz, Ar-Me), 124.9 (vt, $J = 4$ Hz, Ar-Me), 122.5 (vt, $J = 18$ Hz, Ar-P), 28.0 (dvt, $J_{C-Rh} = 2$ Hz, $J_{C-P} = 10$ Hz, P(CHMe₂)₂), 22.2 (vt, $J_{C-P} = 13$ Hz, P(CHMe₂)₂), 21.74 (vt, $J_{C-P} = 4$ Hz, P(CHMe₂)), 21.68 (s, Ar-Me), 20.7 (s, Ar-Me), 19.4 (vt, $J_{C-P} = 3$ Hz, P(CHMe₂)), 18.9 (vt, $J_{C-P} = 5$ Hz, P(CHMe₂)), 18.1 (s, P(CHMe₂)). Elem. Anal. Found (Calculated) for C₂₈H₄₆NP₂Rh: C, 59.71(59.89); H, 8.07 (8.26).

Observation of (*o*-MePNP)Rh(HD) (409-Rh(HD)). (409-Rh(Me)(Cl)) (64 mg, 0.11 mmol) and NaBH₄ (22 mg, 0.57 mmol) was combined in a mixture of C₆D₆ and *d*₄-

methanol and stirred at room temperature for 4 h. The volatiles were removed under vacuum and the product was extracted with diethyl ether and filtered through a pad of Celite. The volatiles were removed under vacuum, and the solid was washed with pentane. A mixture containing >85% of (**409-Rh(HD)**) and (**409-Rh(H₂)**) by ³¹P{¹H} NMR was produced. Data for the ¹H signal of the H in HD in **409-Rh(HD)** follow. ¹H NMR (C₆D₆): δ -13.33 (dvt, $J_{\text{Rh-H}} = 20$ Hz, $J_{\text{H-D}} = 20$ Hz, $J_{\text{H-P}} = 9$ Hz).

Synthesis of (PCP^{iPr})Rh(H)(Cl) (410-Rh(H)(Cl)). In a Teflon screw-top flask, **410-H** (270 mg, 0.800 mmol) and [(COD)Rh(OAc)]₂ (216 mg, 0.400 mmol) were dissolved in toluene and heated at 80 °C for 5 h. The reaction mixture was filtered through a pad of Celite, and the volatiles were removed under vacuum to produce **410-Rh(H)(OAc)** as a light reddish-brown solid, which was characterized *in situ*. The solid was dissolved in toluene and Me₃SiCl (150 μL, 1.18 mmol) was added to the solution. After 3 h the volatiles were removed from solution under vacuum, and the resulting solid was dissolved in toluene and filtered through a pad of Celite and silica. **410-Rh(H)(Cl)** (223 mg, 58.5 %) was recrystallized as red square crystals judged to be >97% pure from a minimum amount of toluene layered with pentane in a -35 °C freezer. ³¹P{¹H} NMR (C₆D₆): δ 63.0 (d, $J_{\text{P-Rh}} = 114$ Hz); ¹H NMR (C₆D₆): δ 6.98 (apparent q (heavy second order effects), 1H, $J = 9$ Hz, $J = 6$ Hz, Ar-H), 6.94 (d, 2H, $J = 8$ Hz, Ar-H), 2.82 (dvt, 2H, $J_{\text{H-H}} = 17$ Hz, $J_{\text{H-P}} = 4$ Hz, CH₂P), 2.72 (dvt, 2H, $J_{\text{H-H}} = 18$ Hz, $J_{\text{H-P}} = 4$ Hz, CH₂P), 2.52 (m, 2H, P(CHMe₂)₂), 1.85 (m, 2H, P(CHMe₂)₂), 1.25 (apparent q (dvt), 6H, $J = 8$ Hz, P(CH(CH₃)₂), 1.24 (apparent q (dvt), 6H, $J = 7$ Hz, P(CH(CH₃)₂), 0.91 (apparent q (dvt), 6H, $J = 8$ Hz, P(CH(CH₃)₂), 0.88 (apparent q (dvt), 6H, $J = 8$ Hz, P(CH(CH₃)₂), -

24.85 (dvt, 1H, $J_{\text{H-Rh}} = 44$ Hz, $J_{\text{H-P}} = 13$ Hz); $^{13}\text{C}\{^1\text{H}\}$ NMR (C_6D_6): δ 159.2 (d, $J_{\text{C-Rh}} = 31$ Hz, C-Rh), 150.6 (vt, $J_{\text{C-P}} = 10$ Hz, CCH_2P), 123.4 (s), 123.1 (vt, $J_{\text{C-P}} = 9$ Hz, Ar-C- CH_2P) 32.2 (dvt, $J_{\text{C-P}} = 12$ Hz, $J_{\text{C-Rh}} = 2$ Hz, Ar- CP^iPr_2), 24.33 (vt, $J_{\text{C-P}} = 11$ Hz, PCMe_2), 24.26 (vt, $J_{\text{C-P}} = 11$ Hz, PCMe_2), 19.0 (s, $\text{PCH}(\text{CH}_3)_2$), 18.9 (s, $\text{PCH}(\text{CH}_3)_2$), 18.7 (s, $\text{PCH}(\text{CH}_3)_2$), 17.6 (s, $\text{PCH}(\text{CH}_3)_2$).

(PCP^{iPr})Rh(H)(OAc) (410-Rh(H)(OAc)). $^{31}\text{P}\{^1\text{H}\}$ NMR (C_6D_6): δ 66.6 (d, $J_{\text{P-Rh}} = 115$ Hz); ^1H NMR (C_6D_6): δ 6.89 (t, 1H, $J = 7$ Hz, Ar-H), 6.85 (d, 2H, $J = 7$ Hz, Ar-H), 2.94 (d, 2H, $J_{\text{H-P}} = 16$ Hz, CH_2P), 2.80 (d, 2H, 16Hz, CH_2P), 2.34 (m, 2H, PCHMe_2), 1.97 (s, 3H, O_2CCH_3), 1.85 (m, 2H, PCHMe_2), 1.15 (apparent q (dvt), 6H, $J = 8$ Hz, $\text{PCH}(\text{CH}_3)_2$), 1.08 (m, 12H, $\text{PCH}(\text{CH}_3)_2$), 0.96 (apparent q (dvt), 6H, $J = 7$ Hz, $\text{PCH}(\text{CH}_3)_2$), -21.23 (dvt, 1H, $J_{\text{H-Rh}} = 30$ Hz, $J_{\text{H-P}} = 14$ Hz); $^{13}\text{C}\{^1\text{H}\}$ NMR (C_6D_6): δ 181.8 (s, O_2CMe), 157.5 (d, $J_{\text{C-Rh}} = 31$ Hz, C-Rh), 148.1 (vt, $J_{\text{C-P}} = 8$ Hz, CCH_2P), 122.7 (s, Ar-H), 122.2 (vt, $J_{\text{C-P}} = 8$ Hz, Ar-H), 34.1 (vtd, $J_{\text{C-P}} = 14$ Hz, $J_{\text{C-Rh}} = 3$ Hz, Ar- $\text{CH}_2\text{P}^i\text{Pr}_2$), 25.11 (vt, PCMe_2 , $J_{\text{C-P}} = 10$ Hz), 24.6 (s, O_2CCH_3), 24.4 (vt, PCMe_2 , $J_{\text{C-P}} = 11$ Hz), 19.6 (s, $\text{PCH}(\text{CH}_3)_2$), 19.0 (s, $\text{PCH}(\text{CH}_3)_2$), 18.4 (s, $\text{PCH}(\text{CH}_3)_2$), 18.2 (s, $\text{PCH}(\text{CH}_3)_2$).

Synthesis of (PCP^{iPr})Rh(S^{iPr}Pr₂) (410-Rh(S^{iPr}Pr₂)). In a Schlenk flask, **410-Rh(H)(Cl)** (125.0 mg, 0.262 mmol), NaO^tBu (37.8 mg, 0.393 mmol), and diisopropyl sulfide (75 μL , 0.524 mmol) were dissolved in toluene and stirred at RT for 1 h. The volatiles were removed under vacuum, and the solid was dissolved in pentane and filtered through silica and Celite. **410-Rh(S^{iPr}Pr₂)** was recrystallized from a minimum amount of pentane in a -35 °C freezer to produce orange brown crystals (63 mg, 43%

yield). $^{31}\text{P}\{^1\text{H}\}$ NMR (C_6D_6): δ 56.4 (d, $J_{\text{P-Rh}} = 164$ Hz); ^1H NMR (C_6D_6): δ 7.21 (d, 2H, $J = 8$ Hz, Ar-H), 7.14 (t, 1H, $J = 8$ Hz, Ar-H), 3.05 (br s, 4H, $\text{CH}_2\text{P}^i\text{Pr}_2$), 2.80 (m, 2H, $\text{S}(\text{CHMe}_2)_2$), 1.99 (m, 4H, PCHMe_2), 1.36 (d, 12H, $J = 7$ Hz, $\text{S}(\text{CH}(\text{CH}_3)_2)$), 1.24 (apparent q (dvt), 12H, $J = 7$ Hz, $\text{P}(\text{CHCH}_3)_2$), 1.06 (apparent q (dvt), 12H, $J = 7$ Hz, $\text{P}(\text{CHCH}_3)_2$); $^{13}\text{C}\{^1\text{H}\}$ NMR (C_6D_6): δ 173.8 (br d, $J_{\text{C-Rh}} = 41$ Hz, C-Rh), 150.6 (dvt, Ar- CH_2P , $J_{\text{C-P}} = 11$ Hz, $J_{\text{C-Rh}} = 3$ Hz), 122.2 (s, Ar-H), 120.5 (vt, $J_{\text{C-P}} = 9$ Hz, Ar-H), 40.9 (s, $\text{S}(\text{CMe}_2)_2$), 37.2 (dvt, $J_{\text{C-P}} = 11$ Hz, $J_{\text{C-Rh}} = 5$ Hz, Ar- $\text{CH}_2\text{-P}$), 26.2 (vt, $J_{\text{C-P}} = 8$ Hz, PCHMe_2), 24.8 (s, $\text{S}(\text{CH}(\text{CH}_3)_2)_2$), 20.3 (vt, $J_{\text{C-P}} = 3$ Hz, $\text{P}(\text{CH}(\text{CH}_3)_2)_2$), 18.9 (s, $\text{P}(\text{CH}(\text{CH}_3)_2)_2$). Elem. Anal. Found (Calculated) for $\text{C}_{26}\text{H}_{49}\text{O}_2\text{P}_2\text{RhS}$: C, 55.75 (55.91); H, 8.96 (8.84).

4.4.3 Catalytic Reactions

Catalytic Dimerization of Terminal Alkynes. In a typical run, catalyst (0.0053 mmol), alkyne (0.530 mmol) were mixed in C_6D_6 to make an 800 μL solution in a J. Young tube. The reactions were run at 1% catalyst loading at 80 $^\circ\text{C}$. Upon completion of the reaction, 5 μL 1,4-dioxane was added as an internal standard. Products were identified by ^1H NMR and comparison to literature data.^{219,221,246} The product yield was determined by ^1H NMR integration versus the 1,4-dioxane standard.

CHAPTER V
SYNTHESIS OF PNP RHODIUM COMPLEXES CONTAINING RHODIUM-ZINC
COVALENT BONDS*

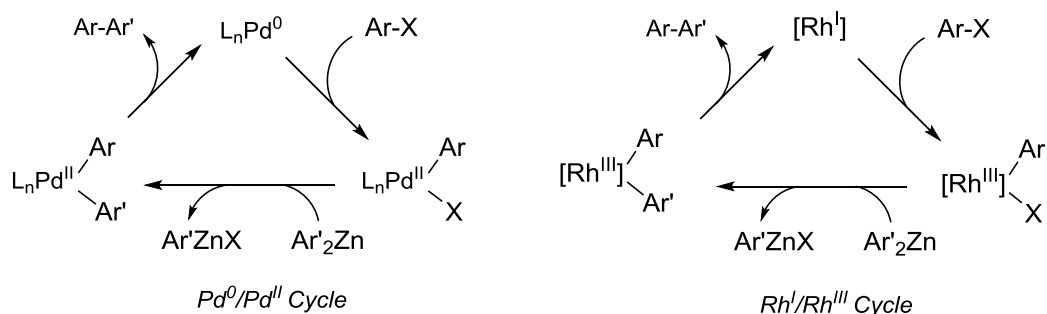
5.1 Introduction

The coupling of organic electrophiles and organozinc reagents is most commonly catalyzed by palladium in a process referred to as Negishi coupling.^{226,247} This process is a highly valuable pathway for making carbon-carbon bonds in organic synthesis.²⁴⁸ While palladium is recognized as the most successful metal for Negishi coupling, other metals have also been reported to catalyze the reaction such as Ni, Fe, Co, and Cu.²⁴⁸ Rhodium-catalyzed Negishi coupling has also been successfully accomplished by the Takagi group.²⁴⁹

Thorough studies of Pd-catalyzed Negishi coupling have provided experimental and computational evidence for a catalytic cycle involving oxidative addition (OA), transmetallation (TM), and reductive elimination (RE).²⁵⁰ We have previously shown that pincer-ligated Rh systems can operate through a Rh(I)/Rh(III) cycle that is analogous to a Pd(0)/Pd(II) catalytic cycle, exploring stoichiometric and catalytic reactions of aryl halides with nucleophiles.^{233,251,252} We hypothesized a possible cycle for Rh-catalyzed Negishi coupling (Scheme V-1), and this chapter reports the results of our investigation into the reactivity of the (PNP)Rh system. Since the OA and RE steps have

* Reproduced by permission of The Royal Society of Chemistry from “Formation of (PNP)Rh complexes containing covalent rhodium-zinc bonds in studies of potential Rh-catalyzed Negishi coupling.” Pell, C. J.; Shih, W.-C.; Gatard, S.; Ozerov, O. V. *Chem. Commun.* **2017**, 53, 6456. DOI: 10.1039/C7CC02707A

already been demonstrated with (PNP)Rh,²⁵¹ we focused on the compatibility of the TM step and the attendant organozinc reagents with catalysis.

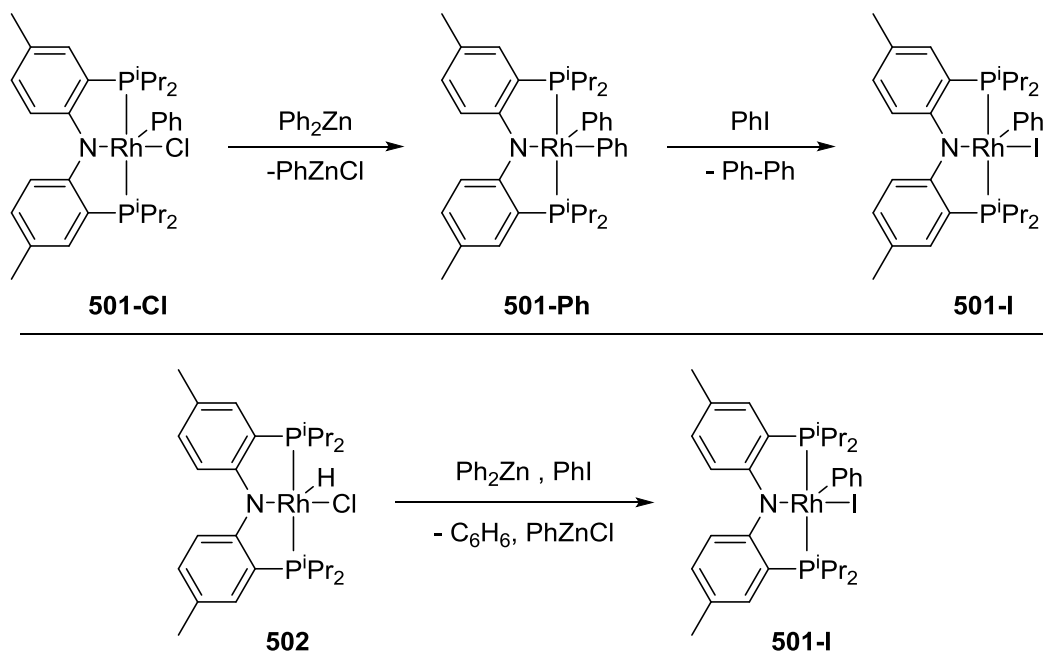


Scheme V-1. Mechanism for Pd-catalyzed Negishi coupling compared to a Rh(I)/Rh(III) mechanism.

5.2 Results and Discussion

5.2.1 Stoichiometric and Catalytic Reactions Relevant to Negishi Coupling

Transmetalation with (PNP)Rh(Ph)(Cl) (**501-Cl**) and Ph₂Zn was observed to occur within minutes in C₆D₆ to form (PNP)Rh(Ph)₂ (**501-Ph**) (Scheme V-2, top). We previously showed that this complex cleanly undergoes Ph-Ph RE and generates the 14-electron (PNP)Rh fragment in solution, which rapidly reacts with aryl halides via OA.²⁵¹



Scheme V-2. (Top) **501-Cl** Transmetalation with Ph_2Zn , reductive elimination of biphenyl, and oxidative addition of iodobenzene. (Bottom) Dehydrohalogenation of **502** with Ph_2Zn and the oxidative addition of iodobenzene.

For catalytic studies we selected $(\text{PNP})\text{Rh}(\text{H})(\text{Cl})$ (**502**), which was observed to undergo dehydrohalogenation with Ph_2Zn and OA with PhI to enter the proposed catalytic cycle via $(\text{PNP})\text{Rh}(\text{Ph})(\text{I})$ (**501-I**) (Scheme V-2, bottom). Initial testing showed little to no 4-fluorobiphenyl formation (^{19}F NMR evidence) after 24 h thermolysis at 90°C of C_6D_6 solutions of $p\text{-FC}_6\text{H}_4\text{X}$ ($\text{X} = \text{Cl}, \text{Br}, \text{I}$) and Ph_2Zn in the presence of 3% of **502** (Table V-1).^{*} Analysis of the reaction mixtures by $^{31}\text{P}\{^1\text{H}\}$ NMR spectroscopy showed the same major Rh product in all reactions as a doublet at 46.2 ppm ($J_{\text{Rh-P}} = 119$

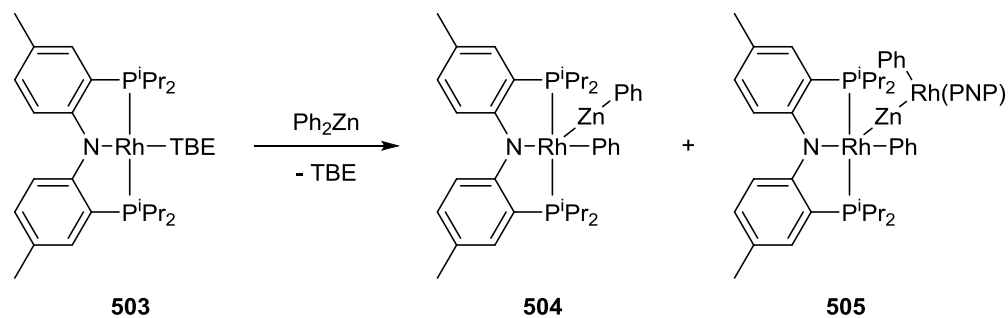
^{*} Slow addition of Ph_2Zn to the 4- $\text{FC}_6\text{H}_4\text{Br}$ coupling reaction did not lead to an improvement.

Hz). Because this did not correspond to a (PNP)Rh(Ar)(X) or (PNP)Rh(Ar)₂ complex it suggested that the catalyst was being sequestered by a reagent in the reaction mixture.

Table V-1. Negishi coupling with **502**

X	Time	ArX Remaining	4-fluoro-biphenyl
Cl	24h	92%	0%
Br	24h	90%	4%
I	44 h	50% ^a	7%
Reactions were performed on a 0.10 mmol scale in J. Young tubes. ^a 36% of the aryl halide was converted to (phenyl)(4-fluorophenyl)zinc, for discussion see ESI.			

We were able to independently synthesize this product through the addition of 1.1 eq. of Ph₂Zn to (PNP)Rh(TBE) (**503**, TBE = *tert*-butylethylene) in C₆D₆ at room temperature (Scheme V-3). This reaction resulted in the displacement of *tert*-butylethylene and the insertion of rhodium into the C-Zn bond of Ph₂Zn to form (PNP)Rh(ZnPh)(Ph) (**504**) in >95% conversion (observed by ¹H NMR spectroscopy) as shown in Scheme V-3. **504** was isolated by recrystallization in a 48% yield as a dark red solid.



Scheme V-3. Synthesis of **504** and **505**.

The structure of **504** was determined by a single crystal X-ray diffraction study on a dark red block crystal (Figure V-2). Possible insertion of Rh into a C-Zn bond of Me_2Zn was previously documented by Heinekey, Goldberg and co-workers, with the product $(\text{PONOP})\text{Rh}(\text{ZnMe})(\text{Me})\text{OTf}$ characterized by ^1H NMR and elemental analysis, but not structurally.²⁵³ Two molecules of **504** are contained within the asymmetric unit, each adopting an approximately square-pyramidal geometry with the $-\text{ZnPh}$ ligand *trans* to the empty site. The Zn-N distances in the two independent molecules differ by ca. 0.3 Å, but the shortest of these distances ($\text{N1}'-\text{Zn1}' = 2.366(4)$ Å) is still >0.2 Å longer than the average Zn-NR₃ bond length (2.16 Å) calculated from a study of the structural characterization of Reformatsky reagents supported by a binucleating bis(amidoamine) ligand.²⁵⁴ The shorter Zn-N distance corresponds to only marginal pyramidalization at N (sum of angles at N is 358° vs 360°) or change in the C-Zn-Rh angle (ca. 173° and 176°). The data suggest that the interaction between N and Zn is not a significant contributor to the overall structural preference of this molecule.

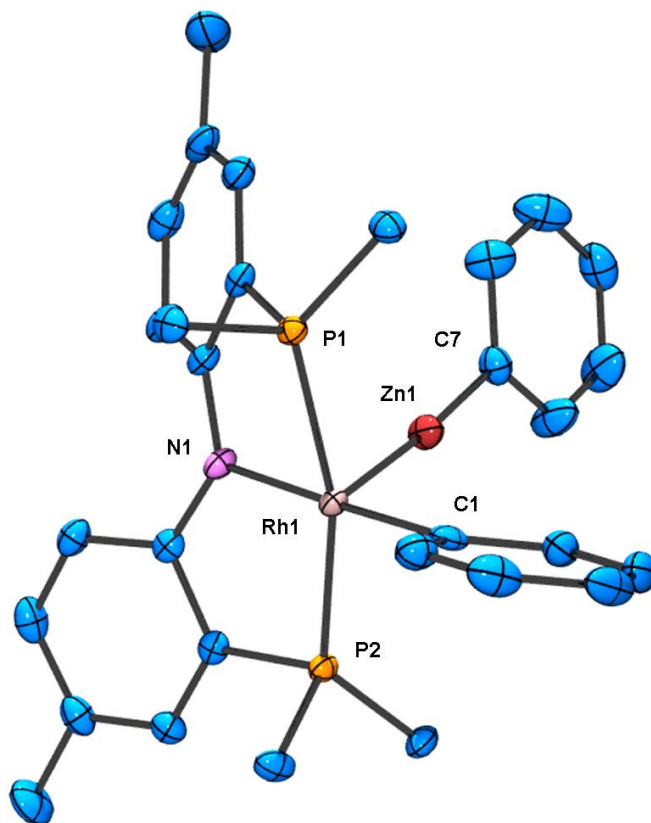


Figure V-1: Left: ORTEP drawing of **504**. The ellipsoids are set at the 50% probability level, and hydrogen atoms and isopropyl methyls have been omitted for clarity. Selected bond distances (Å) and angles (°): Rh1-C1 = 2.048(4), Rh1-Zn1 = 2.3217(6), C7-Zn1-Rh1 = 175.62(14), Zn1-C7 = 1.949(4), N1-Rh1-Zn1 = 73.32(10), Zn1-N1 = 2.664(4), Rh1-N1 = 2.133(3) C1-Rh1-N1 = 178.36(16), P1-Rh1-P2 = 162.62(4), Rh1-P1 = 2.2760(11), Rh1-P2 = 2.2819(11), N1-Zn1-Rh1 = 50.08(8). **Zn-N Contact:** C1'-Rh1'-N1' = 177.57(16), C1'-Rh1' = 2.025(4), N1'-Rh1' = 2.155(3), Zn1'-Rh1' = 2.3478(7), N1'-Rh1'-Zn1' = 63.21(10), N1'-Rh1' = 2.155(3), P1'-Rh1' = 2.2710(11), Rh1'-P2' = 2.2869(11), P1'-Rh1'-P2' = 162.67(4), N1'-Zn1' = 2.366(4), N1'-Rh1'-Zn1' = 63.21(10), N1'-Zn1'-Rh1' = 54.41(8), C7'-Zn1'-Rh1' = 173.15(13). XRD Structure solved by Wei-Chun Shih.

During one of the attempts to crystallize **504** at room temperature in pentane, orange plate crystals were formed. A single crystal X-ray diffraction study determined

this species to be a zinc-bridged dimetallic structure of $[(\text{PNP})\text{Rh}(\text{Ph})]_2(\mu\text{-Zn})$ (**505**) (Figure V-2). The local structure about each Rh is similar to **504**, with the Zn atom occupying the apical position in each square pyramid. Ostensibly, **505** is a product of insertion of two (PNP)Rh fragments into Ph_2Zn ; one into each C-Zn bond. However, thermolysis of **3** with 0.5 eq. of Ph_2Zn only produced a 1:1 mixture of **503**:**504**. We have not been able to reproduce the serendipitous synthesis of **505**.

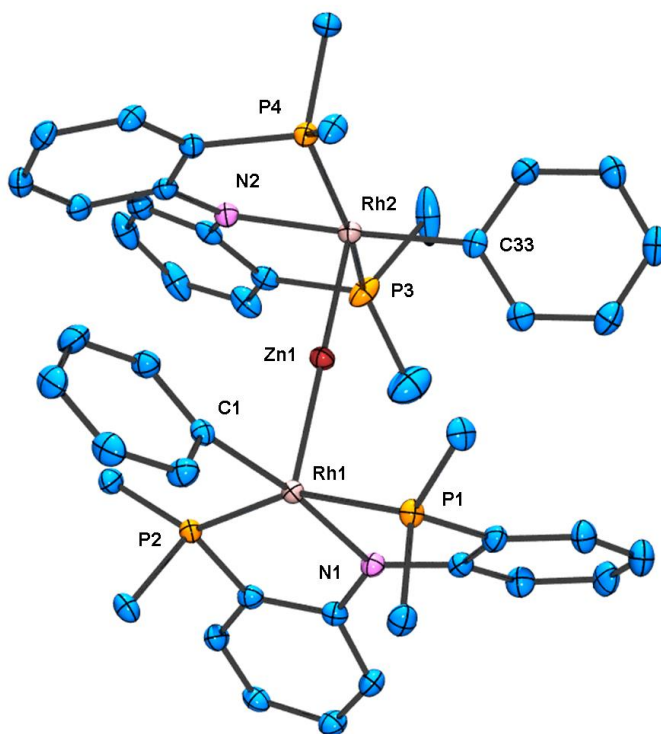


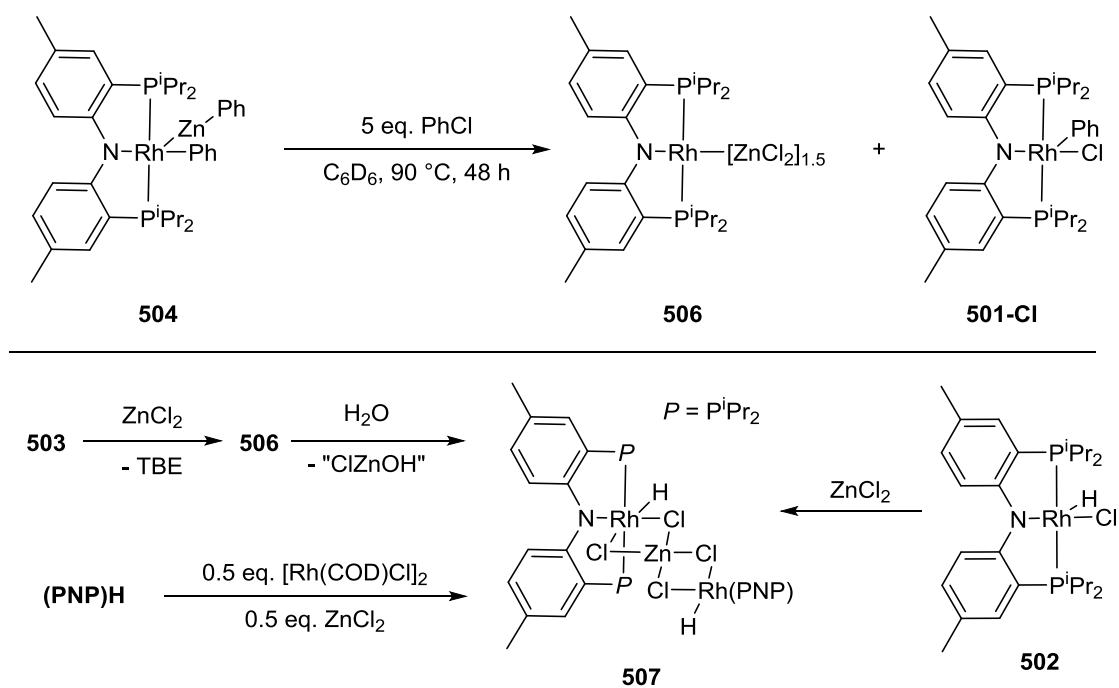
Figure V-2. ORTEP drawing of **505**. The ellipsoids are set at the 50% probability level, and hydrogen atoms and methyls are omitted for clarity. Selected bond distances (Å) and angles (°): Rh1-Zn1 = 2.3738(5), Rh2-Zn1 = 2.3711(5), Rh1-N1 = 2.117(2), Rh2-N2 = 2.114(2), Rh1-C1 = 2.054(3), Rh2-C33 = 2.049(3), Rh1-Zn1-Rh2 = 177.030(16), C1-Rh1-Zn1 = 89.44(8), C33-Rh2-Zn1 = 89.43(8), C1-Rh1-N1 = 172.80(10), C33-Rh2-N2 = 174.33(10), P1-Rh1-P2 = 155.54(3), P3-Rh2-P4 = 158.44(3). XRD structure solved by Wei-Chun Shih.

The Rh-Zn bond lengths in **504** and **505** fall into the 2.32-2.37 Å range, with the shorter Rh-Zn bond (2.3217(6) Å) in **504** apparently being the shortest reported Rh-Zn distance. This range is similar to the unbridged Rh-Zn bond distance of 2.3550(13) Å in Caulton's [MeC(CH₂PPh₂)₃RhH₂ZnN(SiMe₃)₂].²⁵⁵ Rh-Zn bond distances in compounds where they may be bridged by a hydride^{256,257} or are part of a multimetallic cluster^{258,259} tend to be longer. Due to zinc's low electronegativity and the propensity for the zinc ligand to occupy the apical site in compounds **504** and **505**, it is likely that these zinc ligands (e.g., -ZnPh in **504**) exert a strong trans-influence similarly to boryls, stannyls, silyls, and other X-type ligands connected to the transition metal via a single bond to an electropositive element.²⁶⁰

Oxidation state assignments in heterobimetallic compounds can be debatable, and we view valence²⁶¹ as a more relevant concept for discussing these compounds. Both **504** and **505** contain trivalent rhodium and divalent zinc, with the appropriate and common geometries (square-pyramidal for Rh and linear for Zn). We have previously reported a related compound [(^FPNP)Pd]₂(μ-Zn) with a linear Zn bridge connecting two Pd centers, synthesized via photolysis of (^FPNP)Pd-Et in the presence of Et₂Zn.²⁶² A similar mercury-bridged dinickel species has also been recently made with a pyrrolyl/bis(phosphine) PNP pincer ligand.²⁶³ Complexes featuring -ZnR ligands on transition metals other than rhodium are being reported more frequently such as in the work by the Fischer group on organozinc-rich transition metal molecules,^{259a,264} Parkin's dehydrogenative formation of a Mo-Zn bond,²⁶⁵ and a Ru-ZnEt complex recently

synthesized by the Whittlesey group.²⁶⁶ Pt-ZnSiR₃ compounds have also been synthesized via radical pathways from Pt(0) and bis(silyl)zinc reagents.²⁶⁷ Formation of adducts from Pd(II) complexes as Lewis bases and ZnX₂ compounds as Lewis acids have also been described experimentally²⁶⁸ and analyzed computationally.²⁶⁹

We were determined to see if **504** could still react with an aryl chloride to reenter the catalytic cycle as **501-Cl**. Treating **504** with 5 eq. of chlorobenzene and heating at 90 °C for 20 h still showed **504** comprising 25% of the reaction mixture. After 48 h, a mixture composed of about 50% **501-Cl** and 50% of a new product that gave rise to a broad doublet at 46.5 ppm by ³¹P{¹H} NMR spectroscopy. We hypothesized it to be an adduct of the (PNP)Rh fragment with ZnCl₂ (**506**) (Scheme V-4, top). In support of the proposed formulation and stoichiometry, **506** could be independently synthesized by thermolysis of **503** in benzene in the presence of a minimum of 1.5 eq. of ZnCl₂ (Scheme V-4).



Scheme V-4. (Top) Treatment of **504** with chlorobenzene. (Bottom) Synthesis and hydrolysis of **506** and synthesis of **507**.

Attempts to obtain single crystals from **506** were met with the partial decomposition to a purple product containing a hydride resonance observable by ^1H NMR spectroscopy at -19.98 ppm (dt, $J_{\text{Rh-P}} = 26$ Hz, $J_{\text{P-H}} = 10.5$ Hz). This product was identified as $[(\text{PNP})\text{Rh}(\text{H})]_2[\mu\text{-ZnCl}_4]$ (**507**) (Scheme V-4) and was structurally characterized by an XRD study of a purple block crystal (Figure V-3). **507** could be synthesized a) by treating **502** with excess (3 eq.) ZnCl_2 (Scheme V-4), b) via a one-pot synthesis from the (PNP)H ligand in toluene with a half equivalent of $[\text{Rh}(\text{COD})\text{Cl}]_2$ and a half equivalent of ZnCl_2 ; and c) rapid hydrolysis of compound **506** upon treatment with 1.33 eq. of degassed water in C_6D_6 (Scheme 3, middle). The structure of **507** contains two equivalents of **502** combined with an equivalent of ZnCl_2 by four chloride

bridges. We hypothesize that **506** has a similar structure with the $-\text{ZnCl}$ ligand occupying the hydride site in **507**. It is likely that the Rh-Zn bond is hydrolyzed to form a Rh-H and a “Zn(OH)Cl” by-product. Goldberg’s (PONOP)Rh(ZnMe)(Me)OTf was also sensitive to hydrolysis.²⁵³ The (PNP)Rh fragment has previously shown its capacity to insert into metal-halide bonds in our studies of the oxidative addition of early metal-halogen bonds,²⁷⁰ thus it is plausible that **506** arises from insertion of Rh into Zn-Cl bonds, however we could not establish the structure of **506** unambiguously. In another attempt to prove the possibility of insertion into Zn-Cl bonds, thermolysis of **503** with PhZnCl was carried out. The resultant mixture contained ca. 30% of **504** in addition to several other unidentified products. Thus although Rh-Zn bonds were made in this reaction as well, it was not possible to determine whether insertion into Zn-Cl bonds had occurred.

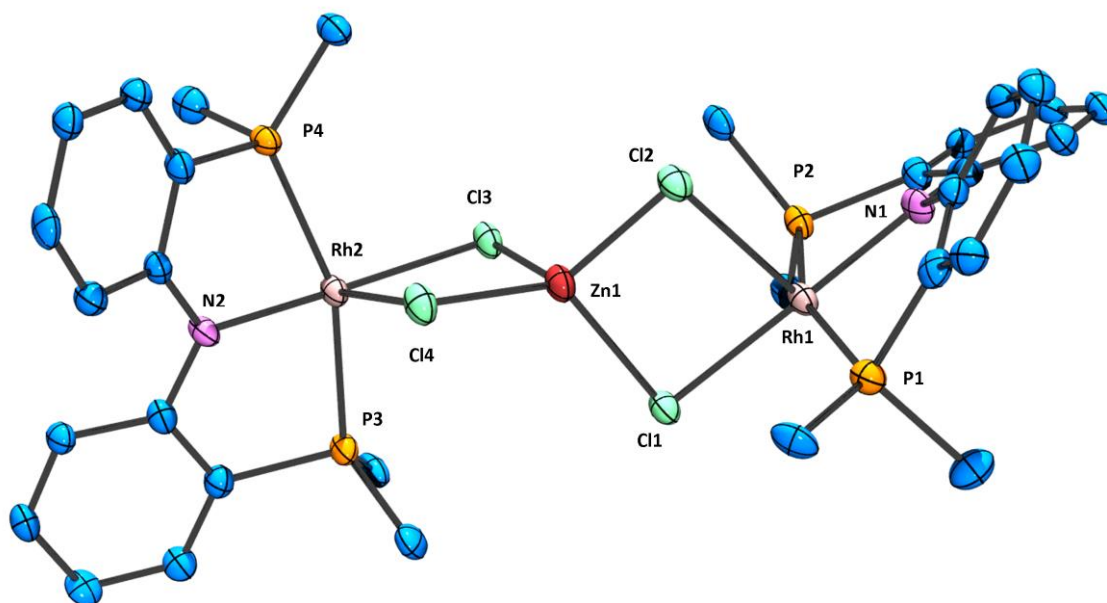
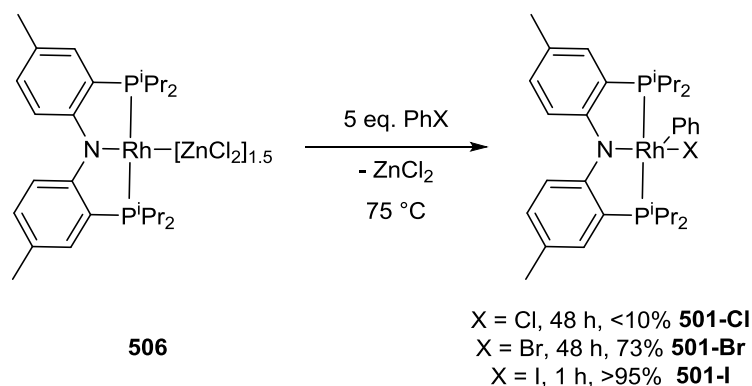


Figure V-3. ORTEP Drawing of **507**. The ellipsoids are set at the 50% probability level. Hydrogens, methyls, and a molecule of pentane are omitted for clarity. Selected bond distances (Å) and angles (°): Rh1-Cl1 = 2.4403(14), Rh1-Cl2 = 2.6114(15), Rh2-Cl3 = 2.4287(14), Rh2-Cl4 = 2.6102(16), Rh1-N1 = 2.038(5), Rh2-N2 = 2.023(4), N1-Rh1-Cl2 = 92.97(14), N2-Rh2-Cl4 = 91.26(15), Zn1-Cl1 = 2.3045(16), Zn1-Cl2 = 2.2585(16), Zn1-Cl3 = 2.3151(17), Zn1-Cl4 = 2.2385(15), N1-Rh1-Cl1 = 176.71(14), N2-Rh2-Cl3 = 176.04(15), Cl1-Zn1-Cl3 = 106.25(6), Cl2-Zn1-Cl3 = 120.67(6), Cl4-Zn1-Cl3 = 97.11(6). The Rh-H could not be located from the difference Fourier maps. XRD structure solved by Wei-Chun Shih.

In relevance to Negishi coupling, **504** and **506** can both be considered adducts between the (PNP)Rh fragment and Zn reagents or by-products. We have previously established that the (PNP)Rh fragment is necessary for the OA of aryl halides to take place.^{251,271,272} Thus the formation of **504** and **506** can be viewed as deactivation of the reactive species necessary for catalysis. Similarly to **504**, **506** reacted only sluggishly with PhCl (<10% conversion after 48 h at 75 °C). The reactions of **506** with PhBr and PhI proceeded faster, as expected, but overall **504** and **506** appear to undergo OA with

aryl halides (Scheme V-5) at a decreased rate compared to **503** or (PNP)Rh(SⁱPr₂).²⁷¹ Although **504** is an adduct formed by oxidative addition (and **506** possibly is, as well), it is nonetheless formulaically analogous to the Lewis acid-base adducts between Pd(0) and divalent Zn compounds that have been implicated in computational investigations into palladium-catalyzed Negishi coupling.^{269a,273} Similar to our findings, it was shown that Pd(0)-ZnX₂ interactions slow the oxidative addition of vinyl bromide and are detrimental to catalysis.²⁷³



Scheme V-5. Treatment of **506** with phenylhalides and percent conversion to **501-X**.

5.2.2 Reactions of Rh-Zn Bimetallic Complexes with Dihydrogen

Heterobimetallic complexes are of interest because they possess two electronically different metals in close proximity. Heterogeneous Cu zinc hydride species are the industry's choice for the hydrogenation of carbon monoxide to methanol.²⁷⁴ Thus there is an interest in the literature to explore heterobimetallic zinc hydride species.^{256,257} There is also an increased interest in molecular zinc hydride characterization and catalytic applications such as hydrosilylation, hydrogenation of imines, and the

dehydrocoupling of alcohols with silanes.²⁷⁵ While there have been only limited examples of defined homogeneous heterobimetallic hydride compounds participating in catalysis,²⁷⁶ the field of heterobimetallics has recently been acknowledged as a relatively unexplored area that could uncover new fundamental reactivity and selectivity for known reactions.²⁷⁷

With this in mind, **504** was exposed to an atmosphere of H₂ and the sample was heated for 20 h at 60 °C. Benzene was observed by ¹H NMR spectroscopy as well as two new C_{2v} (PNP)Rh compounds. When the volatiles were removed from the sample, and redissolved in C₆D₆, it was observed that only one of the C_{2v} products remained (Figure V-4). It contained a complex hydride signal at -15.67 ppm that integrated to 1 proton. Although the product has not been fully characterized, it was observed to form crystals from cold Et₂O.

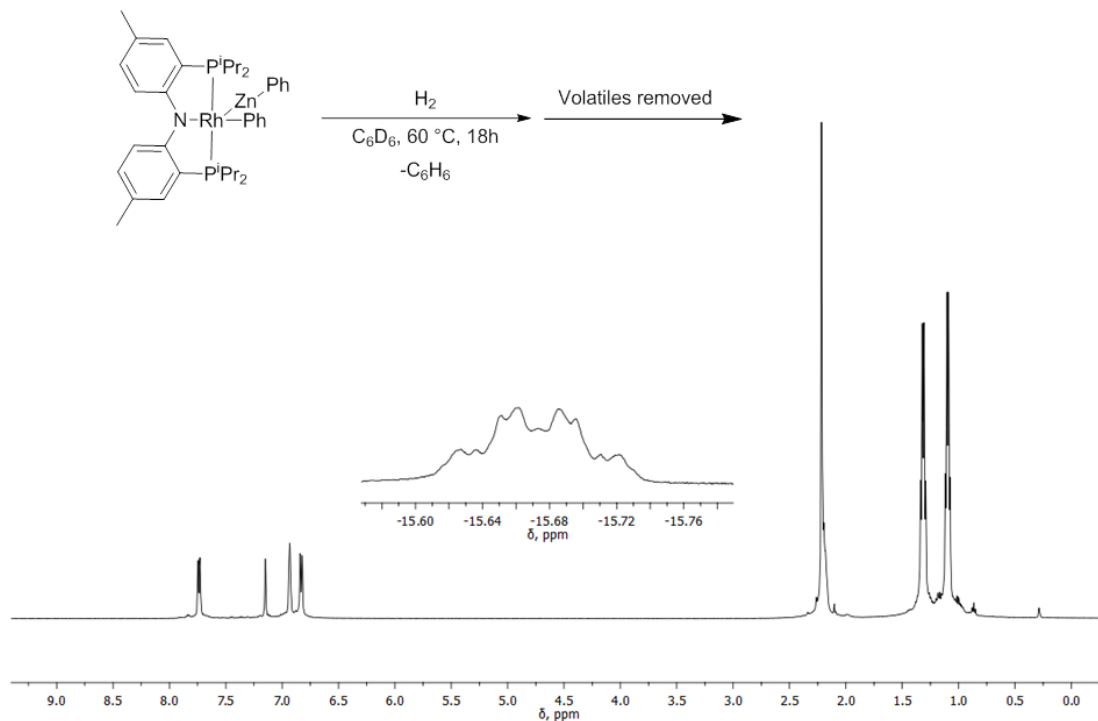


Figure V-4. ^1H NMR spectrum resulting from the treatment of **504** with dihydrogen gas. Inset is the hydride region of the ^1H NMR spectrum.

Rhodium-zinc hydrides could also be synthesized by treating (PNP)Rh(H_2) (**401-Rh(H₂)**) with ZnCl_2 in C_6D_6 at room temperature. This reaction yielded a C_1 product with hydride signals at -13.67 and -18.33 ppm (Figure V-5).

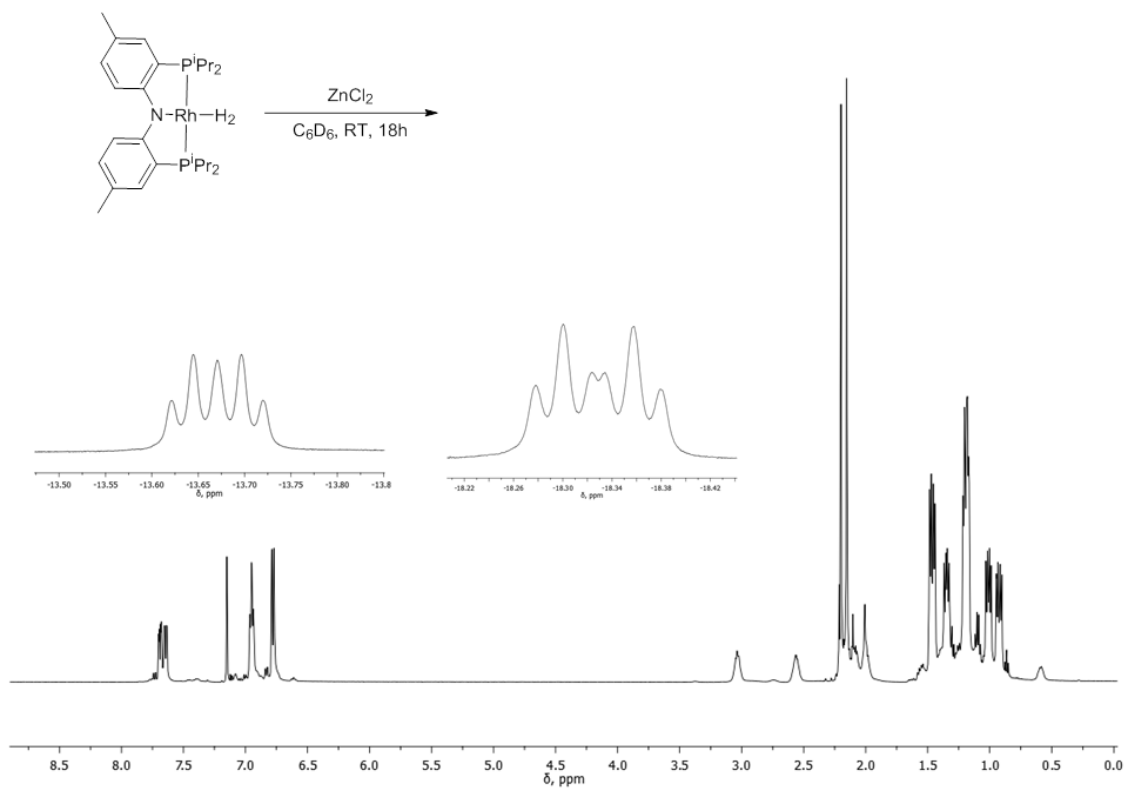


Figure V-5. Crude ^1H NMR spectrum resulting from treating **401-Rh(H₂)** with ZnCl_2 . Inset is the hydride region of the ^1H NMR spectrum.

5.3 Conclusion

In conclusion, we have shown that under potential Negishi coupling conditions, the (PNP)Rh catalyst is sequestered by organozinc reagents or by-products through the formation of adducts of (PNP)Rh with ZnX_2 . In the case of the addition of ZnPh_2 , the Rh center inserts into the Zn-Ph bond while the precise structural outcome of the addition of PhZnCl and ZnCl_2 to (PNP)Rh has not been unambiguously established. The formation of these adducts is deleterious for catalysis as they dramatically diminish the availability of the unsaturated (PNP)Rh intermediate necessary for the step of oxidative

addition of the aryl halide. We have also shown that rhodium-zinc hydride species can be accessed from **504** and the addition of ZnCl₂ to **401-Rh(H₂)**.

5.4 Experimental

5.3.1 General Considerations

Unless otherwise specified, all manipulations were performed under an argon atmosphere using standard Schlenk or glovebox techniques. Toluene, ethyl ether, and pentane were dried and deoxygenated (by purging) using a solvent purification system by MBraun and stored over molecular sieves in an Ar-filled glove box. C₆D₆ was distilled from NaK/Ph₂CO/18-crown-6-ether and stored over molecular sieves in the glovebox. Liquid aryl halides (4-fluorochlorobenzene, 4-fluorobromobenzene, 4-fluoroiodobenzene, chlorobenzene, iodobenzene, and trifluorotoluene) were degassed and introduced into an argon filled glovebox and stored under molecular sieves. **501-Ph**,²⁵¹ **501-Br**,²⁷⁸ and **501-I**²⁷⁸ were previously characterized by our group. **501-Cl**²⁷⁸ and **502**²⁷⁸ were synthesized as described in the literature. Diphenylzinc was prepared as described in the literature.²⁷⁹ Bis(4-fluorophenyl)zinc was prepared as described in the literature.²⁸⁰ Phenylzinc chloride was prepared by mixing a 1:1 ratio of Ph₂Zn and ZnCl₂ in toluene and stirring overnight. ZnCl₂ was dried by refluxing in freshly distilled SOCl₂ followed by the removal of the volatiles via vacuum transfer.

5.3.2 Negishi Coupling Reactions

General procedure for Negishi Coupling Reactions. **502** (0.003 mmol, 100 μL of a 0.030 M solution in C₆D₆) was added to a J. Young tube and treated with *p*-FC₆H₄X

(X= Cl, Br, I) (0.10 mmol, 100 μ L of 1.0 M solution in *p*-FC₆H₄X / 0.33 M in PhCF₃ as an internal standard). Ph₂Zn (22 mg, 0.10 mmol) was added to the J. Young tube, and then the solution was diluted with 300 μ L of C₆D₆). The J. Young tubes were placed in a 90 °C oil bath. Reaction progress was monitored by ¹⁹F NMR spectroscopy.

Coupling of 4-fluoroiodobenzene. In entry 3 there was a 36% conversion to a new product observed at -112.5 ppm by ¹⁹F NMR spectroscopy. We hypothesize that this product is (phenyl)(4-fluorophenyl)zinc that is produced through an aryl-aryl transmetallation step.

Coupling of 4-fluorobromobenzene with slow addition of Ph₂Zn. 502 (0.007 mmol, 230 μ L of a 0.030 M solution in C₆D₆) was added to a 100 mL Schlenk flask and treated with 4-fluorobromobenzene (25 μ L, 0.23 mmol) and trifluorotoluene (10 μ L, 0.08 mmol) was added as an internal standard. The solution was diluted with 1 mL of toluene. Ph₂Zn (50 mg, 0.23 mmol) was dissolved in 50 mL of toluene and transferred to an addition funnel. The addition funnel was mounted onto the Schlenk flask containing the reaction mixture, and the Ph₂Zn solution was added dropwise over a period of 6 hours while the reaction mixture was heated in a 90 °C oil bath. Within the first hour of Ph₂Zn addition, the reaction mixture had turned orange-brown color, which suggests that **504** is present as opposed to green (PNP)Rh species such as **501-Ph** or (PNP)Rh(C₆H₄F)(Br).²⁷² The reaction progress was checked by ¹⁹F NMR spectroscopy after 20 h, which showed no formation of 4-fluorobiphenyl, and >95% of the starting material remaining.

Observation of (*p*-FC₆H₄)Zn(C₆H₅). Bis(4-fluorophenyl)zinc (10 mg, 0.039 mmol) and Ph₂Zn (25 mg, 0.11 mmol) were dissolved in 500 μL of C₆D₆ in order to match the product ratio and concentration in the reaction mixture of the Negishi coupling of 4-fluoroiodobenzene with diphenyl zinc. After mixing the two diarylzinc reagents in solution for 1 hour, analysis by ¹⁹F NMR showed a multiplet at -113.1 ppm.

5.3.3 Synthesis and Characterization

Treatment of 501-Cl with 1 eq. of Ph₂Zn. 501-Cl (38 mg, 0.059 mmol) was dissolved in C₆D₆ in a J. Young tube. Iodobenzene (13 μL, 0.12 mmol) was added to trap the 16-electron rhodium complex after the reductive elimination of biphenyl. The reaction mixture was treated with Ph₂Zn (13 mg, 0.059 mmol). Analysis by ³¹P{¹H} NMR spectroscopy within 15 minutes of mixing showed **501-Ph** as the major product with trace amounts of **501-I** and **504**. The reaction mixture was left overnight at room temperature, and analysis by ¹H NMR spectroscopy in the morning showed the formation of biphenyl and **501-I** as the major rhodium complex.

Treatment of 502 with Ph₂Zn. 502 (10 mg, 0.018 mmol) was dissolved in C₆D₆ with iodobenzene (4 μL, 0.036 mmol) and treated with Ph₂Zn (4 mg, 0.018 mmol). Analysis with ³¹P{¹H} NMR spectroscopy within 45 min. at room temperature showed **501-I** as the major product and **504** and **501-Cl** as minor side products. ¹H NMR spectroscopy showed the formation of C₆H₆.

Synthesis of (PNP)Rh(ZnPh)(Ph) (504). 503 (36 mg, 0.058 mmol) was added to a J. Young tube with Ph₂Zn (15 mg, 0.068 mmol) and dissolved in C₆D₆. The J. Young tube was rotated for 4 hours and was observed by ³¹P{¹H} and ¹H NMR to

convert >95% to **504**. The solution was diluted with pentane and filtered through Celite. The volatiles were removed and the red solid was redissolved in pentane and placed in a -35 °C freezer to recrystallize overnight. The product was isolated as a red solid (21 mg, 48% yield). $^{31}\text{P}\{^1\text{H}\}$ NMR (C_6D_6 , 202 MHz): δ 46.2 (d, $J = 119$ Hz). ^1H NMR (C_6D_6 , 500 MHz): δ 7.92 (d, $J = 7.5$ Hz, 2H, Ar-*H* of PNP), 7.76 (d, $J = 7$ Hz, 2H, Ar-*H*), 7.23 (d, $J = 6.5$ Hz, Ar-*H*), 7.18 (t, $J = 7$ Hz, 2H, Ar-*H*), 7.12 (m, 3H, Ar-*H*), 6.99 (t, $J = 7$ Hz, 1H, Ar-*H*), 6.95 (s, 2H, Ar-*H* of PNP), 6.86 (d, $J = 8.5$ Hz, 2H, Ar-*H* of PNP), 2.44 (m, 2H, *CHMe*₂), 2.19 (s, 6H, Ar-*Me*), 2.19 (m, 2H, *CHMe*₂), 1.12 (app. q (dvt), $J = 8$ Hz, 6H, *PCHMe*₂), 1.08 (app. q (dvt), $J = 7$ Hz, 6H, *PCHMe*₂), 0.95 (app. q (dvt), $J = 6$ Hz, 6H, *PCHMe*₂), 0.89 (app. q (dvt), $J = 7.5$ Hz, 6H, *PCHMe*₂). $^{13}\text{C}\{^1\text{H}\}$ NMR (C_6D_6 , 100.6 MHz): δ 161.1 (dvt, $J = 10$ Hz, $J = 1$ Hz, C-N of PNP), 158.2 (dvt, $J = 30.9$ Hz, $J = 9.9$ Hz, *i*-Ph), 145.8 (d, $J = 10.4$ Hz, Zn-C), 140.8 (br. vt, $J = 1.9$ Hz, Ph), 137.3 (s, Ph), 132.4 (s, Ar PNP), 131.8 (s, Ar PNP), 128.6 (s, Ph), 126.7 (s, Ph), 125.9 (s, Ph), 125.1 (vt, $J = 3.1$ Hz, Ar PNP), 123.3 (vt, $J = 18.2$ Hz, Ar PNP), 121.2 (s, Ph), 116.5 (vt, $J = 4.7$ Hz, Ar of PNP), 20.61 (vt, $J = 2.3$ Hz, *PCHMe*₂), 20.57 (s, Ar-*Me*), 20.0 (vt, $J = 2.4$ Hz, *PCHMe*₂), 18.5 (vt, $J = 2.7$ Hz, *PCHMe*₂), 17.8 (s, *PCHMe*₂). Anal. Calcd for $\text{C}_{38}\text{H}_{50}\text{NP}_2\text{RhZn}$: C, 60.77; H, 6.71; N, 1.86 Found: C, 59.67; H, 6.34; N, 1.76.

Treatment of 503 with 0.5 eq. Ph_2Zn . **503** (28 mg, 0.045 mmol) was dissolved in C_6D_6 in a J. Young tube and treated with Ph_2Zn (5 mg, 0.023 mmol). The reaction was mixed overnight at room temperature and examined by ^1H and $^{31}\text{P}\{^1\text{H}\}$ NMR spectroscopy. The mixture was observed to be a 1:1 mixture of **503** and **504** with 0.5 equivalents of free *tert*-butylethylene. The solution was transferred to a 10 mL Schlenk

flask and the volatiles were removed. The solid residue was redissolved in C₆D₆ and transferred to a J. Young tube. The reaction was heated at 90 °C overnight. ¹H and ³¹P{¹H} NMR showed no change in the distribution of products.

Treatment of 503 with 1 eq. of PhZnCl. 503 (31 mg, 0.05 mmol) was dissolved in C₆D₆ in a J. Young tube and treated with PhZnCl (9 mg, 0.05 mmol). Analysis by ³¹P{¹H} NMR spectroscopy 20 minutes after mixing showed that about 34% of the reaction mixture was composed of **504**. The reaction was left for 24 h at room temperature and the color of the solution became brown. The mixture was analyzed by ³¹P{¹H} NMR spectroscopy. Broad doublets were observed at 47.0 ppm ($J_{\text{Rh-P}} = 101$ Hz) and 45.3 ppm ($J = 116$ Hz) and **504** still composed about 30% of the reaction mixture. The reaction was heated at 80 °C for 1 h, at which point the reaction turned green. Analysis by ³¹P{¹H} NMR spectroscopy showed a mixture of approximately ten compounds. Compound **504** still composed about 30% of the mixture.

Treatment of 504 with PhCl. 504 (11 mg, 0.015 mmol) was dissolved in C₆D₆ in a J. Young tube and treated with chlorobenzene (8 μL, 0.079 mmol) and refluxed for 48 h. ³¹P{¹H} NMR spectroscopy showed a 1:1 distribution of **506** and **501-Cl**. ¹H NMR spectroscopy showed the formation of approximately 1.5 equivalents of biphenyl.

In Situ observation of (PNP)Rh(ZnCl₂)_{1.5} (506). Method 1: **503** (18 mg, 0.029 mmol) was dissolved in C₆D₆ in a J. Young tube and treated with anhydrous ZnCl₂ (30 mg, 0.22 mmol) and mixed for 2 days at room temperature. The reaction had turned from an orange-red color to bright green. Analysis of the mixture by ¹H NMR spectroscopy shows complete consumption of **503** and free *tert*-butyl ethylene. Analysis

by $^{31}\text{P}\{^1\text{H}\}$ NMR spectroscopy showed a broad doublet at 46.5 ppm (approximate $J_{\text{Rh-P}} = 100$ Hz). Method 2: **503** (74 mg, 0.12 mmol) was dissolved in C_6D_6 and treated with anhydrous ZnCl_2 (24 mg, 0.18 mmol) in a J. Young tube and refluxed for 8 hours. The product could also be made in a shorter period of time by using >1.5 eq of anhydrous ZnCl_2 and refluxing the solution. Attempts to isolate the product via filtration through Celite and the removal of the volatiles under vacuum led to the partial formation of **7**. $^{31}\text{P}\{^1\text{H}\}$ NMR (202 MHz, C_6D_6): δ 46.5 (br. d, $J_{\text{Rh-P}} = 100$ Hz); ^1H NMR (500 MHz, C_6D_6): δ 7.71 (br, 4H, Ar-H), 6.83 (br, 4H, Ar-H), 6.70 (d, $J = 7$ Hz, 4H, Ar-H), 2.52 (br, 4H, PCHMe_2), 2.27 (br, 4H, PCHMe_2), 2.14 (s, 12H, Ar-Me), 1.49 (br, 6H, PCHMe_2), 1.37 (br, 12H, PCHMe_2), 1.23 (br, 18H, PCHMe_2), 0.98 (br, 6H, PCHMe_2), 0.93 (br, 6H, PCHMe_2); $^{13}\text{C}\{^1\text{H}\}$ NMR (128 MHz, C_6D_6): δ 162.7 (br, Ar-N), 132.0 (s, Ar), 131.5 (br, Ar), 131.3 (br, Ar), 126.5 (s, Ar), 119.1 (br, Ar), 118.6 (br, Ar), 27.3 (br, PCHMe_2), 23.5 (br, PCHMe_2), 20.5 (s, Ar-Me), 20.3 (s, Me), 20.1 (s, Me), 18.7 (s, Me), 18.0 (s, Me).

Treatment of 503 with 0.6 eq. of ZnCl_2 . **503** (75 mg, 0.12 mmol) was dissolved in C_6D_6 and treated with anhydrous ZnCl_2 (10 mg, 0.07 mmol). The mixture was heated overnight at 80 °C and produced a mixture of intractable products observed by ^1H NMR and $^{31}\text{P}\{^1\text{H}\}$ NMR containing **503** (~30%) and several other products. **506** accounted for ~5% of the reaction mixture.

Treatment of 503 with 1 eq. of ZnCl_2 . **503** (75 mg, 0.11 mmol) was dissolved in C_6D_6 and treated with anhydrous ZnCl_2 (15 mg, 0.11 mmol) the reaction was heated at 80 °C for 48 hours. After this time, $^{31}\text{P}\{^1\text{H}\}$ NMR spectroscopy showed a mixture of products containing 23% **506** and 9% **503**.

Synthesis of [(PNP)Rh(H)]₂[μ-ZnCl₄] (507). Method 1: **503** (74 mg, 0.12 mmol) was dissolved in C₆D₆ and treated with anhydrous ZnCl₂ (24 mg, 0.18 mmol) in a J. Young tube and refluxed for 8 hours. Analysis by ¹H NMR spectroscopy indicated that the starting material had been converted to the product **506**. The reaction mixture was diluted with toluene and filtered through Celite and the volatiles were removed under vacuum. Analysis by ¹H and ³¹P{¹H} NMR spectroscopy showed a mixture of **506** and **507**. The volatiles were removed from the reaction to leave a fine flowing powder, which was exposed to the glovebox atmosphere and stirred as a solid for 5 days at which point the powder had turned purple. The product was extracted with pentane and filtered through Celite to yield **507** (48 mg, 63%). Method 2: **503** (26 mg, 0.042 mmol) was dissolved in C₆D₆ and treated with anhydrous ZnCl₂ (15 mg, 0.11 mmol) was refluxed for 8 h and showed complete conversion to **506**. The solution was then filtered through Celite to remove excess ZnCl₂ and transferred into a new J. Young tube. Water (1 μL, 0.056 mmol) was added to the solution and shaken vigorously for five seconds. Within less than a minute, the green solution had turned purple and contained a precipitate. Analysis by ¹H and ³¹P{¹H} NMR spectroscopy showed complete conversion to **507**. The solution was diluted with pentane and filtered through Celite and the volatiles were removed under vacuum. The purple solid was recrystallized from pentane in a -35 °C freezer (16 mg, 63% yield). Method 3: **502** (14 mg, 0.025 mmol) was dissolved in C₆D₆ and treated with ZnCl₂ (10 mg, 0.073 mmol). Within 15 min. of mixing, the solution had turned from green to purple. Analysis by ¹H and ³¹P{¹H} NMR spectroscopy showed >95% conversion to **7**. Method 4: **(PNP)H** (300 mg, 0.70 mmol) and [Rh(COD)Cl]₂

(172 mg, 0.35 mmol) were dissolved in toluene and treated with ZnCl₂ (47 mg, 0.35 mmol) and stirred vigorously overnight at room temperature. The resulting solution was diluted with pentane and filtered through a pad of Celite and then the volatiles were removed under vacuum. The resulting solid was recrystallized by dissolving in diethyl ether and layering with pentane. **507** was isolated as a purple solid (352 mg, 80% yield). ³¹P{¹H} NMR (121 MHz, C₆D₆): δ 49.6 (d, *J*_{Rh-P} = 104 Hz), 49.5 (d, *J*_{Rh-P} = 104 Hz); ¹H NMR (500 MHz, C₆D₆): δ 7.42 (br, 4H, Ar-*H*), 6.89 (br, 4H, Ar-*H*), 6.61 (dd, *J* = 8.5 Hz, *J* = 1.5 Hz, 4H, Ar-*H*), 3.05 (br, 2H, PCHMe₂), 2.83 (br, 2H, PCHMe₂), 2.22 (br, 2H, PCHMe₂), 2.14 (br, 2H, PCHMe₂), 2.10 (s, 12H, PCHMe₂), 1.53 (dt (apparent q.), *J* = 7.5 Hz, 12H, PCHMe₂), 1.45 (br, 6H, PCHMe₂), 1.36 (br, 6H, PCHMe₂), 1.30 (br, 12H, PCHMe₂), 1.12 (br, 6H, PCHMe₂), 1.07 (br, 6H, PCHMe₂), -19.98 (dt, *J*_{Rh-H} = 26 Hz, *J*_{P-H} = 10.5 Hz, 2H, Rh-H); ¹³C{¹H} NMR (128 MHz, C₆D₆): δ 161.5 (br., C-N), 161.1 (br., C-N), 131.4 (s), 130.9 (s), 125.4 (br.), 124.9 (br.), 122.5 (s), 122.4 (s), 122.2 (s), 117.7 (br.), 116.2 (br.), 26.4 (br.), 25.5 (overlapping br.), 25.1 (br.), 20.6 (s, Ar-*Me*), 19.4 (s), 19.2 (s), 19.0 (s), 18.9 (s), 18.6 (br.). Anal. Calcd for C₅₂H₈₂Cl₄N₂P₄Rh₂Zn: C, 49.10; H, 6.50; N, 2.20 Found: C, 48.83; H, 5.95; N, 2.09.

Treatment of 506 with chlorobenzene. **503** (23 mg, 0.037 mmol) was treated with ZnCl₂ (15 mg, 0.11 mmol) in C₆D₆. The reaction was heated at 80 °C for 4 h, at which time complete conversion to **506** was observed. The reaction was then filtered through Celite in toluene, and the volatiles were removed. The residue was dissolved in 600 μL of C₆D₆ and transferred to a J. Young tube. Chlorobenzene (19 μL, 0.185 mmol)

was added to the reaction and heated at 75 °C for 48 hours. Conversion to **501-Cl** was observed to be <10% by ^1H NMR spectroscopy.

Treatment of 506 with bromobenzene. 503 (23 mg, 0.037 mmol) was treated with ZnCl_2 (15 mg, 0.11 mmol) in C_6D_6 . The reaction was heated at 80 °C for 4 h, at which time complete conversion to **506** was observed. The reaction was then filtered through Celite in toluene, and the volatiles were removed. The residue was dissolved in 600 μL C_6D_6 and transferred to a J. Young tube. Phenyl bromide (20 μL , 0.185 mmol) was added to the reaction which was then heated at 75 °C for 48 hours. At this time, conversion to **501-Br** was observed to be 73% by ^1H NMR spectroscopy.

Treatment of 506 with iodobenzene. 503 (23 mg, 0.037 mmol) was treated with ZnCl_2 (15 mg, 0.11 mmol) in C_6D_6 . The reaction was heated at 80 °C for 4 h, at which time complete conversion to **506** was observed. The reaction was then filtered through Celite in toluene, and the volatiles were removed. The residue was dissolved in 600 μL C_6D_6 and transferred to a J. Young tube. Phenyl iodide (21 μL , 0.185 mmol) was added to the reaction, which was then heated for 1 h at 75 °C. Analysis by ^1H and $^{31}\text{P}\{^1\text{H}\}$ NMR spectroscopy showed complete conversion to **1-I**. A precipitate was also observed, presumably ZnCl_2 .

Treatment of 503 with chlorobenzene. 503 (23 mg, 0.037 mmol) was dissolved in 600 μL of C_6D_6 in a J. Young tube and treated with chlorobenzene (19 μL , 0.185 mmol). The reaction was heated at 75 °C for 45 min. and was observed by $^{31}\text{P}\{^1\text{H}\}$ NMR spectroscopy to be >95% converted to **501-Cl**.

5.3.4 Reactions with Dihydrogen

Treatment of 504 with H₂. **504** (28 mg, 0.037 mmol) was dissolved in C₆D₆ in a J. Young tube. The headspace was evacuated through the freeze-pump-thaw method and was refilled with 1 atm of H₂. The sample was heated for 18 h at 60 °C. Analysis by ¹H and ³¹P{¹H} NMR showed the formation of two C_{2v} products in a 1:2 ratio and the formation of C₆H₆. **Product 504-A:** ³¹P{¹H} NMR (121 MHz, C₆D₆): δ 63.7 (br. d, *J* = 126 Hz); ¹H NMR (500 MHz, C₆D₆): δ 7.73 (d, *J* = 8.5 Hz, 2H, Ar-*H*), 6.93 (br, 2H, Ar-*H*), 8.38 (d, *J* = 8.5 Hz, Ar-*H*), 2.21 (s, 6H, Ar-*Me*), 2.05 (m, 4H, PCHMe₂), 1.31 (dvt (ap. q), *J* = 7.5 Hz, PCHMe₂), 1.09 (dvt (ap. q), *J* = 7 Hz, PCHMe₂), -15.67 (br, 1H, Rh-*H*). **Product 504-B:** ³¹P{¹H} NMR (121 MHz, C₆D₆): δ 68.0 (d, *J* = 122 Hz); ¹H NMR (500 MHz, C₆D₆): δ 7.83 (d, *J* = 9 Hz, 2H, Ar-*H*), 7.65 (d, *J* = 6.5 Hz, 2H, Ar-*H*), 7.33 (t, *J* = 7.5 Hz, 2H, Ar-*H*), 7.26 (t, *J* = 7.5 Hz, 1H, Ar-*H*), 6.90 (br, 2H, Ar-*H*), 6.86 (d, *J* = 8.5 Hz, 2H, Ar-*H*), 2.21 (s, 6H, Ar-*Me*), 2.20 (m, 4H, PCHMe₂), 1.19 (dvt (ap. q), *J* = 7.5 Hz, 12H, PCHMe₂), 0.97 (dvt (ap. q), *J* = 7 Hz, 12H, PCHMe₂), -15.38 (dt, *J*_{Rh-H} = 20 Hz, *J*_{P-H} = 13 Hz, 1H, Rh-*H*).

The solution was filtered through Celite and the volatiles were removed under vacuum, and the residue was redissolved in C₆D₆ and analyzed by ¹H and ³¹P{¹H} NMR spectroscopy, where it appeared that the product **504-B** had disappeared and product **504-A** was the only product present with a sharper hydride signal integrating to 1 proton. The product could be recrystallized from Et₂O at -35 °C.

Treatment of 410-Rh(H₂) with ZnCl₂. **410-Rh(H₂)** (19 mg, 0.036 mmol) was dissolved in C₆D₆ in a J. Young tube and treated with ZnCl₂ (10 mg, 0.073 mmol). The

reaction was mixed at room temperature overnight. The reaction mixture was analyzed by ^1H and $^{31}\text{P}\{^1\text{H}\}$ NMR spectroscopy. $^{31}\text{P}\{^1\text{H}\}$ NMR (121 MHz, C_6D_6): δ 64.0 (dd, $J_{\text{P-P}} = 347$ Hz, $J_{\text{Rh-P}} = 100$ Hz), 60.8 (dd, $J_{\text{P-P}} = 348$ Hz, $J_{\text{Rh-P}} = 100$ Hz); ^1H 7.69 (dd, $J = 8.5$ Hz, $J = 3.5$ Hz, 1H, Ar-*H*), 7.64 (dd, $J = 8.5$ Hz, $J = 3.5$ Hz, 1H, Ar-*H*), 6.95 (br. overlapping dd, $J = 6.5$ Hz, 2H, Ar-*H*), 6.78 (d, $J = 8.5$ Hz, 2H, Ar-*H*), 3.04 (m, 1H, *PCHMe*₂), 2.56 (m, 1H, *PCHMe*₂), 2.20 (s, 3H, Ar-*Me*), 2.15 (s, 3H, Ar-*Me*), 2.08 (m, 1H, *PCHMe*₂), 2.00 (m, 1H, *PCHMe*₂), 1.46 (overlapping dd, $J = 6.5$ Hz, $J = 15$ Hz, 6H, *PCHMe*₂), 1.35 (dd, $J = 7.5$ Hz, $J = 14$ Hz, 3H, *PCHMe*₂), 1.19 (overlapping signals, 9H, *PCHMe*₂), 1.01 (dd, $J = 15$ Hz, $J = 7$ Hz, 3H, *PCHMe*₂), 0.92 (dd, $J = 16$ Hz, $J = 6.5$ Hz, 3H, *PCHMe*₂), -13.67 (ddd apparent dt, $J = 26$ Hz, $J = 12$ Hz, 1H, Rh-*H*), -18.33 (ddd apparent dt, $J = 29$ Hz, $J = 11$ Hz, 1H, Rh-*H*).

5.3.5 X-ray Crystallography

X-ray data collection, solution, and refinement for (PNP)Rh(Ph)(ZnPh) (504). A dark red, multi-faceted block of suitable size (0.24 x 0.14 x 0.11 mm) was selected from a representative sample of crystals of the same habit using an optical microscope and mounted onto a nylon loop. Low temperature (110 K) X-ray data were obtained on a Bruker APEXII CCD based diffractometer (Mo sealed X-ray tube, $K_{\alpha} = 0.71073$ Å). All diffractometer manipulations, including data collection, integration and scaling were carried out using the Bruker APEXII software.²⁸¹ An absorption correction was applied using SADABS.²⁸² The space group was determined on the basis of systematic absences and intensity statistics and the structure was solved by direct methods and refined by full-matrix least squares on F^2 . The structure was solved in the

monoclinic C c space group using XS²⁸³ (incorporated in SHELXLE). All non-hydrogen atoms were refined with anisotropic thermal parameters. All hydrogen atoms were placed in idealized positions and refined using riding model. The structure was refined (weighted least squares refinement on F^2) and the final least-squares refinement converged. Twin was found by using TwinRotMat incorporated in PLATON program with a twin matrix of -1 0 0 0 -1 0 1 0 1 and a BASF number of 0.07, which refined to 0.12 as final refinement.²⁸⁴

X-ray data collection, solution, and refinement for [(PNP)Rh(Ph)]₂(μ -Zn) (505). An orange, multi-faceted plate of suitable size (0.30 x 0.17 x 0.03 mm) was selected from a representative sample of crystals of the same habit using an optical microscope and mounted onto a nylon loop. Low temperature (110 K) X-ray data were obtained on a Bruker APEXII CCD based diffractometer (Mo sealed X-ray tube, K_{α} = 0.71073 Å). All diffractometer manipulations, including data collection, integration and scaling were carried out using the Bruker APEXII software.²⁸¹ An absorption correction was applied using SADABS.²⁸² The space group was determined on the basis of systematic absences and intensity statistics and the structure was solved by direct methods and refined by full-matrix least squares on F^2 . The structure was solved in the monoclinic P 2₁/c space group using XS²⁸³ (incorporated in SHELXLE). All non-hydrogen atoms were refined with anisotropic thermal parameters. All hydrogen atoms were placed in idealized positions and refined using riding model. The structure was refined (weighted least squares refinement on F^2) and the final least-squares refinement converged. No additional symmetry was found using ADDSYM incorporated in

PLATON program.²⁸⁴ The SQUEEZE protocol included in PLATON was used to account for disordered solvent molecules found in the crystal lattice that could not be satisfactorily modeled.²⁸⁵

X-ray data collection, solution, and refinement for [(PNP)Rh(H)]₂[μ-ZnCl₄] (507). A purple, multi-faceted block of suitable size (0.21 x 0.12 x 0.11 mm) was selected from a representative sample of crystals of the same habit using an optical microscope and mounted onto a nylon loop. Low temperature (110 K) X-ray data were obtained on a Bruker APEXII CCD based diffractometer (Cu sealed X-ray tube, $K_{\alpha} = 1.54178 \text{ \AA}$). All diffractometer manipulations, including data collection, integration and scaling were carried out using the Bruker APEXII software.²⁸¹ An absorption correction was applied using SADABS.²⁸² The space group was determined on the basis of systematic absences and intensity statistics and the structure was solved by direct methods and refined by full-matrix least squares on F^2 . The structure was solved in the monoclinic P 2₁/c space group using XS²⁸³ (incorporated in SHELXLE). All non-hydrogen atoms were refined with anisotropic thermal parameters. All hydrogen atoms were placed in idealized positions and refined using riding model. Hydrogen atoms on Rh could not be located from difference Fourier maps and were removed. The structure was refined (weighted least squares refinement on F^2) and the final least-squares refinement converged. No additional symmetry was found using ADDSYM incorporated in PLATON program.²⁸⁴ The SQUEEZE protocol included in PLATON was used to account for disordered solvent molecules found in the crystal lattice that could not be satisfactorily modeled.

CHAPTER VI
SYNTHESIS OF FLUOROCARBYENE, FLUOROOLEFIN, AND
FLUOROCARBYNE COMPLEXES OF RHODIUM*

6.1 Introduction

Organofluorine chemistry's major impact on the world of industrial chemistry has inspired many investigations into the unique properties that are inherent to molecules and materials containing C-F bonds. Transition metal complexes containing perfluorocarbon ligands are an important subset of these studies since they exhibit distinctive bonding properties²⁸⁶ and can mediate perfluoroalkyl-carbon bond forming processes.^{286,287} Group 9 perfluoroalkylidenes have garnered interest in the past decade after Hughes developed a simple reductive method for making Ir=CFR complexes (Figure VI-1, top) from iridium-fluoroalkyl precursors.²⁸⁸ These complexes have been analyzed in the context of their potential intermediacy in perfluoroolefin metathesis,²⁸⁹ and more recently the Baker group has shown that analogous cobalt perfluorocarbenes (Figure VI-1, top)²⁹⁰ are capable of undergoing a [2+1] cycloaddition with :CF₂²⁹¹ and [2+2] cycloaddition with C₂F₄.²⁹² Analogous chemistry was also reported for a difluorocarbene complex of Ni(0).²⁹³ Baker has also shown that cationic cobalt (III)

* Reproduced in part from "Fluorocarbene, fluoroolefin, and fluorocarbyne complexes of Rh." Pell, C. J.; Zhu, Y.; Huacuja, R.; Herbert, D. E.; Hughes, R. P.; Ozerov, O. V. *Chem. Sci.* **2017**, 8, 3178 with the permission of the Royal Society of Chemistry. DOI: 10.1039/C6SC05391B

difluorocarbenes could undergo migratory insertion into perfluoroalkyl ligands, possibly providing a blueprint for transition metal catalyzed perfluoroolefin polymerization.²⁹⁴

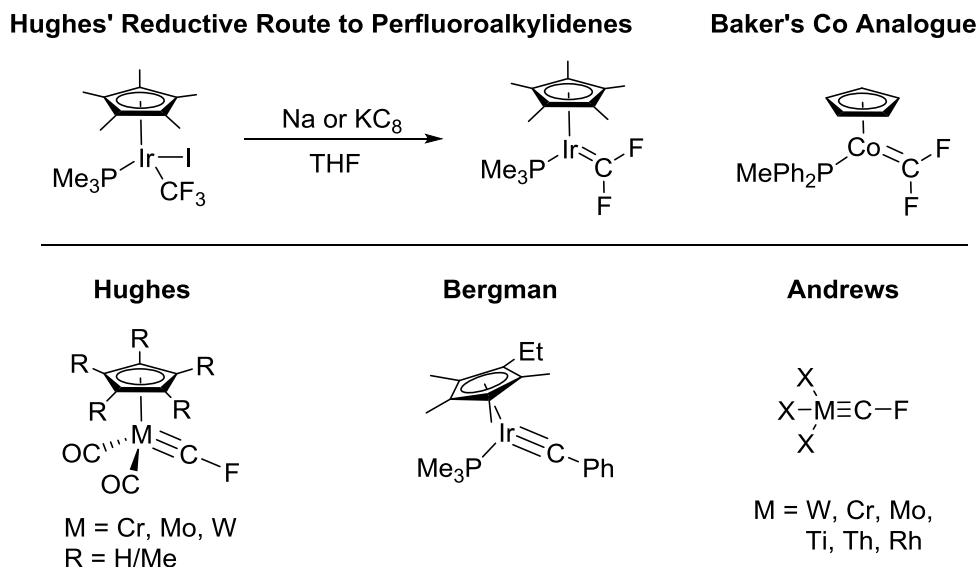


Figure VI-1. Perfluoroalkylidenes from Hughes and Baker. Isolated fluorocarbyne by Hughes, the iridium carbyne by Bergman, and matrix-trapped fluorocarbynes by Andrews.

The only family of isolable terminal fluoromethylidyne complexes known to date are the $\text{Cp}^*\text{M}(\text{CO})_2(\text{CF})$ compounds (M = Cr, Mo, W) reported by Hughes and co-workers (Figure VI-1, bottom).²⁹⁵ The Andrews group has reported a number of fluoromethylidyne complexes of the general formula $\text{X}_3\text{M}(\text{CF})$ (Figure VI-1, bottom; X = halogen) via trapping laser ablated metal atoms in argon/halocarbon matrices at ca. 10 K.²⁹⁶ Most of the isolable terminal carbyne complexes are complexes of metals of groups 6,^{297,298} 7,^{298,299} and 8.^{300,301} A few examples are known for group 5.³⁰² In group 9, one 18-electron complex has been fully characterized for Ir by Bergman et al. (Figure

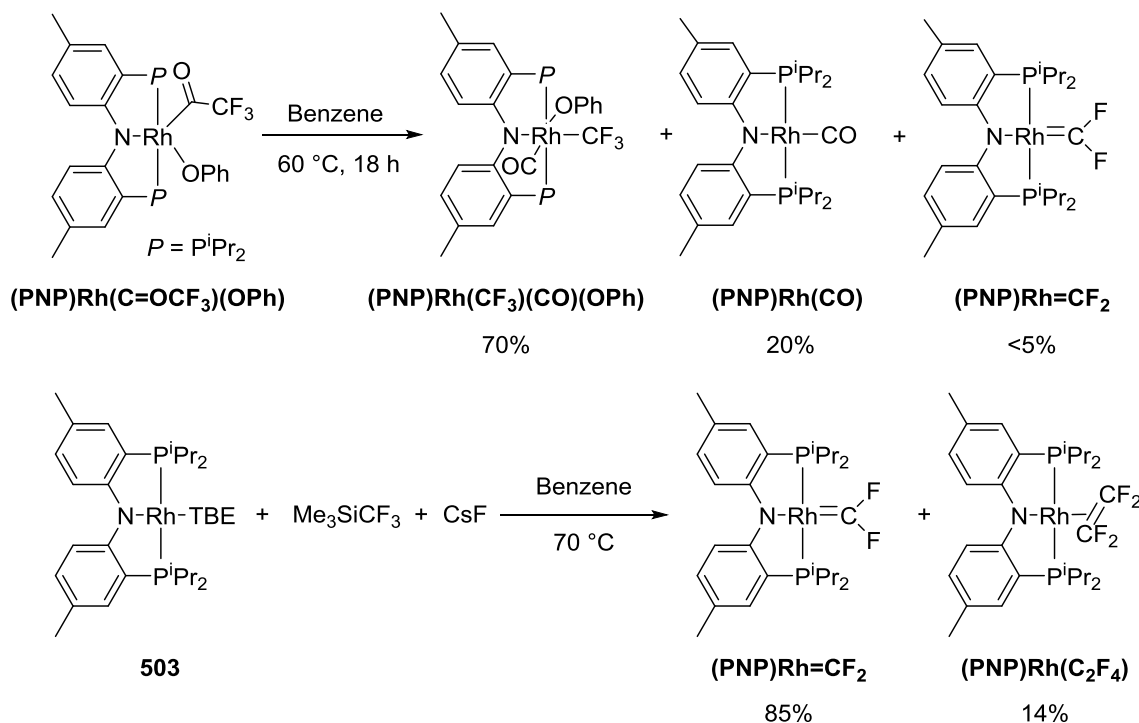
VI-1, bottom),³⁰³ and one square planar 16-electron complex was mentioned in passing for Rh by Werner et al.,³⁰⁴ as a component of a reaction mixture. The “concentration” of metal carbyne complexes in the middle of the transition metal series can be compared with similar trends for other metal-element multiple bonds.^{305,306} Discussed within this chapter is the synthesis, characterization, and analysis of electronic structure of a rare cationic fluoromethyldiene complex of Rh, as well as related Rh perfluoroalkylidene complexes. All computations were performed by Dr. Russell P. Hughes.

6.2 Results and Discussion

6.2.1 Synthesis of CF_2 , C_2F_4 , and CF_2CF_3 Complexes

Graduate student Yanjun Zhu from our group reported in 2011 reactions of the (PNP)Rh fragment with aryl carboxylates, including aryl-oxygen oxidative addition.³⁰⁷ The (PNP)Rh acyl-oxygen oxidative addition product of phenyl trifluoroacetate, **(PNP)Rh(C=OCF₃)(OPh)**, could be thermalized to produce **(PNP)Rh(CO)** and **(PNP)Rh(CF₃)(CO)(OPh)** as major products (Scheme VI-1). During this work, Yanjun noted that some other unidentified products were evident in trace amounts. One particular trace product was consistently observed in 2-5% yield. For it, a doublet of triplets was observed both in the ³¹P{¹H} NMR and ¹⁹F NMR spectra (coupling constants: ¹J_{Rh-P} = 146 Hz, ²J_{Rh-F} = 49 Hz, ³J_{P-F} = 30 Hz). These multiplicities implied a P₂RhF₂ NMR spin system – rather unexpected given the *three* fluorines in the CF₃ group of the starting material. It was noted that the ¹⁹F NMR chemical shift was itself uncommon (95.6 ppm) and in the range reported for various difluorocarbene complexes

(i.e., $M=CF_2$).^{290,295a,308,309} The observed $^2J_{Rh-F} = 49$ Hz was also similar to that of Grushin's *trans*-(Ph_3P)₂(F)Rh=CF₂, which possessed a $^2J_{Rh-F}$ of 33 Hz.³⁰⁸



Scheme VI-1. Initial observation of $(PNP)Rh=CF_2$, and synthesis of $(PNP)Rh=CF_2$ initially performed by Yanjun Zhu.

Yanjun hypothesized that this minor side product might be $(PNP)Rh=CF_2$ and attempted an independent synthesis of it based on the procedure of Grushin et al. that yielded *trans*-(F)(PPh_3)₂Rh=CF₂.³⁰⁸ Indeed, treatment of $(PNP)Rh(TBE)$ (**503**) (TBE = tert-butylethylene) with CsF/ Me_3SiCF_3 (Rupert's reagent) resulted in complete consumption of **503** and the formation of $(PNP)Rh=CF_2$ and $(PNP)Rh(C_2F_4)$ in about

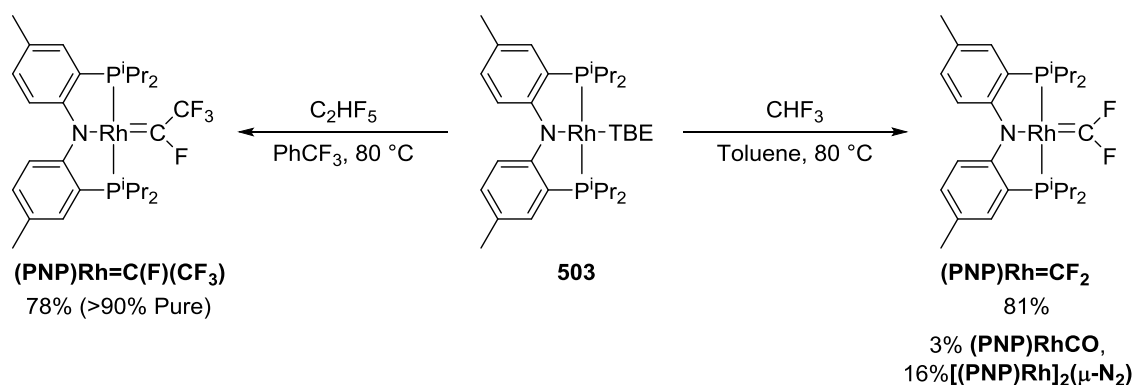
85:15 ratio as observed by NMR spectroscopy (Scheme VI-1).* **(PNP)Rh=CF₂** could be isolated in 52% yield and of >98% purity by recrystallization. The ³¹P{¹H} NMR and ¹⁹F NMR spectra of **(PNP)Rh=CF₂** so obtained were identical to that of the impurity we observed in the reaction in Scheme VI-1.

503 showed no reaction with Me₃SiCF₃ alone. Similar to the other cases of use of CsF/Me₃SiCF₃, we propose that these reagents generate a CF₃ anion equivalent that displaces TBE and then loses fluoride, resulting in the formal transfer of CF₂ to Rh. Alternatively, CsF/Me₃SiCF₃ could be generating free CF₂ which then binds to Rh. Using the CsF/Me₃SiCF₃ protocol, we could not avoid the formation of **(PNP)Rh(C₂F₄)** due to the generation of free C₂F₄ from the CsF/Me₃SiCF₃ mixture. C₂F₄ was observed by ¹⁹F NMR spectroscopy in control experiments where CsF and Me₃SiCF₃ were mixed in C₆D₆ and heated at 80 °C. No reaction was observed when **(PNP)Rh=CF₂** was treated with another equivalent of CsF/Me₃SiCF₃. This contrasts the reactivity of Baker's difluorocarbene cobalt (I) complexes²⁹¹ which undergo a [2+1] cycloaddition with free :CF₂ to form cobalt tetrafluoroethylene complexes.

To date, we have not been able to formulate a reasonable proposal for how **(PNP)Rh=CF₂** could be formed from **(PNP)Rh(COCF₃)(OPh)** (Scheme VI-1). The formation of M=CF₂ by fluoride migration from M-CF₃ is well precedented and is likely the key step in forming **(PNP)Rh=CF₂**; the difficulty is with conceiving of a plausible fate for the other atoms of the original phenyl trifluoroacetate molecule.

* **(PNP)Rh(CO)** accounted for approximately 1% of the reaction mixture.

Goldman et al. documented formation of (PCP)Ir=CF₂ in a reaction of a (PCP)Ir source with HCF₃.³⁰⁹ This reaction proceeded via C-H oxidative addition of HCF₃ to Ir followed by loss of HF. In a similar vein, we found that **503** reacted with HCF₃ at 80 °C to provide a mixture of compounds containing (PNP)Rh=CF₂ as a major product (>80%) with (PNP)Rh(CO) and [(PNP)Rh]₂(μ-N₂) as minor products (Scheme VI-2). Commercial HCF₃ contains dinitrogen as an impurity. Hydrolysis of a difluorocarbene complex to a carbonyl complex has precedent,³¹⁰ but attempts to purposefully hydrolyze (PNP)Rh=CF₂ proved to be unsuccessful, reminiscent of Baker's cobalt fluorocarbene complexes.²⁹⁰ It is possible that hydrolysis of (PNP)Rh=CF₂ only takes place in the presence of HF (a by-product of (PNP)Rh=CF₂ generation). We observed no intermediates* in the reaction of **503** with HCF₃, which may indicate that dissociation of TBE²⁷¹ is the rate-limiting step.

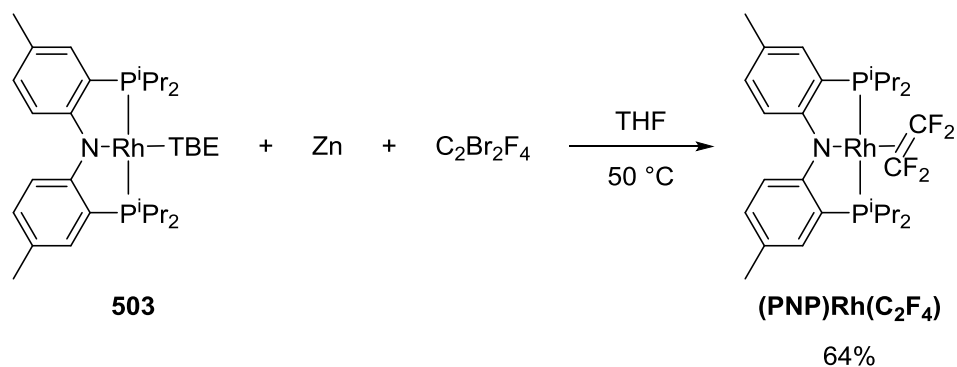


Scheme VI-2. Reactions of **503** with pentafluoroethane and fluoroform to synthesize perfluoroalkylidnes.

* We do not observe the HF by-product spectroscopically, but it is possible it is consumed by a reaction with borosilicate glass.

An analogous reaction of **503** with C_2HF_5 was attempted as a potential means to access $(PNP)Rh(C_2F_4)$. However, the major product of this reaction turned out to be a tetrafluoroethylidene complex $(PNP)Rh=C(F)(CF_3)$ (Scheme VI-2). Dinitrogen impurity in C_2HF_5 led to the known $[(PNP)Rh]_2(\mu-N_2)$ as a major side product, whose content could be reduced by degassing C_2HF_5 using the “freeze-pump-thaw” technique. $(PNP)Rh=CF_2$ was also observed as a side product composing 13% of the reaction mixture when **503** was treated with 2 atm of C_2HF_5 and heated overnight at 80 °C. $(PNP)Rh=C(F)(CF_3)$ could be isolated in >90% purity with $(PNP)Rh(CO)$ composing the rest of the mixture.

The synthesis of $(PNP)Rh(C_2F_4)$ was instead accomplished by thermolysis of **503** in a solution containing C_2F_4 which was generated *in situ* by reducing $C_2F_4Br_2$ with 1.5 eq. of Zn powder at 50 °C in THF. $(PNP)Rh(C_2F_4)$ was isolated in 64% yield as a pure solid (Scheme VI-3).



Scheme VI-3. Synthesis of $(PNP)Rh(C_2F_4)$.

The presence of multiple NMR-active nuclei provided for information-rich NMR spectra of **(PNP)Rh=CF₂**, **(PNP)Rh=C(F)(CF₃)**, and **(PNP)Rh(C₂F₄)**. All three complexes displayed C_{2v}-symmetric NMR spectra in solution at ambient temperature. The carbene complexes **(PNP)Rh=CF₂** and **(PNP)Rh=C(F)(CF₃)** displayed characteristic ¹³C NMR resonances at 206.3 and 225.0 ppm. In the CF₂ complex the observation that the two fluorines couple identically to both phosphorus nuclei, and vice versa, is consistent with rapid rotation about the Rh=CF₂ bond on the NMR timescale at room temperature. Likewise the observation of identical coupling of both P-nuclei to all four fluorines in the C₂F₄ complex is consistent with rapid rotation about the Rh-alkene bond axis. Small energy barriers to these rotations are calculated by DFT (*vide infra*).

The identity of **(PNP)Rh=CF₂** and **(PNP)Rh(C₂F₄)** was confirmed by X-ray diffraction studies on suitable single crystals (Figure VI-2). Treating the CF₂ or C₂F₄ ligands as occupying a sole coordination site, the coordination environment about Rh is approximately square planar in both molecules. The CF₂ unit in **(PNP)Rh=CF₂** lies approximately in that plane, while the C-C vector of the C₂F₄ ligand in **(PNP)Rh(C₂F₄)** is approximately perpendicular to it. The CF₂ and C₂F₄ ligands evidently exert similar *trans*-influence as the Rh-N distances in **(PNP)Rh=CF₂** and **(PNP)Rh(C₂F₄)** are only different by ca. 0.01 Å. In general, the metrics of the Rh=CF₂ unit in **(PNP)Rh=CF₂** are very similar to the Rh=CF₂ unit in *trans*-(Ph₃P)₂(F)Rh=CF₂. The structures of **(PNP)Rh=CF₂** and **(PNP)Rh(C₂F₄)** contain some close C-F...H contacts (C-F...H distances of 2.33-2.45) (F...C distances of 3.1-3.3 Å). While they are probably unavoidable in these molecules, these distances are short enough to be considered weak

F...H interactions.³¹¹ C-F...H interactions have been observed in pincer-ligated zirconium complexes bearing a trifluoromethyl as a pendant group, which have also exhibited through-space H-F coupling visible in their ¹H NMR spectra.³¹² However **(PNP)Rh(C₂F₄)** and **(PNP)Rh=CF₂** showed no through-space ¹⁹F-¹H coupling to the isopropyl arms.

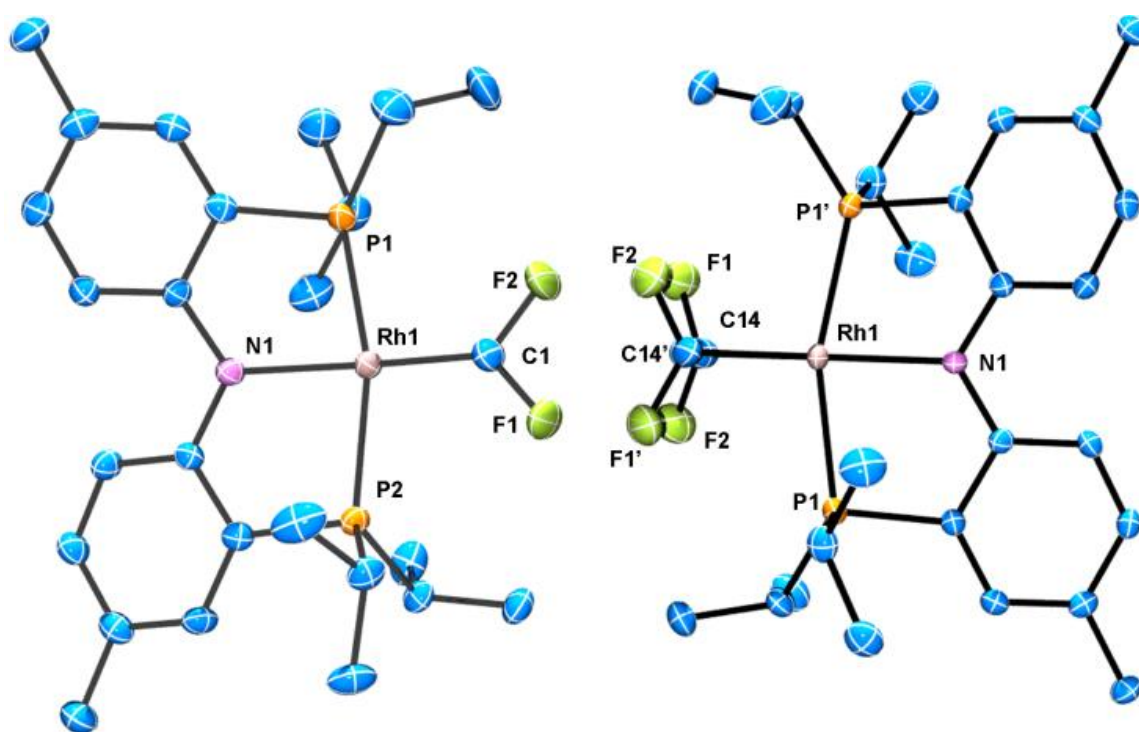


Figure VI-2 ORTEPs of **(PNP)Rh=CF₂** (left) and **(PNP)Rh(C₂F₄)** (right). The ellipsoids are set at the 50% probability level, and hydrogen atoms are omitted for clarity. Selected bond distances (Å) and angles (°) for **(PNP)Rh=CF₂**: Rh1–C1, 1.821(4); Rh1–N1, 2.043(3); C1–F1, 1.335(4); C1–F2, 1.348(5); N1–Rh–C1, 171.39(15); F2–C1–F1, 100.8(3); Rh1–C1–F2, 130.1(3); Rh1–C1–F1, 128.6. **(PNP)Rh(C₂F₄)**: Rh1–C14, 2.006(3); Rh1–N1, 2.054(3); C14–F1, 1.378(3); C14–F2, 1.361(3); C14–C140, 1.354(7); C14–Rh–C140, 39.4(2); C14–Rh–N1, 160.28(10). XRD structures solved by David Herbert.

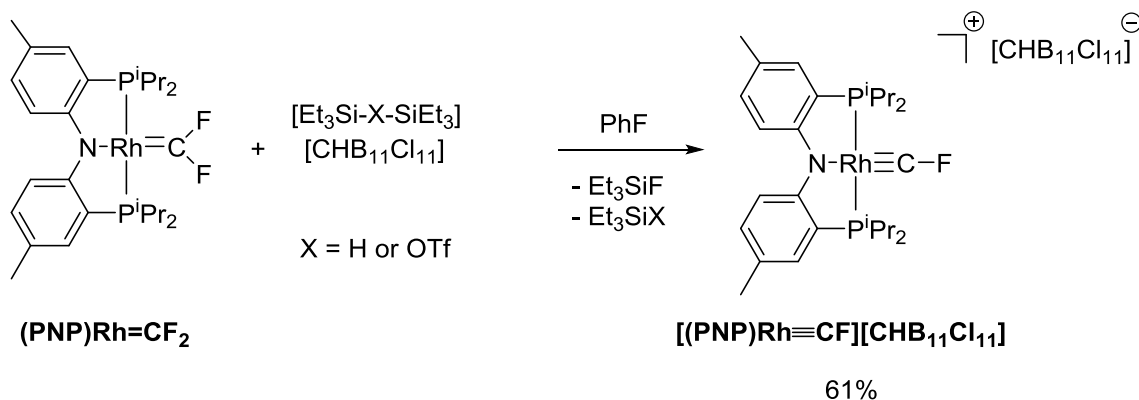
6.2.2 Synthesis of Cationic Fluoromethylidyne

With compounds **(PNP)Rh=CF₂**, **(PNP)Rh=C(F)(CF₃)**, and **(PNP)Rh(C₂F₄)** in hand, we contemplated whether one of the fluorides could be removed to yield cationic C_xF_y complexes. Hughes et al. previously demonstrated proton-induced loss of fluoride from α -positions of Ir perfluoroalkyls,^{288a} and Baker recently demonstrated a Lewis-acid abstraction of a fluoride from N-heterocyclic fluoroalkenes to yield polyfluoroalkenyl imidazolium salts.³¹³ There is significant precedent for electrophilic abstraction of an anionic heteroatom substituent from late-metal carbene complexes by a Lewis acid.^{303,314} Trialkylsilylium cations, in the form of their salts with halogenated carborane anions, are powerful Lewis acids with high affinity for fluoride.³¹⁵ We and others have exploited them in catalytic C-F activation reactions³¹⁶ and thus a [R₃Si]⁺ reagent appeared perfect for fluoride abstraction.

Reactions of **(PNP)Rh=CF₂**, **(PNP)Rh(C₂F₄)**, and **(PNP)Rh=C(F)(CF₃)** with **[Et₃Si-H-SiEt₃][HCB₁₁Cl₁₁]**³¹⁷ or **[(Et₃Si)₂OTf][HCB₁₁Cl₁₁]**³¹⁸ all generated the Et₃SiF by-product, indicating that fluoride abstraction took place in all three cases. However, reactions of **(PNP)Rh(C₂F₄)** and **(PNP)Rh=C(F)(CF₃)** resulted in mixtures of several products as seen by ¹⁹F NMR spectroscopy and typically broad or no signals were observed by ³¹P{¹H} NMR spectroscopy. The reaction mixtures produced from the reaction of **(PNP)Rh(C₂F₄)** or of **(PNP)Rh=C(F)(CF₃)** with **[(Et₃Si)₂OTf][HCB₁₁Cl₁₁]** did regenerate the corresponding starting material when treated with CsF. This indicates that fluoride abstraction from these two isomeric complexes generates isomers of **[(PNP)Rh(C₂F₃)]⁺** that do not interconvert on the experimental time scale. Although we

were not able to identify these compounds experimentally, DFT computational studies were used to investigate possible structures of the $[(\text{PNP})\text{Rh}(\text{C}_2\text{F}_3)]^+$ isomers (*vide infra*).

On the other hand, reaction of $(\text{PNP})\text{Rh}=\text{CF}_2$ with $[\text{Et}_3\text{Si}-\text{H}-\text{SiEt}_3][\text{HCB}_{11}\text{Cl}_{11}]$ cleanly and reproducibly generated a new Rh complex that displayed a P_2RhF NMR spin system (Scheme VI-4). The key NMR spectroscopic features of this compound were the unusual ^{19}F NMR chemical shift (66.2 ppm), the very high $^1J_{\text{C-F}}$ coupling constant of 470 Hz,^{*} and the rather substantial $^2J_{\text{Rh-F}} = 136$ Hz.



Scheme VI-4. Synthesis of $(\text{PNP})\text{RhCF}^+$ via fluoride abstraction. Initially performed by Yanjun Zhu.

These spectroscopic data are similar to those exhibited by $\text{Cp}^*(\text{CO})_2\text{Mo}\equiv\text{CF}$, whose ^{19}F NMR spectrum contained a singlet at 78.15 ppm, with a large $^1J_{\text{C-F}}$ coupling

^{*} $^1J_{\text{C-F}}$ coupling constant was determined in an experiment using $[\text{BArF}_{20}]^-$ as a counter anion for $[(\text{PNP})\text{Rh}\equiv\text{CF}]^+$. This particular experiment was performed by Rafael Huacuja.

constant of 556 Hz evident by ^{13}C NMR spectroscopy.^{295a} Hughes's other $\text{Cp}(\text{CO})_2\text{M}\equiv\text{CF}$ ($\text{M} = \text{Cr}, \text{W}$) complexes also exhibited ^{19}F NMR chemical shifts in this region with high $J_{\text{C-F}}$ coupling constants.^{295b} Due to limited solubility in non-interactive solvents and the extensive coupling inherent to the fluoromethylidyne ^{13}C NMR resonance in $[(\text{PNP})\text{Rh}\equiv\text{CF}]^+$, it was not observed by $^{13}\text{C}\{^{31}\text{P}\}$, $^{13}\text{C}\{^1\text{H}\}$, nor $^{13}\text{C}\{^{19}\text{F}\}$ NMR spectroscopy.

X-ray quality crystals of $[(\text{PNP})\text{Rh}\equiv\text{CF}][\text{HCB}_{11}\text{Cl}_{11}]$ were studied using X-ray diffraction to yield a structure fully supportive of a fluorocarbyne formulation (Figure VI-3). The structural and NMR spectroscopic features of $[(\text{PNP})\text{Rh}\equiv\text{CF}]^+$ are best

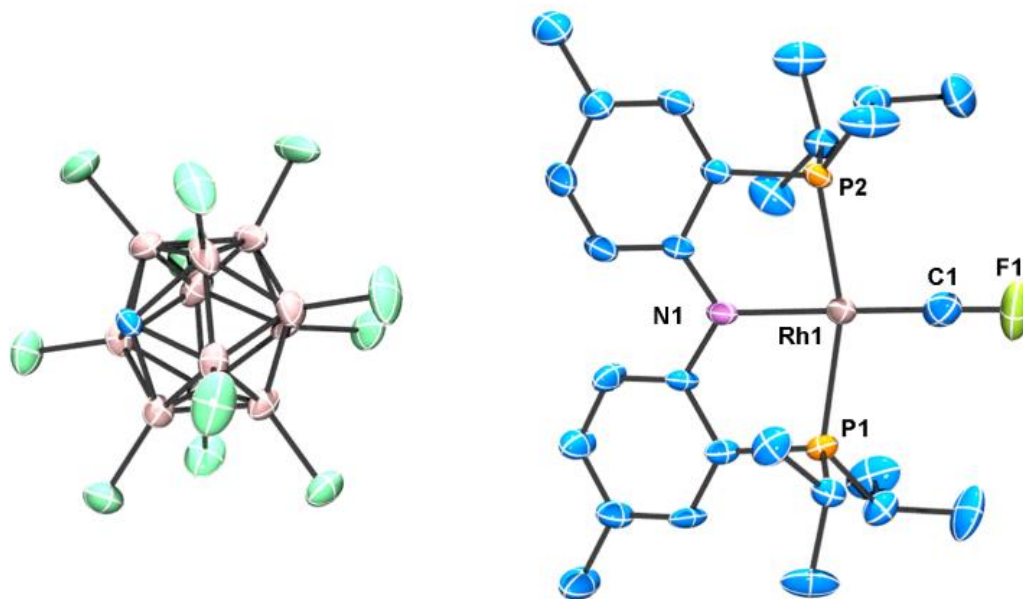


Figure VI-3. ORTEP of $[(\text{PNP})\text{Rh}\equiv\text{CF}][\text{HCB}_{11}\text{Cl}_{11}]$. The ellipsoids are set at the 50% probability level, and hydrogen atoms are omitted for clarity. Selected bond distances (Å) and angles ($^\circ$): Rh1–C1, 1.702(7); Rh1–N1, 2.019(4); C1–F1, 1.257(8); C1–Rh1–N1, 174.1(3); F1–C1–Rh1, 173.4(7). XRD Structure solved by David Herbert.

reviewed in comparison with $\text{Cl}_3\text{Rh}\equiv\text{CF}$ and a few other relevant compounds. Andrews et al. observed IR spectroscopic evidence for $\text{Cl}_3\text{Rh}\equiv\text{CF}$ in reactions of laser-ablated rhodium atoms with CFCl_3 . A DFT calculation of this product predicted a Rh-C bond length of 1.740 Å and a Rh-C-F bond angle of 143.4°. ^{296d} This compares with our observed Rh-C bond length of 1.702(7) Å and a Rh-C-F bond angle of 173.46°. Although both $[(\text{PNP})\text{Rh}\equiv\text{CF}]^+$ and $\text{Cl}_3\text{Rh}\equiv\text{CF}$ are four-coordinate, they contain different numbers of valence electrons: from a hypothetical point of view of a $[\text{CF}]^+$ ligand, it is attached to a d^8 Rh center in $[(\text{PNP})\text{Rh}\equiv\text{CF}]^+$, but to a d^7 $[\text{Cl}_3\text{Rh}]^-$ fragment in $\text{Cl}_3\text{Rh}\equiv\text{CF}$. The geometry of the RhCF unit in $[(\text{PNP})\text{Rh}\equiv\text{CF}]^+$ is similar to Bergman's iridium carbyne complex (Figure VI-1), which possesses an Ir-C bond length of 1.734(6) Å and an Ir-C-C bond angle of 175.7(4). ³⁰³ The Rh-C distance in $[(\text{PNP})\text{Rh}\equiv\text{CF}]^+$ is ca. 0.12 Å shorter than that in $(\text{PNP})\text{Rh}=\text{CF}_2$, consistent with the increase in the Rh-C bond order. The Rh-C bond distance in $[(\text{PNP})\text{Rh}\equiv\text{CF}]^+$ is also ca. 0.07 Å shorter than that in Werner's *trans*-(P^iPr_3)₂ClRh=C=C(Me)(H) square planar vinylidene complex. ³¹⁹

6.3 Computational Studies and Discussion*

6.3.1 DFT Structural Studies

Modern Density Functional Theory (DFT) is a powerful tool with which to examine electronic structures and bonding trends in organometallic compounds. ^{320,321} In addition, application of Natural Bond Orbital (NBO) ³²²⁻³²⁷ methods allows insight into

* All computational studies were performed by Professor Russell P. Hughes at Dartmouth College.

some of the subtleties of metal-ligand bonding.^{322,324,326} The NBO analysis also generates Wiberg Bond Indices (WBI),³²⁸ determined within the natural atomic orbital basis, providing one means of estimating bond orders between atoms. Trends in WBI values are also useful in tracking variations in bond multiplicities. The newly synthesized family of fluorocarbon complexes **(PNP)Rh(C₂F₄)**, **(PNP)Rh=CF₂**, and **[(PNP)Rh≡CF]⁺** prompted a computational comparison with their (hypothetical) hydrocarbon analogues **(PNP)Rh(C₂H₄)**, **(PNP)Rh=CH₂** and **[(PNP)Rh≡CH]⁺** in order to assess the effects of fluorination on the metal-carbon bonding, and, for the carbene and carbyne complexes, to probe the nature and extent of the multiple bonding between the metal and carbon. In addition, since the CF⁺ ligand is isoelectronic with the well-known ligands NO⁺ and CO, it was of interest to establish trends in metal ligand and intraligand bonding between **[(PNP)Rh≡CF]⁺**, **[(PNP)Rh(NO)]⁺**, and **(PNP)Rh(CO)**. Full molecule DFT studies were performed using the M06 functional^{329,330} and the triple- ζ LACV3P**++ basis set, which uses extended core potentials³³¹⁻³³⁴ on heavy atoms and a 6-311G**++ basis³³⁵⁻³³⁸ for other atoms, as implemented in the Jaguar^{339,340} suite of programs. Full details are available as Supplementary Information.

Selected bond lengths and computed WBI values for the calculated complexes are provided in Table VI-1, with metric comparisons to the available crystallographic structures reported here. The DFT calculated metrics are in good agreement with crystallographic numbers, giving confidence in the DFT metrics for the unknown complexes. One exception appears in **(PNP)Rh(C₂F₄)** in which the C-C distance for the coordinated alkene (1.354 Å) is only slightly longer than that in C₂F₄ itself (1.318 Å)³⁴¹

and is much shorter than all other transition metal complexes of this perfluoroalkene in the Cambridge Structure Database.³⁴² In contrast, the DFT calculated value (1.416 Å) is in good agreement with other crystallographically determined values³⁴² and is much more sensible with respect to calculated WBI values (see below).

Table VI-1. Calculated and crystallographic bond lengths (Å)^a and Wiberg Bond Indices^b (WBI) for (PNP)Rh compounds.

Compound	Rh-P _{ave}	Rh-N	Rh-C _{ave}	C-C	C-X _{ave} (ligand)
(PNP)Rh(C ₂ H ₄)	2.332 <i>0.462</i>	2.098 <i>0.378</i>	2.165 <i>0.453</i>	1.394 <i>1.474</i>	1.088 <i>0.930</i>
(PNP)Rh(C ₂ F ₄)	2.378 2.3309(11) <i>0.436</i>	2.100 2.054(3) <i>0.352</i>	2.048 2.006(3) <i>0.594</i>	1.416 1.354(7)^c <i>1.186</i>	1.346 1.369(3) <i>0.858</i>
(PNP)Rh=CH ₂	2.338 <i>0.476</i>	2.216 <i>0.225</i>	1.850 <i>1.250</i>	-	1.104 <i>0.955</i>
(PNP)Rh=CF ₂	2.331 2.302(12) <i>0.462</i>	2.156 2.043(3) <i>0.297</i>	1.864 1.821(4) <i>1.168</i>	-	1.325 1.341(5) <i>0.911</i>
[(PNP)Rh≡CH] ⁺	2.378 <i>0.440</i>	2.075 <i>0.332</i>	1.728 <i>1.714</i>	-	1.110 <i>0.942</i>
[(PNP)Rh≡CF] ⁺	2.384 2.337(16) <i>0.432</i>	2.061 2.019(4) <i>0.341</i>	1.740 1.702(7) <i>1.587</i>	-	1.247 1.257(8) <i>1.065</i>
[(PNP)Rh≡C-CF ₃] ⁺	2.384 <i>0.453</i>	2.054 <i>0.330</i>	1.734 <i>1.770</i>	-	1.499 <i>0.960</i>
(PNP)Rh(CO)	2.336 <i>0.462</i>	2.117 <i>0.291</i>	1.855 <i>1.041</i>	-	1.152 <i>2.031</i>
[(PNP)Rh(NO)] ⁺	2.393 <i>0.439</i>	2.019 <i>0.445</i>	1.778 (Rh-N) <i>1.151</i>	-	1.141 (NO) <i>1.917</i>
^a DFT calculated (M06/LACV3P**++) values are in plain text; X ray crystallographic values are in bold. ^b WBI values are in italics ^c This crystallographic value is questionable. See discussion in the text.					

All the complexes examined here can be formally viewed as square planar d^8 compounds, i.e., as complexes of a d^8 , three-coordinate fragment (PNP)Rh with neutral or cationic ligands. The NBO perspective of bonding interactions in such compounds^{322,326} requires 4-electron/3-center bonds between the pair of *trans* ligands such that the alkene, carbene, and carbyne ligands of interest are always involved in a shared bonding interaction with the N of the PNP pincer. Clearly contributions to this shared interaction may be weighted differently in each case, and the WBI values should reflect this.

6.3.2 Comparison of C_2H_4 and C_2F_4 Ligands

The bonding between alkenes and transition metal fragments is well understood,³⁴³ but a comparison between C_2H_4 and C_2F_4 coordinated to identical metal-ligand fragments is rare. A classic intramolecular example involves $CpRh(C_2H_4)(C_2F_4)$ ³⁴⁴ but the hydrocarbon and fluorocarbon alkenes are necessarily bound to different fragments in this molecule. Figure VI-4 illustrates the key Natural Localized Molecular Orbitals (NLMOs)^{322,325,326} arising from NBO calculations of interactions between C_2H_4 and C_2F_4 and the truncated^{*,345} (PNP)Rh fragment. The bonding orbitals (σ and π) are essentially localized on Rh and the alkene ligand, while the corresponding antibonding NLMOs show significant “tailing” involving the σ and π

* We refer to a PNP ligand in which the P^iPr_2 groups have been replaced by PMe_2 groups and the aryl part of the pincer replaced by P-CH=CH-N linkers as “truncated.” It was used in calculations from which the NLMO Figures were derived and for calculations of rotational barriers in the $C_2H_4/C_2F_4/CH_2/CF_2$ complexes. All other calculations used the full version of the ligand. The truncated PNP ligands has been previously used by Wu and Hall.

orbitals on the *trans*-N of the pincer ligand. This “tailing” is indicative of delocalization of these N electrons into the corresponding σ^* and π^* components of the Rh-alkene interaction; it is significantly greater for the σ^* component and corresponds to the 3-center/4-electron bonding expected between *trans*-ligands in a d^8 Rh(I) complex. The WBI values indicate significantly greater reduction in C-C bonding and increase in Rh-C

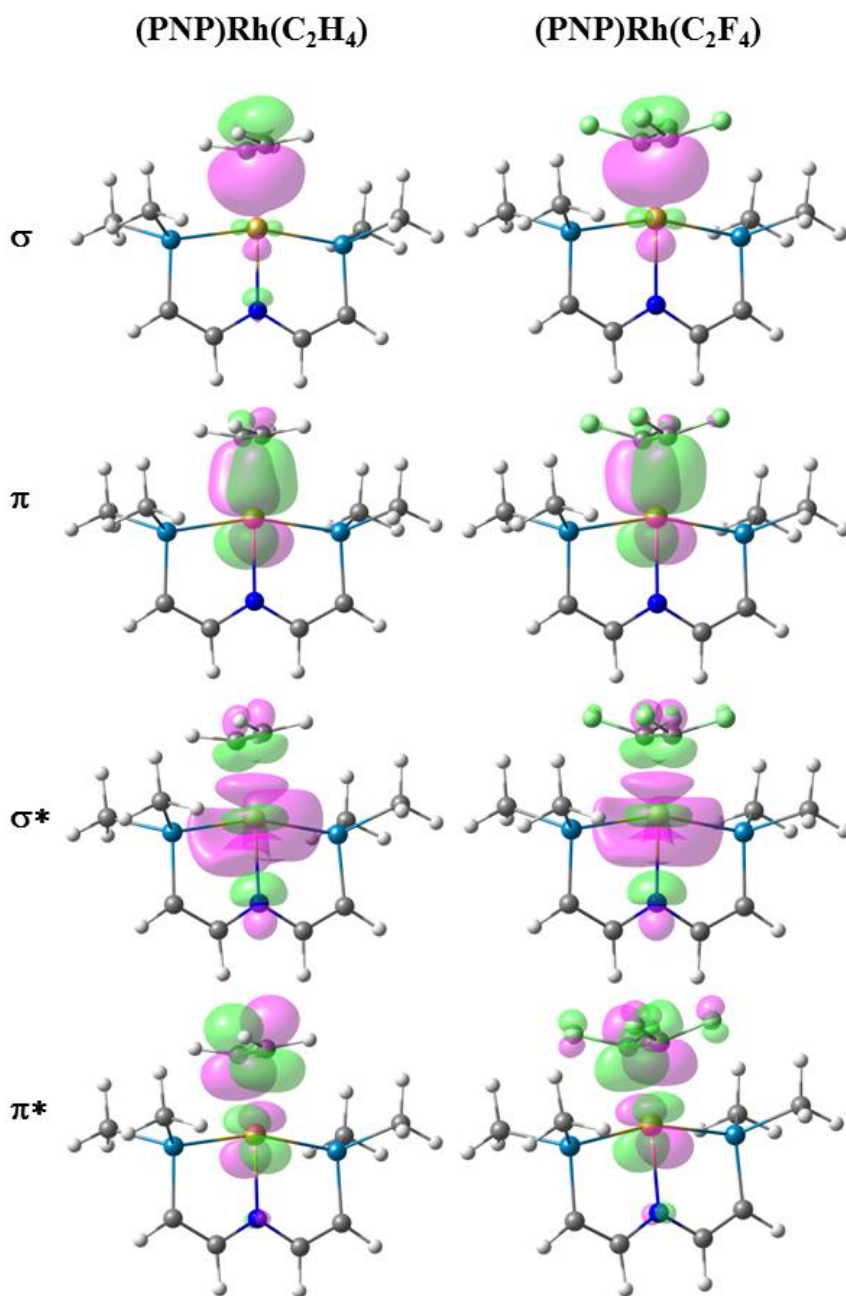


Figure VI-4. NLMOs for the bonding and antibonding interactions between C₂H₄ (column 1) and C₂F₄ (column 2) and the (PNP)Rh fragment. For clarity the PⁱPr₂ groups have been replaced by PMe₂ groups and the aryl part of the pincer truncated to P-CH=CH-N linkers.

bonding in coordinated C_2F_4 than in C_2H_4 . This is consistent with the shorter Rh-C distances and with the idea of a more metallacyclopropane structure and stronger Rh-C bonding for the fluorinated alkene complex. Not surprisingly, stronger bonding to the fluorinated alkene results in weaker bonding to the *trans* ligand, with correspondingly lower WBI values for the Rh-N bonds (Table VI-1). In the π^* -perp NMLO for the C_2F_4 there is also evidence for delocalization from F-lone pairs.

There are two Rh \rightarrow alkene backbonding options involving π^* -perp or π^* -inplane. Clearly the ground state conformation of the C_2F_4 complex utilizes the former, but the latter is available for an in-plane C_2F_4 conformation, leading to a low barrier for C_2F_4 rotation. Similar arguments for facile rotation of C_2F_4 ligands in Ru(II) complexes have been put forth elsewhere.³⁴⁶ The free energy profile for C_2F_4 rotation was calculated using a truncated* version of the PNP ligand (identical to that shown in Figure VI-4), and is unusual. Relative to the perpendicular conformation observed in the ground state there were two transition states located. The first, lying 7.1 kcal/mol above the ground state corresponds to a 45 degree rotation about the Rh-alkene bond axis, and the second, lying 8.7 kcal/mol above the ground state is the conformation in which the fluoroalkene lies in the coordination plane. Very shallow minima, higher in energy than the ground state, were observed between these transition states. These barriers are low enough in energy that rotation should be fast on the NMR timescale, consistent with the observed NMR data. The barriers contrast with those for the corresponding C_2H_4 analogue, for which the in-plane conformation is a minimum, lying only 0.4 kcal/mol above the

ground state, and the 45 degree conformation is a transition state lying 2.5 kcal/mol above the ground state.

6.3.3 Comparison of CH₂ and CF₂ Ligands

Figure VI-5 presents the corresponding NLMOs for the CF₂ and the CH₂ complex with a truncated* PNP ligand. These complexes are very similar except for the fluorine delocalizations into the π*-NLMO. The σ and π NLMOs are consistent with a formal double bond between Rh and the CF₂ (or CH₂) ligands, with the p-orbital on C and d-orbital on Rh providing the π-component. These NLMOs look essentially identical to those in Figure VI-4, except for a more significant delocalization of the fluorine lone pairs in the π*-perp NLMO. But now there is competition between the rhodium d-orbital and the fluorine lone pair p-orbitals for π-bonding with the carbene carbon, as expected; in (PNP)Rh=CH₂ only the metal can provide this π-bonding. Consequently π-bonding with fluorines diminishes π-bonding with Rh and, relative to the CH₂ complex, the Rh-C WBI decreases significantly and the Rh-C distance increases; notably the C-F WBI is greater than in the previously discussed C₂F₄ complex. In contrast to the alkene ligands discussed above there is overall weaker metal-carbon bonding to CF₂ than CH₂ and the corresponding *trans* Rh-N WBI value is larger for **(PNP)Rh=CF₂**.

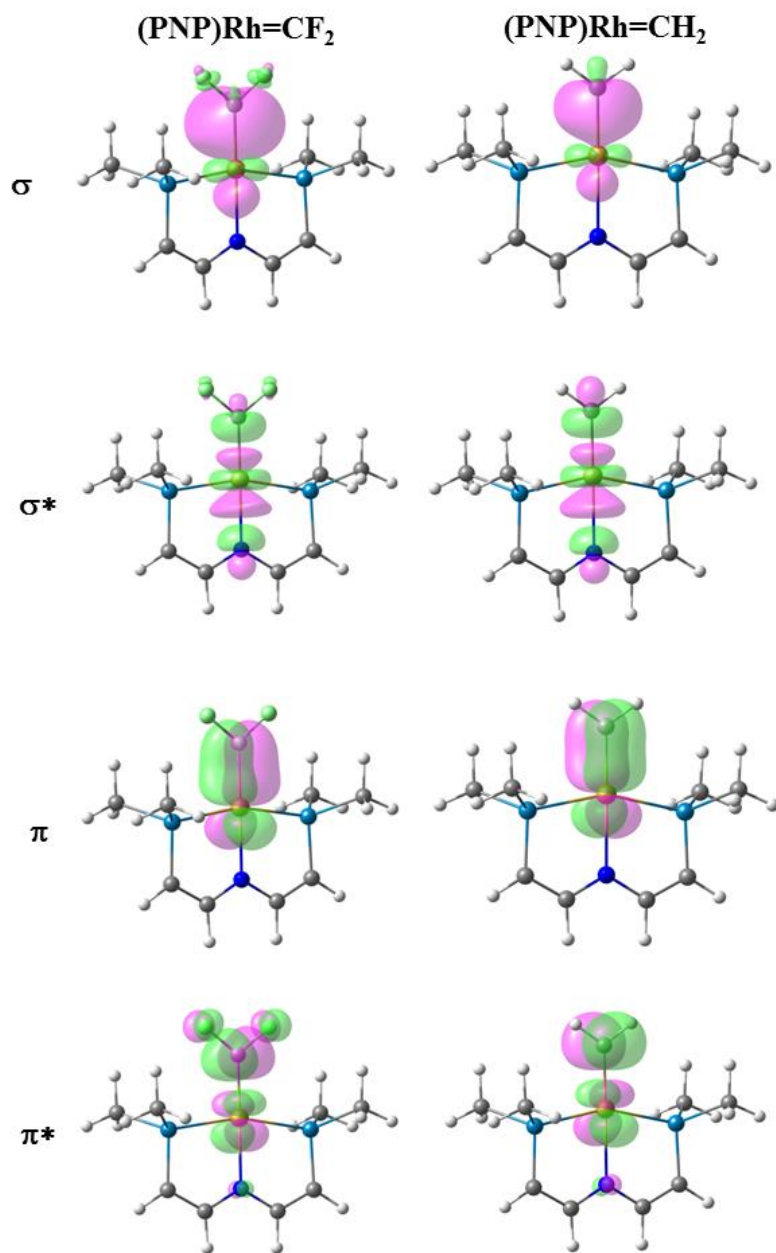


Figure VI-5. NLMOs for the bonding and antibonding interactions between the CF₂ ligand and the (PNP)Rh fragment (left) and for the CH₂ ligand and the (PNP)Rh fragment (right). For clarity the PⁱPr₂ groups have been replaced by PMe₂ groups and the aryl part of the pincer truncated to P-CH=CH-N linkers.

Facile CF₂ ligand rotation is expected due to the availability of the π*-perp and π*-inplane interactions. Calculations on the truncated* ligand analogue of the CF₂ complex reveal the same trend in conformational energetics observed for the C₂F₄ complex (*vide supra*). The in-plane CF₂ conformation, with the π*-perp interaction, is the ground state, with two transition states at 45 degree and 90 degree (perpendicular to the coordination plane) lying 2.0 and 4.8 kcal/mol higher in energy, respectively. Shallow minima were calculated between these transition states, which were higher in energy than the ground state conformation. The barriers are consistent with the experimental observation of fast rotation on the NMR timescale. In contrast, the rotation of the corresponding CH₂ ligand is even more facile, with the perpendicular, 45 degree and in-plane conformations lying at essentially equal energies.

6.3.4 Comparison of CH⁺, CF⁺, and CCF₃⁺ Ligands

Figure VI-6 presents the corresponding NLMOs for [(PNP)Rh≡CF]⁺. As with the carbene complexes, those for [(PNP)Rh≡CH]⁺ are similar except for enhanced “tailing” in the antibonding NLMOs for the CF⁺ complex. In contrast to the alkene and carbene complexes (*vide supra*) there is now a second fully engaged π-component for the Rh-C bond involving the in-plane d-orbital and a second p-orbital on the CF⁺ (or CH⁺) ligand. In the antibonding NLMOs we see the expected σ-donation from the trans-N in σ*, a small π-donation from *trans*-N in π*(perp), and a small donation from the Rh-P bonds in π*(in-plane). But once again the largest delocalizations in the π* NLMOs comes from the F lone pairs, interactions that cannot occur in [(PNP)Rh≡CH]⁺. Consequently the Rh-C WBI for [(PNP)Rh≡CH]⁺ is substantially larger than that for the

6.3.5 Degree of Rh-C Multiple Bonding

The Rh-C bonding in these carbene and carbyne complexes is inextricably linked to interactions with the *trans* N since there are necessarily shared bonding components between *trans* ligands, with additional complexities introduced by the fluorine substituents on carbon. So we cannot expect the Rh=CX₂ interaction to be a true double bond, or that in the cationic Rh≡CX to be a triple bond, even though we may draw resonance structures that reflect these prejudices. However, the WBI values for both Rh=CX₂ bonds (CH₂ 1.250; CF₂ 1.168) are significantly larger than unity, though not close to two, while those for the Rh≡CX cations are significantly larger still (CH 1.714; CF 1.587; CCF₃ 1.770), though not close to the bond order of three. Clearly there is significant multiple bonding between Rh and these unsaturated carbon ligands with higher bond orders to these ligands being reflected in lower bond orders to the *trans* N.

6.3.6 Comparison of CF⁺, NO⁺, and CO Ligands

The NLMOs for the CO and NO⁺ complexes are similar to those of the CF⁺ compounds discussed previously and are not shown here. Considering this series of isoelectronic complexes as involving a linear Rh-X-Y array the three resonance forms (**A**, **B**, **C**) for the contiguous π-system are shown in Figure VI-7, along with the WBI values for the appropriate bonds in the Rh-C-O, Rh-N-O and Rh-C-F complexes. The WBI values are consistent with progressively increased contributions of resonance forms **C**>**B**>**A** on changing the ligand from CO to NO⁺ to CF⁺, as expected from their relative π-acceptor abilities. Similar conclusions were reached for the fragments M(CO)₂(XY) [M = Cr, Mo, W; XY = CO, NO⁺, CF⁺] in a previous study.^{295b}

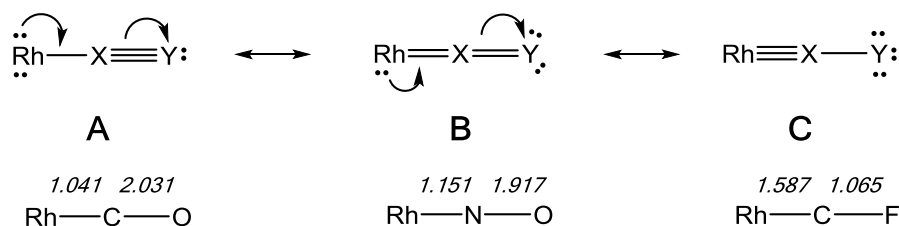


Figure VI-7. Resonance forms for the π -system in a linear Rh–X–Y ligand array, with WBI values for the bonds in Rh–C–O, Rh–N–O, and Rh–C–F complexes. All three complexes are isoelectronic and no formal charges are shown.

6.3.7 Relative Energies of Isomeric Fluorocarbon Ligands

It was of interest to compare the relative energies of the **(PNP)Rh(C₂F₄)** complex with its carbene isomer **(PNP)Rh=C(F)(CF₃)**. At the DFT/M06/LACV3P**++ level the free energy of the carbene isomer is found to be 2.4 kcal/mol uphill from its alkene analogue. Interestingly the carbene CFCF₃ ligand lies perpendicular to the (PNP)Rh plane, in contrast to the CF₂ analogue described above, presumably due to steric interactions between the CF₃ and the cis PR₂ groups.

Potential products arising from fluoride abstraction from these isomeric complexes were also subjected to DFT evaluation. Abstraction of fluoride from **(PNP)Rh=C(F)(CF₃)** could occur from the α -position to yield a carbyne complex **(PNP)Rh(CCF₃)⁺**, analogous to the characterized CF⁺ complex described above, or from the β -position to afford the corresponding isomeric η^1 -perfluorovinyl cation **(PNP)Rh(CF=CF₂)⁺**. These are found to have almost identical free energies, with the carbyne complex lying only 0.4 kcal/mol higher than its perfluorovinyl isomer. An η^2 -perfluorovinyl isomer, the potential initial product of fluoride abstraction from the

(PNP)Rh(C₂F₄) was found to lie 12.1 kcal/mol above its η^1 -perfluorovinyl analogue. Structures of all these compounds and their relative energies are provided in Figure VI-8.

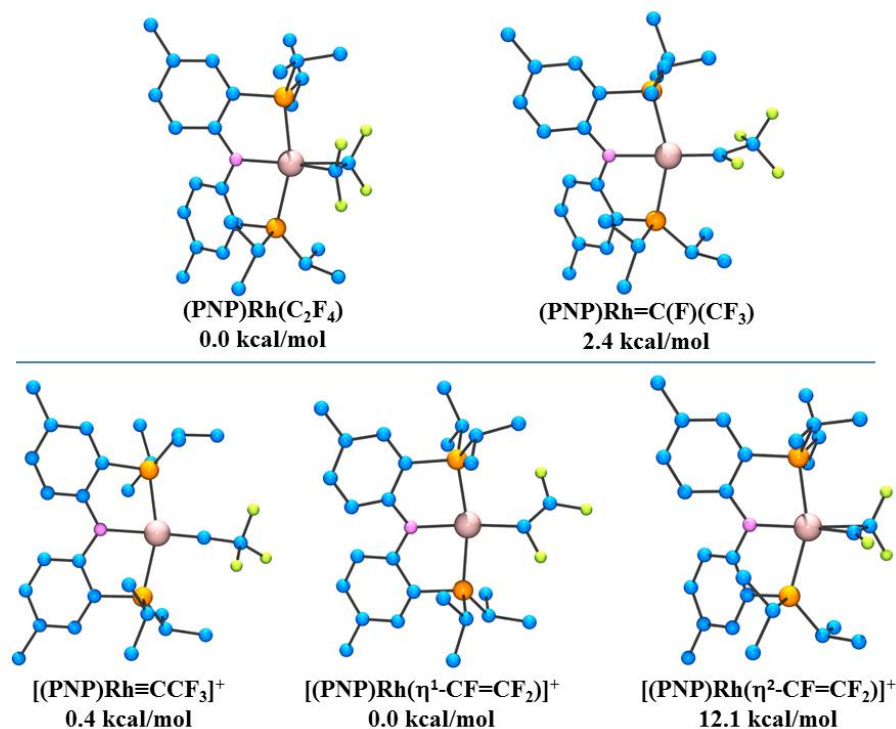


Figure VI-8. (Top) Calculated structures and relative energies for (PNP)Rh(C₂F₄) isomers. (Bottom) Calculated structures and relative energies for proposed structures resulting from fluoride abstraction from (PNP)Rh=C(F)(CF₃).

6.4 Conclusions

In summary, we have shown that (PNP)Rh perfluorocarbene complexes can be synthesized by treating a Rh(I) precursor with Rupert's reagent or a fluoroalkane containing a C-H bond. Using silylium reagents, a fluoride can be abstracted from (PNP)Rh=CF₂ to form a cationic fluoromethylidyne. Thus the (PNP)Rh system

conveniently allows synthesis and comparison of perfluoroolefin, perfluorocarbene, and perfluorocarbyne complexes. Using DFT calculations we were able to compare the Natural Localized Molecular Orbitals of these fluoroorganic complexes to their hypothetical hydrocarbon analogues. We established that the fluorine atoms on the carbene and carbyne ligands participate in π donation to the acceptor orbitals on carbon to compete with back donation from the metal. This resulted in a longer Rh-C bond in the fluorinated complexes compared to their hydrocarbon analogues. However, C_2F_4 was calculated to form a shorter Rh-C bond than the C_2H_4 complex. Calculated Wiberg Bond Indices also showed that although the unsaturated fluorocarbon ligands have bond orders greater than one to rhodium, the nitrogen *trans* to these ligands interacts with their antibonding orbital and decreases the bond order to less than a true double and triple bond.

6.5 Experimental

6.5.1 General Considerations

Unless specified otherwise, all manipulations were performed under an argon atmosphere using standard Schlenk line or glove box techniques. Toluene, pentane, and isooctane were dried and deoxygenated (by purging) using a solvent purification system by MBraun and stored over molecular sieves in an Ar-filled glove box. C_6D_6 and $CDCl_3$ was dried over and distilled from Na/K/ Ph_2CO /18-crown-6 and stored over molecular sieves in an Ar-filled glove box. Fluorobenzene and benzotrifluoride were dried with and then distilled from CaH_2 and stored over molecular sieves in an Ar-filled glove box.

Me_3SiCF_3 was degassed prior to use and stored in an Ar-filled glove box. CsF was grounded and dried at 130 °C under vacuum for 2 days. **503**,²⁷² $[(\text{Et}_3\text{Si})_2(\text{SO}_3\text{CF}_3)][\text{HCB}_{11}\text{Cl}_{11}]$ ³¹⁸, and $[\text{Ph}_3\text{C}][\text{HCB}_{11}\text{Cl}_{11}]$,³¹⁸ was prepared according to the published procedures. $[(\text{PNP})\text{Rh}]_2(\mu\text{-N}_2)$ was previously characterized.²⁷¹ All other chemicals were used as received from commercial vendors unless otherwise specified.

6.5.2 Synthesis and Characterization

Synthesis of (PNP)Rh=CF₂. Method 1. **503** (105 mg, 0.170 mmol), Me_3SiCF_3 (50.0 μL , 0.340 mmol) and CsF (25.0 mg, 0.170 mmol) were placed in a Teflon flask in about 3 mL C_6D_6 . The reaction mixture was stirred vigorously and heated at 70 °C for 6 d. NMR analysis revealed the presence of 85% of **(PNP)Rh=CF₂** and 14% of **(PNP)Rh(C₂F₄)** together with 1% of **(PNP)Rh(CO)**. The same distribution of products (85% **(PNP)Rh=CF₂**, 14% **(PNP)Rh(C₂F₄)**, and 1% **(PNP)Rh(CO)**) was obtained when the mixture was heated for 3 d at 80 °C. The reaction mixture was passed through Celite. The volatiles were removed under vacuum and the residue was extracted with pentane. The pentane solution was passed through Celite again. The volatiles were removed under vacuum. The residue was dissolved in isooctane and placed in the freezer at -35 °C. Small amount of precipitate was formed the next day. The supernatant was filtered through Celite, then the volatiles were removed and the residue dried under vacuum. NMR analysis indicated > 98% purity of **(PNP)Rh=CF₂** (51 mg, 52% yield). **Method 2.** **503** (400 mg, 0.65 mmol) was dissolved in toluene in a 50 mL PTFE screw-top flask with a PTFE-coated stir bar. The solution was degassed and filled with 1 atm of

CHF_3 and heated overnight at 80 °C. The volatiles were removed under vacuum in the morning and the product was extracted with pentane and filtered through a pad of silica and Celite. The volatiles were removed to yield a dark red powder (226 mg) that was composed of 3% **(PNP)Rh(CO)**, 81% **(PNP)Rh=CF₂**, and 16% **[(PNP)Rh]₂(μ-N₂)**. ¹H NMR (C₆D₆): δ 7.66 (d, *J* = 8 Hz, 2H, (PNP)Aryl-H), 7.10 (br, 2H, (PNP)Aryl-H), 6.80 (d, *J* = 8 Hz, 2H, (PNP)Aryl-H), 2.43 (m, 4H, CH(CH₃)₂), 2.19 (s, 6H, Ar-CH₃), 1.27 (dvt (app. q.), *J* = 8 Hz, 12 H, CH(CH₃)₂), 1.13 (dvt (app. q.), *J* = 8 Hz, 12 H, CH(CH₃)₂). ³¹P{¹H}NMR (C₆D₆) : 53.7 (dt, *J*_{Rh-P} = 144 Hz, *J*_{F-P} = 30 Hz). ¹⁹F NMR (C₆D₆): 95.6 (dt, *J*_{Rh-F} = 49 Hz, *J*_{P-F} = 30 Hz). ¹³C{¹H}NMR (C₆D₆): 206.3 (dtt, *J*_{Rh-C} = 85 Hz, *J*_{C-P} = 12 Hz, *J*_{C-F} = 454 Hz), 162.3 (t, *J* = 11 Hz), 132.4, 131.9, 125.8 (t, *J* = 3 Hz), 122.3 (t, *J* = 18 Hz), 116.1 (t, *J* = 3 Hz), 25.4 (t, *J* = 11 Hz), 20.5, 19.3 (t, *J* = 3 Hz), 18.5. Elem. Anal. Found (Calculated) for C₂₇H₄₀F₂NP₂Rh: C, 55.81 (55.77); H, 6.96 (6.93); N, 2.35 (2.41).

Attempted Hydrolysis of (PNP)Rh=CF₂. A 20 mg mixture [91% **(PNP)Rh=CF₂**, 5% **(PNP)Rh(CO)**, 4% **(PNP)Rh]₂(μ-N₂)**] was dissolved in C₆D₆ and H₂O (10 μL) was added. The solution was left for 24 h at room temperature. No decomposition of **(PNP)Rh=CF₂** to **(PNP)Rh(CO)** was observed by ³¹P{¹H} NMR spectroscopy. Heating the sample overnight at 80 °C also led to no visible decomposition of **(PNP)Rh=CF₂** to **(PNP)Rh(CO)**, with **(PNP)Rh=CF₂** still accounting for >90% of the reaction mixture by ³¹P{¹H} NMR spectroscopy.

Treatment of (PNP)Rh(CO) with Me₃SiCF₃ and CsF. **(PNP)Rh(CO)** (28 mg, 0.050 mmol) was dissolved in toluene in a PTFE screw-top vial and treated with

Me_3SiCF_3 (30 μL , 0.20 mol) and CsF (16 mg, 0.10 mmol) and heated at 80 °C for 3 days. No reaction was observed to take place.

Treatment of (PNP)Rh=CF₂ with Me₃SiCF₃ and CsF. A 1:1 mixture of (PNP)Rh=CF₂ and (PNP)Rh(CO) (28 mg, 0.050 [Rh] (0.025 mmol per species)) was dissolved in toluene in a PTFE screw-top vial and treated with Me₃SiCF₃ (30 μL , 0.20 mol) and CsF (16 mg, 0.10 mmol) and heated at 80 °C for 3 days. Analysis by ³¹P{¹H} NMR spectroscopy using (PNP)Rh(CO) as an internal integration standard showed that no reaction had occurred.

Treatment of 1,2-dibromo-tetrafluoroethane with Zinc. Zinc (10 mg, 0.15 mmol) was added to a J. Young tube with 600 μL of THF. 1,2-dibromo-tetrafluoroethane (12 μL , 0.10 mmol) was added to the solution. Bubbles could be seen indicating the formation of tetrafluoroethylene upon mixing the heterogeneous mixture. ¹⁹F NMR spectroscopy was used to observe tetrafluoroethylene as a singlet resonating at -133.67 ppm in THF.

Observation of tetrafluoroethylene in C₆D₆. Zinc (10 mg, 0.15 mmol) was added to a J. Young tube with 600 μL of THF. 1,2-dibromo-tetrafluoroethane (12 μL , 0.10 mmol) was added to the solution. The solution was then frozen in liquid nitrogen and the headspace evacuated under vacuum. The solution was thawed and shaken. Bubbles could be seen forming around the solid zinc particles. After 20 minutes, the produced tetrafluoroethylene was vacuum transferred to another J. Young tube containing 600 μL of C₆D₆. ¹⁹F NMR spectroscopy was used to observe tetrafluoroethylene as a singlet resonating at -132.48 ppm in C₆D₆.

Treatment of Me₃SiCF₃ with CsF in C₆D₆. CsF (25 mg, 0.14 mmol) was added to a J. Young tube containing C₆D₆. Me₃SiCF₃ (50 μL, 0.39 mmol) was added to the J. Young tube and the solution was heated at 80 °C for 1 h. ¹⁹F NMR spectroscopy showed the formation of tetrafluoroethylene. The reaction was heated at 80 °C for 3 d. ¹⁹F NMR spectroscopy showed that tetrafluoroethylene (δ = -132.63 ppm) and Me₃SiF (δ = -158.00) were the two major products.

Synthesis of (PNP)Rh(C₂F₄). Method 1. **503** (300 mg, 0.49 mmol) was dissolved in THF with powdered zinc (240 mg, 3.67 mmol) in a Schlenk flask. The mixture is heated to 50 °C and a solution of 1,2-dibromo-tetrafluoroethane (290 μL, 2.42 mmol) is added dropwise. The solution immediately starts to bubble with the formation of tetrafluoroethylene. The reaction was heated overnight and the volatiles were removed under vacuum in the morning. The product was extracted with toluene and filtered through a plug of silica and Celite. The volatiles were removed again and the product was extracted with pentane and filtered through Celite. The volatiles were removed and the product was isolated as a light orange solid (138 mg, 45% yield). Method 2. An alternative synthesis was performed by dissolving **503** (300 mg, 0.49 mmol) in THF in a PTFE screw-cap flask. Powdered zinc (240 mg, 3.67 mmol) was added to another flask in THF, and 1,2-dibromo-tetrafluoroethane (290 μL, 2.42 mmol) was added dropwise. After 30 minutes of stirring the 1,2-dibromo-tetrafluoroethane over zinc at 50 °C, the produced tetrafluoroethylene was vacuum transferred to the first flask containing **503**. The reaction was stirred overnight at 50 °C and the volatiles were removed under vacuum in the morning. The product was filtered through silica and

Celite in THF and washed with pentane to yield the product as a light orange solid (197 mg, 64% yield). ^1H NMR (C_6D_6): δ 7.45 (d, $J = 8.5$ Hz, 2H, Ar-*H*), 6.81 (br, 2H, Ar-*H*), 6.75 (d, $J = 8.5$ Hz, 2H, Ar-*H*), 2.30 (br, 4H, PCHMe₂), 2.13 (s, 6H, Ar-*Me*), 1.30 (br, 12H, PCHMe₂), 0.96 (overlapping dt (app. q), $J = 7$ Hz, 12H, PCHMe₂). $^{31}\text{P}\{^1\text{H}\}$ NMR (C_6D_6): 52.3 (dq, $J_{\text{Rh-P}} = 137$ Hz, $J_{\text{F-P}} = 23$ Hz); ^{19}F NMR (C_6D_6): 100.7 (br); $^{13}\text{C}\{^1\text{H}\}$ NMR (CDCl_3): 161.5 (dvt, $J_{\text{C-P}} = 11$ Hz, $J_{\text{C-Rh}} = 2$ Hz, C-N), 132.3 (s, Ar), 131.8 (s, Ar), 126.7 (vt, $J_{\text{C-P}} = 3$ Hz, Ar), 119.2 (vt, $J_{\text{C-P}} = 20$ Hz, Ar), 115.1 (vt, $J_{\text{C-P}} = 5$ Hz, Ar), 111.37 (m, C₂F₄), 23.8 (br, PCHMe₂), 20.6 (s, Ar-*Me*), 18.5 (br, PCHMe₂), 16.7 (s, PCHMe₂). Elem. Anal. Found (Calculated) for C₂₈H₄₀F₄NP₂Rh: C, 53.39 (53.26); H, 6.47 (6.38).

Treatment of 503 with C₂HF₅ in a J. Young tube. **503** (22 mg, 0.036 mmol) was dissolved in C₆D₆ and the solution was degassed and charged with 1 atm of C₂HF₅. The solution was heated at 80 °C overnight. Analysis by $^{31}\text{P}\{^1\text{H}\}$ NMR spectroscopy in the morning showed 52% conversion to [(PNP)Rh]₂(μ-N₂) and (PNP)Rh(N₂), 9% (PNP)Rh(CO), 27% (PNP)Rh=C(F)(CF₃).

Synthesis of (PNP)Rh=C(F)(CF₃). **503** (200 mg, 0.32 mmol) was dissolved in benzotrifluoride (5 mL) in a 25 mL PTFE screw top flask, and the solution was degassed under vacuum. A 25 mL PTFE screw top flask was filled with 1 atm of C₂HF₅ and frozen in liquid nitrogen, once the C₂HF₅ (melting point = -103 °C) was frozen in the flask, the volatiles were removed under vacuum to remove dinitrogen from the gas mixture. The C₂HF₅ was freeze-pumped-thawed two more times and then vacuum transferred to the flask containing the **503** solution. The solution was then heated

overnight at 80 °C. The flask was cooled to room temperature and the volatiles were removed under vacuum. A portion of the resulting greenish blue solid was dissolved in C₆D₆ and analyzed by ³¹P{¹H} NMR, which displayed a mixture composed of 62% **(PNP)Rh=C(F)(CF₃)**, 1% **(PNP)Rh(CO)**, and 37% **503**. The solid was redissolved in benzotrifluoride and treated with C₂HF₅ following the previously described procedure. The reaction was heated overnight at 80 °C, and the volatiles were removed under vacuum in the morning. The resulting dark blue solid was dissolved in pentane and filtered through a pad of silica and Celite. The volatiles were removed to yield a blue powder (156 mg, 78% yield >90% pure). Analysis by ³¹P{¹H} NMR spectroscopy determined the mixture to be >90% **(PNP)Rh=C(F)(CF₃)**, the rest of the mixture was composed of **(PNP)Rh(CO)**. Dissolving the mixture in pentane and placing in a -35 °C freezer overnight formed clover-shaped crystals. Analysis of the crystals by ³¹P{¹H} NMR spectroscopy showed the same distribution of products (>90% **(PNP)Rh=C(F)(CF₃)** and <10% **(PNP)Rh(CO)**). Method 2. **503** (200 mg, 0.32 mmol) was dissolved in benzotrifluoride (5 mL) in a 25 mL PTFE screw top flask, and the solution was degassed under vacuum. A 50 mL PTFE screw top flask was filled with 1 atm of C₂HF₅ and frozen in liquid nitrogen, once the C₂HF₅ (melting point = -103 °C) was frozen in the flask, the volatiles were removed under vacuum to remove dinitrogen from the gas mixture. The C₂HF₅ was freeze-pumped-thawed two more times and then vacuum transferred to a 25 mL PTFE capped flask containing the **503** solution. The solution was then heated for 24 h at 80 °C. The flask was cooled to room temperature and an aliquot of the reaction mixture was transferred to J. Young tube for NMR

analysis. $^{31}\text{P}\{^1\text{H}\}$ NMR spectroscopy showed a mixture containing 25% **(PNP)Rh(CO)**, 52% **(PNP)Rh=C(F)(CF₃)**, and 13% **(PNP)Rh=CF₂**. ^1H NMR (C₆D₆): 7.57 (dvt, $J = 8.5$ Hz, $J_{\text{H-P}} = 2$ Hz, 2H, Ar-H), 7.05 (m, 2H, Ar-H), 6.77 (dd, $J = 9$ Hz, $J = 1.5$ Hz, 2H, Ar-H), 2.53 (m, 4H, PCHMe₂), 2.18 (s, 6H, Ar-Me), 1.28 (overlapping dvt (app. q), $J = 7.5$ Hz, PCHMe₂), 1.05 (overlapping dvt (app. q), $J = 7$ Hz, PCHMe₂); ^{19}F NMR (C₆D₆): 75.6 (br. t, $J = 39.5$ Hz, 1F, Rh=C(F)(CF₃)), -74.2 (d, $J = 11.3$ Hz, 3F, Rh=C(F)(CF₃)); $^{31}\text{P}\{^1\text{H}\}$ NMR (C₆D₆): 55.4 (dd, $J_{\text{Rh-P}} = 149.3$ Hz, $J_{\text{F-P}} = 41.0$ Hz); $^{13}\text{C}\{^1\text{H}\}$ NMR (C₆D₆): 225.0 (m, Rh=C), 161.3 (dvt, $J_{\text{C-P}} = 12$ Hz, $J_{\text{C-Rh}} = 2$ Hz, C-N), 132.3 (s, Ar-H), 132.1 (s, Ar-H), 126.2 (vt, $J_{\text{C-P}} = 3$ Hz, Ar), 121.6 (vt, $J_{\text{C-P}} = 19$ Hz, Ar), 116.8 (vt, $J_{\text{C-P}} = 5$ Hz, Ar), 25.3 (vt, $J_{\text{C-P}} = 11$ Hz, PCHMe₂), 20.5 (s, Ar-Me), 19.4 (vt, $J_{\text{C-P}} = 3$ Hz, PCHMe₂), 18.3 (s, PCHMe₂).

Synthesis of [(PNP)Rh≡CF][CHB₁₁Cl₁₁]. [Ph₃C][CHB₁₁Cl₁₁] (31.6 mg, 0.041 mmol) was dissolved in about 1 mL of PhF in a flask followed by the addition of Et₃SiH (8.0 μL, 0.049 mmol). The yellow solution changed to colorless within minutes. **(PNP)Rh(=CF₂)** (24 mg, 0.041 mmol) was added to the reaction mixture. The solution changed to green/blue immediately. The bluish solid was precipitated out by adding excess pentane to the solution. The supernatant was decanted. The solid was washed with pentane (3x3 mL) and dried under vacuum. Yield, 27 mg, 61%. The X-ray quality crystals were obtained by carefully laying pentane to 1,2-difluorobenzene solution of the title compound at room temperature. ^1H NMR (C₆D₆/1,2-difluorobenzene, 1,2-difluorobenzene was added to increase the solubility and it overlapped with the aromatic resonances of the title compound. Only aliphatic region was reported): δ 2.66 (br, 1H,

$\text{CHB}_{11}\text{Cl}_{11}$), 2.41 (m, 4H, CHMe_2), 2.18 (s, 6H, Ar- CH_3), 1.03 (app. q, $J = 11$ Hz, 12H, CHMe_2), 0.90 (app. q, $J = 11$ Hz, 12H, CHMe_2). $^{31}\text{P}\{^1\text{H}\}$ NMR ($\text{C}_6\text{D}_6/1,2$ -difluorobenzene): δ 89.3 (dd, $J_{\text{Rh-P}} = 106$ Hz, $J_{\text{F-P}} = 14$ Hz). ^{19}F NMR: δ 66.2 (dt, $J_{\text{Rh-F}} = 136$ Hz, $J_{\text{P-F}} = 14$ Hz). $^{13}\text{C}\{^1\text{H}, ^{31}\text{P}\}$ NMR ($\text{C}_6\text{D}_5\text{Br}/1,2$ -difluorobenzene): δ 160.1(s), 134.1(s), 132.5 (s), 116.2 (s) 47.3 (broad s, C-H) 26.3 (s, CHMe_2), 20.0(s, Ar- CH_3), 18.7 (s, CHMe_2), 17.6 (s, CHMe_2). (2 aromatic signals are overlapping with solvent). Elem. Anal. Found (Calculated) for $\text{C}_{28}\text{H}_{41}\text{B}_{11}\text{Cl}_{11}\text{FNP}_2\text{Rh}$: C, 31.02 (31.01); H, 3.80 (3.81).

Determination of $J_{\text{C-F}}$ by observation of ^{13}C satellites in ^{19}F NMR for $[(\text{PNP})\text{Rh}\equiv\text{CF}]^+$. In an oven dried, argon cooled J. Young Tube $[\text{Ph}_3\text{C}][\text{BArF}_{20}]$ (19 mg, 0.029 mmol) was dissolved in ~ 0.1 mL of $\text{C}_6\text{H}_5\text{F}$. To the solution Et_3SiH (6 mg, 0.052 mmol) was added and then mixed until the solution became a very pale brown (almost colorless). After five minutes, $(\text{PNP})\text{Rh}=\text{CF}_2$ (17 mg, 0.029 mmol) was added and the NMR tube walls were rinsed with ~ 0.3 mL of $\text{C}_6\text{H}_5\text{F}$ and ~ 0.2 mL of C_6D_6 . Upon mixing the color immediately changed from a dark red to a dark blue. An overnight ^{19}F NMR collection was sufficient to show ^{13}C satellites (shown below). ^{19}F NMR ($\text{C}_6\text{H}_5\text{F}/\text{C}_6\text{D}_6$): 65.1(dt, $J_{\text{Rh-F}} = 136$ Hz, $J_{\text{P-F}} = 12$ Hz, $J_{\text{C-F}} = 470$ Hz).

Treatment of $(\text{PNP})\text{Rh}(\text{C}_2\text{F}_4)$ with $[(\text{Et}_3\text{Si})_2(\text{SO}_3\text{CF}_3)][\text{HCB}_{11}\text{Cl}_{11}]$. $[(\text{Et}_3\text{Si})_2(\text{SO}_3\text{CF}_3)][\text{HCB}_{11}\text{Cl}_{11}]$ (38 mg, 0.042 mmol) was dissolved in fluorobenzene in a vial and $(\text{PNP})\text{Rh}(\text{C}_2\text{F}_4)$ (27 mg, 0.042 mmol) was added to the reaction mixture, which immediately turned blue. The mixture was stirred overnight and transferred to a J. Young tube. Analysis by ^{19}F NMR spectroscopy showed Et_3SiOTf and Et_3SiF , while analysis by $^{31}\text{P}\{^1\text{H}\}$ NMR showed no signals. The reaction mixture was transferred back

to a flask, and the volatiles were removed under vacuum. The dark blue solid was then redissolved in fluorobenzene and precipitated with pentane. A slightly blue-tinted clear solution was decanted from the blue solid, and the solid was dried under vacuum to yield 25 mg of a blue solid. The solid was dissolved in 0.5 mL of toluene and 0.2 mL of *ortho*-dichlorobenzene and transferred to a J. Young tube. Analysis by ^{19}F NMR spectroscopy showed a broad signal at -84.5 ppm. Upon cooling the solution to -30 °C this signal split into two other signals at -83.2 and -85.8 ppm, and other broad signals appeared at -97.6 and -106.1 ppm. Analysis by $^{31}\text{P}\{^1\text{H}\}$ NMR spectroscopy showed one broad peak at 55 ppm, but upon cooling the sample to -30 °C the signal split into two broad peaks around 60 ppm.

The mixture was warmed to room temperature and CsF (10 mg, 0.66 mmol) was added to the J. Young tube and rotated overnight. By morning the solution had turned from dark blue to a brownish green. Analysis by ^{19}F NMR spectroscopy showed that 98% of the visible signals had been converted back to **(PNP)Rh(C₂F₄)** (as judged by integration versus a residual FPh peak). The solution in the J. Young tube was transferred to a vial and pentane was added to precipitate any cationic species and the solution was filtered through celite to form an orange filtrate. ^1H , $^{31}\text{P}\{^1\text{H}\}$, and ^{19}F NMR spectroscopy all confirmed that **(PNP)Rh(C₂F₄)** was the resulting product.

Treatment of (PNP)Rh=C(F)(CF₃) with [(Et₃Si)₂(SO₃CF₃)] [HCB₁₁Cl₁₁]. A mixture of **(PNP)Rh=C(F)(CF₃)** and **(PNP)Rh(CO)** (21 mg, 9:1) was dissolved in fluorobenzene in a J. Young tube and treated with [(Et₃Si)₂(SO₃CF₃)] [HCB₁₁Cl₁₁] (30 mg, 0.033 mmol). Analysis by ^{19}F NMR spectroscopy after 2 h at RT showed Et₃SiOTf

and Et₃SiF. Analysis by ³¹P{¹H} NMR showed a broad doublet at about 60 ppm. The reaction was left overnight and in the morning the volatiles were removed and the resulting solid was washed with pentane. The resulting solid was dissolved in C₆D₅Br for NMR analysis. Analysis by ³¹P{¹H} NMR spectroscopy showed a broad doublet at 60.3 ppm (d, *J* = 148 Hz) as the major signal. Analysis by ¹⁹F NMR spectroscopy showed a singlet at -71.8 ppm as the major signal. The ¹H NMR spectrum showed broad aliphatic peaks and no characteristic signals. This mixture was transferred to a 10 mL Schlenk flask and the volatiles were removed under vacuum. The solid was then dissolved in *ortho*-difluorobenzene and treated with CsF (5 mg, 0.033 mmol) and stirred for 4 days at room temperature. The volatiles were removed and the resulting solid was dissolved in fluorobenzene and pentane and filtered through Celite. The volatiles were removed and the solid was dissolved in C₆D₆ for NMR analysis. Analysis by ¹⁹F NMR spectroscopy showed **(PNP)Rh=C(F)(CF₃)** as the major fluorine containing product. Analysis by ³¹P{¹H} NMR spectroscopy showed **(PNP)Rh(CO)**, **(PNP)Rh=C(F)(CF₃)**, and **(PNP)Rh(C₆D₅)(Br)** in a (20:51:28 ratio). ¹H NMR spectroscopy verified the identity and composition of this mixture. Method 2. A mixture of **(PNP)Rh=C(F)(CF₃)** and **(PNP)Rh(CO)** (11 mg, 1:1) was dissolved in fluorobenzene in a J. Young tube and treated with [(Et₃Si)₂(SO₃CF₃)] [**HCB₁₁Cl₁₁**] (15 mg, 0.017 mmol). The reaction was left overnight and in the morning the volatiles were removed and the reaction mixture was dissolved in *ortho*-difluorobenzene and treated with CsF (5 mg, 0.033 mmol). The reaction was stirred for 4 days at room temperature. The volatiles were removed under vacuum and the resulting solid was dissolved in fluorobenzene. Pentane was added to

the solution to precipitate any cesium salts, and the supernatant was passed through Celite. The volatiles were removed under vacuum, and the resulting solid was dissolved in C₆D₆ for NMR analysis. Analysis by ³¹P{¹H} NMR showed **(PNP)Rh(CO)** and **(PNP)Rh=C(F)(CF₃)**. ¹H NMR spectroscopy showed that these products were present in a ((**(PNP)Rh(CO)**) : (**(PNP)Rh=C(F)(CF₃)**) = 3:1 ratio). ¹⁹F NMR spectroscopy showed **(PNP)Rh=C(F)(CF₃)** as the major fluorine-containing product. **(PNP)Rh(C₂F₄)** was not observed.

6.5.3 X-ray Crystallography

X-Ray data collection, solution, and refinement for (PNP)Rh=CF₂. A red block crystal of suitable size (0.30 x 0.21 x 0.15 mm) was selected from a representative sample of crystals of the same habit using an optical microscope, mounted onto a nylon loop and placed in a cold stream of nitrogen. Low temperature (110 K) X-ray data were obtained on a Bruker APEXII CCD based diffractometer (Mo sealed X-ray tube, K_α = 0.71073 Å). All diffractometer manipulations, including data collection, integration and scaling were carried out using the Bruker APEXII software.²⁸¹ An absorption correction was applied using SADABS.²⁸² The structure was solved in the *Pna2*₁ space group using XS²⁸³ (incorporated in SHELXTL). The solution was refined by full-matrix least squares on *F*². No additional symmetry was found using ADDSYMM incorporated into the PLATON program.²⁸⁴ All non-hydrogen atoms were refined with anisotropic thermal parameters. All hydrogen atoms were placed in idealized positions and refined using a riding model. The structure was refined (weighted least squares refinement on *F*²) and

the final least-squares refinement converged to $R_1 = 0.0357$ ($I > 2\sigma(I)$, 6606 data) and $wR_2 = 0.0751$ (F^2 , 30909 data, 298 parameters).

X-Ray data collection, solution, and refinement for (PNP)Rh(C₂F₄). A red block crystal of suitable size (0.17 x 0.14 x 0.11 mm) was selected from a representative sample of crystals of the same habit using an optical microscope, mounted onto a nylon loop and placed in a cold stream of nitrogen. Low temperature (110 K) X-ray data were obtained on a Bruker APEXII CCD based diffractometer (Mo sealed X-ray tube, $K_\alpha = 0.71073$ Å). All diffractometer manipulations, including data collection, integration and scaling were carried out using the Bruker APEXII software.²⁸¹ An absorption correction was applied using SADABS.²⁸² The structure was solved in the monoclinic C2/c space group using XS²⁸³ (incorporated in SHELXTL). The solution was refined by full-matrix least squares on F^2 . No additional symmetry was found using ADDSYMM incorporated into the PLATON program.²⁸⁴ All non-hydrogen atoms were refined with anisotropic thermal parameters. All hydrogen atoms were placed in idealized positions and refined using a riding model. The structure was refined (weighted least squares refinement on F^2) and the final least-squares refinement converged to $R_1 = 0.0293$ ($I > 2\sigma(I)$, 2775 data) and $wR_2 = 0.0862$ (F^2 , 3031 data, 169 parameters).

X-Ray data collection, solution, and refinement for [(PNP)Rh≡CF][CHB₁₁Cl₁₁]. A blue prism (0.20 x 0.17 x 1.00 mm) was selected from a representative sample of crystals of the same habit using an optical microscope, mounted onto a nylon loop and placed in a cold stream of nitrogen (110 K). Low-temperature X-ray data were obtained on a Bruker APEXII CCD based diffractometer (Mo sealed X-ray

tube, $K\alpha = 0.71073 \text{ \AA}$). All diffractometer manipulations, including data collection, integration and scaling were carried out using the Bruker APEXII software.²⁸¹ The space group was determined on the basis of systematic absences and intensity statistics and the structure was solved in the orthorhombic space group $Pna2_1$ by direct methods using XS²⁸³ (incorporated in SHELXTL) and refined by full-matrix least-squares on F^2 . No obvious missed symmetry was reported by PLATON.²⁸⁴ All non-hydrogen atoms were refined with anisotropic thermal parameters. Hydrogen atoms were placed in idealized positions and refined using riding model. The structure was refined (weighted least squares refinement on F^2) and the final least-squares refinement converged to $R_1 = 0.0590$ ($I > 2\sigma(I)$, 9513 data) and $wR_2 = 0.1511$ (F^2 , 10849 data, 511 parameters).

6.5.4 Computational Methods

Full molecule DFT studies were performed using the M06 functional^{329,330} and the triple- ζ LACV3P**++ basis set, which used extended core potentials³³¹⁻³³⁴ on Rh and a 6-311G**++ basis³³⁵⁻³³⁸ for other atoms, as implemented in the Jaguar^{339,340} suite of programs. NBO 6.0³²²⁻³²⁷ and WBI calculations,³²⁸ as implemented in Jaguar, were performed on each optimized structure. Computed structures were confirmed as energy minima by calculating the vibrational frequencies using second derivative analytic methods, and confirming the absence of imaginary frequencies. DFT calculations on the energetics of rotation barriers in CX_2 and C_2X_4 ligands ($X = F, H$) were performed on complexes containing a truncated form of the pincer ligand (see text of manuscript).

Non-default options chosen in Jaguar:

- SCF calculation type: DFT(M06)

- Vibrational frequencies and related properties will be computed from analytic second derivatives
- Molecular symmetry not used
- Energy convergence criterion: 1.00E-05 hartrees
- RMS density matrix convergence criterion: 1.00E-06
- Highest accuracy cutoffs used in SCF

CHAPTER VII

CONCLUSION

The catalytic dehydrogenative borylation of terminal alkynes (DHBTA) using (POCOP)Pd complexes has been demonstrated. While these complexes are the only group 10 catalysts for DHBTA, the system is limited by the propensity for pincer-ligated palladium complexes to leach palladium(0) into solution. This Pd(0) can then catalyze the hydrogenation of the terminal alkyne. However, hydrogenation can be prevented with the addition of phosphines to the reaction mixture. The system also suffers from the reversible nature of the product forming step, which leads to longer reaction times and incomplete conversions.

Second generation iridium DHBTA catalysts based on (PNP)Ir were demonstrated to be superior to both the (SiNN)Ir first generation catalyst and our palladium DHBTA catalyst. These second generation Ir catalysts have been used to increase the substrate scope of DHBTA to include a number of 1,6-enynes and 1,6-diyne, including propargyl ethers and amines. The borylated enynes and diynes were subjected to rhodium-catalyzed reductive cyclization. However the alkynylboron substituent seems to promote an alkene isomerization in the heteroatom-tethered enynes and diynes during the cyclization reaction. This double bond isomerization was difficult to gain control of with 1,6-enynes, and these reactions usually resulted in a mixture of products. However, the reductive cyclization of borylated 1,6-diyne was a well-behaved reaction, and a number of amine-tethered borylated 1,6-diyne were found to undergo

reductive cyclization to form pyrroles. Investigating reductive cyclization using amine-derived 1,6-diynes without alkynylboron moieties led to the discovery that the absence of an alkynylboron substituent can lead to a mixture of pyrrolidine and pyrrole products. However, thermolysis of the mixture after reductive cyclization has completed will isomerize the pyrrolidines to pyrroles. Ultimately, through the combination of DHBTA and reductive cyclization, we have devised a two-step, atom-economical route to borylated pyrroles.

A series of (pincer)Rh complexes have been synthesized for study as potential catalysts for alkyne dimerization to 1,3-enynes. Our findings indicate that aryl/bis(phosphine/phosphinite) PCP or POCOP pincer ligands do result in Rh catalysts capable of alkyne dimerization. Similarly to the PNP-based catalysts reported previously, the PCP/POCOP systems produce little to no *Z*-enynes as products. PCP- and POCOP-based Rh compounds with PⁱPr₂ side arms are faster catalysts than the PNP-based Rh complexes. However, none of the compounds under study in this work displayed notable selectivity for either *E*- or *gem*-enyne isomer. Isomeric ratios vary considerably as a function of the catalyst and the alkyne substrate, thus clear trends are not apparent.

In the study of (PNP)Rh as a potential catalyst for Negishi coupling, the (PNP)Rh complex is sequestered by organozinc reagents or by-products through the formation of adducts of (PNP)Rh with ZnX₂. In the case of the addition of ZnPh₂, the Rh center inserts into the Zn-Ph bond. The precise structural outcome of the addition of PhZnCl and ZnCl₂ to (PNP)Rh has not been unambiguously established. The formation

of these adducts is deleterious for catalysis as they dramatically diminish the availability of the unsaturated (PNP)Rh intermediate necessary for the step of oxidative addition of the aryl halide.

The synthesis of (PNP)Rh perfluorocarbene complexes has been accomplished by treating a Rh(I) precursor with Rupert's reagent or a fluoroalkane containing a C-H bond. Using silylium reagents, a fluoride can be abstracted from these perfluorocarbenes, and the abstraction of fluoride from the CF₂ ligand forms an isolable cationic fluoromethyldyne. Thus the (PNP)Rh system conveniently allows synthesis and comparison of perfluoroolefin, perfluorocarbene, and perfluorocarbyne complexes. Using DFT calculations we were able to compare the Natural Localized Molecular Orbitals of these fluoroorganic complexes to their hypothetical hydrocarbon analogues. It was established that the fluorine atoms on the carbene and carbyne ligands participate in π donation to the acceptor orbitals on carbon to compete with back donation from the metal. This resulted in a longer Rh-C bond in the fluorinated complexes compared to their hydrocarbon analogues. However, C₂F₄ was calculated to form a shorter Rh-C bond than the C₂H₄ complex. Calculated Wiberg Bond Indices also showed that although the unsaturated fluorocarbon ligands have bond orders greater than one to rhodium, the nitrogen *trans* to these ligands interacts with their antibonding orbital and decreases the bond order to less than a true double and triple bond.

REFERENCES

- (1) Brewster, J. H.; Negishi, E.-I. *Science* **1980**, *207*, 44.
- (2) Suzuki, A. *Angew. Chem. Int. Ed.* **2011**, *50*, 6722.
- (3) Brown, H. C.; Zweifel, G. *J. Am. Chem. Soc.* **1959**, *81*, 247.
- (4) Dhillon, R. S. *Hydroboration and Organic Synthesis*; Springer-Verlag: Berlin, 2007.
- (5) Beletskaya, I.; Pelter, A. *Tetrahedron* **1997**, *53*, 4957.
- (6) Trost, B. M.; Ball, Z. T. *Synthesis* **2005**, *2005*, 853.
- (7) Miyaura, N.; Yamada, K.; Suzuki, A. *Tetrahedron Lett.* **1979**, *20*, 3437.
- (8) Lennox, A. J. J.; Lloyd-Jones, G. C. *Chem. Soc. Rev.* **2014**, *43*, 412.
- (9) Johansson Seechurn, C. C. C.; Kitching, M. O.; Colacot, T. J.; Snieckus, V. *Angew. Chem. Int. Ed.* **2012**, *51*, 5062.
- (10) Akama, T.; Zhang, Y. K.; Ding, C. Z.; Plattner, J. J.; Maples, K. R.; Freund, Y.; Sanders, V.; Xia, Y.; Baker, S. J.; Nieman, J. A. Boron-Containing Small Molecules as Anti-Inflammatory Agents. US 2009/0291917 A1, November 26, 2009.
- (11) Hall, D. G. *Boronic Acids: Preparation and Applications in Organic Synthesis, Medicine and Materials*; 2 ed.; Wiley-VCH Verlag GmbH & Co. KGaA: Weinheim, 2011.
- (12) Desai, A. A. *Angew. Chem. Int. Ed.* **2012**, *51*, 9223.
- (13) Ishiyama, T.; Murata, M.; Miyaura, N. *J. Org. Chem.* **1995**, *60*, 7508.

- (14) Nguyen, P.; Blom, H. P.; Westcott, S. A.; Taylor, N. J.; Marder, T. B. *J. Am. Chem. Soc.* **1993**, *115*, 9329.
- (15) Mkhaliid, I. A. I.; Barnard, J. H.; Marder, T. B.; Murphy, J. M.; Hartwig, J. F. *Chem. Rev.* **2009**, *110*, 890.
- (16) Cho, J.-Y.; Tse, M. K.; Holmes, D.; Maleczka, R. E.; Smith, M. R. *Science* **2002**, *295*, 305.
- (17) Ishiyama, T.; Takagi, J.; Ishida, K.; Miyaura, N.; Anastasi, N. R.; Hartwig, J. F. *J. Am. Chem. Soc.* **2002**, *124*, 390.
- (18) Hartwig, J. F. *Chem. Soc. Rev.* **2011**, *40*, 1992.
- (19) Kuninobu, Y.; Ida, H.; Nishi, M.; Kanai, M. *Nat Chem* **2015**, *7*, 712.
- (20) Hartwig, J. F. *Acc. Chem. Res.* **2017**, *50*, 549.
- (21) Preshlock, S. M.; Ghaffari, B.; Maligres, P. E.; Krska, S. W.; Maleczka, R. E.; Smith, M. R. *J. Am. Chem. Soc.* **2013**, *135*, 7572.
- (22) Press, L. P.; Kosanovich, A. J.; McCulloch, B. J.; Ozerov, O. V. *J. Am. Chem. Soc.* **2016**, *138*, 9487.
- (23) Hartwig, J. F. *Acc. Chem. Res.* **2012**, *45*, 864.
- (24) Campeau, L.-C.; Chen, Q.; Gauvreau, D.; Girardin, M.; Belyk, K.; Maligres, P.; Zhou, G.; Gu, C.; Zhang, W.; Tan, L.; O'Shea, P. D. *Org. Process Res. Dev.* **2016**, *20*, 1476.
- (25) Maleczka, R. E.; Shi, F.; Holmes, D.; Smith, M. R. *J. Am. Chem. Soc.* **2003**, *125*, 7792.

- (26) Murphy, J. M.; Liao, X.; Hartwig, J. F. *J. Am. Chem. Soc.* **2007**, *129*, 15434.
- (27) (a) Liskey, C. W.; Liao, X.; Hartwig, J. F. *J. Am. Chem. Soc.* **2010**, *132*, 11389. (b) Zhang, G.; Zhang, L.; Hu, M.; Cheng, J. *Adv. Synth. Catal.* **2011**, *353*, 291. (c) Kim, J.; Choi, J.; Shin, K.; Chang, S. *J. Am. Chem. Soc.* **2012**, *134*, 2528.
- (28) Tzschucke, C. C.; Murphy, J. M.; Hartwig, J. F. *Org. Lett.* **2007**, *9*, 761.
- (29) Qiao, J. X.; Lam, P. Y. S. *Synthesis* **2011**, *2011*, 829.
- (30) Coutts, S. J.; Adams, J.; Krolkowski, D.; Snow, R. J. *Tetrahedron Lett.* **1994**, *35*, 5109.
- (31) Furuya, T.; Ritter, T. *Org. Lett.* **2009**, *11*, 2860.
- (32) Preshlock, S.; Tredwell, M.; Gouverneur, V. *Chem. Rev.* **2016**, *116*, 719.
- (33) Chen, H.; Schlecht, S.; Semple, T. C.; Hartwig, J. F. *Science* **2000**, *287*, 1995.
- (34) Ishiyama, T.; Ishida, K.; Takagi, J.; Miyaura, N. *Chem. Lett.* **2001**, *30*, 1082.
- (35) Olsson, V. J.; Szabó, K. J. *Angew. Chem. Int. Ed.* **2007**, *46*, 6891.
- (36) Brown, J. M.; Lloyd-Jones, G. C. *J. Am. Chem. Soc.* **1994**, *116*, 866.
- (37) Lee, C.-I.; Zhou, J.; Ozerov, O. V. *J. Am. Chem. Soc.* **2013**, *135*, 3560.
- (38) Trost, B. M.; Masters, J. T. *Chem. Soc. Rev.* **2016**, *45*, 2212.
- (39) Esteruelas, M. A.; Herrero, J.; López, A. M.; Oliván, M. *Organometallics* **2001**, *20*, 3202.
- (40) Chopade, P. R.; Louie, J. *Adv. Synth. Catal.* **2006**, *348*, 2307.
- (41) Liu, J.; Lam, J. W. Y.; Tang, B. Z. *Chem. Rev.* **2009**, *109*, 5799.

- (42) Crespo-Quesada, M.; Cárdenas-Lizana, F.; Dessimoz, A.-L.; Kiwi-Minsker, L. *ACS Catalysis* **2012**, *2*, 1773.
- (43) Jiao, J.; Nishihara, Y. *J. Organomet. Chem.* **2012**, 721-722, 3.
- (44) Ishida, N.; Murakami, M., Reactions of Alkynylboron Compounds. In *Synthesis and Application of Organoboron Compounds*, Fernández, E.; Whiting, A., Eds. Springer International Publishing: Cham, 2015; pp 93.
- (45) Brown, H. C.; Bhat, N. G.; Srebnik, M. *Tetrahedron Lett.* **1988**, *29*, 2631.
- (46) Hu, J.-R.; Liu, L.-H.; Hu, X.; Ye, H.-D. *Tetrahedron* **2014**, *70*, 5815.
- (47) Ijadi-Maghsoodi, S.; Pang, Y.; Barton, T. J. *J. Polym. Sci., Part A: Polym. Chem.* **1990**, *28*, 955.
- (48) Kang, Y. K.; Deria, P.; Carroll, P. J.; Therien, M. J. *Org. Lett.* **2008**, *10*, 1341.
- (49) Mancilla, T.; Contreras, R.; Wrackmeyer, B. *J. Organomet. Chem.* **1986**, 307, 1.
- (50) Lee, S. J.; Anderson, T. M.; Burke, M. D. *Angew. Chem. Int. Ed.* **2010**, *49*, 8860.
- (51) Struble, J. R.; Lee, S. J.; Burke, M. D. *Tetrahedron* **2010**, *66*, 4710.
- (52) Vedejs, E.; Chapman, R. W.; Fields, S. C.; Lin, S.; Schrimpf, M. R. *J. Org. Chem.* **1995**, *60*, 3020.
- (53) Darses, S.; Michaud, G.; Genêt, J.-P. *Eur. J. Org. Chem.* **1999**, 1999, 1875.
- (54) Bardin, V. V.; Adonin, N. Y.; Frohn, H.-J. *J. Fluorine Chem.* **2007**, *128*, 699.
- (55) Britt A. Vanchura, I.; Preshlock, S. M.; Roosen, P. C.; Kallepalli, V. A.; Staples, R. J.; Robert E. Maleczka, J.; Singleton, D. A.; Smith, M. R. *Chem. Commun.* **2010**, 46, 7724.

- (56) Lee, C.-I.; DeMott, J. C.; Pell, C. J.; Christopher, A.; Zhou, J.; Bhuvanesh, N.; Ozerov, O. V. *Chem. Sci.* **2015**, *6*, 6572.
- (57) Pell, C. J.; Ozerov, O. V. *Inorg. Chem. Front.* **2015**, *2*, 720.
- (58) Tsuchimoto, T.; Utsugi, H.; Sugiura, T.; Horio, S. *Adv. Synth. Catal.* **2015**, *357*, 77.
- (59) Iwadate, N.; Suginome, M. *J. Am. Chem. Soc.* **2010**, *132*, 2548.
- (60) Romero, E. A.; Jazzar, R.; Bertrand, G. *Chem. Sci.* **2017**, *8*, 165.
- (61) Jin, L.; Tolentino, D. R.; Melaimi, M.; Bertrand, G. *Sci. Adv.* **2015**, *1*, e1500304.
- (62) Romero, E. A.; Jazzar, R.; Bertrand, G. *J. Organomet. Chem.* **2017**, *829*, 11.
- (63) Wang, C.; Leng, X.; Chen, Y. *Organometallics* **2015**, *34*, 3216.
- (64) Stephan, D. W.; Erker, G. *Angew. Chem. Int. Ed.* **2015**, *54*, 6400.
- (65) (a) G. C. Welch, R. R. S. Juan, J. D. Masuda, D. W. Stephan, *Science* **2006**, *314*, 1124. (b) G. C. Welch, D. W. Stephan, *J. Am. Chem. Soc.* **2007**, *129*, 1880 (c) P. Spies, G. Erker, G. Kehr, K. Bergander, R. Fröhlich, S. Grimme, D. W. Stephan, *Chem. Commun.* **2007**, 5072.
- (66) (a) Dureen, M. A.; Stephan, D. W. *J. Am. Chem. Soc.* **2009**, *131*, 8396. (b) Dureen, M. A.; Brown, C. C.; Stephan, D. W. *Organometallics* **2010**, *29*, 6594.
- (67) Mömning, C. M.; Frömel, S.; Kehr, G.; Fröhlich, R.; Grimme, S.; Erker, G. *J. Am. Chem. Soc.* **2009**, *131*, 12280.
- (68) Jiang, C.; Blacque, O.; Berke, H. *Organometallics* **2010**, *29*, 125.
- (69) Voss, T.; Mahdi, T.; Otten, E.; Fröhlich, R.; Kehr, G.; Stephan, D. W.; Erker, G. *Organometallics* **2012**, *31*, 2367.

- (70) Lawson, J. R.; Clark, E. R.; Cade, I. A.; Solomon, S. A.; Ingleson, M. J. *Angew. Chem. Int. Ed.* **2013**, *52*, 7518.
- (71) Iashin, V.; Chernichenko, K.; Pápai, I.; Repo, T. *Angew. Chem. Int. Ed.* **2016**, *55*, 14146.
- (72) (a) Deloux, L.; Srebnik, M. *J. Org. Chem.* **1994**, *59*, 6871. (b) Desurmont, G.; Klein, R.; Uhlenbrock, S.; Laloë, E.; Deloux, L.; Giolando, D. M.; Kim, Y. W.; Pereira, S.; Srebnik, M. *Organometallics* **1996**, *15*, 3323. (c) Quntar, A. A. A.; Srebnik, M. *Org. Lett.* **2004**, *6*, 4243. (d) Quntar, A. A. A.; Botvinik, A.; Rubinstein, A.; Srebnik, M. *Chem. Commun.* **2008**, 5589. (e) Botvinik, A.; Quntar, A. A. A.; Rubinstein, A.; Srebnik, M. *J. Organomet. Chem.* **2009**, *694*, 3349.
- (73) Nishihara, Y.; Miyasaka, M.; Okamoto, M.; Takahashi, H.; Inoue, E.; Tanemura, K.; Takagi, K. *J. Am. Chem. Soc.* **2007**, *129*, 12634.
- (74) Nishihara, Y.; Okada, Y.; Jiao, J.; Suetsugu, M.; Lan, M.-T.; Kinoshita, M.; Iwasaki, M.; Takagi, K. *Angew. Chem. Int. Ed.* **2011**, *50*, 8660.
- (75) Nishihara, Y.; Suetsugu, M.; Saito, D.; Kinoshita, M.; Iwasaki, M. *Org. Lett.* **2013**, *15*, 2418.
- (76) Iwasaki, M.; Nishihara, Y. *Chem. Rec.* **2016**, *16*, 2031.
- (77) Neeve, E. C.; Geier, S. J.; Mkhaliid, I. A. I.; Westcott, S. A.; Marder, T. B. *Chem. Rev.* **2016**, *116*, 9091.

- (78) Ali, H. A.; El Aziz Al Quntar, A.; Goldberg, I.; Srebnik, M. *Organometallics* **2002**, *21*, 4533.
- (79) Hyodo, K.; Suetsugu, M.; Nishihara, Y. *Org. Lett.* **2014**, *16*, 440.
- (80) Jiao, J.; Nakajima, K.; Nishihara, Y. *Org. Lett.* **2013**, *15*, 3294.
- (81) Jiao, J.; Hyodo, K.; Hu, H.; Nakajima, K.; Nishihara, Y. *J. Org. Chem.* **2014**, *79*, 285.
- (82) Lee, C.-I.; Shih, W.-C.; Zhou, J.; Reibenspies, J. H.; Ozerov, O. V. *Angew. Chem. Int. Ed.* **2015**, *54*, 14003.
- (83) Suginome, M.; Shirakura, M.; Yamamoto, A. *J. Am. Chem. Soc.* **2006**, *128*, 14438.
- (84) Barata-Vallejo, S.; Lantaño, B.; Postigo, A. *Chem. Eur. J.* **2014**, *20*, 16806.
- (85) Umemoto, T.; Ishihara, S. *J. Am. Chem. Soc.* **1993**, *115*, 2156.
- (86) Zheng, H.; Huang, Y.; Wang, Z.; Li, H.; Huang, K.-W.; Yuan, Y.; Weng, Z. *Tetrahedron Lett.* **2012**, *53*, 6646.
- (87) Presset, M.; Oehlich, D.; Rombouts, F.; Molander, G. A. *J. Org. Chem.* **2013**, *78*, 12837.
- (88) Nishihara, Y.; Okamoto, M.; Inoue, Y.; Miyazaki, M.; Miyasaka, M.; Takagi, K. *Tetrahedron Lett.* **2005**, *46*, 8661.
- (89) Paixão, M. W.; Weber, M.; Braga, A. L.; de Azeredo, J. B.; Deobald, A. M.; Stefani, H. A. *Tetrahedron Lett.* **2008**, *49*, 2366.
- (90) Ahammed, S.; Kundu, D.; Ranu, B. C. *J. Org. Chem.* **2014**, *79*, 7391.
- (91) Sonogashira, K. *J. Organomet. Chem.* **2002**, *653*, 46.

- (92) Ogawa, D.; Li, J.; Suetsugu, M.; Jiao, J.; Iwasaki, M.; Nishihara, Y. *Tetrahedron Lett.* **2013**, *54*, 518.
- (93) Shynkaruk, O.; Qi, Y.; Cottrell-Callbeck, A.; Torres Delgado, W.; McDonald, R.; Ferguson, M. J.; He, G.; Rivard, E. *Organometallics* **2016**, *35*, 2232.
- (94) Oh, C. H.; Reddy, V. R. *Tetrahedron Lett.* **2004**, *45*, 8545.
- (95) Molander, G. A.; Traister, K. M. *Org. Lett.* **2013**, *15*, 5052.
- (96) Nishihara, Y.; Saito, D.; Inoue, E.; Okada, Y.; Miyazaki, M.; Inoue, Y.; Takagi, K. *Tetrahedron Lett.* **2010**, *51*, 306.
- (97) Taylor, C.; Bolshan, Y. *Org. Lett.* **2014**, *16*, 488.
- (98) Baxter, M.; Bolshan, Y. *Chem. Eur. J.* **2015**, *21*, 13535.
- (99) Fisher, K. M.; Bolshan, Y. *J. Org. Chem.* **2015**, *80*, 12676.
- (100) Wan, M.; Meng, Z.; Lou, H.; Liu, L. *Angew. Chem. Int. Ed.* **2014**, *53*, 13845.
- (101) William, R.; Wang, S.; Mallick, A.; Liu, X.-W. *Org. Lett.* **2016**, *18*, 4458.
- (102) (a) Mundal, D. A.; Lutz, K. E.; Thomson, R. J. *J. Am. Chem. Soc.* **2012**, *134*, 5782.
(b) Diagne, A. B.; Li, S.; Perkowski, G. A.; Mrksich, M.; Thomson, R. J. *ACS Combinatorial Science* **2015**, *17*, 658.
- (103) Wang, H.; Grohmann, C.; Nimphius, C.; Glorius, F. *J. Am. Chem. Soc.* **2012**, *134*, 19592.
- (104) Gandon, V.; Leca, D.; Aechtner, T.; Vollhardt, P. C., Malacria M., Aubert, C. *Org. Lett.* **2004**, *6*, 3405.

- (105) Gandon, V.; Leboeuf, D.; Amslinger, S.; Vollhardt, K. P. C.; Malacria, M.; Aubert, C. *Angew. Chem. Int. Ed.* **2005**, *44*, 7114.
- (106) Geny, A.; Leboeuf, D.; Rouquié, G.; Vollhardt, K. P. C.; Malacria, M.; Gandon, V.; Aubert, C. *Chem. Eur. J.* **2007**, *13*, 5408.
- (107) Iannazzo, L.; Vollhardt, P. C.; Malacria, M.; Aubert, C.; Gandon, V. *Eur. J. Org. Chem.* **2011**, 3283.
- (108) Melnes, S.; Bayer, A.; Gautun, O. R. *Tetrahedron* **2013**, *69*, 7910.
- (109) Seath, C. P.; Wilson, K. L.; Campbell, A.; Mowat, J. M.; Watson, A. J. B. *Chem. Commun.* **2016**, *52*, 8703.
- (110) Altenburger, K.; Arndt, P.; Spannenberg, A.; Baumann, W.; Rosenthal, U. *Eur. J. Inorg. Chem.* **2013**, *2013*, 3200.
- (111) Altenburger, K.; Arndt, P.; Spannenberg, A.; Rosenthal, U. *Eur. J. Inorg. Chem.* **2015**, *2015*, 44.
- (112) He, G.; Kang, L.; Torres Delgado, W.; Shynkaruk, O.; Ferguson, M. J.; McDonald, R.; Rivard, E. *J. Am. Chem. Soc.* **2013**, *135*, 5360.
- (113) Renaud, J.; Graf, C.-D.; Oberer, L. *Angew. Chem. Int. Ed.* **2000**, *39*, 3101.
- (114) Comas-Barceló, J.; Harrity, J. P. A. *Synthesis* **2017**, *49*, 1168.
- (115) Kirkham, J. D.; Edeson, S. J.; Stokes, S.; Harrity, J. P. A. *Org. Lett.* **2012**, *14*, 5354.
- (116) Fricero, P.; Bialy, L.; Brown, A. W.; Czechtizky, W.; Méndez, M.; Harrity, J. P. A. *J. Org. Chem.* **2017**, *82*, 1688.

- (117) Foster, R. S.; Adams, H.; Jakobi, H.; Harrity, J. P. A. *J. Org. Chem.* **2013**, *78*, 4049.
- (118) Harker, W. R. R.; Delaney, P. M.; Simms, M.; Tozer, M. J.; Harrity, J. P. A. *Tetrahedron* **2013**, *69*, 1546.
- (119) Crépin, D. F. P.; Harrity, J. P. A.; Jiang, J.; Meijer, A. J. H. M.; Nassoy, A.-C. M. A.; Raubo, P. *J. Am. Chem. Soc.* **2014**, *136*, 8642.
- (120) Bachollet, S. P. J. T.; Vivat, J. F.; Cocker, D. C.; Adams, H.; Harrity, J. P. A. *Chem. Eur. J.* **2014**, *20*, 12889.
- (121) Leon, T.; Fernandez, E. *Chem. Commun.* **2016**, *52*, 9363.
- (122) Mkhallid, I. A. I.; Barnard, J. H.; Marder, T. B.; Murphy, J. M.; Hartwig, J. F. *Chem. Rev.* **2010**, *110*, 890.
- (123) Davan, T.; Corcoran, E. W.; Sneddon, L. G. *Organometallics* **1983**, *2*, 1693.
- (124) Kadlecsek, D. E.; Carroll, P. J.; Sneddon, L. G. *J. Am. Chem. Soc.* **2000**, *122*, 10868.
- (125) Takaya, J.; Kirai, N.; Iwasawa, N. *J. Am. Chem. Soc.* **2011**, *133*, 12980.
- (126) Ohmura, T.; Kijima, A.; Suginome, M. *J. Am. Chem. Soc.* **2009**, *131*, 6070.
- (127) Kuninobu, Y.; Iwanaga, T.; Omura, T.; Takai, K. *Angew. Chem. Int. Ed.* **2013**, *52*, 4431.
- (128) Furukawa, T.; Tobisu, M.; Chatani, N. *Chem. Commun.* **2015**, *51*, 6508.
- (129) Lee, C.-I.; Hirscher, N. A.; Zhou, J.; Bhuvanesh, N.; Ozerov, O. V. *Organometallics* **2015**, *34*, 3099.

- (130) Johansson, R.; Wendt, O. F. *Organometallics* **2007**, *26*, 2426.
- (131) Adhikari, D.; Huffman, J. C.; Mindiola, D. J. *Chem. Commun.* **2007**, 4489.
- (132) Zhu, Y.; Chen, C.-H.; Fafard, C. M.; Foxman, B. M.; Ozerov, O. V. *Inorg. Chem.* **2011**, *50*, 7980.
- (133) Adhikary, A.; Schwartz, J. R.; Meadows, L. M.; Krause, J. A.; Guan, H. *Inorg. Chem. Front.* **2014**, *1*.
- (134) van der Boom, M. E.; Milstein, D. *Chem. Rev.* **2003**, *103*, 1759.
- (135) Morales-Morales, D. The Chemistry of PCP Pincer Phosphinite Transition Metal Complexes. In *The Chemistry of Pincer Compounds*; Morales-Morales, D.; Jensen, C. M., Eds Elsevier: Amsterdam, 2007; pp 151-179.
- (136) Chakraborty, S.; Zhang, J.; Patel, Y. J.; Krause, J. A.; Guan, H. *Inorg. Chem.* **2012**, *52*, 37.
- (137) Wang, Z.; Eberhard, M. R.; Jensen, C. M.; Matsukawa, S.; Yamamoto, Y. *J. Organomet. Chem.* **2003**, *681*, 189.
- (138) Wilson, G. L. O.; Abraha, M.; Krause, J. A.; Guan, H. *Dalton Trans.* **2015**, *44*, 12128.
- (139) Eberhard, M. R. *Org. Lett.* **2004**, *6*, 2125.
- (140) Yu, K.; Sommer, W.; Richardson, J. M.; Weck, M.; Jones, C. W. *Adv. Synth. Catal.* **2005**, *347*, 161.
- (141) de Vries, J. G. *Dalton Trans.* **2006**, 421.
- (142) Bolliger, J. L.; Blacque, O.; Frech, C. M. *Chem. Eur. J.* **2008**, *14*, 7969.

- (143) Melero, C.; Martinez-Prieto, L. M.; Palma, P.; Rio, D. d.; Alvarez, E.; Campora, J. *Chem. Commun.* **2010**, *46*, 8851.
- (144) Pun, D.; Diao, T.; Stahl, S. S. *J. Am. Chem. Soc.* **2013**, *135*, 8213.
- (145) Martinez-Prieto, L. M.; Melero, C.; Rio, D. d.; Palma, P.; Campora, J.; Alvarez, E. *Organometallics* **2012**, *31*, 1425.
- (146) Choi, J.; MacArthur, A. H. R.; Brookhart, M.; Goldman, A. S. *Chem. Rev.* **2011**, *111*, 1761.
- (147) Braunschweig, H.; Guethlein, F.; Mailänder, L.; Marder, T. B. *Chem. Eur. J.* **2013**, *19*, 14831.
- (148) Pässler, P.; Hefner, W.; Buckl, K.; Meinass, H.; Meiswinkel, A.; Wernicke, H.-J.; Ebersberg, G.; Müller, R.; Bässler, J.; Behringer, H.; Mayer, D., Acetylene. In *Ullmann's Encyclopedia of Industrial Chemistry*, Wiley-VCH Verlag GmbH & Co. KGaA: 2000.
- (149) Morales-Morales, D.; Grause, C.; Kasaoka, K.; Redón, R. o.; Cramer, R. E.; Jensen, C. M. *Inorg. Chim. Acta.* **2000**, *300–302*, 958.
- (150) Wang, Z.; Sugiarti, S.; Morales, C. M.; Jensen, C. M.; Morales-Morales, D. *Inorg. Chim. Acta.* **2006**, *359*, 1923.
- (151) Bedford, R. B.; Betham, M.; Charmant, J. P. H.; Haddow, M. F.; Orpen, A. G.; Pilaraski, L. T.; Coles, S. J.; Hursthouse, M. B. *Organometallics* **2007**, *26*, 6346.
- (152) Lai, K.-T.; Ho, W.-C.; Chiou, T.-W.; Liaw, W.-F. *Inorg. Chem.* **2013**, *52*, 4151.
- (153) Cid, J.; Carbó, J. J.; Fernández, E. *Chem. Eur. J.* **2012**, *18*, 1512.

- (154) Stewart, S. K.; Whiting, A. J. *Organomet. Chem.* **1994**, *482*, 293.
- (155) Ohmura, T.; Torigoe, T.; Suginome, M. *J. Am. Chem. Soc.* **2012**, *134*, 17416.
- (156) Miyaura, N. Metal-Catalyzed Cross-Coupling Reactions of Organoboron Compounds with Organic Halides. In *Metal-Catalyzed Cross-Coupling Reactions*; de Meijere, A., Diederich, F., Eds.; Wiley-VCH Verlag GmbH: Weinheim, 2008; p 41.
- (157) Marinetti, A.; Jullien, H.; Voituriez, A. *Chem. Soc. Rev.* **2012**, *41*, 4884.
- (158) Delaney, P. M.; Huang, J.; Macdonald, S. J. F.; Harrity, J. P. A. *Org. Lett.* **2008**, *10*, 781.
- (159) (a) Jang, H.-Y.; Krische, M. J. *J. Am. Chem. Soc.* **2004**, *126*, 7875. (b) Jang, H.-Y.; Hughes, F. W.; Gong, H. Zhang, J.; Brodbelt, J. S., Krische, M. J. *J. Am. Chem. Soc.* **2005**, *127*, 6174.
- (160) Wender, P. A.; Buschmann, N.; Cardin, N. B.; Jones, L. R.; Kan, C.; Kee, J.-M.; Kowalski, J. A.; Longcore, K. E. *Nat Chem* **2011**, *3*, 615.
- (161) Ham, Y. J.; Yu, H.; Kim, N. D.; Hah, J.-M.; Selim, K. B.; Choi, H. G.; Sim, T. *Tetrahedron* **2012**, *68*, 1918.
- (162) Martos-Redruejo, A.; López-Durán, R.; Buñuel, E; Cárdenas, D. J. *Chem. Commun.* **2014**, *50*, 10094.
- (163) Kinder, R. E.; Widenhoefer, R. A. *Org. Lett.* **2006**, *8*, 1967.
- (164) Xi, T.; Lu, Z. *ACS Catalysis* **2017**, *7*, 1181.
- (165) Chakrapani, H.; Liu, C.; Widenhoefer, R. A. *Org. Lett.* **2003**, *5*, 157.

- (166) Ishida, M.; Shibata, Y.; Noguchi, K.; Tanaka, K. *Chem. Eur. J.* **2011**, *17*, 12578.
- (167) Bhardwaj, V.; Gumber, D.; Abbot, V.; Dhiman, S.; Sharma, P. *RSC Adv.* **2015**, *5*, 15233.
- (168) Estevez, V.; Villacampa, M.; Menendez, J. C. *Chem. Soc. Rev.* **2014**, *43*, 4633.
- (169) Gulevich, A. V.; Dudnik, A. S.; Chernyak, N.; Gevorgyan, V. *Chem. Rev.* **2013**, *113*, 3084.
- (170) Sawano, T.; Thacker, N. C.; Lin, Z.; McIsaac, A. R.; Lin, W. *J. Am. Chem. Soc.* **2015**, *137*, 12241.
- (171) Sylvester, K. T.; Chirik, P. J. *J. Am. Chem. Soc.* **2009**, *131*, 8772.
- (172) Bauer, R. A.; DiBlasi, C. M.; Tan, D. S. *Org. Lett.* **2010**, *12*, 2084.
- (173) Lin, A.; Zhang, Z.-W.; Yang, J. *Org. Lett.* **2014**, *16*, 386.
- (174) Trost, B. M.; Rise, F. *J. Am. Chem. Soc.* **1987**, *109*, 3161.
- (175) Denmark, S. E.; Liu, J. H.-C. *J. Am. Chem. Soc.* **2007**, *129*, 3737.
- (176) Fan, B.-M.; Xie, J.-H.; Li, S.; Wang, L.-X.; Zhou, Q.-L. *Angew. Chem. Int. Ed.* **2007**, *46*, 1275.
- (177) Park, J. H.; Kim, S. M.; Chung, Y. K. *Chem. Eur. J.* **2011**, *17*, 10852.
- (178) Fairlamb, I. J. S. *Angew. Chem. Int. Ed.* **2004**, *43*, 1048.
- (179) Watson, I. D. G.; Toste, F. D. *Chem. Sci.* **2012**, *3*, 2899.
- (180) Jung, I. G.; Seo, J.; Lee, S. I.; Choi, S. Y.; Chung, Y. K. *Organometallics* **2006**, *25*, 4240.
- (181) Cao, P.; Zhang, X. *Angew. Chem. Int. Ed.* **2000**, *39*, 4104.

- (182) Nguiefack, J.-F.; Bolitt, V.; Sinou, D. *Tetrahedron Lett.* **1996**, *37*, 5527.
- (183) Kawai, H.; Oi, S.; Inoue, Y. *Heterocycles* **2006**, *67*, 101.
- (184) Tanaka, K.; Otake, Y.; Sagae, H.; Noguchi, K.; Hirano, M. *Angew. Chem. Int. Ed.* **2008**, *47*, 1312.
- (185) Evans, P. A.; Sawyer, J. R.; Lai, K. W.; Huffman, J. C. *Chem. Commun.* **2005**, 3971.
- (186) Ojima, I.; Zhu, J.; Vidal, E. S.; Kass, D. F. *J. Am. Chem. Soc.* **1998**, *120*, 6690.
- (187) Chatani, N.; Asaumi, T.; Ikeda, T.; Yorimitsu, S.; Ishii, Y.; Kakiuchi, F.; Murai, S. *J. Am. Chem. Soc.* **2000**, *122*, 12882.
- (188) Vessally, E. *RSC Adv.* **2016**, *6*, 18619.
- (189) Tanaka, K.; Otake, Y.; Hirano, M. *Org. Lett.* **2007**, *9*, 3953.
- (190) Yukiteru, I.; Mitsuhiro, Y. *Chemistry Letters* **2014**, *43*, 1758.
- (191) Anderson, W. K.; Corey, P. F. *J. Med. Chem.* **1977**, *20*, 1691-1694.
- (192) Tenaglia, A.; Gaillard, S. *Angew. Chem. Int. Ed.* **2008**, *47*, 2454.
- (193) Clavier, H.; Nolan, S. P. *Chem. Eur. J.* **2007**, *13*, 8029.
- (194) Yang, Q.; Alper, H.; Xiao, W.-J. *Org. Lett.* **2007**, *9*, 769.
- (195) Tran-Van, A.-F.; Huxol, E.; Basler, J. M.; Neuburger, M.; Adjizian, J.-J.; Ewels, C. P.; Wegner, H. A. *Org. Lett.* **2014** *16*, 1594.
- (196) Kang, S.-K.; Baik, T.-G.; Kulak, A. N.; Ha, Y.-H.; Lim, Y.; Park, J. *J. Am. Chem. Soc.* **2000**, *122*, 11529.

- (197) Strom, K. R.; Impastato, A. C.; Moy, K. J.; Landreth, A. J.; Snyder, J. K. *Org. Lett.* **2015**, *17*, 2126.
- (198) Tran-Van, A.-F.; Götz, S.; Neuburger, M.; Wegner, H. A. *Org. Lett.* **2014**, *16*, 2410.
- (199) Dai, H.; Liu, G.; Zhang, Z.; Yan, H.; Lu, C. *Organometallics* **2016**, *35*, 1488.
- (200) Sakai, N.; Suzuki, H.; Hori, H.; Ogiwara, Y. *Tetrahedron Lett.* **2017**, *58*, 63.
- (201) Bonomi, P.; Attieh, M. D.; Gonzato, C.; Haupt, K. *Chem. Eur. J.* **2016**, *22*, 10150.
- (202) Castillo, J.-C.; Orrego-Hernández, J.; Portilla, J. *Eur. J. of Org. Chem.* **2016**, 3824.
- (203) Preetz, A.; Drexler, H.-J.; Schulz, S.; Heller, D. *Tetrahedron: Asymmetry* **2010**, *21*, 1226.
- (204) Kong, J.-R.; Ngai, M.-Y.; Krische, M. J. *J. Am. Chem. Soc.* **2006**, *128*, 718.
- (205) Kang, B.; Kim, D.-h.; Do, Y.; Chang, S. *Org. Lett.* **2003**, *5*, 3041.
- (206) Miller, K. M.; Luanphaisarnnont, T.; Molinaro, C.; Jamison, T. F. *J. Am. Chem. Soc.* **2004**, *126*, 4130.
- (207) Li, H.; Walsh, P. J. *J. Am. Chem. Soc.* **2005**, *127*, 8355.
- (208) Trost, B. M. *Angew. Chem. Int. Ed. Engl.* **1995**, *34*, 259.
- (209) Leroyer, L.; Maraval, V.; Chauvin, R. *Chem. Rev.* **2012**, *112*, 1310.
- (210) Saito, S.; Yamamoto, Y. *Chem. Rev.* **2000**, *100*, 2901.
- (211) For iron catalysis: (a) Midya, G. C.; Paladhi, S.; Dhara, K.; Dash, J. *Chem. Commun.* **2011**, *47*, 6698. (b) Midya, G. C.; Parasar, B.; Dharab, K.; Dash, J. *Org. Biomol. Chem.* **2014**, *12*, 1812.

- (212) For rhenium catalysis: Kawata, A.; Kuninobu, Y.; Takai, K. *Chem. Lett.* **2009**, *38*, 836.
- (213) For ruthenium catalysis: (a) Chen, X.; Xue, P.; Sung, H. H. Y.; Williams, I. D.; Peruzzini, M.; Bianchini, C.; Jia, G. *Organometallics* **2005**, *24*, 4330. (b) Katayama, H.; Yari, H.; Tanaka, M.; Ozawa, F. *Chem Commun.* **2005**, 4336. (c) Bassetti, M.; Pasquini, C.; Raneri, A.; Rosato, D. *J. Org. Chem.* **2007**, *72*, 4558. (d) Hijazi, A.; Parkhomenko, K.; Djukic, J.-P.; Chemmi, A.; Pfeffer, M. *Adv. Synth. Catal.* **2008**, *350*, 1493. (e) Field, L. D.; Magill, A. M.; Shearer, T. K.; Dalgarno, S. J.; Bhadbhade, M. M. *Eur. J. Inorg. Chem.* **2011**, 3503. (f) Coniglio, A.; Bassetti, M.; García-Garrido, S. E.; Gimeno, J. *Adv. Synth. Catal.* **2012**, *354*, 148. (g) Alós, J.; Bolaño, T.; Esteruelas, M. A.; Oliván, M.; Oñate, E.; Valencia, M. *Inorg. Chem.* **2014**, *53*, 1195.
- (214) For iridium catalysis: (a) Ogata, K.; Toyota, A. *J. Organomet. Chem.* **2007**, *692*, 4139. (b) Forsyth, C. D.; Kerr, W. J.; Paterson, L. C. *Synlett*, **2013**, *24*, 587.
- (215) For nickel catalysis: Ogoshi, S.; Ueta, M.; Oka, M.-A.; Kurosawa, H. *Chem. Commun.* **2004**, 2732.
- (216) For palladium catalysis: (a) Wu, Y.-T.; Lin, W.-C.; Liu, C.-J.; Wu, C.-Y. *Adv. Synth. Catal.* **2008**, *350*, 1841. (b) Jahier, C.; Zatulochnaya, O. V.; Zvyagintsev, N. V.; Ananikov, V. P.; Gevorgyan, V. *Org. Lett.* **2012**, *14*, 2846. (c) Chen, T.; Guo, C.; Goto, M.; Han, L.-B. *Chem. Commun.* **2013**, *49*, 7489. (d) Xu, C.; Du, W.; Zeng, Y.; Dai, B.; Guo, H. *Org. Lett.* **2014**, *16*, 948.

- (217) For rhodium catalysis: (a) Katagiri, T.; Tsurugi, H.; Satoh, T.; Miura, M. *Chem. Commun.* **2008**, 3405. (b) Peng, H. M.; Zhao, J.; Li, X. *Adv. Synth. Catal.* **2009**, *351*, 1371. (c) Rubio-Pérez, L.; Azpíroz, R.; Di Giuseppe, A.; Polo, V.; Castarlenas, R.; Pérez-Torrente, J. J.; Oro, L. A. *Chem. Eur. J.* **2013**, *19*, 15304. (d) Mochizuki, K.; Sakai, K.; Kochi, T.; Kakiuchi, F. *Synthesis*, **2013**, *45*, 2088. (e) Xu, H.-D.; Zhang, R.-W.; Li, X.; Huang, S.; Tang, W. Hu, W.-H. *Org. Lett.* **2013**, *15*, 840.
- (218) For zirconium catalysis: Platel, R. H.; Schafer, L. L. *Chem. Commun.* **2012**, *48*, 10609.
- (219) Dash, A.; Eisen, M. S. *Org. Lett.* **2000**, *2*, 737.
- (220) (a) Nishiura, M.; Hou, Z.; Wakatsuki, Y.; Yamaki, T.; Miyamoto, T. *J. Am. Chem. Soc.* **2003**, *125*, 1184. (b) Nishiura, M.; Hou, Z. *J. Mol. Catal. A: Chem.* **2004**, *213*, 101. (c) Tazelaar, C. G. J.; Bambirra, S.; van Leusen, D.; Meetsma, A.; Hessen, B.; Teuben, J. H. *Organometallics* **2004**, *23*, 936. (d) Komeyama, K. K., T.; Takehira, K.; Takaki, K. *J. Org. Chem.* **2005**, *70*, 7260. (e) Ge, S.; Quiroga Norambuena, V. F.; Hessen, B. *Organometallics* **2007**, *26*, 6508. (f) Ge, S. M., A.; Hessen, B. *Organometallics* **2009**, *28*, 719.
- (221) Weng, W.; Guo, C.; Çelenligil-Çetin, R.; Foxman, B. M.; Ozerov, O. V. *Chem. Commun.* **2006**, 197.

- (222) These compounds were originally reported as dihydrides, but later work showed them to be stretched dihydrogen compounds. See: Smith, D.; Herbert, D. E.; Walensky, J. R.; Ozerov, O. V. *Organometallics*, **2013**, *32*, 2050.
- (223) Morales-Morales, D.; Redón, R.; Yung, C.; Jensen, C. M. *Inorg. Chim. Acta*. **2004**, *357*, 2953.
- (224) Bedford, R. B.; Betham, M.; Blake, M. E.; Coles, S. J.; Draper, S. M.; Hursthouse, M. B.; Scully, P. N. *Inorg. Chim. Acta*. **2006**, *359*, 1870.
- (225) See: Fryzuk, M. D.; MacNeil, P. A. *J. Am. Chem. Soc.* **1981**, *103*, 3592.
- (226) Negishi, E. I., Ed. *Handbook of Organopalladium Chemistry for Organic Synthesis*; Wiley-Interscience: New York, 2002.
- (227) Fan, L. PNP pincer ligands and their late transition metal complexes in the context of strong bond activation and catalysis. Ph. D. Thesis, Brandeis University, Waltham, MA, 2006.
- (228) (a) Ma, L.; Woloszynek, R. A.; Chen, W.; Ren, T.; Protasiewicz, J. D. *Organometallics*, **2006**, *25*, 3301. (b) Ma, L.; Imbesi, P. M.; Updergraff, J. B.; Hunter, A. D.; Protasiewicz, J. D. *Inorg. Chem.* **2007**, *46*, 5220.
- (229) Gründemann, S.; Albrecht, M.; Loch, J. A.; Faller, J. W.; Crabtree, R. H. *Organometallics*, **2001**, *20*, 5485.
- (230) Zhang, Y.; Song, G.; Ma, G.; Zhao, J.; Pan, C.-L.; Li, X. *Organometallics*, **2009**, *28*, 3233.

- (231) (a) Gründemann, S.; Limbach, H. H.; Buntkowsky, G.; Sabo-Etienne, S.; Chaudret, B. *J. Chem. Phys. A* **1999**, *103*, 4752. (b) Gelabert, R.; Moreno, M.; Lluch, J. M.; Lledós, A.; Pons, V.; Heinekey, D. M. *J. Am. Chem. Soc.* **2004**, *126*, 8813.
- (232) Kubas, G. J. *Proc. Natl. Acad. Sci.* **2007**, *104*, 6901.
- (233) Timpa, S. D.; Fafard, C. M.; Herbert, D. E.; Ozerov, O. V. *Dalton Trans.* **2011**, *40*, 5426.
- (234) Montag, M.; Schwartsburd, L.; Cohen, R.; Leitius, G.; Ben-David, Y.; Martin, J. M. L.; Milstein, D. *Angew. Chem. Int. Ed.* **2007**, *46*, 1901.
- (235) Gatard, S.; Chen, C.-H.; Foxman, B. M.; Ozerov, O. V. *Organometallics*, **2008**, *27*, 6257.
- (236) Göttker-Schnetmann, I.; White, P.; Brookhart, M. *J. Am. Chem. Soc.* **2004**, *126*, 1804.
- (237) Salem, H.; Ben-David, Y.; Shimon, L. J. W.; Milstein, D. *Organometallics*, **2006**, *25*, 2292.
- (238) Polzhaev, A. V.; Kuklin, S. A.; Ivanov, D. M.; Petrovskii, P. V.; Dolgushin, F. M.; Ezernitskaya, M. G.; Koridze, A. A. *Russ. Chem. Bull. Int. Ed.* **2009**, *58*, 1847.
- (239) For a discussion of issues in using CO as a reporter of electron density at the metal, see Gusev, D. G. *Organometallics* **2009**, *28*, 763 and references therein.
- (240) Werner, H.; Baum, M.; Schneider, D.; Windmüller, B. *Organometallics*, **1994**, *13*, 1089.

- (241) Ghosh, R.; Zhang, X.; Achord, P.; Emge, T. J.; Krogh-Jespersen, K.; Goldman, A. *S. J. Am. Chem. Soc.* **2007**, *129*, 853.
- (242) (a) Carlton, L.; Read, G. *J. Chem. Soc., Perkin Trans. 1*, **1978**, 1631. (b) Ohshita, J.; Furumori, K.; Matsuguchi, A.; Ishikawa, M. *J. Org. Chem.* **1990**, *55*, 3277.
- (243) Giordano, G.; Crabtree, R. H. *Inorg. Synth.* **1990**, *28*, 88.
- (244) Sheldrick, W. S.; Günther, B. *J. Organomet. Chem.*, **1989**, *375*, 233.
- (245) Van der Ent, A.; Onderdelinden, A. L. *Inorg. Synth.* **1990**, *28*, 90.
- (246) (a) Hatakeyama, T.; Toshimoto, Y.; Gabriel, T.; Nakamura, M. *Org. Lett.*, **2008**, *23*, 5341-5344. (b) Yang, C.; Nolan, S. *J. Org. Chem.*, **2002**, *67*, 591.
- (247) Negishi, E.-i. *Angew. Chem. Int. Ed.* **2011**, *50*, 6738.
- (248) Haas, D.; Hammann, J. M.; Greiner, R.; Knochel, P. *ACS Catalysis* **2016**, *6*, 1540.
- (249) (a) Takahashi, H.; Inagaki, S.; Yoshii, N.; Gao, F.; Nishihara, Y.; Takagi, K. *J. Org. Chem.* **2009**, *74*, 2794. (b) Ejiri, S.; Odo, S.; Takahashi, H.; Nishimura, Y.; Gotoh, K.; Nishihara, Y.; Takagi, K. *Org. Lett.* **2010**, *12*, 1692.
- (250) García-Melchor, M.; Braga, A. A. C.; Lledós, A.; Ujaque, G.; Maseras, F. *Acc. Chem. Res.* **2013**, *46*, 2626.
- (251) Gatard, S.; Celenligil-Cetin, R.; Guo, C.; Foxman, B. M.; Ozerov, O. V. *J. Am. Chem. Soc.* **2006**, *128*, 2808.
- (252) (a) Timpa, S. D.; Pell, C. J.; Zhou, J.; Ozerov, O. V. *Organometallics* **2014**, *33*, 5254. (b) Timpa, S. D.; Pell, C. J.; Ozerov, O. V. *J. Am. Chem. Soc.* **2014**, *136*, 14772. (c) Pell, C. J.; Ozerov, O. V. *ACS Catalysis* **2014**, *4*, 3470.

- (253) Hanson, S. K.; Heinekey, D. M.; Goldberg, K. I. *Organometallics* **2008**, *27*, 1454.
- (254) Hlavinka, M. L.; Hagadorn, J. R. *Organometallics* **2005**, *24*, 4116.
- (255) Geerts, R. L.; Huffman, J. C.; Westerberg, D. E.; Folting, K.; Caulton, K. G. *New J. Chem.* **1988**, *12*.
- (256) Ekkert, O.; White, A. J. P.; Toms, H.; Crimmin, M. R. *Chem. Sci.* **2015**, *6*, 5617.
- (257) Geerts, R. L.; Huffman, J. C.; Caulton, K. G. *Inorg. Chem.* **1986**, *25*, 590.
- (258) (a) Fryzuk, M. D.; McConville, D. H.; Rettig, S. J. *Organometallics* **1990**, *9*, 1359. (b) Fryzuk, M. D.; McConville, D. H.; Rettig, S. J. *Organometallics* **1993**, *12*, 2152.
- (259) (a) Cadenbach, T.; Bollermann, T.; Gemel, C.; Tombul, M.; Fernandez, I.; Hopffgarten, M. v.; Frenking, G.; Fischer, R. A. *J. Am. Chem. Soc.* **2009**, *131*, 16063. (b) Molon, M.; Cadenbach, T.; Bollermann, T.; Gemel, C.; Fischer, R. A. *Chem. Commun.* **2010**, *46*, 5677.
- (260) Zhu, J.; Lin, Z.; Marder, T. B. *Inorg. Chem.* **2005**, *44*, 9384.
- (261) Smith, D. W. *J. Chem. Ed.* **2005**, *82*, 1202.
- (262) Fafard, C. M.; Chen, C.-H.; Foxman, B. M.; Ozerov, O. V. *Chem. Commun.* **2007**, 4465.
- (263) Kreye, M.; Freytag, M.; Jones, P. G.; Williard, P. G.; Bernskoetter, W. H.; Walter, M. D. *Chem. Commun.* **2015**, *51*, 2946.

- (264) (a) Bollermann, T.; Gemel, C.; Fischer, R. A. *Coord. Chem. Rev.* **2012**, *256*, 537.
(b) Molon, M.; Gemel, C.; Seidel, R. W.; Jerabek, P.; Frenking, G.; Fischer, R. A. *Inorg. Chem.* **2013**, *52*, 7152. (c) Molon, M.; Gemel, C.; Jerabek, P.; Trombach, L.; Frenking, G.; Fischer, R. A. *Inorg. Chem.* **2014**, *53*, 10403.
- (265) Kreider-Mueller, A.; Quinlivan, P. J.; Rauch, M.; Owen, J. S.; Parkin, G. *Chem. Commun.* **2016**, *52*, 2358.
- (266) Riddlestone, I. M.; Rajabi, N. A.; Lowe, J. P.; Mahon, M. F.; Macgregor, S. A.; Whittlesey, M. K. *J. Am. Chem. Soc.* **2016**, *138*, 11081.
- (267) Kratish, Y.; Molev, G.; Kostenko, A.; Sheberla, D.; Tumanskii, B.; Botoshansky, M.; Shimada, S.; Bravo-Zhivotovskii, D.; Apeloig, Y. *Angew. Chem. Int. Ed.* **2015**, *54*, 11817.
- (268) Oeschger, R. J.; Chen, P. *Organometallics* **2017**, *36*, 1465.
- (269) (a) Chass, G. A.; O'Brien, C. J.; Hadei, N.; Kantchev, E. A. B.; Mu, W.-H.; Fang, D.-C.; Hopkinson, A. C.; Csizmadia, I. G.; Organ, M. G. *Chem. Eur. J.* **2009**, *15*, 4281. (b) Fuentes, B.; García-Melchor, M.; Lledós, A.; Maseras, F.; Casares, J. A.; Ujaque, G.; Espinet, P. *Chem. Eur. J.* **2010**, *16*, 8596.
- (270) Smith, D. A.; Ozerov, O. V. *Chem. Commun.* **2011**, *47*, 10779.
- (271) Gatard, S.; Guo, C.; Foxman, B. M.; Ozerov, O. V. *Organometallics* **2007**, *26*, 6066.
- (272) Puri, M.; Gatard, S.; Smith, D. A.; Ozerov, O. V. *Organometallics* **2011**, *30*, 2472.

- (273) González-Pérez, A. B.; Álvarez, R.; Faza, O. N.; de Lera, Á. R.; Aurrecochea, J. M. *Organometallics* **2012**, *31*, 2053.
- (274) Behrens, M.; Studt, F.; Kasatkin, I.; Köhl, S.; Hävecker, M.; Abild-Pedersen, F.; Zander, S.; Girgsdies, F.; Kurr, P.; Knief, B.-L.; Tovar, M.; Fischer, R. W.; Nørskov, J. K.; Schlögl, R. *Science* **2012**, *336*, 893.
- (275) Wiegand, A.-K.; Rit, A.; Okuda, J. *Coord. Chem. Rev.* **2016**, *314*, 71.
- (276) Cammarota, R. C.; Lu, C. C. *J. Am. Chem. Soc.* **2015**, *137*, 12486.
- (277) Butler, M. J.; Crimmin, M. R. *Chem. Commun.* **2017**, *53*, 1348.
- (278) Ozerov, O. V.; Guo, C.; Papkov, V. A.; Foxman, B. M. *J. Am. Chem. Soc.* **2004**, *126*, 4792.
- (279) Kimura, M.; Tatsuyama, Y.; Kojima, K.; Tamaru, Y. *Org. Lett.* **2007**, *9*, 1871.
- (280) Schley, N. D.; Fu, G. C. *J. Am. Chem. Soc.* **2014**, *136*, 16588.
- (281) APEX2, Version 2 User Manual, M86-E01078, Bruker Analytical X-ray Systems, Madison, WI, June 2006.
- (282) G.M. Sheldrick “SADABS (version 2008/1): Program for Absorption Correction for Data from Area Detector Frames”, University of Göttingen, 2008
- (283) Sheldrick, G. M. *Acta Crystallogr. Sect. A* **2008**, *64*, 112.
- (284) Spek, A. L. (1998) PLATON – A Multipurpose Crystallographic Tool, Utrecht University: Utrecht, The Netherlands.
- (285) Spek, A. L. *Acta Cryst. C* **2005**, *71*, 9.

- (286) Taw, F. L.; Clark, A. E.; Mueller, A. H.; Janicke, M. T.; Cantat, T.; Scott, B. L.; Hay, P. J.; Hughes, R. P.; Kiplinger, J. L. *Organometallics* **2012**, *31*, 1484.
- (287) (a) Zhu, W.; Wang, J.; Wang, S.; Gu, Z.; Aceña, J. L.; Izawa, K.; Liu, H.; Soloshonok, V. A. *J. Fluorine Chem.* **2014**, *167*, 37. (b) Ohashi, M.; Shirataki, H.; Kikushima, K.; Ogoshi, S. *J. Am. Chem. Soc.* **2015**, *137*, 6496.
- (288) (a) Hughes, R. P.; Laritchev, R. B.; Yuan, J.; Golen, J. A.; Rucker, A. N.; Rheingold, A. L. *J. Am. Chem. Soc.* **2005**, *127*, 15020. (b) Bourgeois, C. J.; Hughes, R. P.; Yuan, J.; DiPasquale, A. G.; Rheingold, A. L. *Organometallics* **2006**, *25*, 2908. (c) Hughes, R. P. *J. Fluorine Chem.* **2010**, *131*, 1059.
- (289) Yuan, J.; Hughes, R. P.; Golen, J. A.; Rheingold, A. L. *Organometallics* **2010**, *29*, 1942.
- (290) Harrison, D. J.; Gorelsky, S. I.; Lee, G. M.; Korobkov, I.; Baker, R. T. *Organometallics* **2013**, *32*, 12.
- (291) Lee, G. M.; Harrison, D. J.; Korobkov, I.; Baker, R. T. *Chem. Commun.* **2014**, *50*, 1128.
- (292) (a) Harrison, D. J.; Lee, G. M.; Leclerc, M. C.; Korobkov, I.; Baker, R. T. *J. Am. Chem. Soc.* **2013**, *135*, 18296. (b) Fuller, J. T.; Harrison, D. J.; Leclerc, M. C.; Baker, R. T.; Ess, D. H.; Hughes, R. P. *Organometallics* **2015**, *34*, 5210.
- (293) Harrison, D. J.; Daniels, A. L.; Korobkov, I.; Baker, R. T. *Organometallics* **2015**, *34*, 4598.

- (294) Leclerc, M. C.; Bayne, J. M.; Lee, G. M.; Gorelsky, S. I.; Vasiliu, M.; Korobkov, I.; Harrison, D. J.; Dixon, D. A.; Baker, R. T. *J. Am. Chem. Soc.* **2015**, *137*, 16064.
- (295) (a) Huang, H.; Hughes, R. P.; Landis, C. R.; Rheingold, A. L. *J. Am. Chem. Soc.* **2006**, *128*, 7454. (b) Huang, H.; Hughes, R. P.; Rheingold, A. L. *Dalton Trans.* **2011**, *40*, 47.
- (296) (a) Lyon, J. T.; Andrews, L. *Inorg. Chem.* **2006**, *45*, 9858. (b) Lyon, J. T.; Cho, H.-G.; Andrews, L. *Organometallics* **2007**, *26*, 6373. (c) Lyon, J. T.; Andrews, L. *Eur. J. Inorg. Chem.* **2008**, *2008*, 1047.
- (297) Schrock, R. R. *Acc. Chem. Res.* **1986**, *19*, 342.
- (298) Schrock, R. R. *Chem. Rev.* **2002**, *102*, 145.
- (299) Ozerov, O. V.; Watson, L. A.; Pink, M.; Caulton, K. G. *J. Am. Chem. Soc.* **2007**, *129*, 6003.
- (300) Jia, G. *Coord. Chem. Rev.* **2007**, *251*, 2167.
- (301) (a) Caskey, S. R.; Stewart, M. H.; Ahn, Y. J.; Johnson, M. J. A.; Rowsell, J. L. C.; Kampf, J. W. *Organometallics* **2007**, *26*, 1912. (b) Shao, M.; Zheng, L.; Qiao, W.; Wang, J.; Wang, J. *Adv. Synth. Catal.* **2012**, *354*, 2743.
- (302) (a) Ramírez-Contreras, R.; Bhuvanesh, N.; Ozerov, O. V. *Organometallics* **2015**, *34*, 1143 and references within. (b) Kurogi, T.; Carroll, P. J.; Mindiola, D. J. *J. Am. Chem. Soc.* **2016**, *138*, 4306.
- (303) Luecke, H. F.; Bergman, R. G. *J. Am. Chem. Soc.* **1998**, *120*, 11008.

- (304) Rappert, T.; Nuernberg, O.; Mahr, N.; Wolf, J.; Werner, H. *Organometallics* **1992**, *11*, 4156.
- (305) Nugent, W. A.; Mayer, J. M. *Metal-Ligand Multiple Bonds*; John Wiley & Sons: New York, 1988.
- (306) (a) Holm, R. H. *Chem. Rev.* **1987**, *87*, 1401. (b) Mayer, J. M. *Comments on Inorg. Chem.* **1988**, *8*, 125. (c) Betley, T. A.; Wu, Q.; Van Voorhis, T.; Nocera, D. G. *Inorg. Chem.* **2008**, *47*, 1849.
- (307) Zhu, Y.; Smith, D. A.; Herbert, D. E.; Gatard, S.; Ozerov, O. V. *Chem. Commun.* **2012**, *48*, 218.
- (308) Goodman, J.; Grushin, V. V.; Larichev, R. B.; Macgregor, S. A.; Marshall, W. J.; Roe, D. C. *J. Am. Chem. Soc.* **2009**, *131*, 4236.
- (309) Choi, J.; Wang, D. Y.; Kundu, S.; Choliy, Y.; Emge, T. J.; Krogh-Jespersen, K.; Goldman, A. S. *Science* **2011**, *332*, 1545.
- (310) (a) Hughes, R. P. *Eur. J. Inorg. Chem.* **2009**, 4591. (b) Brothers, P. J.; Roper, W. R. *Chem. Rev.* **1988**, *88*, 1293.
- (311) Reichenbacher, K.; Suss, H. I.; Hulliger, J. *Chem. Soc. Rev.* **2005**, *34*, 22.
- (312) Kui, S. C. F.; Zhu, N.; Chan, M. C. W. *Angew. Chem. Int. Ed.* **2003**, *42*, 1628.
- (313) Leclerc, M. C.; Gorelsky, S. I.; Gabidullin, B. M.; Korobkov, I.; Baker, R. T. *Chem. Eur. J.* **2016**, *22*, 8063.

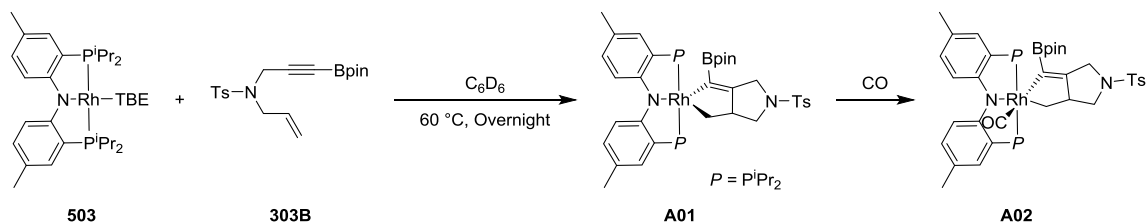
- (314) (a) Fischer, E. O.; Kreis, G.; Kreiter, C. G.; Mülle, J.; Huttner, G.; Lorenz, H. *Angew. Chem.* **1973**, *85*, 618. (b) Fischer, E. O.; Schubert, U.; Kleine, W.; Fischer, H. *Inorg. Synth.* **1979**, *19*, 172.
- (315) Gusev, D. G.; Ozerov, O. V. *Chem. Eur. J.* **2011**, *17*, 634.
- (316) Douvris, C.; Ozerov, O. V. *Science* **2008**, *321*, 1188.
- (317) Hoffmann, S. P.; Kato, T.; Tham, F. S.; Reed, C. A. *Chem. Commun.* **2006**, 767.
- (318) Press, L. P.; McCulloch, B. J.; Gu, W.; Chen, C.-H.; Foxman, B. M.; Ozerov, O. V. *Chem. Commun.* **2015**, *51*, 14034.
- (319) Alonso, F. J. G.; Höhn, A.; Wolf, J.; Otto, H.; Werner, H. *Angew. Chem. Int. Ed.* **1985**, *24*, 406.
- (320) Harvey, J. N. *Annu. Rep. Prog. Chem., Sect. C*, **2006**, *102*, 203.
- (321) Cundari, T. R. *Comprehensive Organometallic Chemistry III*, **2007**, *1*, 639.
- (322) Landis, C. R.; Weinhold, F. in *The Chemical Bond: Fundamental Aspects of Chemical Bonding*; Frenking, G.; Shaik, S. Ed.; Wiley-VCH Verlag GmbH & Co. KGaA: Weinheim, 2014; vol. 1, p 91-119.
- (323) Glendening, E. D.; Badenhop, J. K.; Reed, A. K.; Carpenter, J. E.; Bohmann, J. A.; Morales, C. M.; Landis, C. R.; Weinhold F. *NBO 6.0*, Theoretical Chemistry Institute, University of Wisconsin, Madison, 2013.
- (324) Weinhold, F.; Landis, C. R. *Discovering Chemistry with Natural Bond Orbitals*; John Wiley & Sons: Hoboken, 2012.

- (325) Glendening, E. D.; Landis, C. R.; Weinhold, F. *Wiley Interdisciplinary Reviews: Computational Molecular Science*, **2012**, 2, 1.
- (326) Weinhold F.; and Landis, C. R. *Valency and Bonding: A Natural Bond Orbital Donor-Acceptor Perspective*, Cambridge University Press: Cambridge, 2005.
- (327) Reed, A. E.; Curtiss, L. A.; Weinhold, F. *Chem. Rev.* **1988**, 88, 899.
- (328) Wiberg, L. A. *Tetrahedron* **1968**, 24, 1083.
- (329) Zhao, Y.; Truhlar, D. G. *Theor. Chem. Acc.* **2008**, 120, 215.
- (330) Zhao, Y.; Truhlar, D. G. *Acc. Chem. Res.* **2008**, 41, 157.
- (331) Wadt, W. R.; Hay, P. J. *J. Chem. Phys.* **1985**, 82, 284.
- (332) Hay, P. J.; Wadt, W. R. *J. Chem. Phys.* **1985**, 82, 299.
- (333) Hay, P. J.; Wadt, W. R. *J. Chem. Phys.* **1985**, 82, 270.
- (334) Dunning, T. H.; Hay, P. J. in *Modern Theoretical Chemistry, Vol. 4: Applications of Electronic Structure Theory*; Schaefer III, H. F. Ed.; Plenum, 1977, p 461.
- (335) Frisch, M. J.; Pople, J. A.; Binkley, J. S. *J. Chem. Phys.* **1984**, 80, 3265.
- (336) Clark, T.; Chandrasekhar, J.; Spitznagel, G. W.; Schleyer, P. V. R. *J. Comput. Chem.* **1983**, 4, 294.
- (337) McLean, A. D.; Chandler, G. S. *J. Chem. Phys.* **1980**, 72, 5639.
- (338) Krishnan, R.; Binkley, J. S.; Seeger, R.; Pople, J. A. *J. Chem. Phys.* **1980**, 72, 650.
- (339) Bochevarov, A. D.; Harder, E.; Hughes, T. F.; Greenwood, J. R.; Braden, D. A.; Philipp, D. M.; Rinaldo, D.; Halls, M. D.; Zhang, J.; Friesner, R. A. *Int. J. Quantum Chem.* **2013**, 113, 2110.

- (340) *Jaguar, versions 7.0-9.3*; Schrödinger, LLC: New York, 2007-2016.
- (341) Lentz, D.; Bach, A.; Buschmann, J.; Luger, P.; Messerschmidt, M. *Chem. Eur. J.* **2004**, *10*, 5059.
- (342) Groom, C. R.; Bruno, I. J.; Lightfoot, M. P.; Ward, S. C. *Acta Crystallogr.* **2016**, *B72*, 171.
- (343) Crabtree, R. H.; Mingos, M. *Comprehensive Organometallic Chemistry III*, Elsevier: New York, 2006.
- (344) Guggenberger, L. J.; Cramer, R. *J. Am. Chem. Soc.* **1972**, *94*, 3779.
- (345) Wu, H.; Hall, M. B. *Dalton Trans.* **2009**, 5933.
- (346) (a) Curnow, O. J.; Hughes, R. P.; Rheingold, A. L. *J. Am. Chem. Soc.* **1992**, *114*, 3153. (b) Curnow, O. J.; Hughes, R. P.; Mairs, E. N.; Rheingold, A. L. *Organometallics*, **1993**, *12*, 3102.

APPENDIX A

SYNTHESIS OF BORYLATED METALLACYCLOPENTENES AND ATTEMPTS AT PAUSON KHAND CYCLIZATION WITH ALKYNYLBORONATES



Scheme A-1. Synthesis of **A01** and observation of **A02**.

Synthesis of (PNP)Rhodacycle (A01). **503** (125 mg, 0.20 mmol) was dissolved in fluorobenzene in a screw-top flask and was treated with **303B** (75 mg, 0.20 mmol). The reaction was heated at 60 °C overnight. The solution was filtered through a pad of Celite and the volatiles were removed to yield a brown solid. The resulting solid was rinsed with pentane. The pentane dissolved a red product that was decanted from a green solid that was insoluble in pentane. The green solid was dissolved in toluene, and layered with pentane before being placed in a -35 °C freezer to recrystallize overnight. The product was isolated as a green solid (61 mg, 34% yield). $^{31}\text{P}\{^1\text{H}\}$ NMR (C_6D_6): δ 44.9 (dd, $J_{\text{P-P}} = 353$ Hz, $J_{\text{P-Rh}} = 124$ Hz, 1P), 41.6 (dd, $J_{\text{P-P}} = 353$ Hz, $J_{\text{P-Rh}} = 124$ Hz, 1P); ^1H NMR (C_6D_6): δ 7.77 (d, $J = 8$ Hz, 2H, tosyl Ar-*H*), 7.65 (dd, $J = 8.5$ Hz, $J = 4$ Hz, 1H, Ar-*H*), 7.57 (dd, $J = 8.5$ Hz, $J = 4$ Hz, 1H, Ar-*H*), 6.89 (d, $J = 7$ Hz, 1H, Ar-*H*), 6.83 (m, 3H, overlapping Ar-*H*), 6.72 (d, $J = 8$ Hz, 2H, tosyl Ar-*H*), 4.53 (d, $J = 15.5$ Hz, 1H,

C(sp²)-CH_aH_b-N), 4.25 (d, *J* = 15 Hz, C(sp²)-CH_aH_b-N), 3.88 (dd, *J* = 10.5 Hz, *J* = 6 Hz, 1H, C(sp³)-CH_aH_b-N), 3.18 (m, 1H, Rh-CH₂-C-H), 2.91 (m, 1H, PCHMe₂), 2.61 (dd apparent t, *J* = 10.5 Hz, C(sp³)-CH_aH_b-N), 2.39 (m, 1H, PCHMe₂), 2.31 (m, 1H, PCHMe₂), 2.24 (m, 1H, Rh-CH_aH_b, signal obscured by Ar-Me peak, cross peak was observed by HSQC), 2.21 (s, 3H, Ar-Me), 2.17 (s, 3H, Ar-Me), 2.16 (m, 1H, Rh-CH_aH_b, signal obscured by Ar-Me peak, cross peak observed by HSQC experiment), 2.04 (m, 2H, PCHMe₂), 1.86 (s, 3H, Ar-Me), 1.24 (m, 1H, 1.18 (dd, *J* = 14 Hz, *J* = 7 Hz, 3H, PCHMe₂), 1.11 (dd, *J* = 14.5 Hz, *J* = 7 Hz, 3H, PCHMe₂), 1.022 (s, 6H, Me of Bpin), 1.02 (dd, 3H, overlapped by Bpin methyls), 1.016 (s, 6H, Me of Bpin), 0.96 (m, overlapping PCHMe₂), 0.89 (dd, *J* = 11 Hz, *J* = 7 Hz, 3H, PCHMe₂), 0.85 (dd, 3H, coupling obscured by residual pentane in the solvent). ¹³C{¹H} NMR (C₆D₆): δ 163.5 (dvt, *J* = 21.6 Hz, *J* = 8.4 Hz, C-N of PNP), 160.4 (dvt, *J* = 18.1 Hz, *J* = 2.4 Hz, C-N of PNP), 141.9 (s), 136.8 (s), 132.8 (s, Ar-H), 132.5 (s, Ar-H), 132.2 (s, Ar-H), 132.1 (s, Ar-H), 129.5 (s, Ar-H on tosyl), 127.7 (s, Ar-H on tosyl), 124.5 (d, *J* = 6.0 Hz), 123.3 (d, *J* = 6.2 Hz), 121.9 (d, *J* = 36.0 Hz, Ar-P), 119.8 (d, *J* = 38.1 Hz, Ar-P), 117.6 (d, *J* = 8.9 Hz), 116.0 (bs, C(sp²)-C-Bpin), 114.4 (d, *J* = 9.3 Hz), 82.5 (s, quaternary carbon on Bpin), 56.8 (t, 4.0 Hz, Rh-CH₂-CH), 48.8 (s, C(sp²)-CH₂-N), 46.0 (s, C(sp³)-CH₂-N), 26.1 (dd, *J* = 16 Hz, *J* = 3.5 Hz, PCHMe₂), 25.6 (s, Me on Bpin), 24.4 (s, Me on Bpin), 23.2 (dd, *J* = 20.9 Hz, *J* = 5.3 Hz, PCHMe₂), 22.2 (m, 2x overlapping PCHMe₂), 21.4 (s, Ar-Me), 20.7 (s, Ar-Me), 20.6 (s, Ar-Me), 18.8 (m, 4x overlapping PCHMe), 17.7 (d, *J* = 4.2 Hz, PCHMe), 17.5 (d, *J* = 5 Hz, PCHMe), 17.1 (d, *J* = 5 Hz, PCHMe), 17.8 (d, *J* = 4.4 Hz, PCHMe), 1.7 (dt, *J* = 23.5 Hz, *J* = 3.4 Hz, Rh-CH₂).

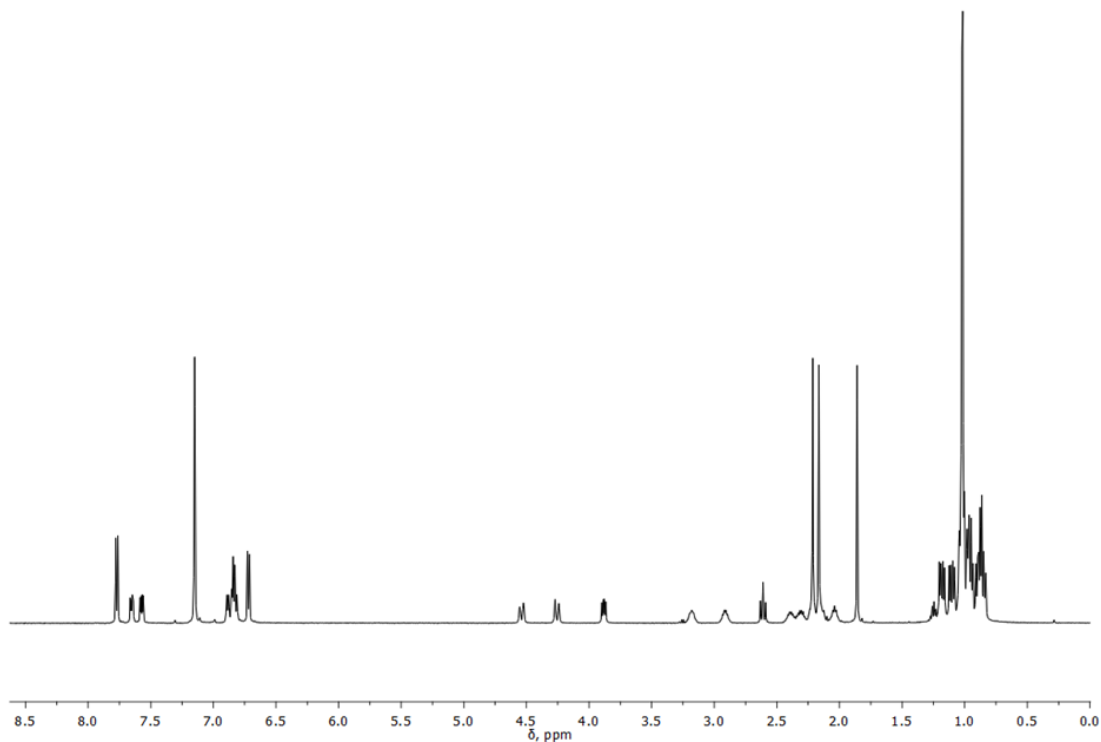
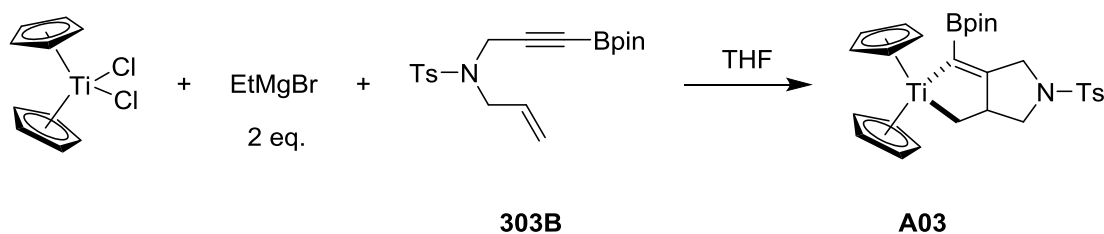


Figure A-1. ^1H NMR of **A01** in C_6D_6 .

Treatment of A01 with an atmosphere of CO. **503** (14 mg, 0.023 mmol) was dissolved in C_6D_6 and treated with **303B** (9 mg, 0.024 mmol) in a J. Young tube. After 5 days at room temperature, **A01** was observed to compose 90% of the mixture by $^{31}\text{P}\{^1\text{H}\}$ NMR spectroscopy. The J. Young tube was degassed using the “freeze-pump-thaw” method, and an atmosphere of CO was added. The solution turned from redish-brown to yellow. Analysis by $^{31}\text{P}\{^1\text{H}\}$ NMR spectroscopy showed about 33% **(PNP)RhCO** and a 66% of a new C_1 symmetric product, presumably **A02** [$^{31}\text{P}\{^1\text{H}\}$ NMR (C_6D_6): δ 51.1

(dd, $J_{P-P} = 357$ Hz, $J_{P-Rh} = 107$ Hz, 1P), 47.1 (dd, $J_{P-P} = 357$ Hz, $J_{P-Rh} = 107$ Hz)]. The reaction mixture was then heated at 60 °C for 1 h at which point complete conversion to (PNP)RhCO was observed by $^{31}\text{P}\{^1\text{H}\}$ NMR spectroscopy. The scale of this reaction precluded isolation of the organic products that result from the displacement of the enyne from rhodium.



Scheme A-2. Synthesis of **A03** from Cp_2TiCl_2 .

Synthesis of A03. This synthetic procedure was adapted from the literature.* In a Schlenk flask, Cp_2TiCl_2 (66 mg, 0.27 mmol) was dissolved in THF. EtMgCl (266 μL , 2.0 M/ether) was added to the reaction mixture at -78 °C followed by a THF solution of **303B** (100 mg, 0.27 mmol). The reaction was allowed to warm to room temperature and was stirred overnight. The solution was filtered through a pad of Celite and the volatiles were removed under vacuum. The solid was redissolved in THF and layered with pentane and placed in a -35 °C freezer. **A03** was isolated as a red solid (70 mg, 48% yield, 85% purity). ^1H NMR 7.83 (d, $J = 8$ Hz, 2H, Ar-*H*), 6.77 (d, $J = 8$ Hz, 2H, Ar-*H*),

* Grossman, R. B.; Buchwald, S. L. *J. Org. Chem.* **1992**, *57*, 5803.

5.83 (s, 5H, Cp), 5.79 (s, 5H, Cp), 4.17 (dd, $J = 15$ Hz, $J = 1.5$ Hz, 1H, NCH_aH_b), 3.75 (dd, $J = 8.5$ Hz, $J = 8.5$ Hz, 1H, $\text{NCH}_a\text{H}_b\text{CH}$), 3.68 (dd, $J = 15$ Hz, $J = 2.5$ Hz, 1H, NCH_aH_b), 2.68 (m, 1H, CH), 2.37 (dd, $J = 10$ Hz, 8.5 Hz, $\text{NCH}_a\text{H}_b\text{CH}$), 1.88 (dd, $J = 11$ Hz, $J = 11$ Hz, 1H, TiCH_aH_b), 0.99 (dd, $J = 11$ Hz, $J = 7$ Hz, TiCH_aH_b).

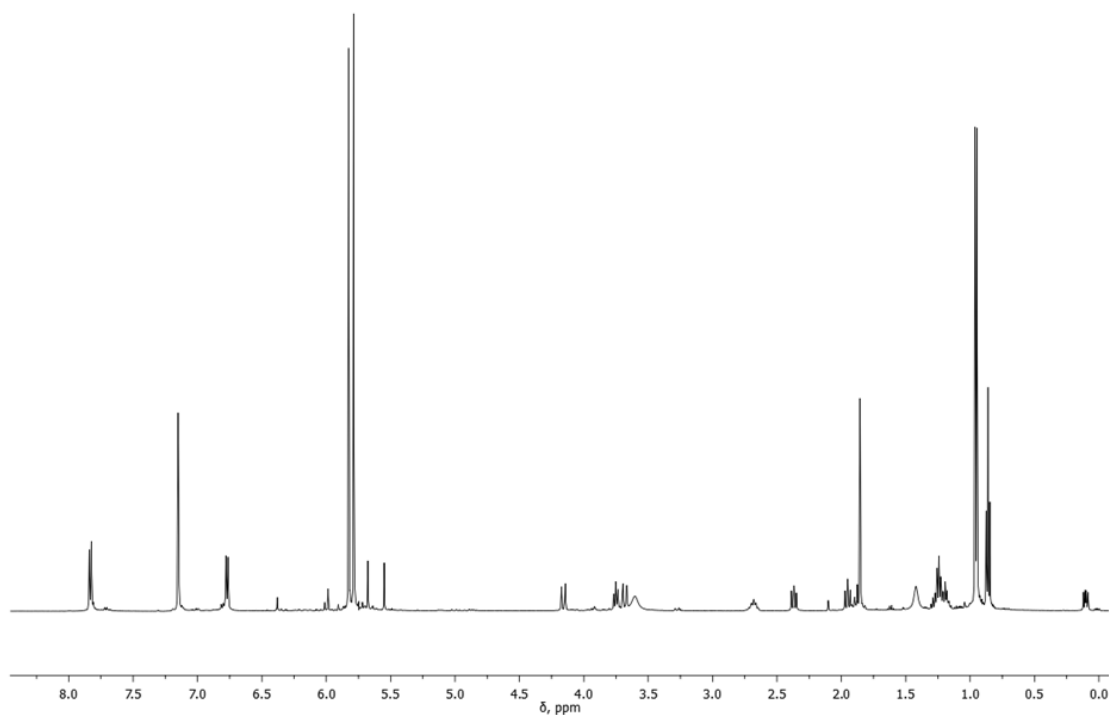
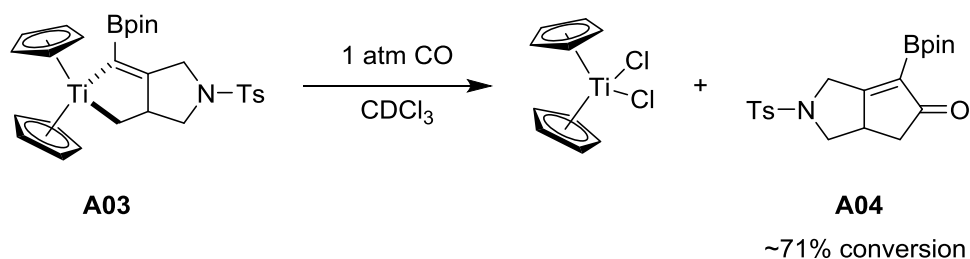


Figure A-2. ^1H NMR of **A03** in C_6D_6 .

Treatment of A03 with CO in C_6D_6 . **A03** (10 mg, 0.018 mmol) was dissolved in C_6D_6 in a J. Young tube, and the vessel was degassed using the “freeze-pump-thaw” method. The headspace was refilled with an atmosphere of CO. The next day, Cp_2TiCO

was the dominant product observed by ^1H NMR spectroscopy. An intractable mixture of organic products was also observed by ^1H NMR.



Scheme A-3. Synthesis of borylated cyclopentenone **A04** from **A03**.

Treatment of A03 with CO in CDCl₃. **A03** (20 mg, 0.036 mmol) was dissolved in CDCl₃ in a J.Young tube, with 5 mL of 1,4-dioxane as an internal standard. The vessel was degassed using the “freeze-pump-thaw” method. The headspace was refilled with an atmosphere of CO. The reaction was left overnight at room temperature. Analysis by ^1H NMR spectroscopy of the reaction mixture showed that Cp₂TiCl₂ was the dominant organometallic product, and there was 71% conversion to the cyclopentanone. **A04** observed *in situ* ^1H NMR (CDCl₃, 500 MHz): δ 7.72 (d, $J = 8$ Hz, 2H, Ar-*H*), 7.32 (d, $J = 8$ Hz, 2H, Ar-*H*), 4.38 (d, $J = 18$ Hz, 1H, NCH_aH_b), 4.28 (d, $J = 18$ Hz, 1H, NCH_aH_b), 3.72 (m, 1H, obscured by 1,4-dioxane), 3.95 (m, 1H, CH), 2.60 (dd, $J = 9.5$ Hz, $J = 9.5$ Hz, 1H, CH_aH_b), 2.42 (s, 3H, Ar-*Me*), 2.05 (dd, $J = 18$ Hz, $J = 3.5$ Hz, 1H, CH_aH_b), 1.26 (s, 12H, *Me* on Bpin).

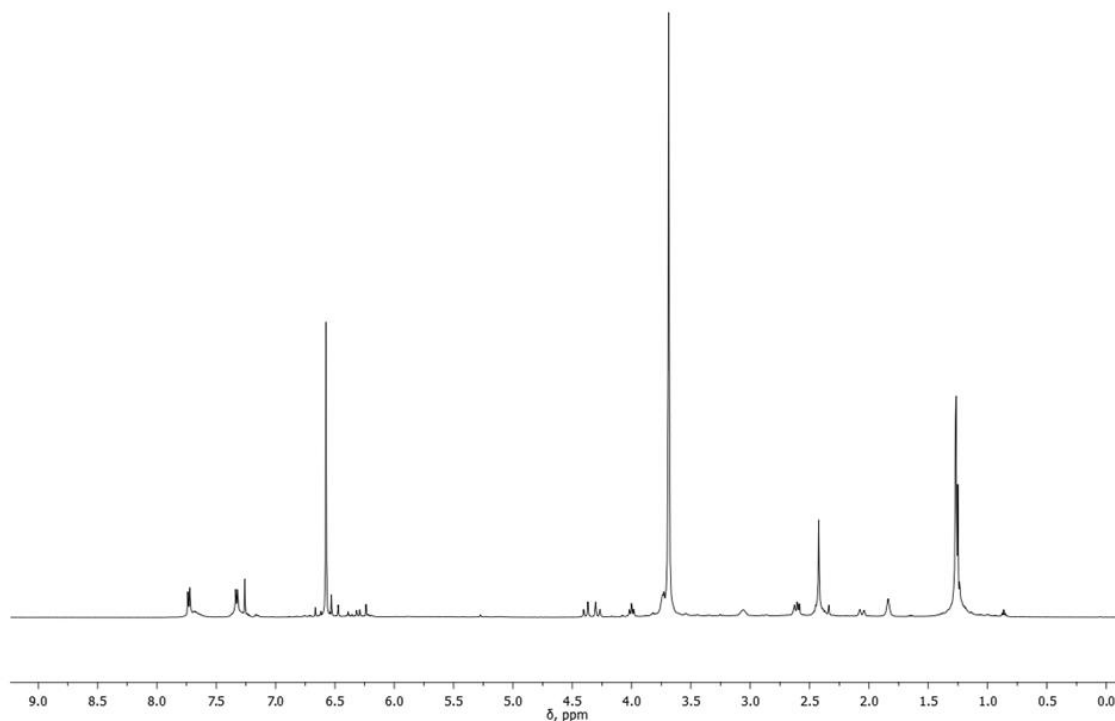
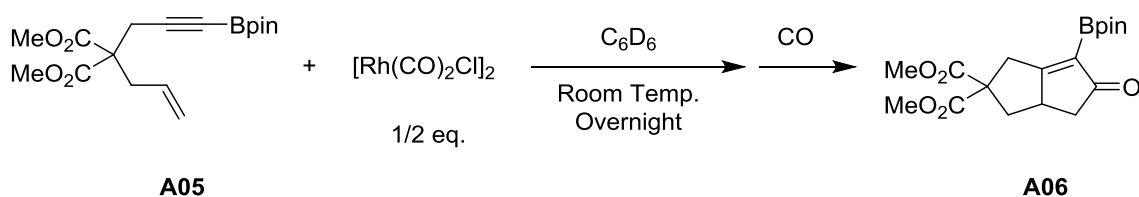


Figure A-3. *in situ* ^1H NMR of **A04** in CDCl_3 . Cp_2TiCl_2 is present at 6.58 ppm, and 1,4-dioxane is present at 3.73 ppm.

Treatment of 303B with $\text{Cp}_2\text{Ti}(\text{CO})_2$. In a J. Young tube, **303B** (23 mg, 0.06 mmol) was dissolved in C_6D_6 and treated with $\text{Cp}_2\text{Ti}(\text{CO})_2$ (14 mg., 0.06 mmol). The J. Young tube was placed in a 90 °C oil bath overnight. Analysis by ^1H NMR spectroscopy the next day showed a singlet at 4.58 corresponding to $\text{Cp}_2\text{Ti}(\text{CO})_2$ and broad low-intensity signals signifying the decomposition of the starting material.



Scheme A-4. Synthesis of borylated cyclopentenone **A06** with stoichiometric $[\text{Rh}(\text{CO})_2\text{Cl}]_2$.

Treatment of A05 with 0.5 eq. of $[\text{Rh}(\text{CO})_2\text{Cl}]_2$. **A05** (36 mg, 0.11 mmol) was dissolved in C_6D_6 in a J. Young tube and $[\text{Rh}(\text{CO})_2\text{Cl}]_2$ (21 mg, 0.05 mmol) was added. The reaction was left overnight at room temperature. In the morning, the solution was a dark brown color. The headspace of the vessel was removed using the “freeze-pump-thaw” method and the headspace was refilled with an atmosphere of CO. The solution turned yellow. The reaction was filtered through a pad of Celite and silica and redissolved in C_6D_6 . Analysis by ^1H NMR spectroscopy showed the formation of **A06**. ^1H NMR (C_6D_6 , 500 MHz): δ 3.77 (d, $J = 19.5$ Hz, 1H, CH_aH_b), 3.54 (d, $J = 19.5$ Hz, 1H, CH_aH_b), 3.26 (s, 3H CO_2Me), 3.22 (s, 3H, CO_2Me), 2.64 (m, 1H, CH), 2.56 (dd, $J = 12$ Hz, 7.4 Hz, CH_aH_b), 2.26 (dd, $J = 16.5$ Hz, $J = 6$ Hz, 1H, CH_aH_b), 1.67 (dd, $J = 16.5$ Hz, $J = 3$ Hz, 1H, CH_aH_b), 1.34 (dd apparent t, $J = 12.5$ Hz, 1H, CH_aH_b), 1.07 (s, 12H, Me on Bpin).

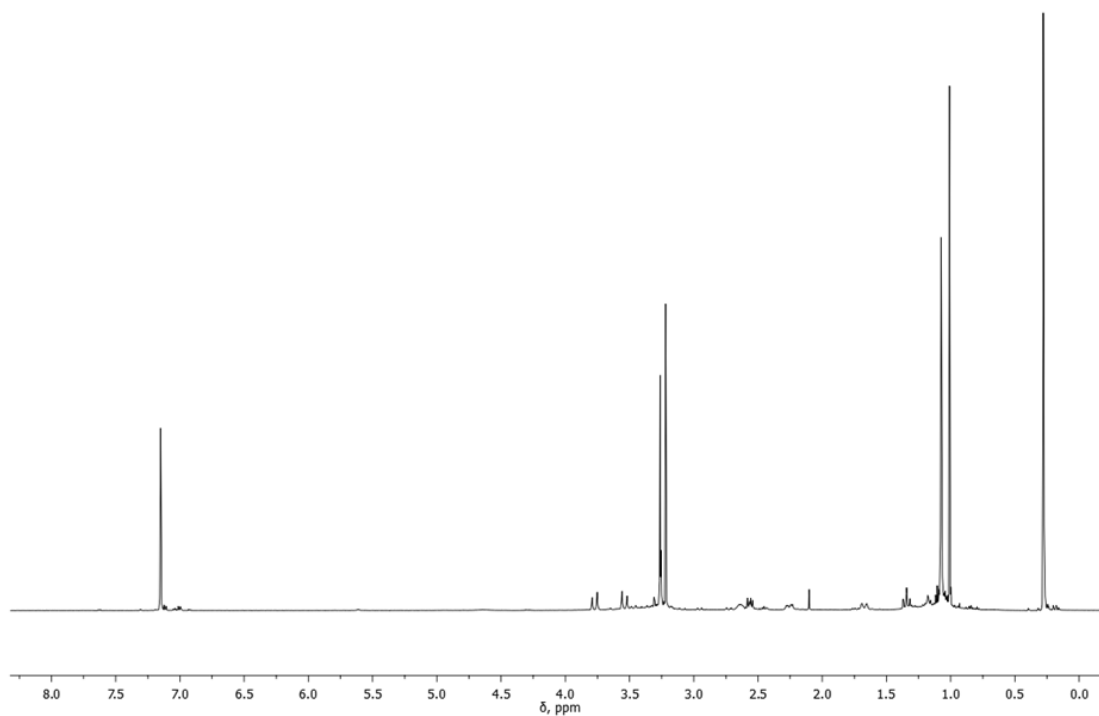


Figure A-4. ^1H NMR of **A06** in C_6D_6 . Bpin decomposition product can be observed at 1.01 and silicone grease is present at 0.29 ppm.

Attempts at Pauson Khand cyclization with borylated 1,6-enynes. Table A-1 shows several attempts at performing catalytic and cobalt-mediated Pauson Khand reactions with borylated 1,6-enynes. Each reaction was performed in a 0.1-0.2 mmol scale in a Teflon screw-top flask under the conditions described.

Table A-1. Attempts at stoichiometric and catalytic Pauson Khand reactions with alkynylboronates.

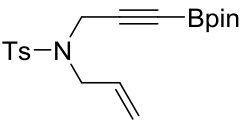
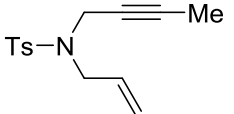
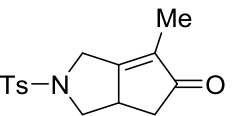
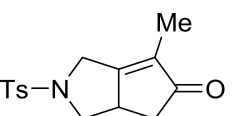
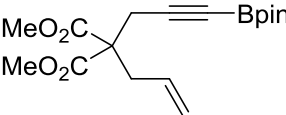
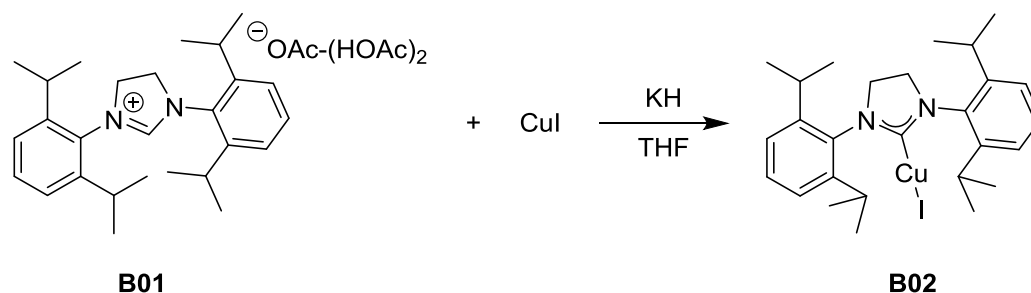
Substrate	Catalyst	Conditions	Result
 <p>303B</p>	5% [Rh(CO) ₂ Cl] ₂	PhF, 70 °C, 20 hours, 1 atm 15% CO in Ar	20% yield of A04
	5% [Rh(CO) ₂ Cl] ₂	PhF, 70 °C, 20 hours, 1 atm 10% CO in Ar	Trace yield of A04
	110% Co ₂ (CO) ₂	1,4-dioxane, 70 °C overnight	black tar after removing volatiles, Bpin decomposition product at 1.00 ppm.
	110% Co ₂ (CO) ₂	1,4-dioxane, 70 °C overnight, Dark	black tar after removing volatiles, Bpin decomposition product at 1.00 ppm.
	5% [Rh(CO) ₂ Cl] ₂ 10% dppe 15% AgOTf	THF, 80 °C, overnight, 10% CO in Ar	4 major products no trace of A04
	10% [Rh(CO) ₂ Cl] ₂ 20% BINAP 24% AgOTf	THF, 40 °C, 5h, 10% CO in Ar	No Reaction
	5% [Rh(CO) ₂ Cl] ₂	nBu ₂ O, 130 °C, 16 h, 1 atm CO	Mixture of intractable products, Bpin decomposition product observed at 1.00 ppm.
	5% Rh(dppe)Cl	Cinnamaldehyde 130 °C	Only starting material observed by ¹¹ B{ ¹ H} NMR spectroscopy
	5% [Ir(COD)Cl] ₂ 10% BINAP	Toluene, 110 °C, 1 atm CO, overnight	30% Bpin decomposition product at 1.00 ppm.
	5% Cp ₂ Ti(CO)	Toluene, 90 °C, 1 atm CO, overnight	No reaction
	10% Co ₂ (CO) ₂	THF, 80 °C, 1 atm CO	Mixture of intractable organic products, Bpin decomposition product at 1.00 ppm.

Table A-1. Continued

Substrate	Catalyst	Conditions	Result
 <p>A07</p>	5% $[\text{Rh}(\text{CO})_2\text{Cl}]_2$	nBu ₂ O, 130 °C, 16 h, 1 atm CO	>90% conversion to  <p>A08</p>
	5% Cp ₂ Ti(CO) ₂	Toluene, 90 °C, 1 atm CO, overnight	66% conversion to  <p>A08</p>
 <p>A05</p>	110% Co ₂ (CO) ₂	1,4 dioxane, 70 °C, 1 atm CO	Black tar produced Bpin decomposition product observed at 1.00 ppm.
	5% $[\text{Rh}(\text{CO})_2\text{Cl}]_2$	nBu ₂ O, 130 °C, 16 h, 1 atm CO	Intractable mixture of products, Bpin decomposition product observed at 1.00 ppm.

APPENDIX B

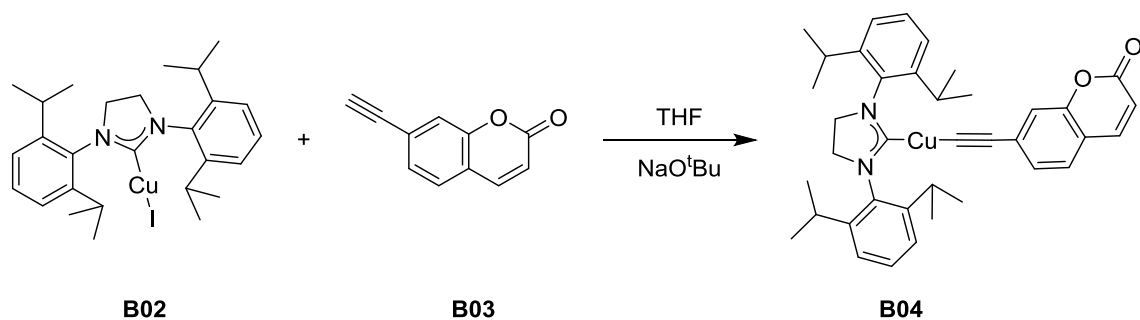
SYNTHESIS OF (NHC)CU ALKYNYL COMPLEXES



Scheme B-1. Synthesis of **B02**.

Synthesis of (SIPr)CuI (B02). In a Schlenk flask, 1,3-bis-(2,6-diisopropylphenyl)imidazolium diacetic acid acetate (**B01**) (350 mg, 0.613 mmol) was dissolved in THF and treated with potassium hydride (125 mg, 3.12 mmol) and CuI (295 mg, 1.55 mmol). The reaction was stirred overnight and the volatiles were removed under vacuum in the morning. The product was extracted with dichloromethane and passed through a pad of Celite. The volatiles were removed from the filtrate and the resulting powder was dissolved in a minimum amount of dichloromethane, which was layered with pentane and placed into a -35 °C freezer to recrystallize (347 mg, 97% yield). The ¹H NMR spectra matched that originally reported.*

* Díez-González, S.; Escudero-Adán, E. C.; Benet-Buchholz, J.; Stevens, E. D.; Slawin, A. M. Z.; Nolan, S. P. *Dalton Trans.* **2010**, 39, 7595-7606.



Scheme B-2. Synthesis of **B04**.

Synthesis of B04. In a Schlenk flask, **B02** (100 mg, 0.172 mmol) was dissolved in THF and treated with NaO^tBu (25 mg, 0.258 mmol) and **B03** (30 mg, 0.176 mmol) and stirred overnight. The volatiles were removed under vacuum in the morning. The product was extracted with dichloromethane and filtered through a pad of Celite. The volatiles were removed and **B04** was recrystallized from dichloromethane layered with pentane in a -35 °C freezer to yield a light yellow solid (70 mg, 65% yield). ¹H NMR (CDCl₃): δ 7.53 (d, *J* = 9.5 Hz, 2H, C=OCH=CH), 7.40 (t, *J* = 7.5 Hz, 2H, Ar-*H*), 7.25 (d, *J* = 7.5 Hz, 4H, Ar-*H*), 7.14 (d, *J* = 8 Hz, 1 Hz, Ar-*H*), 7.12 (s, 1H, Ar-*H*), 7.07 (dd, *J* = 8 Hz, *J* = 1.5 Hz, 1H, Ar-*H*), 6.20 (d, *J* = 9.5 Hz, C=OCH=CH), 4.00 (s, 4H, SiPr), 3.09 (m, 4H, CHMe₂), 1.38 (m, 24H, CHMe₂); ¹³C{¹H} NMR (CDCl₃): δ 204.5 (s, C=Cu), 161.4 (s, C=O), 153.9 (s, Ar-O), 146.7 (s, N-Ar), 143.4 (s), 134.6 (s), 131.6 (s), 129.8 (s), 128.4 (s), 126.9 (s), 119.6 (s), 116.5 (s), 114.7 (s), 104.9 (s), 53.9 (s, NCH₂), 29.1 (s, CHMe₂), 25.7 (s, CHMe₂), 24.0 (s, CHMe₂).

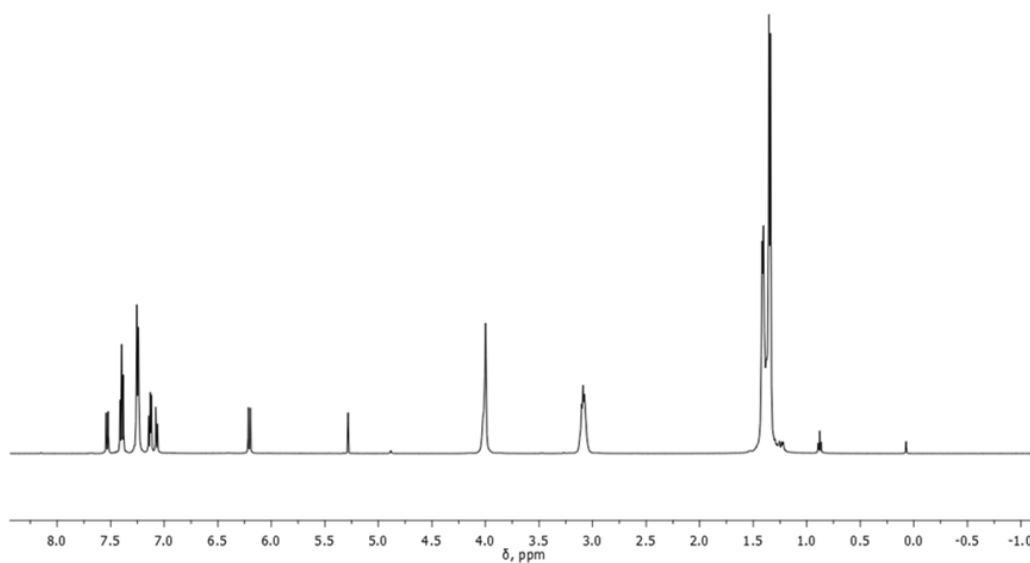
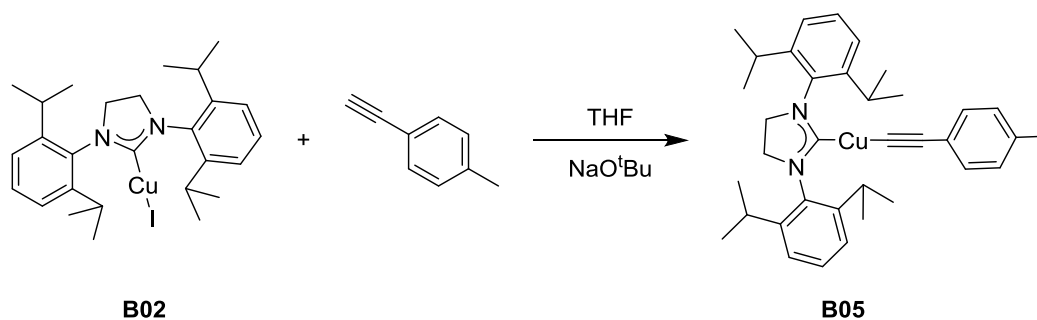


Figure B-1. ^1H NMR of **B04** in CDCl_3 . Residual dichloromethane visible at 5.30 ppm, residual pentane resonances visible at 0.88 ppm and 1.27 ppm. Residual silicone grease visible at 0.07 ppm.



Scheme B-3. Synthesis of **B05**.

Synthesis of B05. In a Schlenk flask, **B02** (100 mg, 0.172 mmol) was dissolved in THF and treated with NaO^tBu (25 mg, 0.258 mmol) and 4-ethynyltoluene (22 μ L, 0.173 mmol) and stirred overnight. The volatiles were removed under vacuum in the morning. The product was extracted with dichloromethane and filtered through a pad of Celite. The volatiles were removed and the product was recrystallized from dichloromethane layered with pentane in a -35 °C freezer to yield a light yellow-white solid (51 mg, 52% yield). ¹H NMR (CDCl₃): δ 7.39 (t, J = 7.5 Hz, 2H, Ar-*H*), 7.25 (d, J = 7.5 Hz, 4H, Ar-*H*), 7.11 (d, J = 8 Hz, 2H, Ar-*H*), 6.86 (d, J = 7.5 Hz, 2H, Ar-*H*), 3.67 (s, 4H, SiPr), 3.10 (sept., J = 7 Hz, 4H, CHMe₂), 2.20 (s, 3H, Ar-*Me*), 1.42 (d, J = 7 Hz, 12H, CHMe₂), 1.35 (d, J = 7 Hz, 12H, CHMe₂); ¹³C{¹H} NMR (CDCl₃): δ 205.0 (s, C=Cu), 146.8 (s, N-*Ar*), 134.9 (s), 134.8 (s), 131.9 (s), 129.7 (s), 128.3 (s), 124.6 (s), 124.2 (s), 119.9 (s), 105.7 (s), 53.9 (s, NCH₂), 29.1 (s, CHMe₂), 25.7 (s, CHMe₂), 24.1 (s, CHMe₂), 21.4 (s, Ar-*Me*).

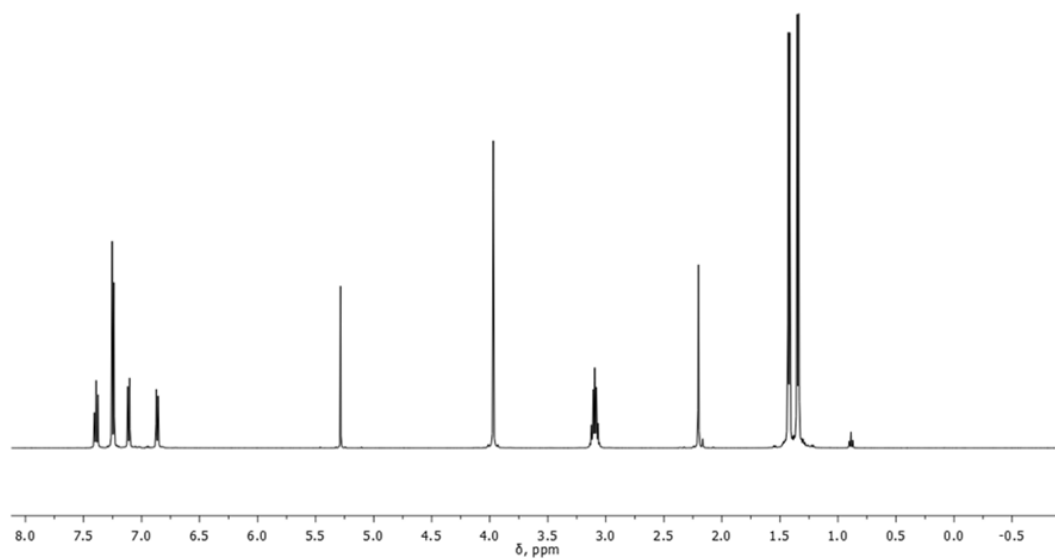


Figure B-2. ^1H NMR spectrum of **B05** in CDCl_3 . Residual dichloromethane visible at 5.30 ppm, residual pentane resonances visible at 0.88 ppm and 1.27 ppm.

APPENDIX C

LIST OF PUBLICATIONS RESULTING FROM PHD WORK

- (1) Pell, C. J.; Shih, W.-C.; Gatard, S.; Ozerov, O. V. "Formation of (PNP)Rh Complexes Containing Covalent Rhodium-Zinc Bonds in Studies of Potential Rh-Catalysed Negishi Coupling", *Chem. Commun.* **2017**, *53*, 6456.
- (2) Pell, C. J.; Zhu, Y.; Huacuja, R.; Herbert, D. E.; Hughes, R. P.; Ozerov, O. V. "Fluorocarbene, Fluoroolefin, and Fluorocarbyne Complexes of Rh", *Chem. Sci.* **2017**, *8*, 3178.
- (3) Lee, C.-I.; DeMott, J. C.; Pell, C. J.; Christopher, A.; Zhou, J.; Bhuvanesh, N.; Ozerov, O. V. "Ligand Survey Results in Identification of PNP Pincer Complexes of Iridium as Long-lived and Chemoselective Catalysts for Dehydrogenative Borylation of Terminal Alkynes", *Chem. Sci.* **2015**, *6*, 6572.
- (4) Pell, C. J.; Ozerov, O. V. "Catalytic Dehydrogenative Borylation of Terminal Alkynes by POCOP-Supported Palladium Complexes", *Inorg. Chem. Front.* **2015**, *2*, 720.
- (5) Timpa, S. D.; Pell, C. J.; Ozerov, O. V. "A Well-Defined (POCOP)Rh Catalyst for the Coupling of Aryl Halides with Thiols", *J. Am. Chem. Soc.* **2014**, *136*, 14772.
- (6) Timpa, S. D.; Pell, C. J.; Zhou, J.; Ozerov, O. V. Fate of Aryl/Amido Complexes of Rhodium(III) Supported by a POCOP Pincer Ligand: C–N Reductive Elimination, β -Hydrogen Elimination, and Relevance to Catalysis *Organometallics* **2014**, *33*, 5254.

(7) Pell, C. J.; Ozerov, O. V. “A Series of Pincer-Ligated Rhodium Complexes as Catalysts for the Dimerization of Terminal Alkynes”, *ACS Catalysis* **2014**, *4*, 3470.